THE MECHANISTIC EFFECTS OF BAICALEIN ON AQUEOUS HUMOR DRAINAGE AND ITS OCULAR HYPOTENSIVE RESPONSE

LI HOI LAM

Ph.D

The Hong Kong Polytechnic University

2021

The Hong Kong Polytechnic University

School of Optometry

The Mechanistic Effects of Baicalein on Aqueous Humor Drainage and Its Ocular Hypotensive Response

Li Hoi Lam

A thesis submitted in partial fulfillment of the requirements for the degree of Doctor of Philosophy

August 2019

CERTIFICATE OF ORIGINALITY

I hereby declare that this thesis is my own work and that, to the best of my knowledge and belief, it reproduces no material previously published or written, nor material that has been accepted for the award of any other degree or diploma, except where due acknowledgement has been made in the text.

Li Hoi Lam

Abstract

Glaucoma is a multifactorial eye disease characterized by gradual loss of vision resulting from progressive optic neuropathy. Despite the fact that glaucoma is a leading cause of blindness worldwide, there is currently no cure yet for glaucoma. Lowering intraocular pressure (IOP) is the only clinical intervention known to slow the progression of glaucomatous blindness. Reduced treatment efficacy and adverse ocular side effects are; however, frequently reported after prolong use of existing anti-glaucoma medications. This strongly suggests an urgent need for a more potent agent with minimal side effects. Baicalein (5,6,7-trihydroxyflavone) is a natural flavonoid derived from the dried roots of *Scutellaria baicalensis Georgi*. It is frequently found in vegetables and commonly used in traditional Chinese medicine. It has been previously reported that baicalein inhibits swelling-activated Cl^- channels in non-pigmented ciliary epithelial cells, potentially reducing the rate of aqueous humor secretion. In addition, it is anticipated that baicalein may affect cell contractility and cell volume regulation as well as extracellular matrix (ECM) remodeling. There have been no literatures to date reporting the effects of baicalein on outflow facility. The primary aim of this study was to elucidate the mechanistic effects of baicalein on conventional outflow facility. The secondary aim was to observe its potential IOP-lowering effects when administered to living rodents.

First, the acute effect of baicalein on outflow facility was studied using constant pressure perfusion system in freshly enucleated C57BL/6J mouse eyes. Outflow facility was determined by measuring the flow rates at sequential pressure steps. Results demonstrated that baicalein elicited a concentration-dependent increase in outflow facility. At 10 μM, baicalein enhanced the outflow facility by approximately 90%, suggesting that baicalein may affect conventional outflow facility, in addition to its inhibitory effect on aqueous humor secretion.

Second, the mechanisms underlying the effects of baicalein on cell volume regulation, cell contractility and cell migration was studied using human trabecular meshwork (hTM) cells. It was shown that baicalein did not affect the cell volume under isometric conditions while a significant inhibition of regulatory volume decrease (RVD) was observed when subjected to hypotonic solution in hTM cells. Likewise, it was found that baicalein triggered a concentration-dependent hTM cell relaxation and retardation of cell migration when compared to the control group. These results suggested that baicalein may enhance the outflow facility by reducing its outflow resistance through the regulation of RVD, cell contractility and migration in hTM cells.

Next, we examined the patterns of differential protein expression and identified specific and novel pathways mediated by baicalein using isobaric tag for relative and absolute quantitation (iTRAQ) based quantitative proteomics. Selected candidate proteins were validated by quantitative polymerase chain reaction (qPCR). The 47 and 119 proteins were significantly regulated after a 3-hour and a 2-day baicalein treatment in hTM cells, respectively. In agreement with our foregoing results, baicalein was shown to alter the expressions of pre-B-cell leukemia transcription factor-interacting protein 1 (PBXIP1) and arylsulfatase B (ARSB), supporting the notion of baicalein-mediated inhibition of TM cell migration. Apart from that, baicalein increased the expressions of matrix metalloproteinase-14 (MMP-14) and cathepsin B that are responsible for extracellular matrix (ECM) digestion, suggesting that baicalein may decrease the outflow resistance by modulating ECM composition. In addition, novel protein changes and pathways of human TM cells related to oxidative phosphorylation, clathrin-mediated endocytosis and mitochondrial dysfunction were observed.

Finally, the *in vitro* findings were validated by measuring IOP changes in rodents. Baicalein, when administrated intraperitoneally, topically or intravitreally, caused a significant reduction in IOP. The largest IOP-lowering effect was achieved with

intravitreal injection of baicalein, in which IOP was lowered by ~9 mmHg in Sprague Dawley (SD) rats.

Taken together, these findings suggest that baicalein may regulate the contractility and volume of hTM cells and the composition of the ECM in the outflow pathway; thereby, enhancing the outflow facility and potentially leading to a reduction of IOP.

Publications, presentations and award arising from the thesis

Research manuscripts:

Shan SW, Do CW, Lam TC, **Li HL**, Stamer WD, To CH. Thrombospondin-1 mediates Rho-kinase inhibitor-induced increase in outflow-facility. J Cell Physiol. 2021 Jun 27. doi: 10.1002/jcp.30492. Epub ahead of print. PMID: 34180057.

Shan SW, Do CW, Lam TC, **Li HL**, Stamer WD, To CH. Data on differentially expressed proteins in ROCK inhibitor-treated human trabecular meshwork cells using SWATH-based proteomics. Data Brief. 12(31):105846, 2020.

Li SKL, Shan SW, **Li HL**, Cheng AKW, Pan F, Yip SP, Civan MM. To CH, Do CW. Characterization and regulation of gap junctions in porcine ciliary epithelium. Invest Ophthalmol Vis Sci. 59(8):3461-3468, 2018.

Conference presentations:

Shan SW, Lam TC, Stamer WD, **Li HL**, Do CW, To CH. The effects of a Rho-associated protein kinase (ROCK) inhibitor (Y39983) on human trabecular meshwork cells – a morphological and proteomic study. Association for Research in Vision and Ophthalmology (ARVO). E-Abstract 5138, May 2019.

Li HL, Dey A, Yu SS, Shan SW, Stamer WD, Chan HL, To CH, Kin C, Do CW. Effects of intravitreal administration of baicalein on intraocular pressure and retinal

thickness in Sprague-Dawley rats. Association for Research in Vision and Ophthalmology (ARVO). E-Abstract 4466, May 2017.

Li HL, Navarro ID, Ashpole NE, Lam C, Chan HL, To CH, Stamer WD, Do CW. Baicalein lowers intraocular pressure and increases outflow facility in mouse eye. Association for Research in Vision and Ophthalmology (ARVO). E-Abstract 2174960, May 2015.

Li HL, Chan HL, To CH, Do CW. Effects of topical baicalein on intraocular pressure in rodents. 12th Association for Ocular Pharmacology and Therapeutics (AOPT). Charleston, South Carolina, Feb 2015.

Li HL, Leung CT, Chan HL, To CH, Do CW. Ocular hypotensive effect of baicalein in Sprague-Dawley rats. Association for Research in Vision and Ophthalmology (ARVO). E-Abstract 1916964, 2014.

Awards:

ARVO 2015 Annual Meeting: Emerging Trends and Hot Topics

Acknowledgements

I would like to express my sincere thanks to my principal supervisor, Dr. Chi-wai Do, and my co-supervisors, Prof. Chi-ho To, and Dr. Dr Henry Chan for their guidance and suggestions on my research study. Their encouragement, patience and continuous support are indispensable for me to complete my study.

My special thanks to Prof. W Daniel Stamer for providing me with a valuable and unforgettable overseas experience at Duke University. I am extremely grateful to Prof. Stamer and his team members for their inspiration, supports and comments. I would also like to thank Dr. Kin Chiu for her teaching and guidance. Thanks also to Dr. Thomas Lam for his patience and precious suggestions especially on the proteomic studies. This project could not be possible without their generous help.

I very much appreciate working with Dr. Samantha Shan, Dr. Rachel Chun, Dr. Tracy Ho, Mr. KK Li, Mr. Jimmy Cheung, Dr. Lily Chan and all my colleagues. They provided me with care, comments and encouragement. Their extended supports have brightened up my research study life.

Last but not least, I would like to express my gratitude to my parents, sister, brother and all relatives. Without their endless love, support and sacrifices, I would not be able to pursuit my study. Thank you very much to all the people who love me and to the people I love.

Li Hoi Lam

Table of contents

List of figures

List of tables

List of abbreviations

A1AR	A1 adenosine receptor
AH	Aqueous humor
ASK1	Apoptosis signal-regulating kinase 1
Ba	Baicalein
BCD	2-hydroxypropyl-β-cyclodextrin
C57 mice	C57BL/6J mice
DDA	Data-dependent acquisition
DMEM	Dulbecco's modified Eagle's medium
ECM	Extracellular matrix
FA	Formic acid
FBS	Fetal bovine serum
FDR	False discovery rate
hTM	Human trabecular meshwork
IL	Interleukin
IOP	Intraocular pressure
IPA	Ingenuity pathway analysis
iTRAQ	Isobaric tag for relative and absolute quantitation
JCT	Juxtacanalicular tissue
MLC	Myosin light chain
MMP	matrix metalloproteinase
MRM	Multiple reaction monitoring
MTT	(3-(4,5-dimethylthiazol-2-yl)-2,5-diphenyltetrazolium bromide) tetrazolium
NPE	Non-pigmented ciliary epithelium

NTG	Normal tension glaucoma
OCT	Optical coherence tomography
PANTHER	Protein ANalysis THrough Evolutionary Relationships
PBS	Phosphate-buffered saline
PCR	Polymerase chain reaction
PE	Pigmented ciliary epithelium
PKC	Protein kinase C
pMLC	Phosphorylated myosin light chain
POAG	Primary open-angle glaucoma
PPI	Protein-protein interaction
RGCs	Retinal ganglion cells
ROCK	Rho kinase
ROS	Reactive oxygen species
RVD	Regulatory volume decrease
SC	Schlemm's canal
SD-OCT	Spectral domain optical coherence tomography
SD rats	Sprague Dawley rats
STRING	Search Tool for the Retrieval of Interacting Genes
TBST	Tris-buffered saline with Tween®20
TGFB1	Transforming growth factor beta-1
TIMP	Tissue inhibitors of metalloproteinase
TM	Trabecular meshwork
TNF	Tumor necrosis factor

Chapter 1 Introduction

1.1 Background

Glaucoma is a common but serious eye disease often resulting in permanent loss of sight. According to findings published by the World Health Organization, it is the leading cause of irreversible blindness worldwide (World Health Organization, 2020). Recent reports indicate that the global number of glaucoma patients aged 40-80 years is expected to increase by 74% from 2013 to 2040, totalling more than 110 million by 2040 (Tham et al., 2014). Vision loss resulting from glaucoma can significantly affect patients' functional mobility and quality of life; thereby, increasing health care, welfare, and economic burdens on our society.

Glaucoma is a group of optic neuropathies with unclear pathogenesis. It is characterized by the progressive loss of retinal ganglion cells (RGCs) and their axons that can be classified into open-angle and angle-closure glaucoma (Weinreb and Khaw, 2004). Both open-angle and angle-closure glaucoma can be the primary disease or secondary to trauma or medications (Weinreb et al., 2014). Among various types of glaucoma, primary open angle glaucoma (POAG) is the most common and is characterized by its insidious onset and progression (Kapetanakis et al., 2016). Raised

intraocular pressure (IOP), family history, aging, diabetes, and high myopia are the major risk factors for glaucoma (Toris and Camras, 1998, Coleman and Miglior, 2008). Among them, elevated IOP has been suggested to be the only modifiable and treatable risk factor. Lowering IOP has been well documented to be a proven effective clinical intervention to retard the onset and progression of glaucomatous blindness (Collaborative Normal-Tension Glaucoma Study Group, 1998b, Collaborative Normal-Tension Glaucoma Study Group, 1998a, The AGIS Investigators, 2000). Despite that, the pathogenesis and pathophysiology of glaucoma remain unclear. As a result, there is still no cure for this disease nor effective treatment to arrest its progression. Without an effective therapy, it is undoubtedly a pressing challenge for the health care system.

1.2 Pathogenesis of glaucoma

Glaucoma is typically characterized with a progressive loss of RGCs and axonal degeneration (Weinreb and Khaw, 2004). Despite the fact that elevated IOP is a major risk factor for glaucoma, normal tension glaucoma (NTG) is not uncommon. In NTG, patients may have an IOP level comparable to that of healthy individuals but still suffer from glaucomatous vision loss (Wang et al., 2012). This suggests that IOP alone cannot fully explain the pathophysiological changes observed in glaucoma

patients. There are a number of theories, including biomechanical, vascular and biochemical theories that may account for the pathogenesis of glaucoma (Ichhpujani and Kumar, 2019, Fechtner and Weinreb, 1994). It is likely that these theories are inter-related, as none of these mechanisms alone can fully explain the variations in glaucomatous damages observed clinically and experimentally.

1.2.1 Biomechanical theory

The biomechanical theory defines IOP as a mechanical force exerted on various tissues that are affected by glaucoma. Particularly, the optic nerve head is quite a vulnerable site when observed in a mechanical perspective since it is where the optic nerve extends from the intraocular space to the subarachnoid space. Here, translaminar pressure is exerted on the optic nerve head from two separate compartments, namely intraocular pressure (IOP) and intracranial / cerebrospinal fluid pressure (Morgan et al., 1995). This can be quite a mechanically stressed spot susceptible to IOP-related changes. Elevated IOP has been regarded as a major risk factor of glaucoma. The prevalence of POAG increases dramatically from 0.65% in subjects with IOP lower than 15 mmHg to 38.92% in those with IOP >30 mmHg (Sommer et al., 1991). It has been demonstrated that elevation of IOP is significantly correlated with structural (Medeiros et al., 2009) and functional (Bergeå et al., 1999)

damages in the retina as observed in glaucoma patients. Retinal damages caused by increased IOP have also been reported in animal studies. For example, sustained elevation of IOP causes a progressive increase in optic nerve cupping, reduction of axon survival and functional retinal responses in rats with chronic ocular hypertension compared to normotensive controls (Chauhan et al., 2002). Moreover, increased IOP can lead to partial or even complete obstruction of axoplasmic transport in the lamina cribrosa region (Anderson and Hendrickson, 1974). It has been shown that elevated IOP in rhesus monkey enhances elastin synthesis in laminar astrocytes. The increased elastin can lead to structural changes in the extra-cellular matrix (ECM), loss of resiliency and deformability of the lamina cribrosa (Pena et al., 2001). These changes in biomechanical properties persist even when IOP is reduced, increasing susceptibility of astrocytes in the development of glaucomatous neuropathy.

Despite the well-established link between IOP and glaucomatous damages, NTG patients with normal IOP (e.g. <21 mmHg) can also suffer from glaucomatous neurodegeneration. This implies that additional factor(s) may be involved in mediating RGC loss rather than elevated IOP alone. It has been revealed that patients with NTG display a significantly lower cerebrospinal fluid pressure compared to those with POAG and healthy subjects (Wang et al., 2012). Thus, both increased IOP

and/or reduced cerebrospinal fluid pressure / intracranial pressure are factors that may generate a pressure difference across the optic nerve head. This, in turn, may lead to deformation and remodeling of lamina cribrosa; thereby, disrupting the axonal transport and inducing RGCs apoptosis (Pena et al., 2001, Weinreb et al., 2014).

1.2.2 Vascular theory

The vascular theory proposes that vascular factors such as ischemia may be involved in the pathogenesis of glaucoma. Maintaining an optimal ocular blood supply is critical due to the high metabolic demands of the retina. It has been suggested that vascular insufficiency may affect the onset and progression of glaucomatous neuropathy (Weinreb and Khaw, 2004). The central retinal artery and short posterior ciliary arteries are the major arteries providing blood supply to the retina. A reduced ocular blood flow and/or velocity may decrease oxygen and nutrient supply as well as metabolic waste removal from the retina. Insufficient blood supply to the retina may result in tissue hypoxia and accumulation of reactive oxygen species (ROS), contributing to subsequent RGC death (Yanagi et al., 2011). The equilibrium between vasodilators such as nitric oxide and vasoconstrictors such as endothelin-1 is important in maintaining vascular function and homeostasis. This disturbance may induce ischemia and reperfusion, further exaggerating oxidative damage (Flammer et

al., 2002). In rodents, retinal ischemia and reperfusion injuries significantly increases RGCs death through necrosis or apoptosis (Slater et al., 2008, Dvoriantchikova et al., 2014).

Reduced systolic and diastolic flow velocities in central retinal artery and short posterior ciliary arteries have been reported in patients with NTG and POAG (Rankin et al., 1995). This has not observed in ocular hypertensive and normal individuals (Akarsu and Bilgili, 2004). In POAG patients with asymmetric visual field defects, while IOPs are comparable, asymmetric flow velocity in central retinal artery and ophthalmic artery are found between the two eyes (Plange et al., 2006). The eyes with more advanced glaucomatous visual field loss demonstrate a lower flow velocity in both ophthalmic artery and central retinal artery, which may be contributed by the increased vascular resistance. This finding suggests that there may be a direct correlation between decreased blood velocity and visual field defect. This also indicates that slower retinal blood supply may contribute to the glaucomatous damage independent of IOP.

1.2.3 Biochemical theory

Glaucoma is a complex multifactorial disease. In additional to biomechanical and vascular theories, ample evidence have demonstrated that increased oxidative stress and inflammatory response contribute to the pathological changes observed in glaucoma patients (Ichhpujani and Kumar, 2019).

1.2.3.1 Oxidative stress

Reactive oxygen species (ROS) is the by-products of mitochondrial oxidative metabolism or cellular response to inflammation and infection (Holmström and Finkel, 2014). Oxidative stress occurs when the production of ROS exceeds the intrinsic anti-oxidative capacity. ROS has been suggested to trigger various chronic diseases, including cardiovascular and ocular diseases, possibly through ROS-mediated damages to lipid, proteins and nucleic acid (Mayne, 2003, Willcox et al., 2004).

It has been reported that there is an increase of ROS in the trabecular meshwork (TM) (Saccà et al., 2005), aqueous humor (AH) (Ferreira et al., 2004, Ghanem et al., 2010) and RGCs (Wax and Tezel, 2009) of glaucoma patients. The increase in ROS may be related to the reduced oxygen supply and metabolic waste removal resulted from the

decreased outflow facility and/or ocular blood flow to the affected tissues (Mozaffarieh et al., 2008). Excessive oxidative stress may increase mitochondrial DNA damage or reduce the number of mitochondria. This may eventually lead to mitochondrial dysfunction triggering apoptosis of TM cells (Izzotti et al., 2010) and RGCs (Kong et al., 2009) in glaucoma patients. It is likely that ROS triggers DNA damage by increasing DNA double-strand breaks (Yu and Anderson, 1997). Significant correlations between DNA oxidative damage and visual defect and IOP have been reported (Saccà et al., 2005). In addition, ROS impairs cell-matrix adhesion, leading to disruption of the cytoskeletal structure, scant cell adhesion and cell loss observed in glaucomatous TM (Zhou et al., 1999, Alvarado et al., 1984). It has been reported that intracellular ROS can trigger an inflammatory response in TM cells. This may be a contributing factor leading to the apoptotic cell death and impairment of AH drainage (Li et al., 2007, Izzotti et al., 2006).

1.2.3.2 Inflammation

There have been ample of evidence suggesting inflammatory response associated with the pathogenesis of glaucoma. In patients with POAG, cytokine levels have been found to be directly proportional to the severity of glaucomatous neuropathy (Huang et al., 2010, Kuchtey et al., 2010). As inflammation is usually triggered by injuries

such as optic nerve transection, it may increase the expression of pro-inflammatory cytokines, eventually causing cell death (Agudo et al., 2009). Studies have demonstrated that there is a significant upregulation of different inflammatory cytokines in serum (Huang et al., 2010), AH (Balaiya et al., 2011, Takai et al., 2012), TM (Taurone et al., 2015) and the retina (Tezel et al., 2001) of POAG patients. In addition, excitotoxicity and inflammatory response can be induced by ischemia, excessive intracellular ROS and dysregulation of blood flow (Ergorul et al., 2010, Evangelho et al., 2019, Li et al., 2007). Vascular dysregulation may lead to hypoxia-induced RGC death by impairing the blood-retinal barrier (Chan-Ling et al., 2007).

It has been shown that inflammation induced by oxidative stress impair the outflow facility in TM and promote RGC loss (Vohra et al., 2013). Moreover, inflammatory response has been shown to alter the expression of matrix metalloproteinases (MMPs). MMPs are essential for the maintenance of IOP homeostasis by regulating ECM turnover (Bradley et al., 2001).

1.3 Treatment of glaucoma

Among the risk factors for glaucoma, IOP is perhaps the only treatable risk factor. Currently, lowering IOP is an effective clinical intervention for delaying the progression of visual field loss regardless of the types of glaucoma (Collaborative Normal-Tension Glaucoma Study Group, 1998b, Collaborative Normal-Tension Glaucoma Study Group, 1998a, The AGIS Investigators, 2000). Glaucoma treatment targeted at IOP reduction can be classified into surgical, laser, and drug treatments. Surgical and laser treatments often produce remarkable and more sustainable IOP lowering effects for a longer period. Nevertheless, they are considered invasive procedures, which can lead to higher risks of complications such as inflammation, local scarring, and pressure spikes (Conlon et al., 2017). Therefore, topical eye medications are often regarded as the first-line treatment for glaucoma.

The AH is a transparent fluid that fills the anterior segment of the eye. IOP level reflects the balance between the rates of AH secretion and its drainage (Do and Civan, 2004, Roy Chowdhury et al., 2015). Elevated IOP in glaucoma is often due to an increased outflow resistance rather than an increased AH secretion (Johnson, 2006). However, majority of the currently-available pharmacologic anti-glaucoma agents lower IOP by either suppressing AH secretion or increasing AH drainage. There are

several classes of drugs used in glaucoma management. They include beta-adrenergic blockers, carbonic anhydrase inhibitors, alpha-adrenergic agonists, prostaglandin analogs and Rho-associated kinase (ROCK) inhibitors (Schehlein and Robin, 2019, Weinreb et al., 2014). The first three classes decrease AH production while prostaglandin analogs and ROCK inhibitors improve fluid drainage (Toris et al., 2008, Rao et al., 2001). It has been demonstrated that the IOP-lowering efficacy reduces after prolonged periods of single drug treatment (Gehr et al., 2006). As a result, more than one medication may be required. For example, studies have shown that combination eye drops targeting different sites can achieve additive IOP-lowering effects (Tanihara et al., 2015). Nevertheless, potential unwanted side effects are similar to each individual drug combined, eventually reducing patient compliance (Conlon et al., 2017). Ocular adverse reactions include blurred vision, stinging sensation, superficial punctate keratitis, corneal erosion, loss of Meibomian gland, and instability of tear film (Arita et al., 2012, Inoue, 2014, Sugrue, 2000). In addition, there is a paradigm of limitations and contraindications related to existing medications. For example, beta-adrenergic blockers are contraindicated in patients with heart and respiratory diseases. It may lead to heart failure, arrhythmia and respiratory arrest (Stewart and Garrison, 1998). Adrenergic agonists and carbonic anhydrase inhibitors are also contraindicated in patients with systemic hypertension, cardiac arrhythmia,

and kidney stones (Lee and Higginbotham, 2005). Therefore, there is a pressing need to develop more potent and safer medications with fewer contraindications and side effects. This relies on a comprehensive understanding of the mechanism and regulation of AH dynamics, which is considered to be scientifically and clinically important.

1.4 Overview of aqueous humor dynamics

IOP levels are governed by a dynamic balance between the rates of AH secretion (inflow) and drainage (outflow). Impairment of the AH inflow and outflow pathways may upset this balance leading to elevated IOP. AH is produced by the ciliary processes and secreted into the posterior chamber. From there, it will pass through the pupil, into the anterior chamber and eventually leaves the eye through two distinct outflow pathways (Goel et al., 2010). The total volume of AH in the human eye is estimated to be 250-375 µl, with a turnover rate of about 100 minutes (Freddo et al., 2020). Maintaining AH circulation is important. It provides oxygen and nutrients to avascular structures of the anterior segment, including the cornea and the crystalline lens. In addition, it removes metabolic wastes from the eye. A stable AH flow and IOP also help inflate the globe and maintain the structural integrity of the eye (To et al., 2002).

1.4.1 Aqueous humor secretion

Several key steps are involved in AH secretion. First, filtrate is formed in the interstitial space of the ciliary stroma from the blood supply to the ciliary processes. Second, solutes are selectively transported by the ciliary epithelium to the posterior chamber. Last, an osmotic fluid flow results from the transport of solutes (Freddo et al., 2020, Bill, 1975).

There are three major physiological processes responsible for AH secretion, namely diffusion, ultrafiltration and active secretion. Diffusion is a passive process by which the solutes move from a region of high to low concentration. Ultrafiltration is also a passive process which allows for the movement of solutes through a membrane. It is driven by a pressure difference between two compartments. In contrast, several lines of evidence show that AH secretion is primarily driven by active transport rather than ultrafiltration and diffusion. Active transport is an energy-dependent mechanism. Solutes and ions are transported against a concentration gradient across the plasma membrane (Bill, 1975). As such, the rate of AH production can be inhibited by anoxia (Chu and Candia, 1988, Krupin et al., 1984), hypothermia (Cole, 1969, Becker, 1960), and metabolic inhibitors (Shahidullah et al., 2003, Kodama et al., 1985).

AH is secreted by the ciliary epithelium. This dual-layered epithelium is comprised of pigmented ciliary epithelium (PE) facing the ciliary stroma and non-pigmented ciliary epithelium (NPE) facing the posterior chamber of the eye. These two cell layers are connected with each other at the apical surface via intercellular gap junctions. It has been demonstrated that active Cl^- secretion is the major driving force for AH secretion (Kong et al., 2006, Do and Civan, 2004, Do and To, 2000). There are a number of transport steps involved in Cl^- movement across the ciliary epithelium. First, Cl^- uptake by PE cells from the ciliary stroma is achieved by two different pathways. They include the Na^+-K^+-$2Cl^-$ symport (Do and To, 2000) and the Na^+/H^+ coupled with Cl^-/HCO_3^- antiports (Counillon et al., 2000), which are powered by the Na^+-K^+-ATPase in the PE cells (Shahidullah et al., 2017, Glynn, 2002). Second, Cl^- is transferred from PE to NPE cells by diffusion (Coca-Prados et al., 1992). Third, Cl^- is released from NPE cells to the posterior chamber via Cl^- channels located at the basolateral membrane. The net Cl^- secretion establishes an osmotic gradient allowing for passive water movement into the eye (To et al., 2002). It has been found that Cl^- concentrations in both PE and NPE cells are similar and substantially higher than the electrochemical equilibrium. This suggests that the rate of Cl^- uptake by PE-cells, as well as Cl^- transfer from PE to NPE cells are quite similar. In addition, the activities of Cl^- channels in NPE cells are relatively low compared with those of K^+ channels

and Na^+-K^+-ATPase under baseline conditions (Do et al., 2005). Thus, out of the three transport steps, the release of Cl^- from NPE cells into the posterior chamber is likely the rate-limiting step in AH secretion (Do and Civan, 2004, Do and To, 2000). We have previously demonstrated that non-selective Cl^- channel blockers, including 5-nitro-2-(3-phenylpropylamino) benzoic acid and niflumic acid, significantly inhibit net Cl^- transport across native bovine and porcine ciliary epithelium by 80-90% (Cheng et al., 2016, Do and To, 2000, Kong et al., 2006). This evidence further supports the crucial role of Cl^- efflux by NPE cells in AH secretion. **Figure 1.1** illustrates a simplified model of ion transport across the ciliary epithelium.

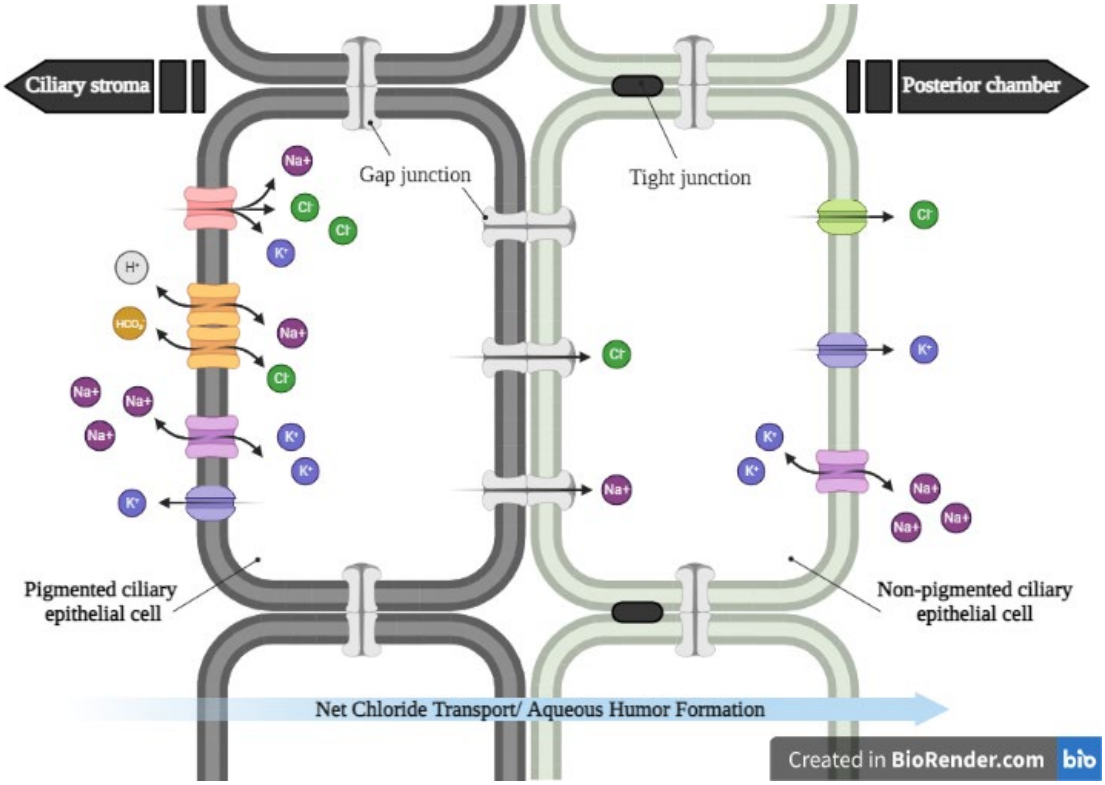

Figure 1.1 A simplified model of ion transport across the ciliary epithelium. Created with BioRender.com

1.4.2 Aqueous humor drainage

After AH is secreted into the posterior chamber, it passes through the pupil and into the anterior chamber. The AH leaves the eye through two independent drainage routes, namely conventional and unconventional outflow pathways (Goel et al., 2010). Similar to AH secretion, AH drainage is temperature-dependent and sensitive to metabolic inhibitors (Boussommier Calleja et al., 2012, Boussommier Calleja et al., 2015). This suggests that the AH outflow pathways are likely to be, by some degree, an active process. The conventional pathway, also known as the trabecular meshwork (TM) pathway, is pressure-dependent. It accounts for ~80-90% of fluid drainage out of the eye (Toris et al., 1999, Pang and Clark, 2008). Here, AH passes through the trabecular meshwork (TM), and enters the Schlemm's canal (SC) and collector channels. It then leaves the eye through the episcleral and conjunctival veins (Goel et al., 2010). It has been reported that TM outflow resistance is often elevated in POAG patients (Rohen et al., 1989). This increase in outflow resistance is considered to be the major cause of IOP elevation in in glaucoma patients.

On the other hand, unconventional pathway, commonly known as the uveoscleral pathway, is pressure-independent. It contributes to 10-20% of the AH drainage in humans (Bill and Phillips, 1971, Bill, 1975, Townsend and Brubaker, 1980). The AH

first enters the root of the iris, and passes through the interstitial spaces of the ciliary muscles. It then enters the suprachoroidal space and lymphatic vessels (Pang and Clark, 2008). Since the conventional pathway is the major route of AH drainage, understanding the location of outflow resistance and its regulatory mechanisms are of paramount importance in developing better treatments for glaucoma.

1.4.2.1 Location of resistance in outflow pathway

For the conventional outflow route, AH passes through the TM before reaching the SC and collector channels (Goel et al., 2010). The TM is a filter-like structure with three major regions, namely the outermost uveal meshwork, middle corneoscleral meshwork and the innermost juxtacanalicular tissue (JCT) regions (Llobet et al., 2003, Tamm, 2009). In the TM, cells are covered and connected by connective tissue lamellae. These lamellae are composed of elastin and collagen fibers (Tamm, 2009). The removal of TM by a surgical procedure to treat glaucoma (termed as trabeculectomy) has been shown to reduce ~70% of the aqueous outflow resistance in human eyes (Van Buskirk, 1977, Rosenquist et al., 1989). TM cells located in the uveal and corneoscleral meshwork are covered by endothelial cells and arranged in sheets with a relatively large space among adjacent trabecular sheets (Tamm, 2009, Gong et al., 1996). It has numerous pores with pore size that can range from 2-75 μm

under normal range of IOP. Therefore, it is considered as a region with low outflow resistance that can generate low impedance to AH drainage (Johnson, 2006). The JCT is the innermost region of the TM adjacent to the SC, whereby TM cells are embedded in the loosely arranged extracellular matrix (ECM) including laminin, fibronectin, collagen, elastin, and myocilin (Acott and Kelley, 2008). The ECM cross-linking helps maintain the integrity and mechanical strength of the tissue; therefore, it is considered a major area of outflow pathway resistance (Stamer and Acott, 2012). However, excessive accumulation and deposition of ECM leads to an increase outflow resistance (Keller and Acott, 2013).

Apart from JCT regions in the TM, about one third of outflow resistance is believed to be generated by the inner wall of the Schlemm's canal (Schuman et al., 1999). The hydraulic conductivity of the basement membrane, pore density in the inner wall endothelium and stiffness of endothelial cells in the SC are the rate limiting factors governing outflow facility (Tamm, 2009). It has been shown that lower hydraulic conductivity, reduced pore density and increased stiffness of SC cells contribute to a higher outflow resistance (Stamer et al., 2015). It is likely that the JCT and SC work together and regulate outflow resistance through a funneling effect (Stamer and Acott, 2012). This funneling effect is primarily affected by pore density and distance

between the two tissues (Stamer, 2012). After passing through the SC, AH enters the collector channels. There are about 30 collector channels in the human eyes (Johnson, 2006). It has been demonstrated that the pressure in the episcleral vein and collector channels are similar in magnitude, suggesting that the collector channel has a minimal influence on outflow resistance (Mäepea and Bill, 1989). It is believed that the collector channel may contribute to distal components of the outflow pathway, but its functional significance remains controversial (Swaminathan et al., 2014).

1.4.2.2 Cellular mechanisms controlling outflow resistance

It has been shown that about one third of the outflow resistance is derived from the region distal to the inner wall of the SC in human eyes (Schuman et al., 1999). The TM is believed to be the diseased tissue involved in glaucoma because of prominent TM thinning and thickening of sheath-derived plaque materials in the JCT observed in POAG subjects (Tektas and Lütjen-Drecoll, 2009). These observed changes may impair outflow drainage and lead to IOP elevation (Vecino et al., 2015). Therefore, it is crucial to understand the potential cellular mechanisms governing outflow resistance.

TM cell volume regulation

Some studies have demonstrated that regulation of TM cell volume may help modulate outflow resistance. It has been shown that there is a correlation between outflow facility and changes in TM cell volume (Dismuke and Ellis, 2009). Perfusion of hypertonic bathing solution can trigger shrinkage of TM cells and increases outflow facility in both calf and human eyes by more than 40%. On the other hand, research have shown that application of hypotonic solution merely reduced outflow facility by 12% (Al-Aswad et al., 1999, Dismuke et al., 2008). In addition to altering the osmolarity of bathing solutions, inhibition of Na^+-K^+-$2Cl^-$ cotransport with bumetanide and bathing Cl^- replacement can also increase outflow facility (Al-Aswad et al., 1999). Similarly, studies also reported that cell shrinkage induced by activation of calcium-activated K^+ (BK_{Ca}) channels can facilitate AH drainage (Dismuke and Ellis, 2009). Nitric oxide has been found to trigger TM cell volume decrease by activating BK_{Ca} channels, potentially leading to an increase in outflow facility (Dismuke et al., 2008). The time course of the cell volume responses are consistent with outflow facility changes, suggesting that altering TM cell volume may have a direct effect on outflow facility. It is noted that changes in outflow facility induced by cell volume changes is transient and reversible (Al-Aswad et al., 1999).

Apart from the direct effect on TM cell volume, volume regulatory response upon hypotonic stimulation can also influence outflow facility. Regulatory volume decrease (RVD) refers to a physiological response of osmotically swollen cells restoring to its original cell volume by activating ion transporters and channels (Hoffmann et al., 2009). Like other cell types, TM cells exhibit RVD and are able to restore cell volume upon hypotonic stimulation by regulating swelling-activated K^+ and Cl^- channels (Mitchell et al., 2002).

It has been shown that slowing RVD of TM cells may increase outflow facility. This may be caused by the stimulation of ATP release when subjected to cell swelling (Li et al., 2012). Studies have shown that the release of ATP promotes the secretion of MMPs such as MMP-2 and MMP-9 (Li et al., 2011a). As a result, increased MMP secretion may reduce the deposition of ECM in the TM, triggering a reduction of outflow resistance (De Groef et al., 2013). The increase of outflow facility induced by prolonged swelling of TM cells can be blocked by MMP inhibitor and A1 adenosine receptor (A1AR) antagonist (Crosson et al., 2005).

TM cell contractility

It has been proposed that outflow resistance can be modulated by regulating TM cell contractility. In human TM, the elastin network within the trabecular lamellae is connected with the elastin fibers of the ciliary muscle (Park et al., 2016). The contraction or relaxation actions of ciliary muscles can induce morphological changes in the TM. For example, contraction of ciliary muscle leads to a widening of TM, resulting in an increase in outflow facility (Bárány, 1962, Overby et al., 2014a).

Apart from the passive effect caused by ciliary muscle, direct modulation of TM cell contractility can alter outflow resistance. Studies have shown that contraction of TM cells triggers a reduction of outflow facility while relaxation of TM cells increases outflow facility in the mammalian eyes (Wiederholt et al., 1995, Rao et al., 2001). TM cell's contractility can be modulated by endothelin-1 (Rosenthal et al., 2005, Dismuke et al., 2014), nitric oxide (Dismuke et al., 2014), ROCK inhibitors (Rosenthal et al., 2005, Koga et al., 2006), and transforming growth factor -β1 (TGFB1) (Nakamura et al., 2002). The relaxation of TM and SC cells leads to a reduction of cell-cell adhesion, cell-ECM interaction, and a loss of actin fibers, causing an increase in outflow facility (Rao et al., 2001).

ECM deposition and remodeling

Various extracellular matrix (ECM) components are found in the TM beams including fibronectin, laminin, elastin, myocilin, and collagen (Sato and Roy, 2002, Lutjen-Drecoll et al., 1981, Ueda and Yue, 2003). The ECM of the TM is thought to be crucial in regulating outflow resistance and IOP. Excessive deposition of ECM in the TM may account for decreased outflow facility in glaucoma (Acott et al., 1988). For example, elevated fibronectin and cross-linked actin networks are found in glaucomatous eyes (Hoare et al., 2009, Babizhayev and Brodskaya, 1989). The continuous turnover and remodeling of the ECM is regulated by the activities of degrading enzymes matrix metalloproteinases (MMPs) and endogenous tissue inhibitors of MMPs (TIMPs) (De Groef et al., 2013). MMPs activities are found to be inhibited in the TM of glaucomatous eyes (De Groef et al., 2013). In parallel with this finding, perfusion of MMPs significantly increase outflow facility while perfusion of TIMPs lower AH drainage (Bradley et al., 1998). In cultured TM cells, the application of mechanical stretch have significantly increased protein expression of MMP-2 and MMP-14 (Bradley et al., 2003). In addition, a decrease of TIMP-2 and an increase of membrane-type 1-MMP have been observed in mechanically-stretched human anterior segment organ culture and TM cell culture. These changes in MMPs activities have been found to alter ECM turnover; hence, outflow resistance (Bradley

et al., 2001). This feedback system helps maintain a stable IOP (Acott and Kelley, 2008). On the contrary, a failure in this feedback system may upset IOP homeostasis, as observed in patients with POAG. For example, MMP-2, MMP-3 and MMP-9 are significantly reduced in the anterior segment of the eyes of POAG patients (Schlötzer-Schrehardt et al., 2003, Määttä et al., 2005), potentially increasing the deposition of ECM for an increased outflow resistance.

Funneling effect

Funneling effect refers to the interaction between JCT region in the TM and the inner wall of SC. When AH passes from JCT to SC through non-uniform and discrete pore size/density, it leads to a segmental flow pattern which is described as a funneling phenomenon (Overby et al., 2009). The distance between TM cells in JCT and inner wall of SC as well as the number of pores in the SC are the two major factors governing funneling effect and AH drainage (Stamer, 2012). It has been shown that application of serine-threonine kinase inhibitor H-7 (1-[5-isoquinoline sulfonyl]-2-methyl piperazine) which affects the actin cytoskeleton and increases the distance between TM and inner wall of SC; thus, facilitate outflow drainage (Sabanay et al., 2000). Moreover, perfusing cationic ferritin, which binds to negatively charged pores on the inner wall of SC, causes an accumulation in the intercellular pores;

thereby, significantly reducing pore numbers and outflow facility in human eyes (Ethier and Chan, 2001). In addition, ROCK inhibitor has been found to widen the separation between JCT and SC regions, increasing the number and size of paracellular pores in SC (Gong and Yang, 2014), potentially reducing outflow resistance.

1.5 Introduction of baicalein

Baicalein (5,6,7-trihydroxyflavone) is a natural flavonoid in the family of flavones. It can be isolated from *Scutellariae radix,* which is a dried root of the medicinal plant *Scutellaria baicalensis Georgi* (Li and Chen, 2005, Ong and Len, 2003). *Scutellariae radix,* also known as Huang-Qin, is commonly used in traditional Chinese medicine (Moon et al., 2006). The therapeutic potential of baicalein is related to its treatment effects on cancers, systemic hypertension, inflammation, and gastrointestinal disorders (Li et al., 2011b, Zhao et al., 2016). Baicalein is frequently found in vegetables such as spinach and green pepper (Ren et al., 2001). The chemical structure of baicalein is illustrated in **Figure 1.2**. It has a molecular formula of $C_{15}H_{10}O_5$ (molecular weight = 270.24 g/mol). Baicalein is a hydrophobic flavonoid and has a limited solubility in water, ranging from 0.43 to 16.82 μg/ml (Liu et al., 2006a, Huang et al., 2014). As suggested by Tu et al., the hydroxyl groups of

baicalein may possibly be the key structures responsible for its actions including radical scavenging and antibacterial activities (Tu et al., 2016).

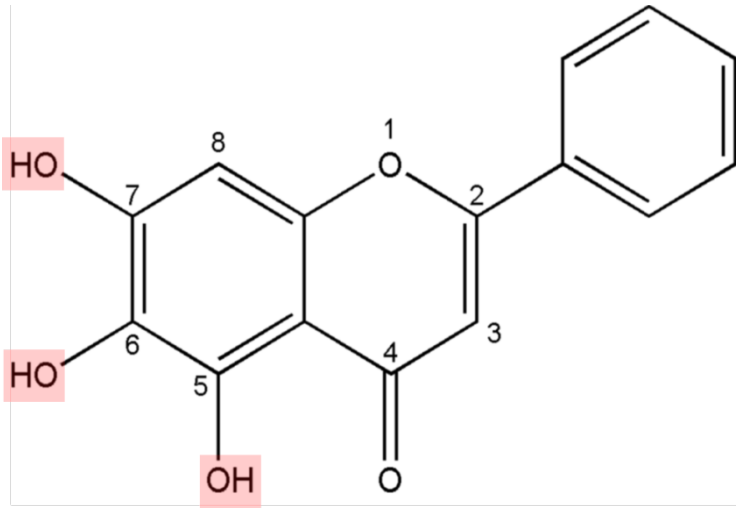

Figure 1.2 Molecular structure of baicalein. The hydroxyl groups are highlighted in red.

1.5.1 Biological functions of baicalein

Baicalein has been used in the treatment of cancers, cardiovascular and inflammatory diseases because of its anti-inflammatory, anti-apoptotic, and anti-oxidant properties (Su et al., 2000, Lee et al., 2015, Dinda et al., 2017, Sowndhararajan et al., 2017). It has been recognized to be safe and is well tolerated by patients (Pang et al., 2016).

1.5.1.1 Anti-oxidation

Evidence suggests that baicalein is a natural antioxidant (Su et al., 2000). The anti-oxidative property of baicalein is related to its molecular structure. As shown in **Figure 1.2**, baicalein has an ortho-dihydroxy group (catechol structure), which serves as an effective radical quencher and provides an intrinsic antioxidant property by electron donation (Foti et al., 1996, Rice-Evans et al., 1996). Cai et al. have indicated that anti-oxidative effects of chalcones and flavones are associated with the position, number, and configuration of hydroxyl groups shown in **Figure 1.3** and baicalein exhibits the highest radical scavenging activity among them (Cai et al., 2006). Similar results are also found in other studies; whereby, baicalein exerts the strongest anti-oxidative effects compared to other flavonoids in *radix of Scutellaria baicalensis* (Gao et al., 1999, Perez et al., 2009).

Previous cellular and animal studies have found that baicalein inhibits oxidative stress-induced damages. For example, some studies have shown that baicalein reduces intracellular ROS-induced damages by H_2O_2 in different cell types; hence, attenuates mitochondrial dysfunction (Kang et al., 2012) and DNA damage (Kim et al., 2012). The protective effect of baicalein against mitochondrial dysfunction is possibly mediated by the inhibition of lipid peroxidation (Zhang et al., 2010). Factors such as

mitochondrial dysfunction have been suggested to play an important role in neurological diseases including Parkinson's disease (Hald and Lotharius, 2005). Studies on baicalein have also demonstrated its ability to reduce the production of ROS and inhibit the 6-hydroxydopamine-induced changes of mitochondrial membrane potential and redox activity (Wang et al., 2013). In addition to *in vitro* studies, baicalein effectively suppresses the myocardial oxidative stress induced by doxorubicin and the cisplatin-induced renal oxidative stress in mice (Sahu et al., 2016, Sahu et al., 2015). Baicalein also ameliorates the oxidative stress in brain and shows neuroprotective effect by promoting the cell survival and preserving the motor and memory functions in different animal models (Lapchak et al., 2007, He et al., 2009). Due to its anti-oxidative property, baicalein is suggested to be a potential treatment for Alzheimer's disease (Zhou et al., 2016) and Parkinson's disease (Sarrafchi et al., 2016).

A **B**

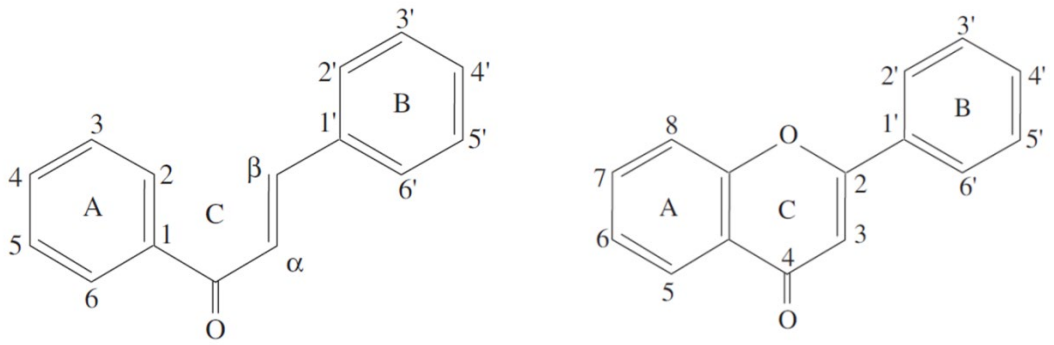

Figure 1.3 Molecular structures of **A**) chalcones and **B**) flavones

1.5.1.2 Anti-inflammation

Previous research have suggested that baicalein has therapeutic potential for various inflammatory diseases including autoimmune hepatitis, osteoarthritis, chronic renal and neurodegenerative diseases (Firuzi et al., 2011, Dinda et al., 2017, Turner et al., 2014). Inflammation causes activation of different pro-inflammatory cytokines such as tumor necrosis factor-α (TNF-α), interleukin-1β (IL-1β) and IL-6 (Jaffer et al., 2010). Data from both *in vivo* and *in vitro* studies have demonstrated that baicalein exhibits anti-inflammatory properties (Lee et al., 2015). For example, it has been observed that baicalein can significantly ameliorate the amount of macrophages and lymphocytes in bronchoalveolar lavage fluid and cytokine expression in lung tissue during pulmonary carcinogenesis-associated inflammation (Chandrashekar et al., 2012). Moreover, it inhibits protein and mRNA expression of cytokines against carbon tetrachloride-induced damage and inflammation in the liver (Huang et al., 2012), and after controlled cortical impact injury in the neurons and microglia of rodents (Chen et al., 2008). In addition, it has been reported that baicalein ameliorates kidney fibrosis by inhibiting pro-inflammatory cytokines such as TNF-α, IL-1β, and monocyte chemotactic proteins by abolishing the activation of nuclear factor-κB and mitogen-activated protein kinase cascades (Wang et al., 2015b). Similarly, studies have shown that baicalein inhibits the expression of cytokines through inhibition of

nuclear factor-κB pathway primary human umbilical vein endothelial cells (Lee et al., 2015), human mast cells (Hsieh et al., 2007) and murine macrophages cells (Fan et al., 2013).

1.5.1.3 Anti-apoptosis

Apoptosis or "programmed cell death" refers to a morphologically distinct form of cell death that involves numerous processes such as cell shrinkage, nuclear condensation, blebs development, membrane fragmentation and phagocytosis of apoptotic cells (Saikumar et al., 1999). Several studies have demonstrated the potential anti-apoptotic effects of baicalein on neurodegenerative disorders including Alzheimer's and Parkinson's diseases (Sowndhararajan et al., 2017, Mattson, 2000, Lebeau et al., 2001). In cancer treatment, baicalein has been shown to have a protective effect by inducing cell cycle arrest in cancer cells (Gao et al., 2016, Min, 2009). Extensive *in vitro* studies have shown that baicalein inhibits apoptosis in 6-hydroxydopamine-treated SH-SY5Y cells (Mu et al., 2009), H_2O_2-treated lung fibroblast cells (Kim et al., 2012) and PC12 cells derived from pheochromocytoma of the rat adrenal medulla (Zhang et al., 2010). It has been found that the anti-apoptotic effects of baicalein in rat cortical neuron cultures treated with amyloid β peptide Aβ (25-35) is associated with c-Jun-dependent apoptotic pathway (Lebeau et al., 2001).

Consistent with *in vitro* results, studies using rats have found that baicalein attenuates amnesia and neuronal loss induced by Aβ (25-35) (Wang et al., 2004). In addition, baicalein has been found to improve retinal functions and reduce apoptotic RGC loss in rats with retinal ischemia (Chao et al., 2013).

1.5.2 Baicalein as a potential anti-glaucoma agent

Recently, increasing evidence demonstrates that baicalein may be a good therapeutic agent for neurological disorders including ischemic brain injury, stroke, Alzheimer's and Parkinson's diseases (Liang et al., 2017, Li et al., 2017). Numerous studies have demonstrated that baicalein possesses the following properties: 1) ameliorate neuronal cell death and brain microvasculature damage induced by 12/15-lipoxygenase (Jin et al., 2008); 2) alleviate mitochondria dysfunction, cognitive and motor impairments in rats with chronic cerebral hypoperfusion (He et al., 2009); and 3) reduce oxidative stress mediated by middle cerebral artery occlusion through the PI3K/Akt and Phosphatase and tensin homolog pathway (Liu et al., 2010a). Recent studies have demonstrated that it can protect neurons from ischemic and oxidative damage in different models of neuropathy (Chao et al., 2013, Hanneken et al., 2006, Maher and Hanneken, 2005), suggesting its potential significance for the prevention of glaucomatous optic neuropathy (Xiao et al., 2014).

A study of seawater killifish has shown that baicalein modulates transepithelial Cl^- secretion in the opercular epithelium (Marshall et al., 1993). Subsequently, baicalein has been reported to increase cyclic adenosine monophosphate-dependent Cl^- secretion across the colonic mucosa of rats (Ko et al., 2002). Consistent with the results obtained from rats, baicalein is also found to regulate Ca^{2+}-dependent Cl^- secretion in human intestinal T84 cells (Yue et al., 2004). Since the secretion of AH is driven primarily by a transepithelial Cl^- transport across the ciliary epithelium (Do and Civan, 2004), there is a possibility that baicalein may regulate AH inflow and IOP. We have previously demonstrated that the addition of baicalein to the aqueous surface unexpectedly inhibits the short-circuit current (Isc) by 60-70% in excised porcine ciliary epithelium (Xiao, 2015); thus, suggesting that baicalein may suppress net Cl^- secretion and AH inflow. In parallel with this finding, baicalein is found to reduce the net fluid movement by ~35% across isolated porcine ciliary body when added to the aqueous surface (Xiao, 2015). The baicalein-triggered Isc inhibition can be abolished when the tissue preparation is pretreated with either aqueous niflumic acid, a Cl^- channel blocker or by replacing Cl^- in the bath. This suggests that its effect may possibly be mediated by the inhibition of NPE Cl^- channel activities. Subsequently, we have demonstrated that baicalein inhibits the swelling-activated Cl^- channels in

native porcine NPE cells using whole-cell patch clamp configuration, further supporting the potential significance of baicalein in reducing AH inflow.

Based on the published literature, baicalein is believed to play a role in the regulation of conventional outflow facility. First of all, baicalein regulates Cl^- secretion (Yue et al., 2004), particularly through swelling-activated Cl^- channels in the ciliary epithelium (Xiao, 2015). This suggests that baicalein may likely be involved in modulating TM cell volume, contributing to the regulation of outflow resistance (Soto et al., 2004). Second, the chemical structure of baicalein shares some similarities to that of genistein, which is a tyrosine kinase inhibitor (Evers et al., 2005, Po et al., 2002). The inhibition of tyrosine kinase has been demonstrated to increase the relaxation of TM at both the cellular and tissue levels (Stumpff et al., 1999, Wiederholt et al., 1998); hence, increasing outflow facility (Wiederholt et al., 2000). Moreover, baicalein has been found to induce ECM remodeling by altering cell-ECM interaction and cell migration in different cell types (Liu et al., 2003, Liu et al., 2016), suggesting that it can potentially modulate ECM deposition in the TM.

The loss of TM cells may also contribute to increased outflow resistance because of reduced degradation of ECM materials (Tektas and Lütjen-Drecoll, 2009, Gabelt and

Kaufman, 2005). The decrease in TM cellularity may be due to damages triggered by oxidation and inflammation. As mentioned before, it has been revealed that oxidative stress and inflammation responses are upregulated in glaucoma (Ichhpujani and Kumar, 2019). Baicalein has been shown to exhibit anti-inflammatory, anti-oxidative, and anti-apoptotic effects in both *in vivo* and *in vitro* studies (Chen et al., 2008, Zhang et al., 2017, Lee et al., 2015, Su et al., 2000, Kang et al., 2012). Therefore, the anti-inflammatory and anti-oxidative properties of baicalein may help improve the survival of TM cells and restore its role in maintaining IOP within the normal range.

1.6 Objective

Glaucoma is a sight-threatening eye disease with unclear pathogenesis. Lowering IOP continues to be the mainstay treatment for glaucoma. Despite this, there are several limitations and constraints with the existing treatment paradigm; thereby, compromising patient compliance and treatment prognosis. As a result, there is an urgent need for developing a safe, potent, and long-lasting anti-glaucoma agent for clinical use.

Currently, all anti-glaucoma medications act by either suppressing AH secretion or facilitating AH drainage. Baicalein is a natural compound that can be readily found in vegetables with low toxicity reported. The therapeutic significance of baicalein against sight-threatening ocular diseases including glaucoma has not been fully explored. We have previously demonstrated that baicalein inhibits the secretion of AH production, supporting its potential role in regulating AH dynamics. It is likely that baicalein may also be involved in the regulation of conventional outflow facility, which is considered as the major factor responsible for elevated IOP. Baicalein has been shown to regulate fluid secretion, cell contraction and migration, as well as ECM composition in other cell types (Ko et al., 2002, Marshall et al., 1993, Oh et al., 2012, Liu et al., 2003, Dinda et al., 2017). We have yet to establish whether or not baicalein mediates its effects by modulating the volume regulation, contractility and migratory properties, and ECM reorganization in TM cells.

Given the complexity of the AH outflow pathway, it is important to adopt a highly sensitive and accurate evaluation of differential protein expression. Hence, we adopted the latest proteomics technology with state-of-the-art bioinformatics platforms to examine the cellular mechanisms underlying baicalein-mediated facilitation of outflow facility. This has been useful to determine the clinical relevance

of baicalein in regulating AH dynamics. By monitoring differential protein expressions at different times, we can evaluate the longitudinal changes in protein profiles after baicalein treatment. The analysis of proteomics data not only provided information regarding targeted candidates but also generated new insights into the involvement of other cellular mechanisms involved in the signaling cascade. As baicalein is known to exhibit anti-apoptotic, anti-inflammatory, and anti-oxidative properties in other cell types, the elucidation of these signaling cascades will provide new insights into novel targets for the restoration of normal functions of TM cells.

In this study, we aimed to establish whether baicalein: 1) increases the conventional outflow facility in *ex vivo* mouse eyes; 2) is involved in the modulation of volume, contractility and migration of TM cells; 3) alters the expression of ECM and cytoskeleton proteins in TM cells; 4) participates in other signaling pathways that may be beneficial to glaucoma through its anti-apoptotic, anti-inflammatory, and anti-oxidative mediated cellular changes; and 5) produces detectable changes in IOP following treatment through various drug administration routes.

Chapter 2 Methodology

2.1 Preparation of baicalein solution

Given that baicalein has a limited solubility in water, it is frequently dissolved in organic solvents such as DMSO. In this study, we attempted to increase its solubility by dissolving it in 20% 2-hydroxypropyl-β-cyclodextrin (BCD). BCD is a cyclic oligosaccharide. It acts by encapsulating the drug inside a hydrophobic cavity to form an inclusion complex; thus, increasing the solubility of the hydrophobic compound (Liu et al., 2006a). BCD has been reported to have minimal adverse effects in animal and human studies (Gould and Scott, 2005).

Transepithelial Cl^- secretion has been considered to be a major driving force for aqueous humor formation across the ciliary epithelium (Kong et al., 2006, Do and To, 2000). With the modified Ussing-Zerahn-type chamber, we have previously demonstrated that baicalein, when dissolved in DMSO, inhibited Isc in a concentration-dependent manner after adding to the aqueous surface (Xiao, 2015). Significant Isc inhibition was only detected when the concentration of baicalein was ≥50 μM. At 50 and 100 μM, baicalein reduced Isc by 24% and 51%, respectively. No significant Isc inhibition was observed at 10 μM or below (Xiao, 2015). Using the same experimental setup, in **Figure 2.1**, we showed that baicalein dissolved in 20%

BCD produced a significant inhibition in Isc from 0.1 μM to 100 μM (n=19, p<0.001). In **Figure 2.2**, we showed that baicalein, when dissolved in 20% BCD, inhibited Isc at a much lower concentration (e.g. from 0.1 μM to 50 μM) compared to baicalein when dissolved in DMSO. At 0.1 μM, baicalein significantly inhibited Isc by 21%. As a result, BCD was chosen as a solvent to enhance the solubility of baicalein in all subsequent studies.

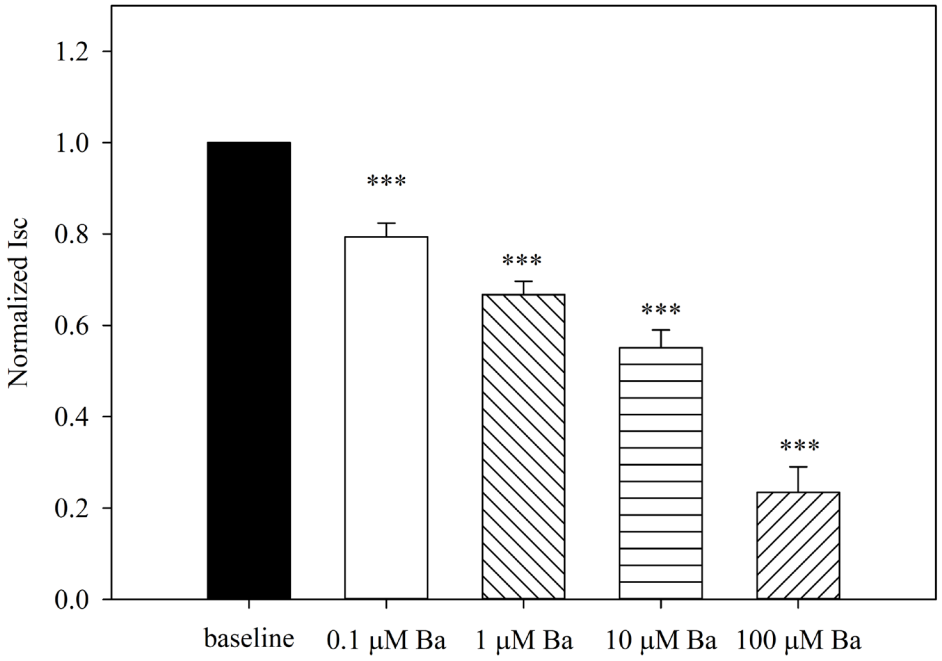

Figure 2.1 Effects of baicalein (0.1, 1, 10 and 100 μM), when administrated to the aqueous side, on normalized short-circuit current (Isc) across the excised porcine ciliary epithelium. Results are expressed as Mean ±SEM (n=19; p<0.001; one-way repeated measures ANOVA).

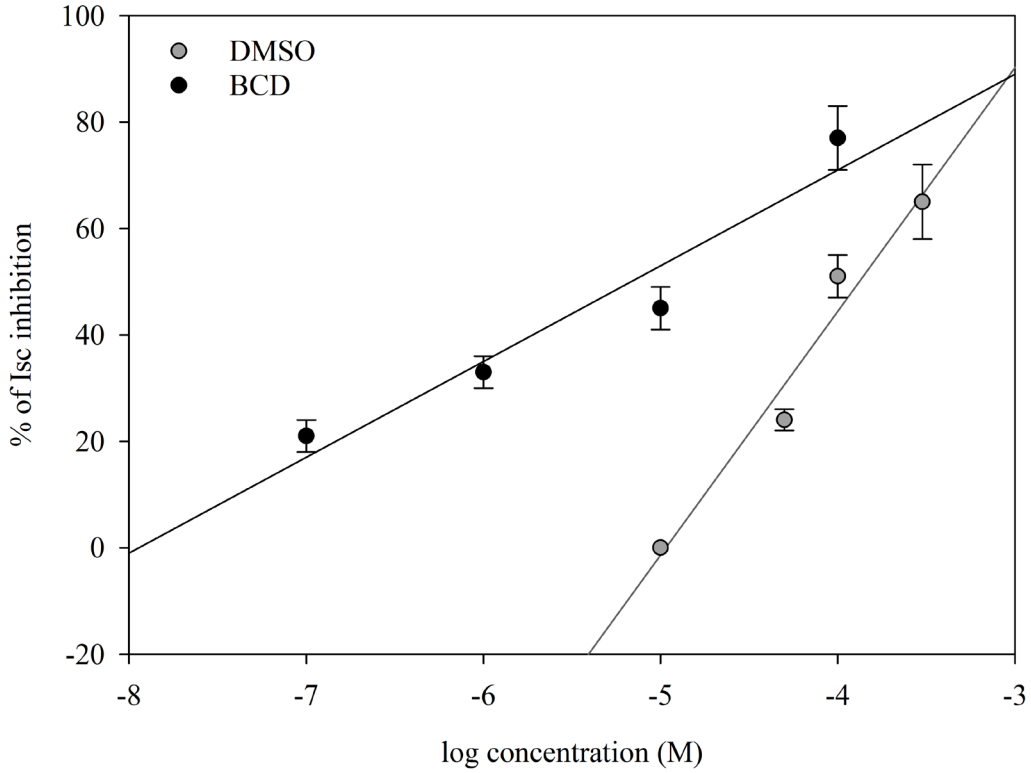

Figure 2.2 Effect of baicalein dissolved in DMSO (Xiao, 2015) compared to 20% BCD corresponding to the percentage Isc inhibition across excised porcine ciliary epithelium when administrated to the aqueous side.

In this project, baicalein was dissolved in PBS with 20% BCD. Hydrochloric acid was used to adjust the pH to 7.4. Baicalein was obtained from Cayman Chemical Co. (Cayman Chemical, MI, USA) while BCD and other drugs were purchased from Sigma-Aldrich (St. Louis, MO, USA).

2.2 *Ex vivo* study

Measurement of conventional outflow facility

Freshly enucleated eyes from adult C57BL/6J mice (C57 mice) were used. C57 mice was chosen because they show similar anatomical structures of the outflow pathway and response to anti-glaucoma drugs as in human eyes (Overby et al., 2014a, Smith et al., 2001, Boussommier Calleja et al., 2012). All experiments were performed in compliance with the Association for Research in Vision and Ophthalmology Statement for the Use of Animals in Ophthalmic and Vision Research. The measurement of conventional outflow facility was determined by the constant-pressure perfusion system. The details of the outflow measurements have been previously summarized (Millard et al., 2011, Sumida and Stamer, 2010, Lei et al., 2011). Briefly, enucleated mouse eye was kept in a water chamber at 37˚C. Then, the eye was cannulated by inserting a 33-gauge beveled NanoFil needle tip (World Precision Instruments) into the anterior chamber through the cornea using a micromanipulator. The needle was connected to a reservoir, a pressure transducer (model 142PC01G; Honeywell, Morristown, NJ) and a glass syringe (50 µl; Hamilton, Reno, NV) connected to a motorized syringe pump (PHD 2000 Syringe Pump, Harvard Apparatus). The flow rate to the perfused eyes could be adjusted under a computerized program (LabVIEW Software; National Instruments) to maintain the

desired pressures. A schematic diagram illustrating the experimental setup for outflow facility measurement is presented in **Figure 2.3**. After the intracameral cannulation, the eye was then perfused with Dulbecco's phosphate-buffered saline (PBS) containing 5.5 mM D-glucose (referred to as "DBG"). Baicalein and vehicle (BCD only) were added to the perfusates of both experimental and control eyes, respectively, and perfused to the eyes for at least 30 minutes at 8 mmHg during the equilibration period. Thereafter, the outflow facilities of both baicalein-treated and vehicle-treated eyes were determined by measuring flow rates at sequential pressure steps (i.e., 4, 8, 12, 16, and 20 mmHg). The outflow facility was then derived from linear regression analysis between flow rates and pressure applied. Comparisons were made between baicalein-treated and vehicle-treated eyes of the same animal. Y39983, a selective ROCK inhibitor, which is known to increase conventional outflow facility, was used as a control for comparison.

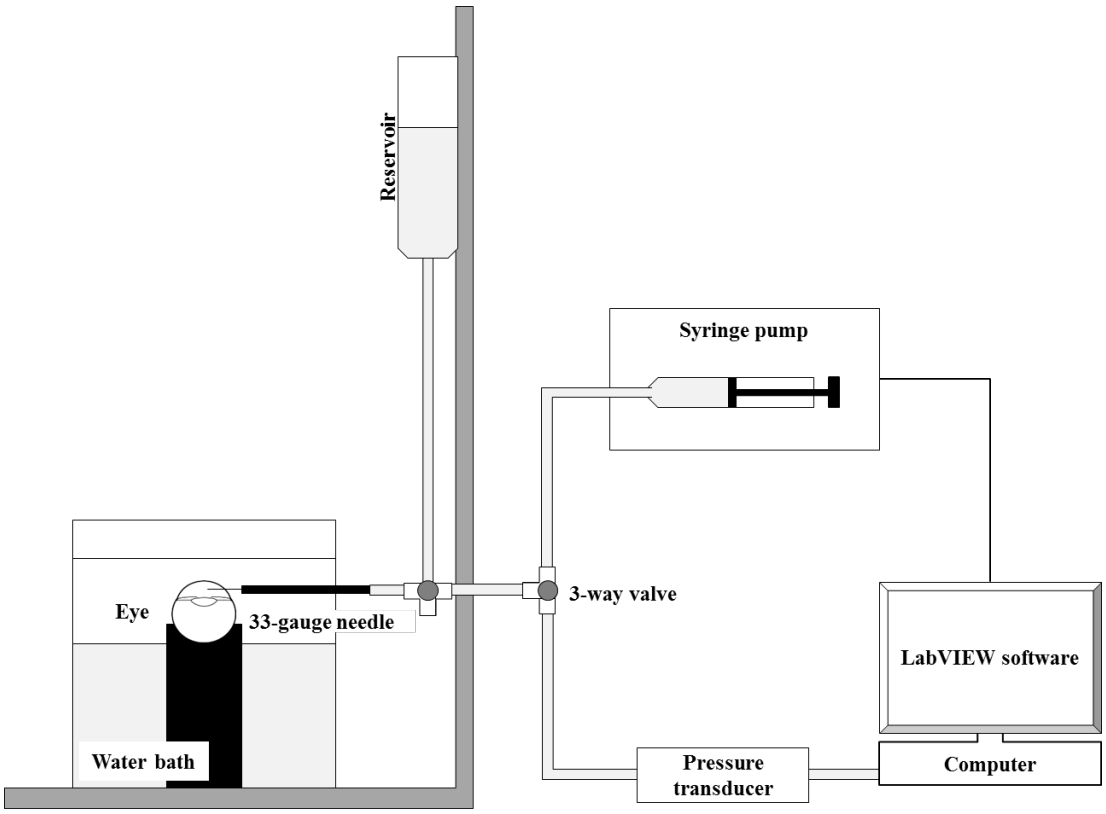

Figure 2.3 Schematic diagram showing the measurement of conventional outflow facility in enucleated mouse eyes.

2.3 *In vitro* study

2.3.1 Human trabecular meshwork (hTM) cell culture

Human trabecular meshwork (hTM) cells were obtained from Prof. W. Daniel Stamer at the Department of Ophthalmology, the Duke University School of Medicine. These hTM cells were isolated from six human donors (aged from 3 months to 88 years old) with no known eye diseases and had been characterized previously (Keller et al., 2018, Stamer et al., 1995, Stamer et al., 2000). The primary hTM cells were maintained in Dulbecco's modified Eagle's medium (DMEM, Low glucose; Invitrogen), containing

penicillin (100 units/ml), streptomycin (100 mg/ml), glutamine (0.29 mg/ml), and 10% fetal bovine serum (FBS) (Invitrogen) and incubated at 37°C until confluence. Subsequently, 1% FBS was used and incubated for at least a week before the experiments.

2.3.2 Measurement of cell viability and proliferation

2.3.2.1 Measurement of cell viability by Trypan blue exclusion assay

The cytotoxicity of baicalein was evaluated by Trypan blue exclusion assay according to the reported methodology (Honjo et al., 2007, Strober, 2015). Confluent hTM cells seeded on 24-well plates were incubated in serum-free DMEM overnight before treatment. Subsequently, 1, 10, and 100 μM baicalein, vehicle, or PBS were added to the cells and incubated for 2 and 4 days. After drug treatment, cells were harvested with 0.25% trypsin at 1,500 rpm for 5 minutes. Cells were then re-suspended in PBS and mixed with 0.4% Trypan blue in a 1:1 ratio for about 3 minutes. Cell counting was conducted within 3-5 minutes after mixing with Trypan blue. 10 μl of Trypan blue/cell mixture was applied to a hemacytometer. A total of 300 unstained (viable) and stained (dead) cells were counted. The cell viability was determined by the following equation:

$$Cell\ viability = \frac{Number\ of\ unstained\ cells}{Number\ of\ total\ cells} \times 100\%$$

2.3.2.2 Measurement of cell proliferation by MTT assay

The proliferation of hTM cells was evaluated by 3-(4,5-dimethylthiazol-2-yl)-2, 5-diphenyltetrazolium bromide (MTT) (Thermo Fisher Scientific) assay according to the manufacturer's instruction (Honjo et al., 2007). MTT assay is a colorimetric assay that provides a rapid and convenient method for evaluating cell proliferation. In MTT assay, a yellow water-soluble tetrazolium salt MTT was reduced to purple water-insoluble formazan crystals by the proliferating cells. The insoluble formazan crystals were subsequently dissolved, resulting in a color change which can be quantified by measuring light absorbance at around 570 nm using a microplate reader or spectrophotometer (Mosmann, 1983, Wang et al., 2010b).

A total of 5 x 10^3 hTM cells per well were seeded in 96-well plates in culture medium. Prior to the experiments, the cells were incubated overnight with serum-free DMEM. Baicalein at various concentrations (1, 10, 100 μM), vehicle or PBS were added to the cells and incubated for 2 and 4 days. After treatment, 10 μl of 12 mM MTT in PBS was added and incubated at 37˚C for 4 hours. 50 μl DMSO was added into the medium and incubated in the dark for 10 minutes with gentle shaking. The absorbance

at 570 nm was measured by an AO microplate reader (Azure Biosystems Inc, CA, USA).

2.3.3 Effects of baicalein on cell volume regulation under isotonic and hypotonic conditions

The effects of baicalein on cell volume was monitored by electronic cell sorting as previously described (Li et al., 2011a, Yantorno et al., 1989). hTM cells were seeded in T-75 culture flask until confluence. Cells were harvested by incubating with 0.25% trypsin for 3 minutes. Afterwards, cells were centrifuged at 1,500 rpm for 5 minutes. The cell pellets were re-suspended in 30 ml of isotonic solution with a 40 μm nylon cell strainer (Falcon, Corning, NT, USA) and settled for 30 minutes. The isotonic bathing solution contained (in mM): 110 NaCl, 1.2 $MgCl_2$, 4.7 KCl, 2.5 $CaCl_2 \cdot H_2O$, 1.2 KH_2PO_4, 30 $NaHCO_3$, 15 HEPES and 10 glucose (290-305 mOsmol/kg H_2O, pH = 7.4) (Mitchell et al., 2002). Real-time cell volume measurements were conducted with a Coulter Counter (Multisizer 3, Beckmann Coulter, Inc., Fullerton, CA) with a 100 μm aperture tube. When the cells passed through the aperture tube, alterations of electrical resistance followed due to the difference in distance between the cells and the aperture wall caused by the cell volume changes (Bryan et al., 2012, Don, 2003). A schematic diagram showing the measurements of cell volume change is presented

in **Figure 2.4**. Cell volume was determined by the peak of distribution function throughout the experiment. Under equilibration period, hTM cell volume was monitored every 5 minutes for 20-30 minutes. Subsequently, baicalein (1, 10, and 100 μM) or vehicle was added to the isotonic bathing solution. Cell volume was monitored at 2.5, 5, 10, 15, 20, 25 and 30 minutes after drug treatment.

The regulatory volume decrease (RVD) was achieved by exposing the hTM cells to hypotonic solution for 30 minutes. The hypotonic solution was prepared similar to that of isotonic solution except that the final NaCl concentration was reduced from 110 mM in the isotonic solution to 37 mM in the hypotonic solution (150-160 mOsmol/kg H_2O, pH = 7.4). Cell volume was continuously monitored at 2.5, 5, 10, 15, 20, 25 and 30 minutes after hypotonicity.

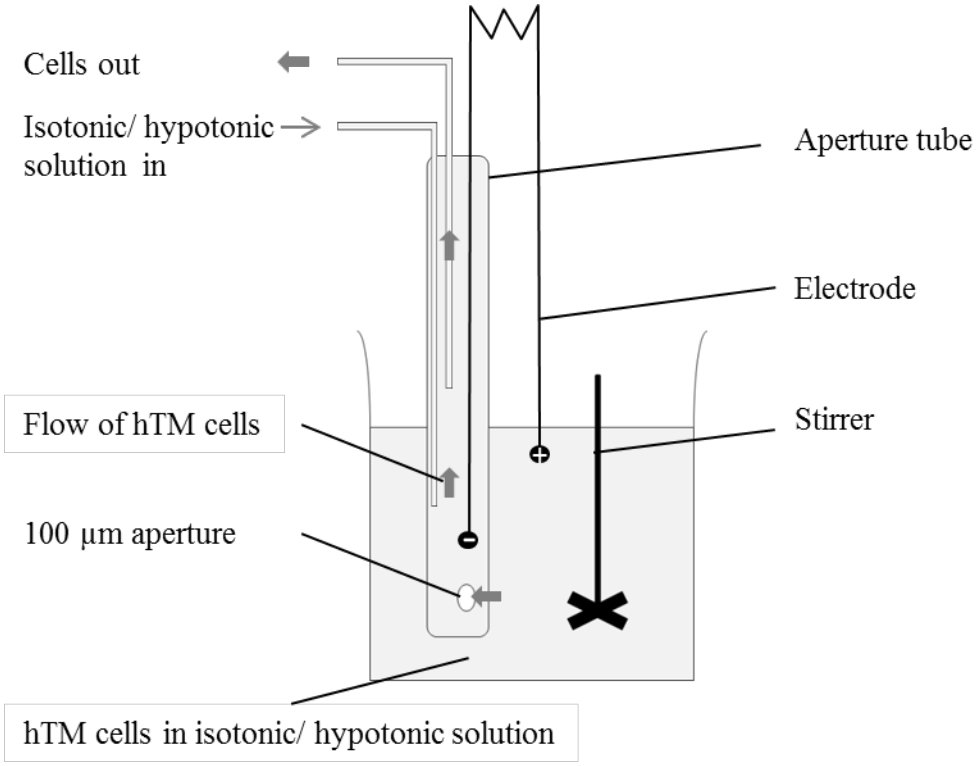

Figure 2.4 Schematic diagram showing the measurements of real-time cell volume changes

2.3.4 Measurement of cell contractility

2.3.4.1 Measurements of hTM cell contractility with collagen gel assay

The collagen gel (1.5 mg/ml) was prepared by mixing 4.42 mg/ml collagen (BD Bioscience, Bedford MA) with 10x PBS, 1M sodium hydroxide and water, according to previously published protocol (Dismuke et al., 2014, Luna et al., 2012). Primary hTM cells were harvested and seeded on the collagen gel (1.5×10^5 cell/cm^2) in a 48-well plate at 37˚C in 5% CO_2 / 95% air for 24 hours. Cells were then changed to serum-free media for an overnight incubation. The collagen gels were detached from the well using 200 µl MultiFlex round tips (Sorenson^{TM} BioScience, Inc.) and settled

in an incubator at 37°C for 9 hours (Dismuke et al., 2014). Baicalein (at various concentrations) and vehicle were added and incubated for 3 and 6 hours. Carbachol (5 μM) was used as a control (Rosenthal et al., 2005). The gel area was monitored at baseline and at 3 hours and 6 hours after drug treatment. Measurements of gel areas were determined using the Motic analysis program (Moticam BTW 8, MMS Microscopes, UK).

2.3.4.2 Measurements of phosphorylated myosin light chain (MLC) expression

Phosphorylation of MLC was used to determine cell contraction in hTM cells. In our experiments, the effect of baicalein on phosphorylated MLC (pMLC) as the percentage of total MLC protein expression was investigated by Western blot analysis (Rosenthal et al., 2005, Dismuke et al., 2014, Rao et al., 2005). The primary hTM cells were plated and incubated at 37°C until confluence. Cells were treated with various concentrations of baicalein (1, 10 and 100 μM) or vehicle for 5 minutes. hTM cells were rinsed with ice-cold PBS, scraped and lysed in lysis buffer (7 M urea, 2 M thiourea, 30 mM TRIS, 2% CHAPS and 1% ASB14, pH = 8.5) with phosphatase and protease inhibitors. Samples were then sonicated in ice water to complete cell lysis, followed by the determination of protein concentrations using Bradford protein assay (Bio-Rad, Hercules, CA, USA). After that, 30 μg proteins were mixed with

β-mercaptoethanol and Laemmli Sample Buffer (BioRad, Hercules, CA, USA). Samples were heated at 95°C for 5 minutes, cooled on ice and loaded into 12% polyacrylamide gels. PageRuler™ Prestained Protein Ladder (10 to 180 kDa) (Thermo Scientific, Waltham, MA, USA) was loaded to the gel for the determination of protein size. After fractionation in SDS-PAGE gel, proteins were transferred onto polyvinylidene fluoride (PVDF) membranes following the published procedures (Mahmood and Yang, 2012). The membranes were blocked with 10% milk in Tris-buffered saline with Tween®20 (TBST) for 1 hour under room temperature in order to block the non-specific binding. It was then incubated overnight with primary (1:1000) antibodies at 4°C for the detection of phosphor-specific MLC 2 (Thr19/Ser18) and MLC 2. The blot was washed by TBST three times (10 minutes each) at room temperature and incubated with secondary antibodies (1:5000) for 1 hour. After washing the blot by TBST three times, the blots were developed using Amersham ECL Select Western Blotting Detection Reagent (GE Healthcare - Life Sciences) for 5 minutes and subsequent exposure in ChemiDoc™ MP Imaging System (Bio-Rad). The changes in signal intensity of pMLC and MLC were determined by Image Studio Lite (version 5.2).

2.3.5 Measurement of cell migration

hTM cells were incubated overnight with serum-free DMEM before the experiments. The hTM cell monolayer was scratched by a 200 µl pipette tip to create a gap area at the center of the well (**Figure 2.5**), similar to previous studies (Koga et al., 2006, Yee et al., 2007). The center of the gap area (cross) was used as the reference point. Subsequently, vehicle and various concentrations of baicalein was added and incubated for a period of up to 4 days. Movement of hTM cells into the gap area was photographed by a light microscope (Nikon Eclipse Ti-S, Melville, NY) at baseline, 2 and 4 days after drug treatment. The gap area was calculated using ImageJ (version 1.49) software and represented as a percentage of the initial gap area. As shown in **Figure 2.6**, the normalized gap area was calculated by the ratio of gap area after treatment to its initial gap area taken at baseline.

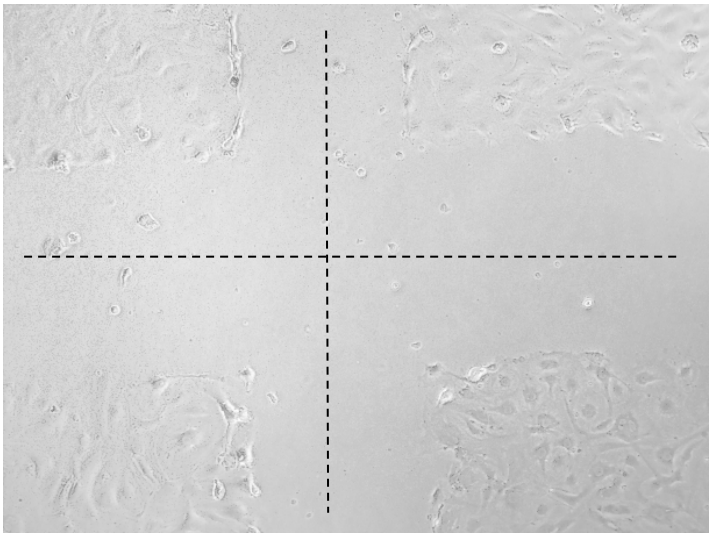

Figure 2.5 The center cross created by a 200 µl pipette tip at the center of the well.

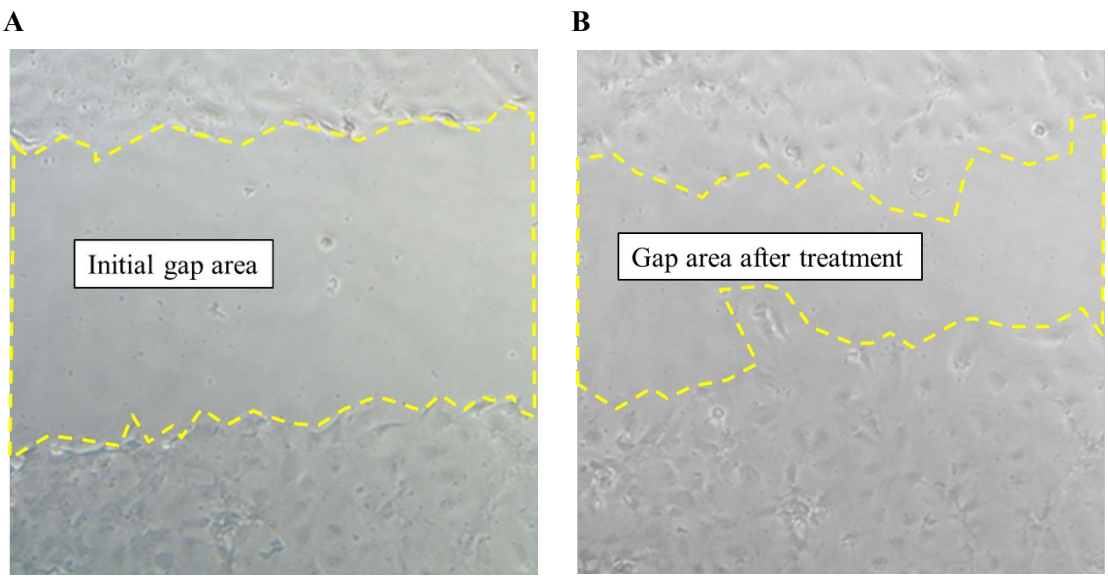

Figure 2.6 The gap area measured by ImageJ for cell migration experiment. **A**) Gap area before treatment on day 0 (initial gap area). **B**) Gap area after treatment. The normalized area gap was derived from the ratio of gap area after treatment to its initial gap area.

2.3.6 Proteomics study of hTM cells following baicalein treatment

2.3.6.1 Cell preparation

In order to determine the acute and relatively long-term effects of baicalein on protein changes in hTM cells, two time points (i.e. 3 hours and 2 days) were chosen. Baicalein (10 μM) or vehicle was added to the preparations and incubated for 3 hours and 2 days, respectively.

Cells were harvested by 0.25% trypsin. Cell pellets were washed twice with PBS before centrifugation at 1,500 rpm for 5 minutes. A 1 ml lysis buffer composed of 7 M urea, 2% CHAPS, 0.1 M TEAB and protease inhibitor was added to the sample.

The lysate was then sonicated on ice for 30 minutes and centrifuged for 15 minutes at 4˚C. Subsequently, supernatants were collected and protein concentration was determinate by Bradford protein assay.

2.3.6.2 Sample preparation for iTRAQ reagent- 8plex

Samples were mixed with 100% acetone in a 1:4 ratio for acetone precipitation overnight at -20˚C. After a 15,000 rpm centrifugation for 30 minutes at 4˚C, supernatants were discarded and 500 µl of 80% acetone was added to the pellets for 5 minutes. Later, the samples were centrifuged for 20 minutes at 4˚C. Supernatants were removed and the pellets were dried up by speed-vac at 4˚C.

After collecting the sample pellets, proteins were reduced and blocked by cysteine according to the following procedures. The pellets were re-suspended in 10 µl 7 M urea in 0.5 M TEAB. Protein concentrations were measured by Bradford protein assay (Bio-Rad, Hercules, CA, USA). 50 µg of protein was collected from each sample and the volume was equalized among samples with the same buffer. A 1 µl reducing reagent, TCEP, was added to all samples and incubated at 37˚C for 1 hour. Then, 0.5 µl cysteine blocking reagent was added to each sample. The samples were thoroughly mixed, spun down and incubated at room temperature for 10 minutes.

Double-distilled water was added to the samples to dilute TEAB from 0.5 M to 0.1 M. Then 0.1 M TEAB was added to obtain a final concentration of 1 M uvea. Proteins blocked by cysteine were digested by trypsin. Samples were incubated at 37˚C with 0.5 µg/µl trypsin (1: 20 trypsin to total protein) for 16 hours with gentle agitation.

Before labeling, a total of 9 µl proteins were collected from all samples. ZipTip (ZipTip C18, Millipore) was used to clean up the samples. 10 µl 100% acetonitrile (ACN) was aspirated and dispensed 3 times. Afterwards, aspiration / dispensation was repeated with 0.1% formic acid (FA). The samples were then pipetted slowly up and down 10 times. After loading the peptides to ZipTip, 0.1% FA was loaded and discarded 3 times, which was repeated with 5% methanol in 0.1% FA. Sample peptides were finally eluted from ZipTip by pipetting up and down 10 µl 60% ACN in 0.1% FA for five times. The peptide concentration was measured by peptide assay (Piece^{TM} Quantitative Colormetric Peptide Assay, Thermo Scientific) and the peptide concentration was equalized to 0.5 µg/µl using 0.1% FA. A peptide ion library was constructed using data-dependent acquisition (DDA) from the collected sample peptides (4 µg).

After DDA, the sample digests were dried at 4˚C by speed-vac. 12.5 µl TEAB (0.5 M) was added to dissolve the peptides. Each digest was labeled by iTRAQ® Reagent-8-plex and mixed with 50 µl isopropanol. The digested sample was labeled by 25 µl of the mixed iTRAQ® Reagent-8plex for 2 hours at room temperature. After labeling each sample, the contents of each iTRAQ® Reagent-8plex-labeled samples were combined and mixed. The combined labeled sample was dried at 4˚C by speed-vac and cleaned by ZipTip.

2.2.6.3. Mass spectrometry acquisition

Analysis was done by using a reverse phase high pressure liquid chromatography electrospray ionization tandem mass spectrometry (RP-HPLC-ESI-MS/MS) TripleTOF® 6600 mass spectrometer (AB SCIEX; Framingham, US) with Analyst TF 1.7 software.

For DDA, iTRAQ labeled peptides (2 µg) were loaded on to a trap column (350 µm x 0.5 mm, C18) by loading buffer (0.1% FA, 2% acetonitrile in water) at 2 µl/min for 15 minutes. It was then separated on a nano-LC column (100 µm x 30 cm, Smartube C18, 5 µm) using an Ekisgent 415 nano-LC system.

Solvent A: 0.1% formic acid, 2% acetonitrile in water and Solvent B: 0.1% formic acid, 98% acetonitrile in water were used in the loading and separating procedures, respectively. The details are listed in **Table 2.1**.

Table 2.1 Details of Solvent A and Solvent B during MS acquisition.

Loading gradient		
Time (min)	**Flow rate of solvent A (µl /min)**	**Flow rate of solvent B (µl /min)**
0	2	0
15	2	0
Separation gradient		
Time (min)	**Solvent A (%)**	**Solvent B (%)**
0	95	5
0.5	90	10
90	80	20
120	72	28
130	55	45
135	20	80
140	20	80
141	95	5
155	95	5

DDA: TOF-MS mass scan was set from 350 m/z to 1,800 m/z with 250 ms accumulation time, followed by 100 m/z – 1,800 m/z for MS/MS scans in high sensitivity mode with 100 ms accumulation time of up to top 20 ion candidates per cycle. Ions with charge state 2 to 5 that exceeded a threshold of 125 count per second

(cps) was counted for MS/MS. Rolling collision energy (CE) was selected to trigger collision-induced dissociation and adjusted CE when using iTRAQ reagent was selected.

2.3.6.4 Liquid Chromatography and MS Analysis

Data-dependent acquisition was searched against Homo sapiens Uniprot reviewed database (version, 26095 entries). Protein identification (ID) was acquired using the ProteinPilot 5.0 software (SCIEX). iTRAQ-8-plex (peptide labeled) was selected as the sample type, and trypsin was selected as the enzyme. Other parameters selected include: cysteine alkylation using MMTS, thorough search effort, biological modification, quantitate, bias correction and background correction. A 1% false discovery rate (FDR) was set as the filter for protein identification. Only proteins containing at least 2 peptides were analyzed for quantification.

The Protein ANalysis THrough Evolutionary Relationships (PANTHER) classification system (version 15 released on Feb, 2020, analysis performed on March 2020) (Geneontology Unifying Biology) was used for the protein classification for all significantly regulated proteins ($p<0.05$) based on gene ontology analysis (homo sapiens). The imported proteins were classified in terms of molecular functions,

protein classes, cellular component-cellular anatomical entity and biological processes.

Online Search Tool for the Retrieval of Interacting Genes (STRING) (version 11 released January 2019, analysis performed on March 2020, http://www.string-db.org/) was used to investigate the protein-protein interaction (PPI) network for all significantly regulated proteins ($p<0.05$). The minimum interaction score was set to medium confidence (0.4) for the PPI network.

To perform a comprehensive analysis of protein database after baicalein treatment at different time points (i.e. 3 hours and 2 days), software ingenuity pathway analysis (IPA, Ingenuity Systems) was used for upstream regulator analysis and ingenuity canonical pathways analysis. Only iTRAQ protein database with at least 2 unique peptides were imported for analysis. The species was set to human and a *p* value of <0.05 (paired t-test) was adopted. The possible upstream regulator and ingenuity canonical pathways were predicted by the calculated significance using the Core Analysis in IPA. It was based on a comparison between database of Ingenuity® Knowledge Base and the input protein list.

2.3.7 Verification of MS results by quantitative polymerase chain reaction

Quantitative PCR (qPCR) was used to validate and quantify the gene expression of the targeted proteins (Wilhelm and Pingoud, 2003, Kubista et al., 2006).

2.3.7.1 Primer design

Pyruvate dehydrogenase E1 component subunit beta (PDHB, P11177), proliferation-associated 2G4 (PA2G4, Q9UQ80) and arylsulfatase B (ARSB, P15848) were selected for validation. Moreover, these protein coding genes were previously reported in the TM and/or potentially involved in signaling pathways related to glaucoma. The corresponding mRNA sequences were searched from the database of National Center for Biotechnology Information, U.S. National Library of Medicine (NCBI). The primers were designed from online Primer3 software tool (Steve Rozen) and confirmed with the database of NCBI (NCBI). Human 18S ribosomal RNA (X03205.1) was used as the internal control for the normalization of target gene expression (Nakajima et al., 2005). **Table 2.2** lists the genes responsible for the target proteins, and the primers sequences of each target gene.

Table 2.2 Primer sequences of pyruvate dehydrogenase E1 component subunit beta, proliferation-associated 2G4, arylsulfatase B and human 18S ribosomal RNA used for qPCR.

Gene	Corresponding proteins	Sequence (5'-3')
huPDHB	Pyruvate dehydrogenase E1 component subunit beta, mitochondrial OS	Forward strand: CTGCAGGTGACAGTTCGTGA
		Reverse strand: TTCTTCCACAGCCCTCGACT
huPA2G4	Proliferation-associated 2G4	Forward strand: AAGGCCTCCAAGACTGCAGA
		Reverse strand: AGTCTGGGGTTTGGTGGGAA
huARSBv1	Arylsulfatase B	Forward strand: ACTGCCATCACCTCCCACTT
		Reverse strand: TGGGAGGACAGCAGCGATAA
huRN18S	Human 18S ribosomal RNA	Forward strand: GTGGTGCATGGCCGTTCTTA
		Reverse strand: ATTGCTCAATCTCGGGTGGC

2.3.7.2 Sample collection and phase separation

hTM cells were treated with baicalein or vehicle and were harvested by 0.25% trypsin. The collected cell pellets were washed twice by PBS. Each sample was lysed by 1 ml TRIzol™ Reagent for 5 minutes at room temperature. 0.2 ml chloroform was then added to each sample and incubated at room temperature for 3 minutes. After centrifuging the samples at 12,000 g for 15 minutes at 4˚C, the upper clear aqueous layer was collected for RNA isolation.

2.3.7.3 RNA isolation

Isopropanol (0.5 ml) was added to the aqueous layer collected from the samples as described in Section 2.2.7.2. It was incubated at room temperature for 10 minutes. After centrifuging the samples at 12,000 g for 10 minutes at 4˚C, the supernatant was discarded. The pellet was washed in 1 ml 70% ethanol and was centrifuged at 7,500 g for 5 minutes at 4˚C. The supernatant was discarded and the remaining RNA pellet collected was air dried and re-dissolved in 30 µl RNAase-free water. Finally, the samples were incubated at 60˚C for 15 minutes and stored at -80˚C before use.

2.3.7.4 Reverse transcription from RNA to cDNA

RNA concentration was measured by NanoDrop™ Spectrometer (Thermo Scientific). The sample RNA concentration was calculated as follow:

$$RNA\ concentration\ (\mu\, g/ml) = \frac{(OD260) \times (dilution\ factor) \times (40 \mu g RNA/ml)}{\frac{1}{OD260}\ unit}$$

OD 260 was a reading taken at the wavelength of 260 nm.

1 µg RNA was collected for the reverse transcription process. High-capacity cDNA Reverse Transcription Kits (Applied Biosystems, Thermo Fisher Scientific) were used. 2 µl 10x Reverse Transcription Buffer, 0.8 µl 25X dNTP mix (100 mM), 2 µl 10x Reverse Transcription Random Primers, and 1 µl MultiScribe Reverse Transcriptase were added to each RNA sample. RNAase-free water was added until the final sample volume reached 20 µl. The RNA samples were then loaded into thermal cycler: 25˚C for 10 minutes, 37˚C for 120 minutes, and 85˚C for 5 minutes. The samples were stored at -20˚C before use.

2.3.7.5 Real-time polymerase chain reaction

The cDNA samples collected from vehicle- and baicalein-treated hTM cells after reverse transcription (described in **section 2.3.7.4**) was diluted 10 times by RNAase-free water prior to measurement. qPCR mixture was prepared by LightCycler® 480 SYBR Green I Master, qPCR graded water, 10 nM forward and reverse primers (listed in **Table 2.2**) in ratio of 5:1:1:1. Then, 2 µl of the diluted cDNA (i.e. 10 ng cDNA) and 8 µl qPCR mixture were loaded into and mixed thoroughly in the LightCycler® 480 Multiwell Plate 96. For negative control, 2 µl of qPCR graded water and 8 µl qPCR mixture were loaded. Three technical replicates were prepared for each cDNA sample and negative control.

The 96-well plates were put into the LightCycler® 480 Instrument (Roche) for pre-incubation and amplification. During pre-incubation, the target temperature was set to 95˚C for 5 minutes in order to activate the DNA polymerase. In order to amplify the target DNA, the temperature was changed to 95˚C, 61˚C and 72˚C, 30 seconds each for 40 cycles. Signal was collected at the end of each cycle. The mRNA expression of the target gene was normalized with the internal control and compared between vehicle- and baicalein-treated samples.

2.4 *In vivo* study

2.4.1 Animals

Adult male Sprague-Dawley rats (SD rats) and C57BL/6J mice (C57 mice) (aged 2-4 months) were used in the experiments. Prior to the experiments, they were kept in cages with daily 12-hour light / dark cycles with unlimited food and water for at least a week. All animals were maintained and handled according to the Association for Research in Vision and Ophthalmology (ARVO) guidelines. All animal work were reviewed and approved by the Animal Subjects Ethics Sub-Committee (ASESC) of The Hong Kong Polytechnic University.

2.4.2 Non-invasive measurements of IOP in rodents

These series of experiments served as a proof-of-concept to determine whether baicalein elicited any detectable reduction of IOP in rodents. Rebound tonometer (Tonolab, iCare, Finland), designed for IOP measurements in rodents was used for IOP measurements. At least three readings were taken and averaged for data analysis. Because of diurnal IOP variations, for some experiments, IOP measurements were conducted both in daytime and nighttime. All IOP measurements were conducted under awake conditions except for the initial experiments with intraperitoneal administration of baicalein. In that experiment, animals were anesthetized with 2% isoflurane inhalation during IOP measurements.

2.4.2.1 Intraperitoneal injection of baicalein

SD rats were used. Measurement of IOP was conducted daily (at the same time of the day) under anesthesia (2% isoflurane inhalation). IOP was monitored daily for at least 3 days before and 4 weeks after drug treatment. There were two groups of animals. In the treatment group, 500 μl of baicalein solution at a concentration of 4 mg/kg was injected via intraperitoneal route once daily for 2 weeks. IOP measurements were conducted immediately before intraperitoneal drug administration. After 2 weeks, the concentration of baicalein was increased to a daily dose of 40 mg/kg for an additional

2 weeks. For the control group, a vehicle (instead of baicalein) was injected daily after IOP measurements.

2.4.2.2 Topical administration of baicalein

Both SD rats and C57 mice were used. IOP was monitored for 3 days both before and after drug treatment under awake condition. Because of diurnal IOP variation, experiments were conducted under daytime and nighttime separately for each species. In other words, changes in IOP were monitored during daytime and nighttime with two different groups of animals. For the daytime group, topical administration of baicalein (10 mM, 20 μl) was applied to the experimental eye twice, separated by a 10-minute interval. A vehicle was used in the contralateral fellow eye as control. IOP measurements were conducted after drug treatment at 1.5, 3, 6, 24, 48, and 72 hour intervals. For the nighttime group, same treatment was given except that all measurements were conducted in the dark.

To determine the bioavailability of baicalein in the eye, the concentration of baicalein in the AH was determined by the multiple reaction monitoring (MRM) approach. C57 mice were used for this experiment. Similar to the above-mentioned experiments, after baseline IOP measurement, baicalein and vehicle (20 μl) was applied topically

twice (separated by 10 minutes) to the experimental and control eyes, respectively. IOP was measured 1.5 hours following drug application. The animal was then sacrificed and the AH was extracted from the anterior chamber by a 33-G needle. Because of the limited volume of AH in mice, three individual samples collected from eyes receiving the same treatment were pooled together as one sample. After 3 times dilution with 100% methanol, baicalein concentration was measured by the MRM approach in a triple quadrupole MS (QTRAP® 6500+ System, Sciex). Eksigent Ekspert UltraLC 110, Sciex QTRAP 6500+ and Kinetex 2.6 µl C18 were used in the MRM system. . During measurement, aqueous solvent (0.1% FA in double-distilled water) and organic solvent (0.1% FA in methanol) were pumped into the system under different proportions. The pump flow rate was set as 0.6 ml/min for 5 minutes in each measurement. In the first 2 minutes, there was 40% of organic solvent of the pump flow. Then the percentage of organic solvent was increased to 98% for 2 minutes. In the final minute of measurement, organic solvent percentage was reduced back to 40%. The source optimization is listed under **Table 2.3** and the selected daughter ions with the conditions are shown in **Table 2.4**. The expected retention time of the daughter ions was 3.9 minute.

Table 2.3 Parameters of MRM source optimization.

Item	Condition	Item	Condition
Curtain Gas	20 psi	Ion Source Gas 1	45 psi
Collision Gas	Medium	Ion Source Gas 2	40 psi
Ionspray Voltage	5200 V	Declustering Potential	96 V
Temperature	500 ˚C	Entrance Potential	10 V

Table 2.4 Details of daughter ions of baicalein.

	Q1 mass (+ve polarity)	Q3 mass	Collision energy	Collision cell exit potential
1	270.992 m/z	123.0 m/z	41 eV	8 V
2	270.992 m/z	168.9 m/z	39 eV	12 V

2.4.2.3 Intravitreal injection of baicalein on IOP

SD rats were used because it has a larger eyeball for intravitreal drug administration. The experiment was divided into two parts. During the intravitreal injection procedures, all animals were anesthetized by intraperitoneal injection of a mixture of ketamine (80 mg/kg) and xylazine (8 mg/kg). The SD rats were divided into 4 groups (n=6 in each group). In each group, 2 µl of vehicle, 7.5 µM, 75 µM, and 750 µM of baicalein was injected to the experimental eye, while the contralateral eye of the same animal was treated as control. Nighttime IOP was measured because baicalein was shown to have a larger ocular hypotensive effect during nighttime. It is estimated that

the total volume of AH and vitreous humor was about 65 to 75 µl (Valderrama et al., 2008, Sha and Kwong, 2006), resulting in an estimated baicalein concentration of 0.2 µM, 2 µM and 20 µM in the anterior chamber. IOP measurements were monitored daily for 3 days before and up to 9 days after drug treatment. Total retinal thickness was measured by a spectral domain optical coherence tomography (SD-OCT) system (Micron IV, Phenix Research Laboratories) at baseline and at the end of the experiment (i.e. day 9) to rule out any retinal cytotoxicity.

For the second part of the experiment, 2 µl of 750 µM baicalein or vehicle was injected intravitreally to the experimental eye while the fellow untreated eye was used as the control. IOP was measured under awake condition every 12 hours for 3.5 days (84 hours) after drug treatment.

2.5 Data analysis

All data were expressed as Mean ±SEM. SigmaPlot for Windows (version 13.0) was used for statistical analysis. When comparing between mean results of two groups, paired or unpaired t-test was used. For multiple groups' comparison, one- or two-way Analysis of Variance (ANOVA) followed by Bonferroni t-test was used. A *p*-value of <0.05 was considered statistically significant (*p<0.05; ** p<0.01; *** p<0.001).

Chapter 3 Results

3.1 *Ex vivo* study

Effect of baicalein on outflow facility in mouse eyes

The effect of baicalein (0.1, 1, 10 μM) on outflow facility *C* (μl/min/mmHg) in enucleated mouse eyes was investigated by constant-pressure perfusion system. The average flow rates of both baicalein-treated and vehicle-treated control eyes at each pressure step are presented in **Figure 3.1**. Since conventional outflow is pressure-dependent, linear regression was adopted to determine the line of best-fit between flow rate (Q, μl/min) and pressure applied (P, mmHg) (Lei et al., 2011, Boussommier Calleja et al., 2012). A good correlation was yielded with $R^2 > 0.9$ in all cases. Subsequently, the outflow facility (C) was determined by calculating the slope of the respective regression line. Our results showed that there was no significant difference of outflow facility in control eyes among different groups (range: 0.023 to 0.029 μl/min/mmHg, $p>0.05$, one-way ANOVA). In order to minimize individual variations among animals, a comparison was made between experimental (baicalein-treated) and their corresponding control (vehicle-treated) eyes of the same animal. As shown in **Figure 3.2**, at 0.1 μM, baicalein had no effect on outflow facility when compared to the vehicle-treated control eye ($p>0.05$, paired t-test). At 1 μM and 10 μM, baicalein significantly increased outflow facility by 37 ±13% ($p<0.01$, paired

t-test) and 89 ±20% (p<0.01, paired t-test), respectively. Our results suggest that administration of baicalein elicited a concentration-dependent increase in outflow facility. The effect of Y39983, a selective ROCK inhibitor, was used for comparison as a control. At 50 µM, Y39983 significantly increased the outflow facility by 74 ±18% (n=3, p<0.05, paired t-test) in paired enucleated eyes. Comparing the results obtained from baicalein, the increase in outflow facilities induced by 1 µM and 10 µM baicalein were no different from that of 50 µM Y39983 (p>0.05, one-way ANOVA).

A

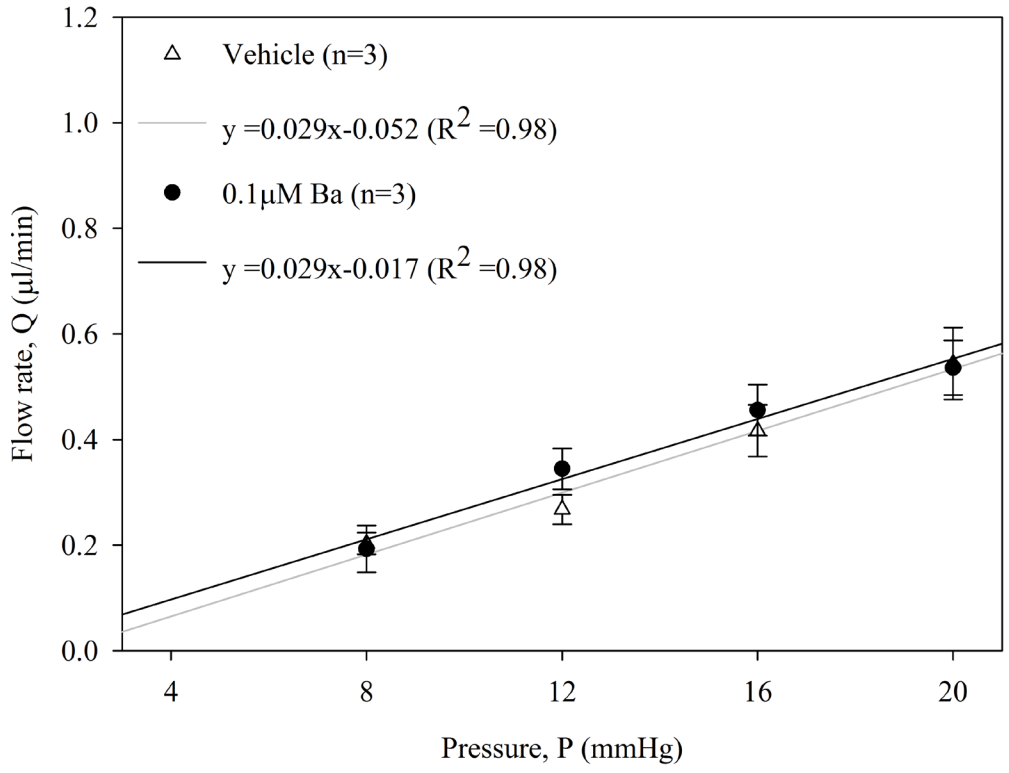

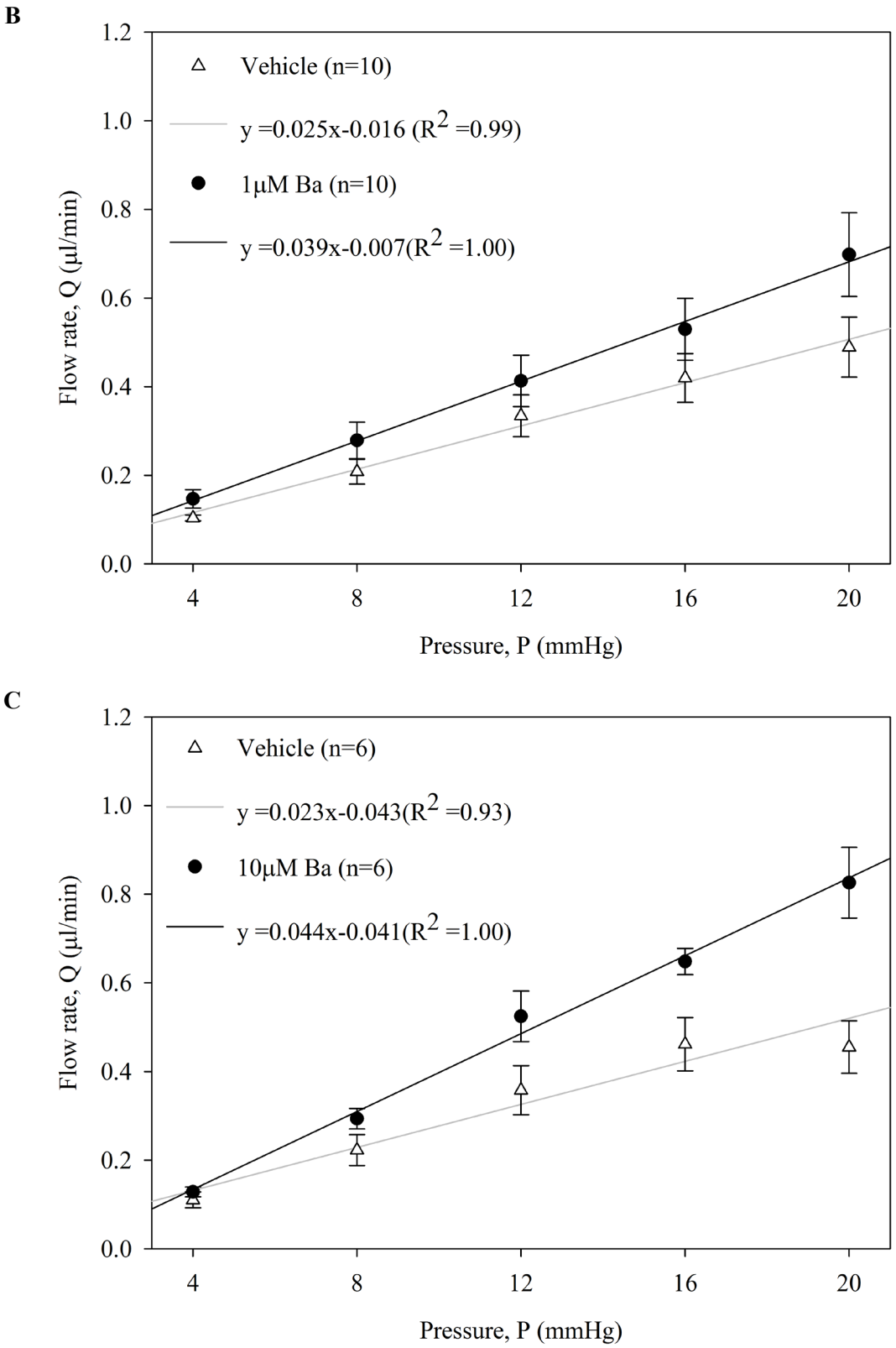

Figure 3.1 Flow rate (Q) measured at different pressures (P) applied in paired enucleated eyes in C57BL/6J mice with different concentrations of baicalein **A**) 0.1 μM (n=3); **B**) 1 μM (n=10); and **C**) 10 μM (n=6). Results are expressed as Mean ±SEM.

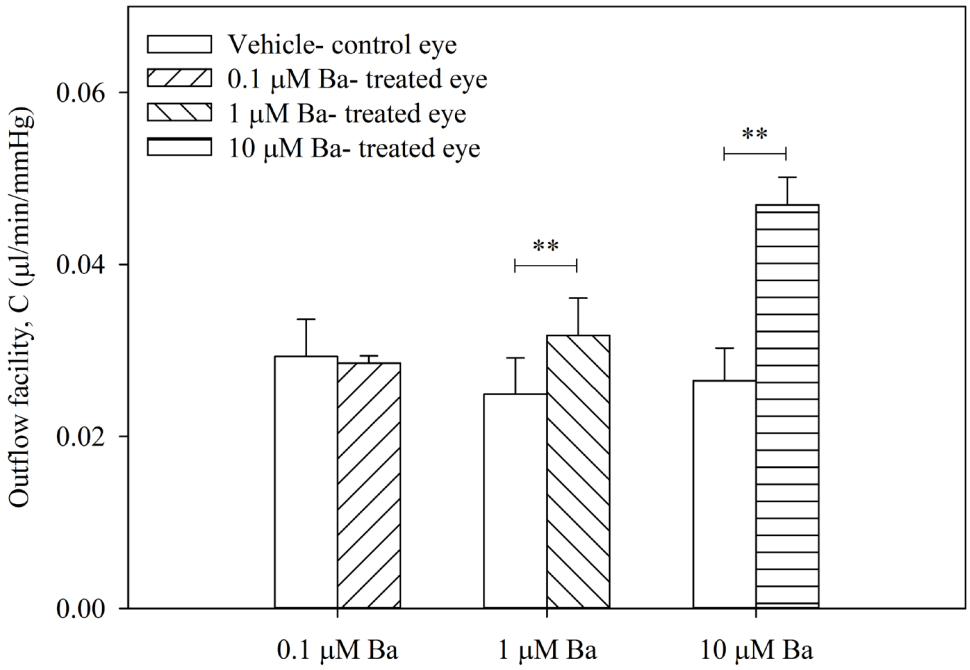

Figure 3.2 The calculated outflow facility of 0.1 μM baicalein (n=3), 1 μM baicalein (n=10) and 10 μM baicalein (n=6) treated eyes and their fellow vehicle-treated control eyes. Results are expressed as Mean ±SEM (**p<0.01, paired t-test).

3.2 *In vitro* study

3.2.1 Effects of baicalein on cell viability and proliferation

To determine whether baicalein influences cell survival and normal cell growth, the effects of baicalein, at various concentrations (1, 10 and 100 μM), on cell viability and proliferation of hTM cells were investigated. Cell viability and cell proliferation were monitored after treatment with baicalein for 2 and 4 days by Trypan blue exclusion test and MTT assay, respectively.

3.2.1.1 Effect of baicalein on cell viability

The cytotoxicity of baicalein was assessed by monitoring the viability of hTM cells using Trypan blue assay. As shown in **Figure 3.3**, cell viability was expressed as a percentage of viable cells (i.e. no. of viable cells / total no. of cells). Our results showed that cell viability after a 2-day PBS treatment and vehicle were 82.7 ±2.8% and 84.8 ±2.1%, respectively, with no significant difference detected (p>0.05). Similarly, we did not observe any significant difference in cell viability between PBS (79.0 ±4.5%) and vehicle (80.0 ±3.4%) after the 4-day treatment. These results reflect the subtle effects of vehicle on hTM cell viability. Likewise, no significant difference was found in cell viability between baicalein-treated (1 to 100 μM) and vehicle-treated hTM cells after a 2-day and 4-day treatment (**Figure 3.3**, p>0.05, one-way ANOVA). Our results indicated that baicalein did not affect the cell viability at both time points.

A. 2 days of treatment

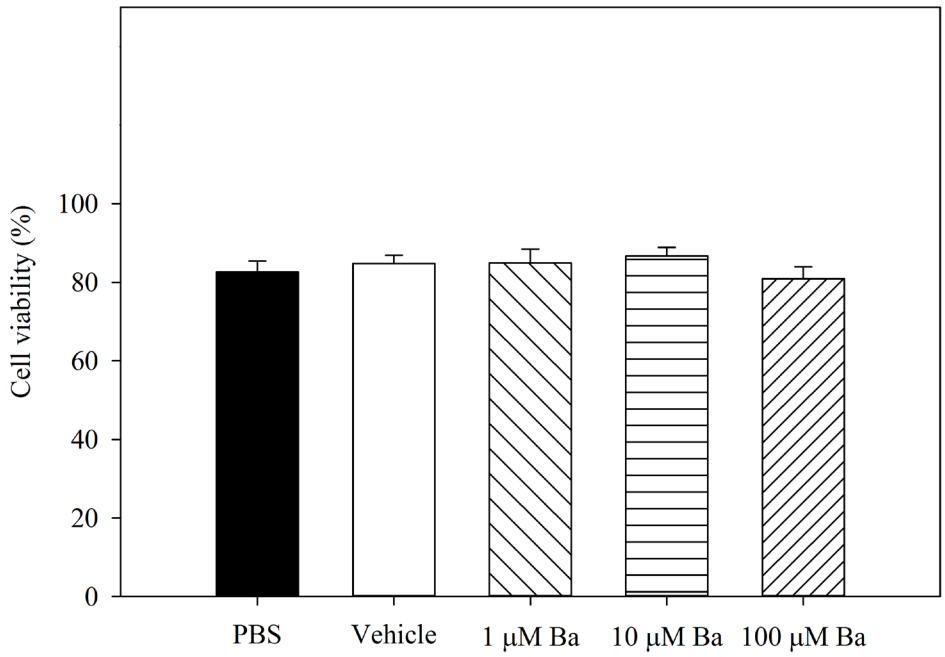

B. 4 days of treatment

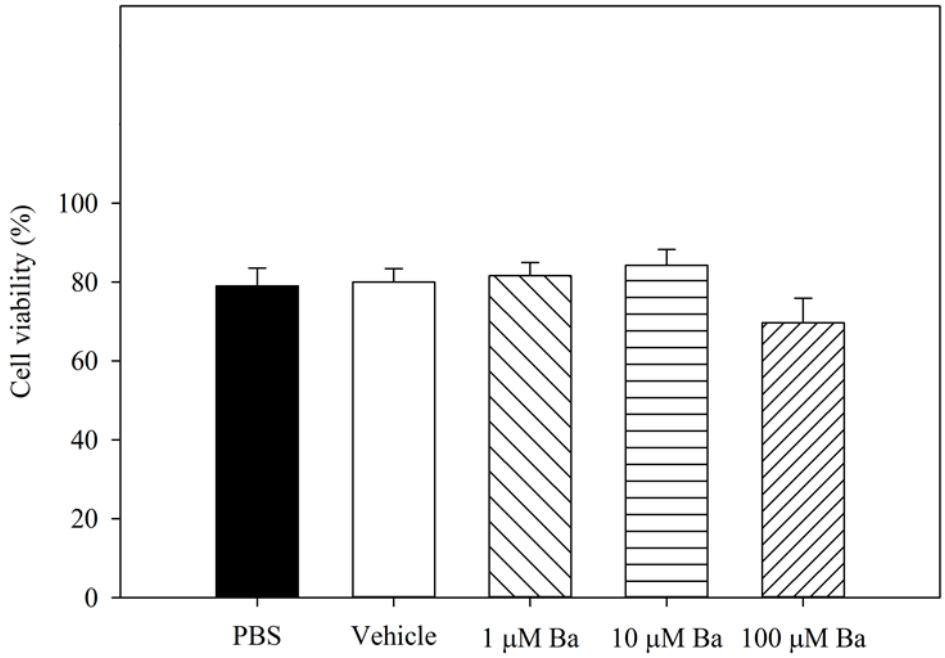

Figure 3.3 Cell viability measured by Trypan blue exclusion test after **A**) 2-day; and **B**) 4-day treatment with PBS, vehicle, and baicalein (1 μM, 10 μM and 100 μM) in hTM cells. Results are expressed as Mean ±SEM (n=4, p>0.05, one-way ANOVA).

3.2.1.2 Effect of baicalein on cell proliferation

The effect of baicalein on cell growth and proliferation was measured by MTT assay. The normalized hTM cell proliferation after 2- and 4-day treatment under various conditions are summarized in **Figure 3.4**. No significant change was observed in proliferation rates between PBS and vehicle after 2-day and 4-day treatments (p>0.05). Our results suggested that vehicle did not affect normal cell proliferation or growth. In addition, there was no significant difference in proliferation rates between vehicle-treated and baicalein-treated at all concentrations (1 to 100 μM) after 2- and 4- day treatment (p>0.05, one-way ANOVA). Thus, baicalein did not affect hTM cell proliferation. These results show that baicalein have minimal effect on both cell viability and proliferation, indicating that baicalein may have low toxicity and viable safety profile as a pharmacologic agent that can be used in subsequent experiments.

A. 2 days of treatment

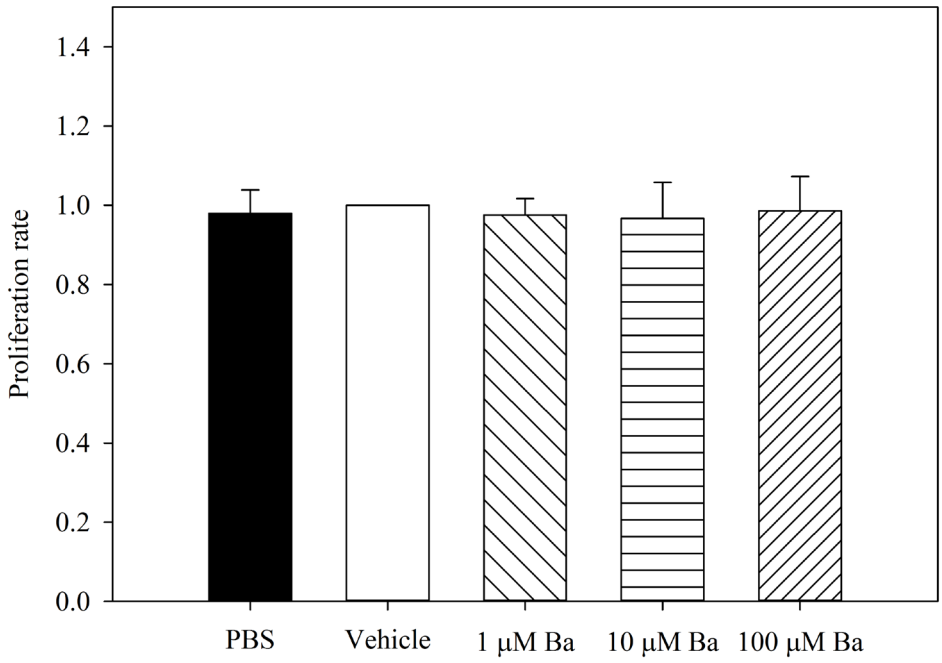

B. 4 days of treatment

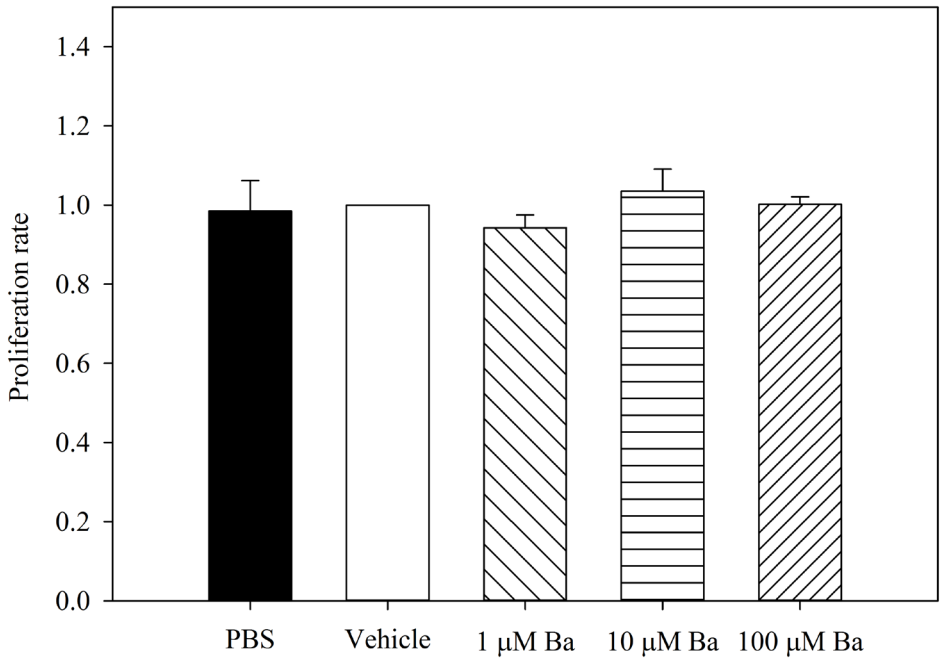

Figure 3.4 Cell proliferation after **A**) 2-day; and **B**) 4-day treatment with PBS, vehicle, and baicalein (1 µM, 10 µM and 100 µM) in hTM cells. Results are expressed as Mean ±SEM (n=4, p>0.05, one-way ANOVA).

3.2.2 Effects of baicalein on volume regulation in hTM cells

Cell volume regulation has been proposed to participate in the regulation of outflow resistance. To test the acute effects of baicalein on volume regulation, hTM cells were treated with baicalein or vehicle under both isotonic and hypotonic conditions. The hTM cells were suspended in isotonic bathing solution (290-305 mOsmol/kg H_2O) for equilibration and then treated with either baicalein (1, 10, and 100 μM) or vehicle for 30 minutes. The relative cell volume changes after different treatments are presented in **Figure 3.5**. Our results demonstrated no significant difference between vehicle-treated and baicalein-treated groups at all concentrations tested (p>0.05, one-way ANOVA).

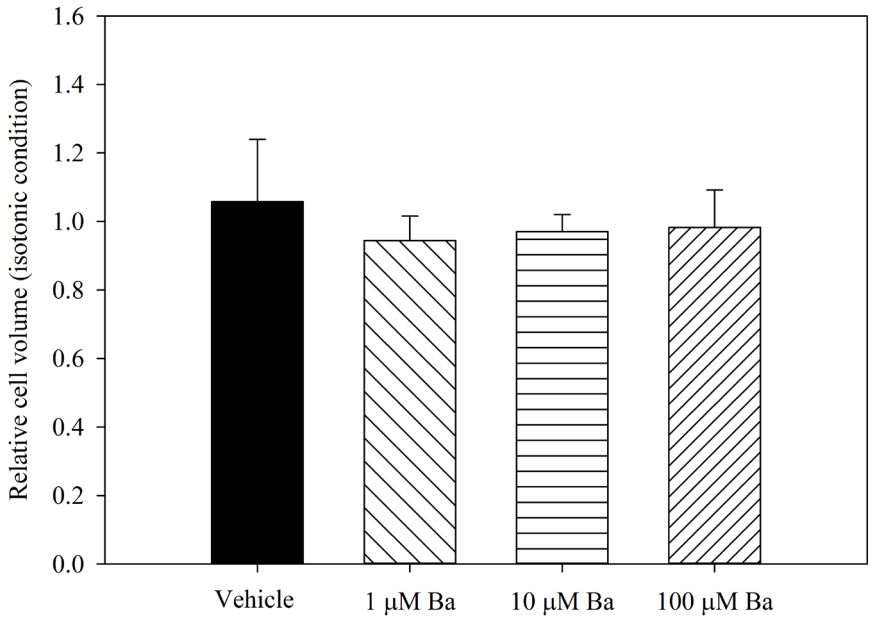

Figure 3.5 Relative hTM cell volume after treatment with vehicle, and baicalein (1 μM, 10 μM, 100 μM) in isotonic condition for 30 minutes. Results are expressed as Mean ±SEM (n=3, p>0.05, one-way ANOVA).

The changes in cell volume over 30 minutes with hypotonic stimulation (150-160 mOsmol/kg H_2O) are summarized in **Figure 3.6**. As expected, reducing the osmolarity of the bathing solution triggered a rapid cell swelling in the first 2-3 minutes followed by a gradual restoration to its initial cell volume (termed as regulatory volume decrease RVD) throughout the experiments. Our results showed that 10 μM and 100 μM baicalein significantly inhibited RVD while 1 μM baicalein had no significant effect on cell volume recovery.

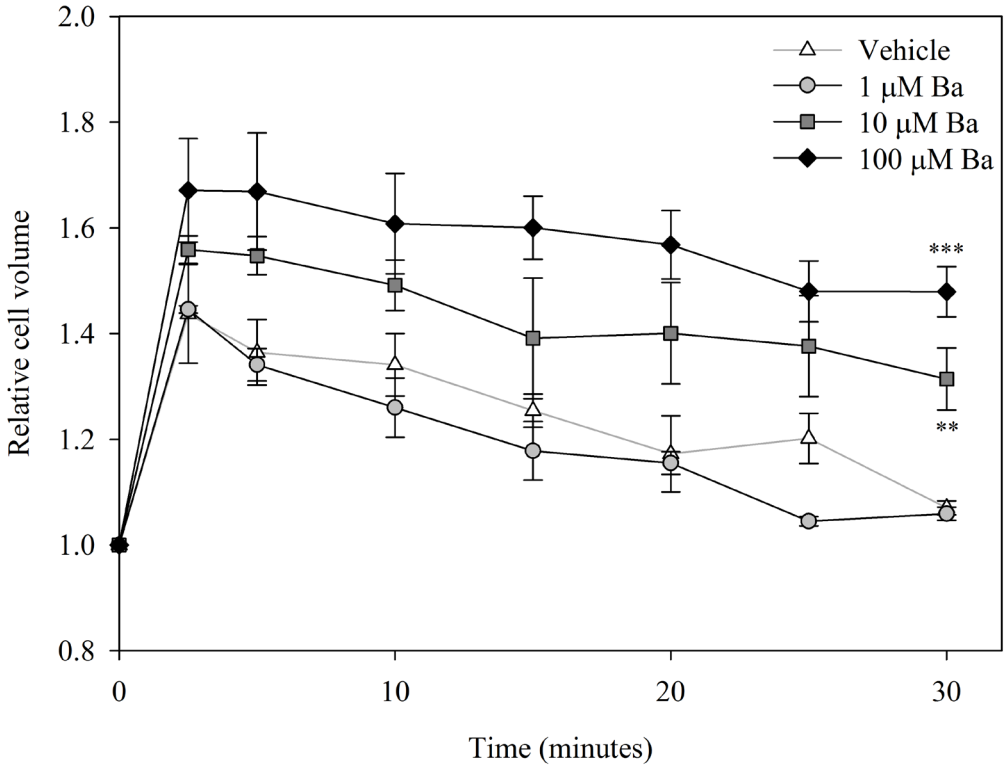

Figure 3.6 Relative cell volume changes in hTM cells after treatment with vehicle, and baicalein (1 μM, 10 μM, and 100 μM) upon hypotonic stimulation. Results are expressed as Mean ±SEM (n=3, ** p<0.01, *** p<0.001, one-way ANOVA followed by Bonferroni t-test).

3.2.3 Effect of baicalein on contractility of hTM cells

3.2.3.1 Effect of baicalein on gel contraction

The effect of baicalein on hTM cell contractility was determined by collagen gel contraction assay. The changes in collagen gel areas measured before and after treatment were normalized for comparison. **Figure 3.7** summarizes the changes in collagen gel areas after baicalein treatment as compared to their respective vehicle-treated controls. We found that baicalein elicited a concentration-dependent relaxation of TM cells after 3- and 6-hour treatment. At 100 μM, baicalein triggered a sustained relaxation of hTM cells by 10 ±3% (p<0.01) and 10 ±3% (p<0.05) after 3- and 6-hour treatment, respectively. The effects of 1 and 10 μM baicalein on hTM cell relaxation were not statistically significant. In this set of experiment, 5 μM carbachol, which was previously demonstrated to induce TM cell contraction (Rosenthal et al., 2005), was used as a control. Consistent with previous finding, our results showed that carbachol triggered a sustained contraction of hTM cells by 14 ±8% and 13 ±8% after 3-hour and 6-hour of treatment, respectively, when compared with PBS-treated cells (n=5, p<0.05, two-way repeated measures ANOVA). Our results indicated that baicalein elicited a concentration-dependent hTM cell relaxation lasted for at least 6 hours.

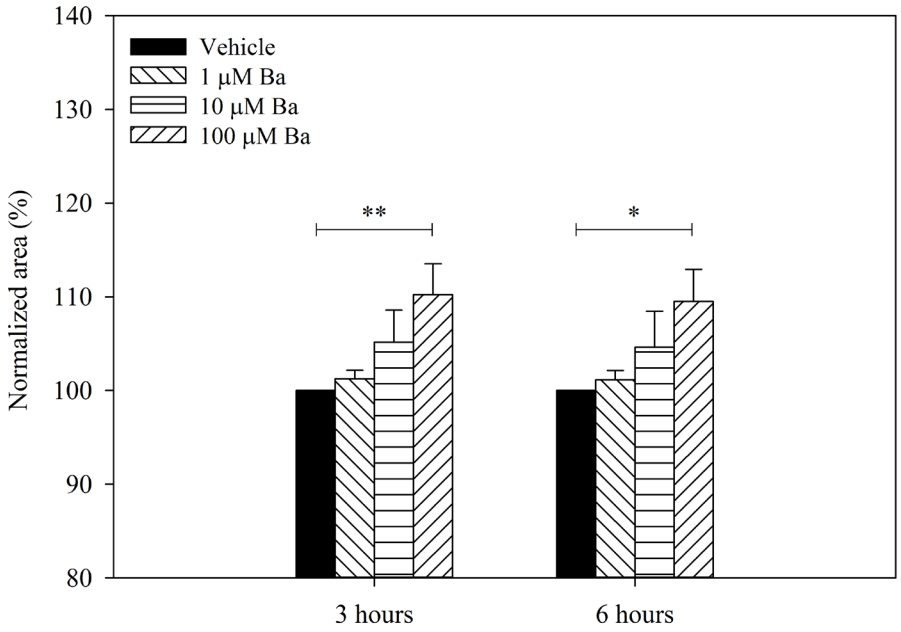

Figure 3.7 Effects of baicalein on the contractility of hTM cells. Results are presented as normalized collagen gel area after treatment with vehicle (n=5), 1 μM (n=3), 10 μM (n=5), and 100 μM (n=5) baicalein for 3 and 6 hours. Results are expressed as Mean ±SEM (*p<0.05, **p<0.01, two-way repeated measures ANOVA followed by Bonferroni t-test).

3.2.3.2 Effect of baicalein on phosphorylated myosin light chain (pMLC)

In addition to gel contraction, the contractility of hTM cells can be measured as a percentage of phosphorylated 20-kDa myosin light chain (pMLC) to total MLC. It was previously shown that there is a positive correlation between the pMLC/MLC level and the magnitude of cell contraction (Rao et al., 2005). **Figure 3.8** shows the expression of pMLC/MLC after baicalein or vehicle treatment by Western blot analyses. Baicalein was found to downregulate the expression pMLC/MLC after 5 minutes of treatment. 100 μM baicalein reduced pMLC/MLC expression by 18 ±9% (p<0.05, paired t-test). As expected, carbachol (5 μM) increased the pMLC/MLC

expression by 85 ±51% (n=4, p<0.05, paired t-test) in hTM cells. Our results were consistent with the findings of gel contraction assay that baicalein elicited a relaxation of hTM cells.

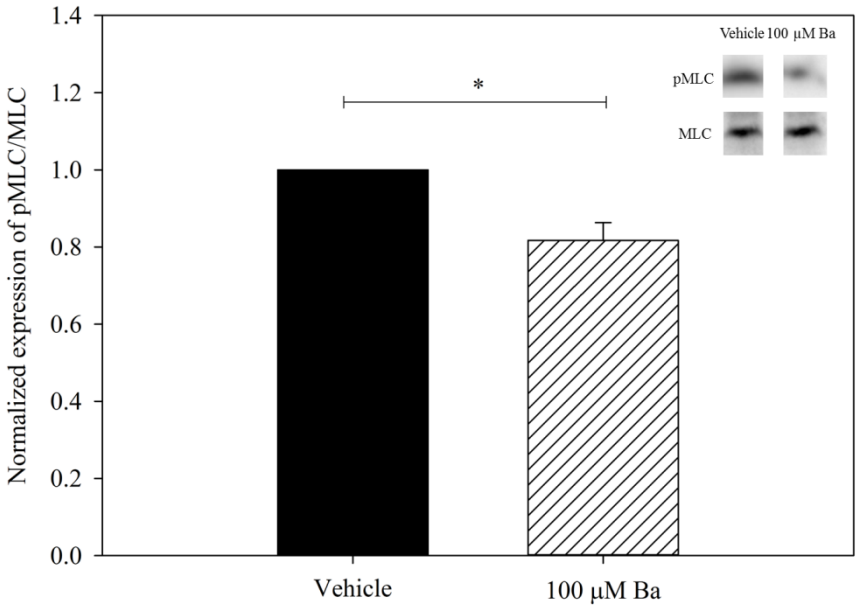

Figure 3.8 Effects of baicalein on percentage expression of phosphorylated myosin light chain (pMLC) to total MLC in hTM cells using Western blot analyses. Results are presented as normalized pMLC/MLC expression after treatment with vehicle and 100 µM baicalein for 5 minutes. A typical experiment showing pMLC and MLC bands is shown on the top right-hand corner of the diagram. Results are expressed as Mean ±SEM (n=4, *p<0.05, paired t-test).

3.2.4 Effect of baicalein on hTM cell migration

To investigate whether baicalein influences hTM cell motility, we measured hTM cell migration after baicalein treatment for a period of 2 to 4 days. This was achieved with

measuring the cell-free gap area after making vertical and horizontal scratches on the confluent hTM cell layer. As mentioned in **Section 3.2.1**, we demonstrated that baicalein had no influence on cell proliferation. Hence, any changes in gap areas were possibly mediated by cell migration. The effects of baicalein on hTM cell migration as compared to vehicle control are summarized in **Figure 3.9**. Our results showed that baicalein triggered a progressive concentration-dependent inhibition of cell migration. After 2 days of treatment, 10 and 100 μM baicalein significantly inhibited cell migration by 35 ±12% (p<0.05) and 60 ±11% (p<0.001, two-way repeated measures ANOVA), respectively, when compared to vehicle-treated control. Likewise, baicalein inhibited the cell migration by 29 ±6% (1 μM, p<0.05), 48 ±4% (10 μM, p<0.001), and 78 ±9% (100 μM, p<0.001) after 4 days of treatment. Y39983 was used as a control. Similar to the results of baicalein treatment, 1 μM of Y39983 inhibited the TM cell migration by 37 ±5% (n=4 p<0.05).

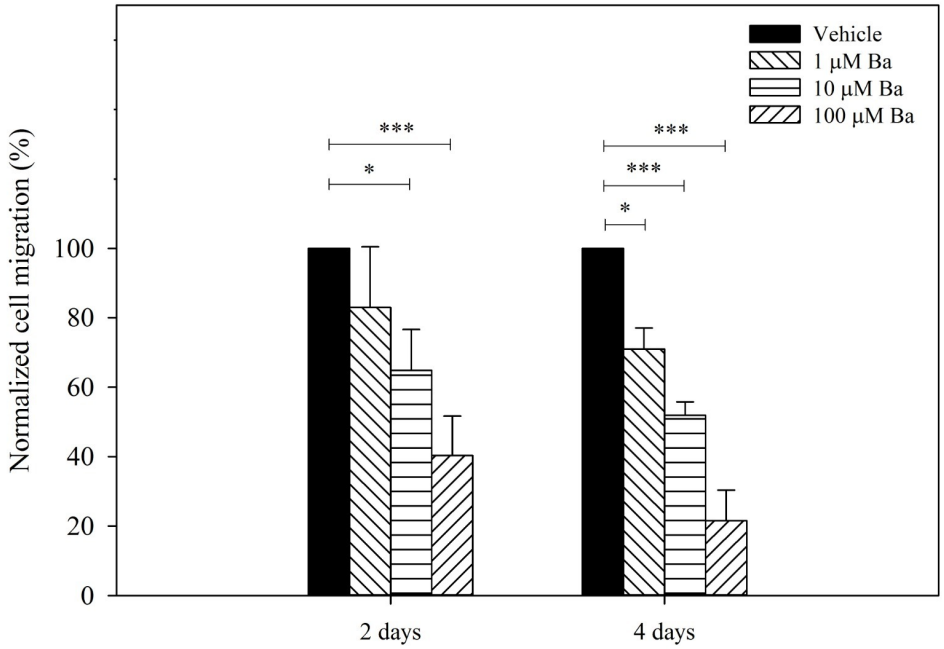

Figure 3.9 Normalized cell migration (%) after 2-day and 4-day treatments with vehicle, and baicalein (1 μM, 10 μM, and 100 μM) in hTM cells. Results are expressed as Mean ±SEM (n=3, **p*<0.05, ****p*<0.001, two-way repeated measures ANOVA followed by Bonferroni t-test).

3.2.5 Proteomic study in hTM cells after treatment of baicalein

In the preceding sections, baicalein was shown to enhance outflow facility in a dose-dependent manner. We proposed several potential mechanisms influencing the observed increase in outflow facility through: 1) cell volume regulation, 2) cell relaxation, and 3) reduced cell migration in the TM. In order to better understand the potential mechanisms involved, we investigated protein expression profiles after baicalein treatment. 10 μM of baicalein was used because it was the lowest concentration shown to elicit changes in TM cells and outflow facility. Two profiling

time points were chosen for the experiments, i.e. 3-hour and 2-day. The protein changes after 3 hours may possibly reflect the underlying mechanisms leading to an acute increase in outflow facility while the 2-day baicalein treatment could provide more insight into the immediate to long-term post treatment effects on hTM cells.

Using LC MS/MS isobaric tags for relative and absolute quantitation (iTRAQ) proteomics, with FDR set to 1%, 1,342 and 1,866 unique hTM cell proteins with at least two unique peptides were identified and quantified after baicalein treatment for 3 hours and 2 days, respectively. The ProteinPilot 5.0 Software (SCIES) was used to support proteomics data analysis. The distribution of all identified proteins is summarized as a volcano plot (**Figure 3.10**). We observed a total of 47 proteins (with 27 upregulated and 20 downregulated) with significantly altered expressions after baicalein treatment for 3 hours ($p<0.05$, paired t-test). For the 2-day treatment, 119 proteins (with 35 upregulated and 84 downregulated) were significantly regulated ($p<0.05$, paired t-test). With a fold change of >1.3 ($\log_2 > 0.31$ or $\log_2 < -0.42$), 17 proteins were upregulated and 14 proteins were downregulated after a 3-hour treatment. For 2-day treatment, 11 proteins were upregulated and 20 proteins were downregulated with a fold change of >1.3.

A. 3-hour treatment **B. 2-day treatment**

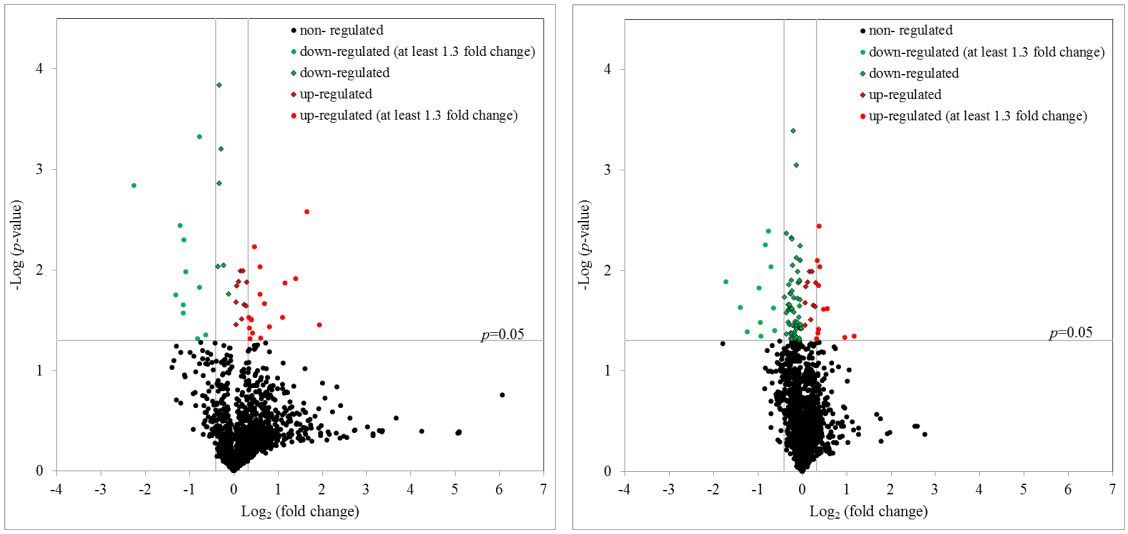

Figure 3.10 Volcano plot based on proteomics data after **A**) 3 hours (1,342 proteins) and **B**) 2 days (1,866 proteins) treatment of baicalein (10 µM). The distribution of all proteins with at least 2 unique peptides is presented. The x-axis shows a $\log_2$ fold change and y-axis shows the negative log10 *p*-value calculated by paired t-test (2 tailed). A total of 47 proteins and 119 proteins were significantly altered in expressions ($p<0.05$) after baicalein treatment for 3 hours and 2 days, respectively. For 3-hour treatment, a total of 17 proteins were upregulated (red circle) while 14 proteins were downregulated (green circle) with at least a 1.3-fold change. For 2-day treatment, a total of 11 proteins were upregulated (red circle) and 20 proteins were downregulated (green circle) with a fold change of >1.3.

All significantly regulated proteins ($p<0.05$), regardless of fold changes were subject to gene ontology (GO) (Homo sapiens) analysis according to the PANTHER classification system (http://www.pantherdb.org). The genes were classified into four categories: molecular functions, cellular components, proteins classes, and biological processes. Under molecular functions (**Figure 3.11 A and B**), 4 and 83 genes were identified among all significantly regulated proteins after the 3-hour and the 2-day time point treatment of baicalein, respectively. GO: 0003824 (catalytic activity) was

the top molecular function aspect regulated. A total of 16 and 42 genes were identified to be responsible for catalytic activity after 3-hour and 2-day baicalein treatment, respectively. The second ranked GO molecular function involved was binding (GO: 0005488), which was related to the interaction of a molecule with another molecule through specific binding sites. There were 23 and 29 genes identified to be related to binding after the 3-hour and the 2-day time point baicalein treatment, respectively.

For protein class classification (**Figure 3.11 C and D**), metabolite inter-conversion enzyme (PC00262) was the top regulated protein class at both time points with 9 and 23 genes identified after 3-hour and 2-day baicalein treatment, respectively. This result was in alignment with a higher number of significantly regulated proteins identified after 2 days as compared to 3 hours' treatment (119 vs 47 proteins). At the 2-day time point, there were additional protein candidates, including protein-binding activity modulator (PC00095) and cell adhesion molecule (PC00069).

Likewise, changes in cellular components were more pronounced after 2-day baicalein treatment as compared to 3-hour treatment. Proteins related to cellular component- cellular anatomical entity are summarized in **Figure 3.11 E and F**. A

total of 20 and 49 genes were identified at these two time points. Organelle (GO: 0043226) including nucleus, mitochondria, vesicles, and cytoskeleton was the highest ranked at both time points. The next top regulated cellular component was membrane (GO: 0016020) with 8 and 27 genes identified after the 3-hour and the 2-day treatment time points, respectively.

The top three biological processes after 3 hours of baicalein treatment were cellular process (GO: 0009987), metabolic process (GO: 0008152) and cellular component organization or biogenesis (GO: 0071840) with 28, 18, and 15 genes identified (**Figure 3.11 G**). Similarly, after 2 days of treatment, the top regulated biological processes were cellular process (53 genes), metabolic process (34 genes), and cellular component organization or biogenesis (18 genes), as shown in **Figure 3.11 H**.

Molecular Function

A. 3 hours

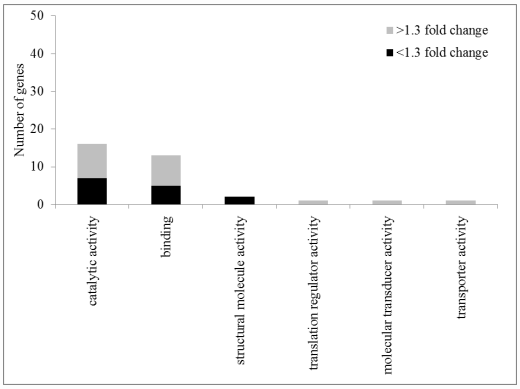

B. 2 days

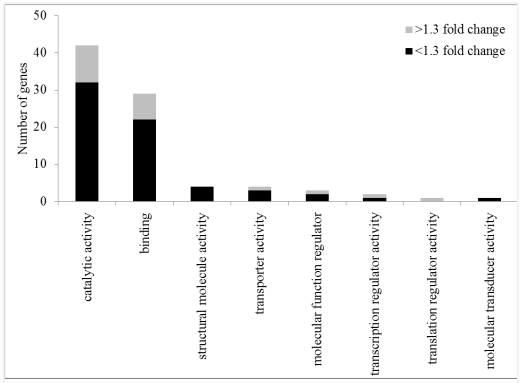

Protein classes

C. 3 hours

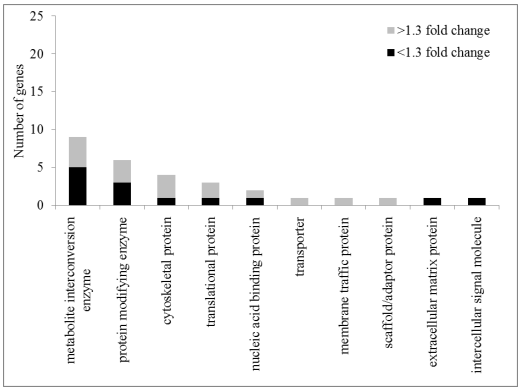

D. 2 days

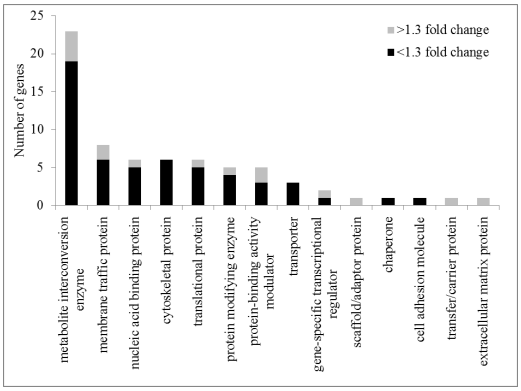

Cellular component- cellular anatomical entity

E. 3 hours

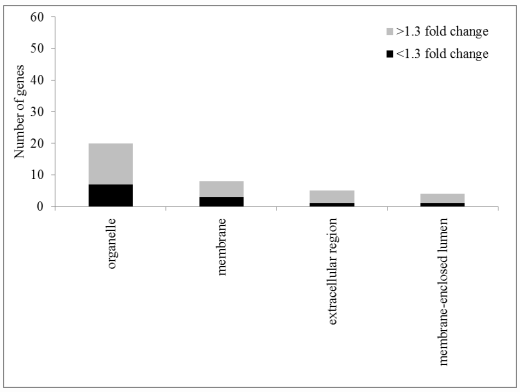

F. 2 days

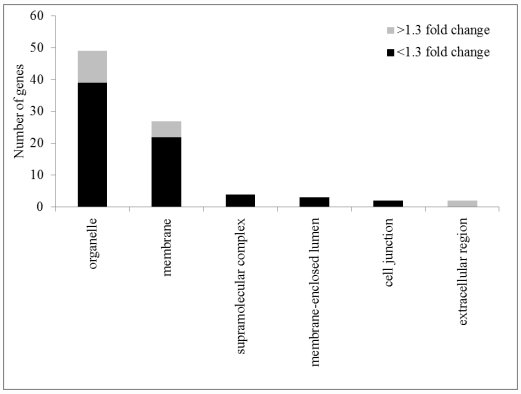

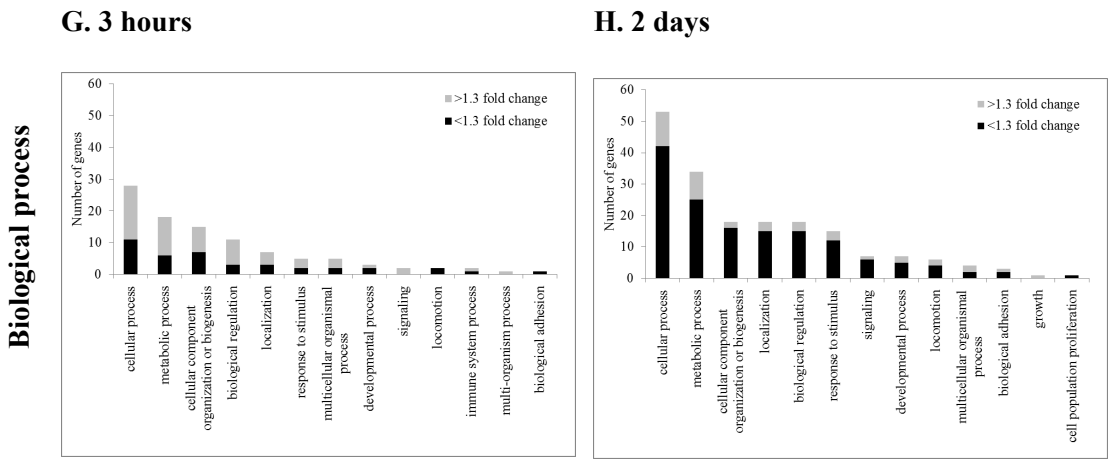

Figure 3.11 PANTHER classification with GO annotation of proteins showed significant expression (n=3, p<0.05, paired t-test). **A**, **C** and **E** represented proteins after 3 hours treatment of 10 µM baicalein. **B**, **D** and **F** represented proteins after 2 days treatment of 10 µM baicalein. **A** and **B** were molecular functions, **C** and **D** were protein classes, E and F were cellular component- cellular anatomical entity, **G** and **H** were biological processes.

Using the PANTHER classification system, despite the fact that a number of significantly regulated proteins were higher after 2 days as compared to the 3-hour treatment, the top regulated molecular functions, protein classes, cellular component and biological process involved: namely catalytic activity, metabolite inter-conversion enzyme, organelle and cellular process, were the same at both time points. This suggested that baicalein exerted similar effects on hTM cells, particularly for molecular functions and biological processes in which the top three functions and processes involved were the same for both time points.

To further elucidate the regulatory system, all differentially expressed proteins with $p<0.05$, regardless of their fold changes were searched to establish a protein-protein interaction (PPI) network. As shown in **Figure 3.12** and **Figure 3.13**, all differentially expressed proteins are presented in different colors according to their potential regulated biological process, molecular function and pathways involved. In addition, different colored lines represent the potential interactions among those proteins. We observed that most of the differentially expressed proteins were closely related and interacted with each other. Of all 47 and 119 significantly regulated proteins, only 13 and 14 "isolated" proteins were found after 3 hours and 2 days baicalein treatment, respectively.

The PPI network after baicalein treatment for 3 hours is shown in **Figure 3.12** and the full list of proteins with altered expression is presented in **Supplementary Table 1**. Of all the 47 identified proteins (nodes), there were 53 edges between the nodes with an average node degree of 2.26 (an index expressing the average interaction among proteins) in the network. The average local clustering coefficient was found to be 0.456, suggesting that the number of edges obtained from our results were significantly higher than the expected number of edges from a random set of proteins

of similar size drawn from the genome (53 vs 23). Our results suggested that the proteins were biologically connected, with a PPI enrichment *p*-value of <0.001.

For biological process, organonitrogen compound metabolic process (GO: 1901564) was the most regulated process with 28 proteins involved with FDR <0.01. There were 8 proteins with FDR= 0.0422 associated with oxidation-reduction process. For molecular function, similar to the results obtained from PANTHER, catalytic activity was one of the top regulated functions with 27 proteins involved (FDR<0.01), while for binding function, there were 38 proteins involved with FDR <0.05.

Likewise, the PPI network of baicalein treatment for 2 days is illustrated in **Figure 3.13** and the full list of proteins with altered expression is presented in **Supplementary Table 2**. There were 119 nodes and 356 edges between the nodes, with an average node degree of 5.98. The average local clustering coefficient was 0.408. The expected number of edges was 203, which was significantly less than the actual 356 edges observed. The PPI enrichment *p*-value was <0.001, which was similar to the 3-hour treatment.

For biological processes, exocytosis (GO: 0006887) was the top regulated process with 23 identified proteins (FDR <0.001). There were 22 proteins that were related to oxidation-reduction process with FDR <0.001. For molecular functions, small molecule binding (GO: 0036094) and nucleotide binding (GO: 0000166) were the top regulated functions with FDR <0.001. There were 66 proteins identified for catalytic activity with FDR <0.001 and 93 proteins identified for binding with FDR <0.01. In addition to molecular functions and biological processes, after 2-day treatment of baicalein, 11 and 8 proteins were identified to be involved in Huntington's disease (hsa05016, purple nodes) and Parkinson's disease (hsa05012, dark green nodes), respectively (FDR <0.001).

Based on the PPI network generated by STRING analysis, more than 70% of the regulated proteins were closely related, affecting molecular functions through binding and catalytic activity, similar to that of PANTHER results. In addition, oxidation-reduction process was involved after baicalein treatment at both time points. It was shown that the 2-day treatment also affected the pathway related to neurodegenerative diseases, including Huntington's disease and Parkinson's disease.

3 hours of treatment

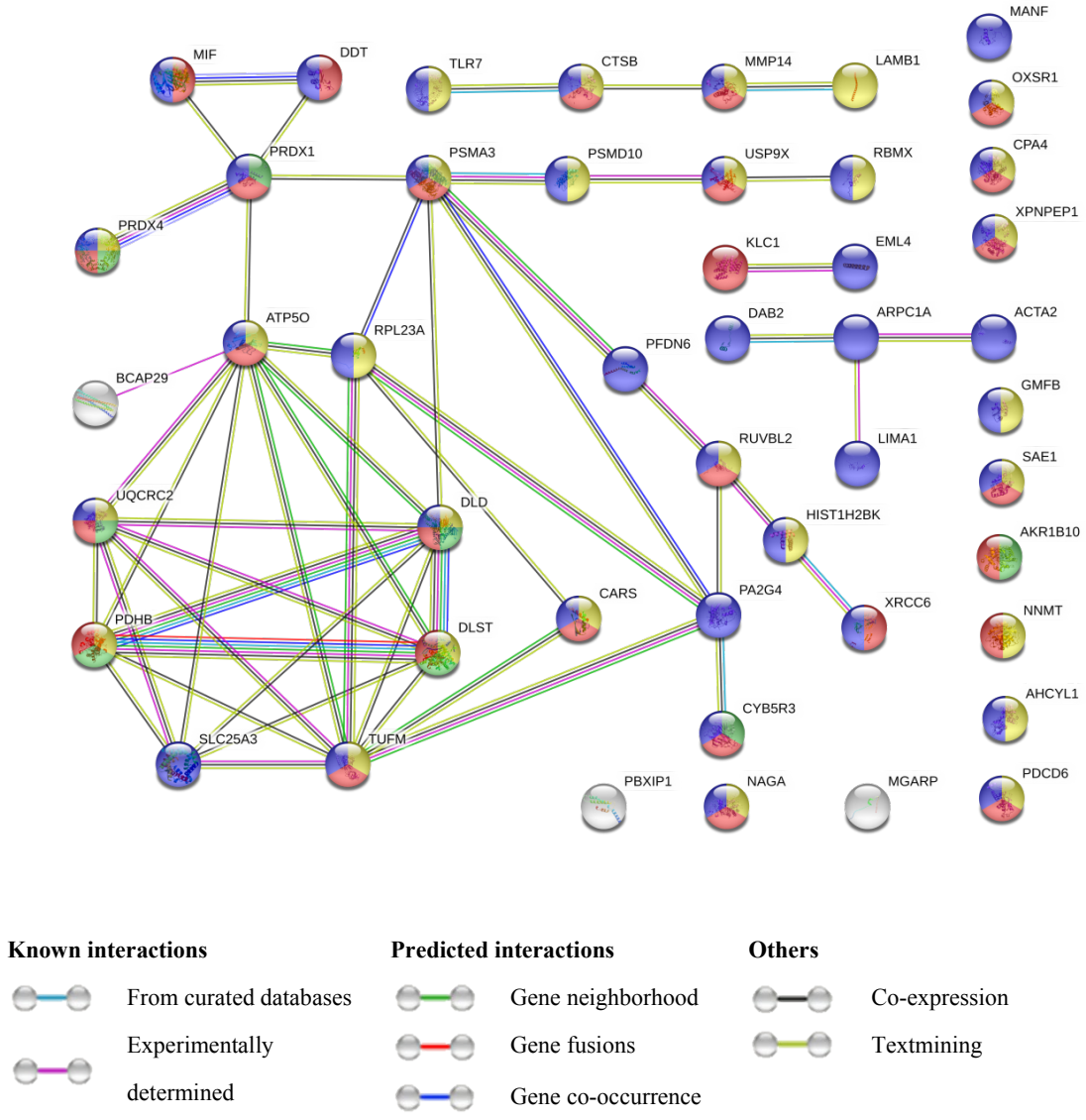

Figure 3.12 Protein-protein interaction network of 47 differentially expressed proteins (p<0.05) after baicalein treatment for 3 hours, as reported in STRING analysis (version 11). Network analysis was set at medium confidence (0.4). The relationships of 34 proteins (presented as nodes) were derived from the curated databases, experimentally determined evidence, gene neighborhood, gene fusions, gene co-occurrence, co-expression and textmining. Proteins related to organonitrogen compound metabolic process, oxidation-reduction process, catalytic activity and binding are presented in yellow, green, red and blue colored (nodes), respectively. A full list of proteins with altered expression is presented in **Supplementary Table 1**.

2 days of treatment

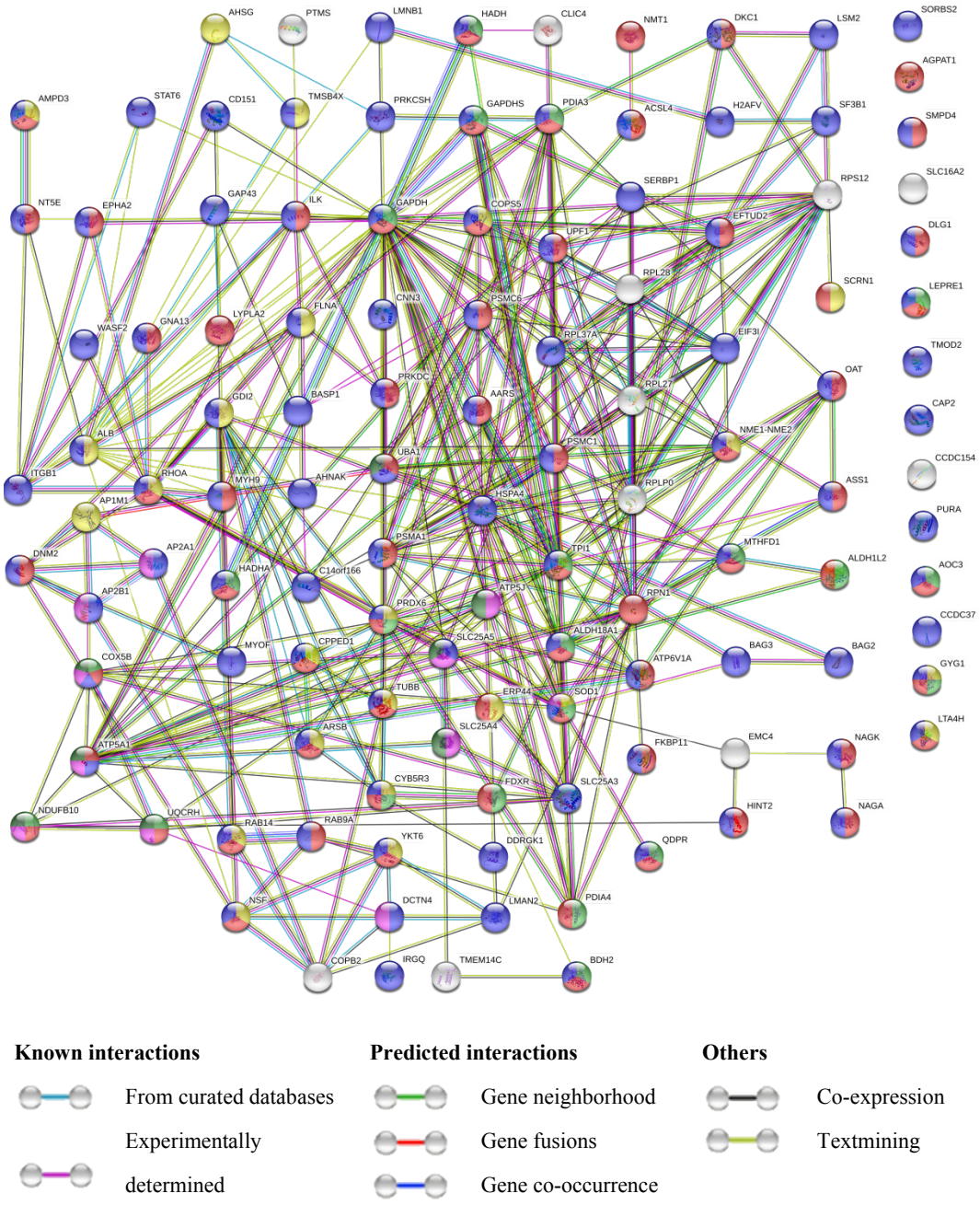

Figure 3.13 Protein-protein interaction network of 119 differentially expressed proteins (p<0.05) after baicalein treatment for 2 days, as reported in STRING software (version 11). Network analysis was set at medium confidence (0.4). The relationships of 105 proteins (presented as nodes) were derived from the curated databases, experimentally determined evidence, gene neighborhood, gene fusions, gene co-occurrence, co-expression and textmining. Proteins related to exocytosis, oxidation-reduction process, catalytic activity, binding, Huntington's disease and Parkinson's disease are presented in yellow, green, red, blue, purple and dark green colored (nodes), respectively. A full list of proteins with altered expression is presented in **Supplementary Table 2**.

Figure 3.14, **Table 3.1** and **Table 3.2** present all differentially expressed proteins (p<0.05) with >1.3 fold change after 3-hour and 2-day of baicalein treatment. Proteins with significant upregulation are represented in green bars while those with significant downregulation are shown in red bars. After 3 hours of baicalein treatment, 17 proteins were upregulated and 14 proteins were downregulated. Likewise, there were 11 upregulated and 20 downregulated proteins after 2 days treatment of baicalein.

A. 3 hours of treatment

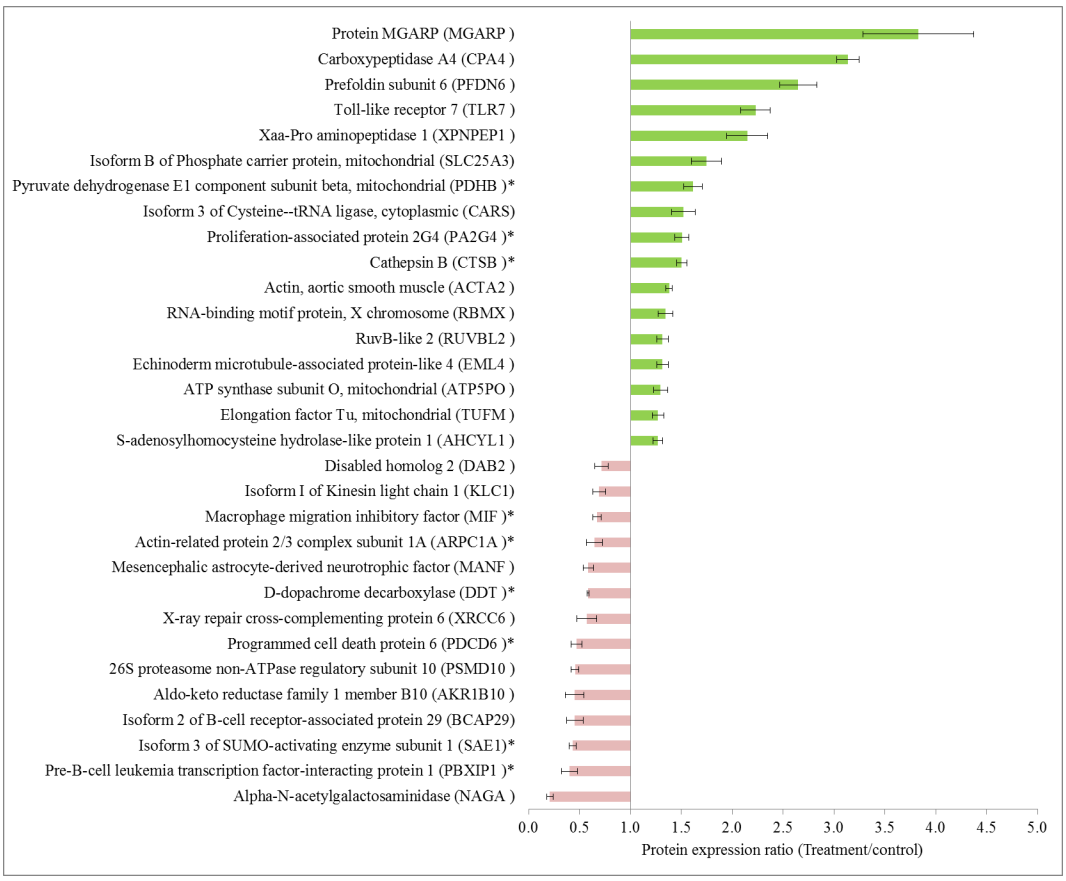

B. 2 days of treatment

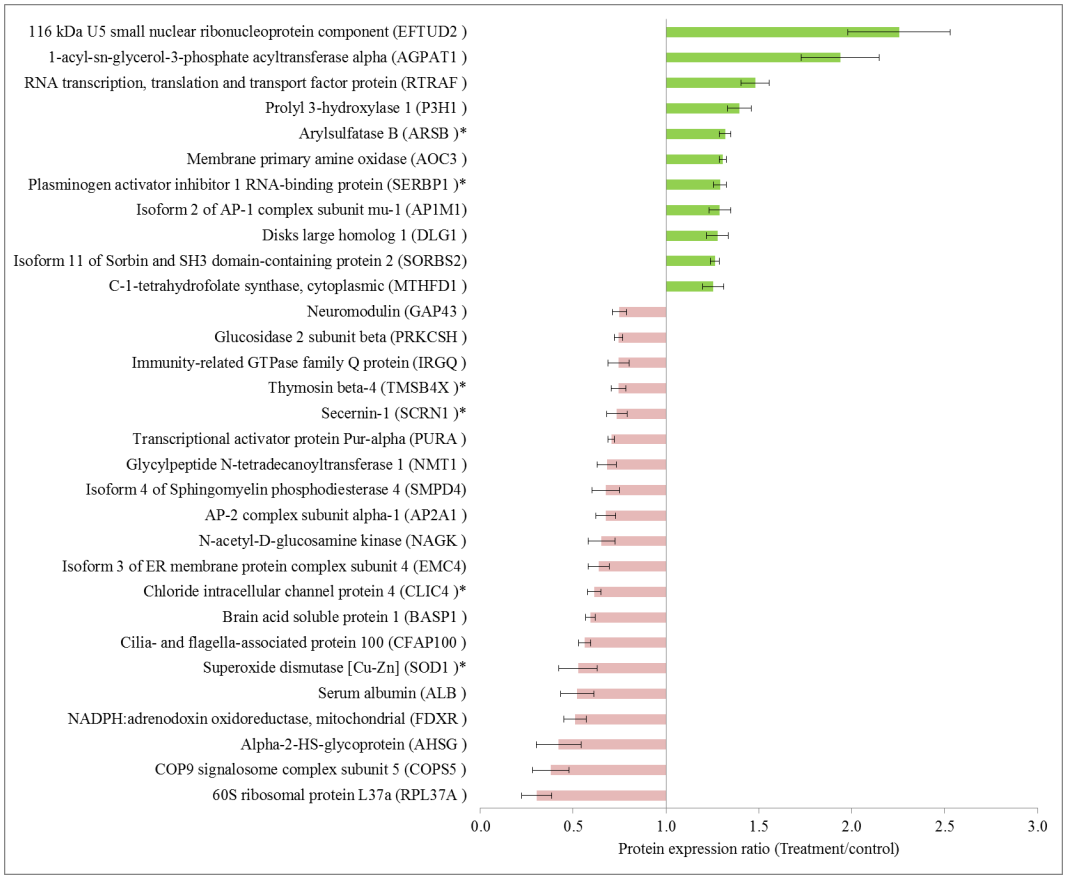

Figure 3.14 Quantitative differential protein expressions with at least 2 unique peptides and >1.3 fold change after baicalein treatment for **A**) 3 hours (17 upregulated and 14 downregulated proteins) and **B**) 2 days (11 upregulated and 20 downregulated proteins). Proteins marked with * are the proteins selected for further discussion. Results are presented as Mean ± SEM (n=3, $p<0.05$, paired t-test).

Table 3.1 Quantitative differential protein expressions with at least 2 unique peptides and >1.3 fold change after 3 hours treatment of baicalein (17 upregulated and 14 downregulated proteins). GN: Gene Name; Δ: Fold change (treatment/ control) (Mean ± SEM); *p*: *p*-value (n=3, paired t-test); proteins highlighted in red are the proteins selected for further discussion.

GN	Protein (UniProt Accession)	Δ	*p*
NAGA	Alpha-N-acetylgalactosaminidase (P17050)	0.2 ±0.0	0.001
PBXIP1	Pre-B-cell leukemia transcription factor-interacting protein 1 (Q96AQ6)	0.4 ±0.1	0.018
SAE1	Isoform 3 of SUMO-activating enzyme subunit 1 (Q9UBE0-3)	0.4 ±0.0	0.004
BCAP29	Isoform 2 of B-cell receptor-associated protein 29 (Q9UHQ4-2)	0.5 ±0.1	0.022
AKR1B10	Aldo-keto reductase family 1 member B10 (O60218)	0.5 ±0.1	0.027
PSMD10	26S proteasome non-ATPase regulatory subunit 10 (O75832)	0.5 ±0.0	0.005
PDCD6	Programmed cell death protein 6 (O75340)	0.5 ±0.1	0.011
XRCC6	X-ray repair cross-complementing protein 6 (P12956)	0.6 ±0.1	0.048
DDT	D-dopachrome decarboxylase (P30046)	0.6 ±0.0	0.000
MANF	Mesencephalic astrocyte-derived neurotrophic factor (P55145)	0.6 ±0.1	0.015
ARPC1A	Actin-related protein 2/3 complex subunit 1A (Q92747)	0.6 ±0.1	0.044
MIF	Macrophage migration inhibitory factor (P14174)	0.7 ±0.0	0.015
KLC1	Isoform I of Kinesin light chain 1 (Q07866-9)	0.7 ±0.1	0.038
DAB2	Disabled homolog 2 (P98082)	0.7 ±0.1	0.050
AHCYL1	S-adenosylhomocysteine hydrolase-like protein 1 (O43865)	1.3 ±0.0	0.030
TUFM	Elongation factor Tu, mitochondrial (P49411)	1.3 ±0.1	0.038
ATP5PO	ATP synthase subunit O, mitochondrial (P48047)	1.3 ±0.1	0.048
EML4	Echinoderm microtubule-associated protein-like 4 (Q9HC35)	1.3 ±0.1	0.032
RUVBL2	RuvB-like 2 (Q9Y230)	1.3 ±0.1	0.031
RBMX	RNA-binding motif protein, X chromosome (P38159)	1.3 ±0.1	0.042
ACTA2	Actin, aortic smooth muscle (P62736)	1.4 ±0.0	0.006
CTSB	Cathepsin B (P07858)	1.5 ±0.0	0.009
PA2G4	Proliferation-associated protein 2G4 (Q9UQ80)	1.5 ±0.1	0.018
CARS	Isoform 3 of Cysteine--tRNA ligase, cytoplasmic (P49589-3)	1.5 ±0.1	0.047
PDHB	Pyruvate dehydrogenase E1 component subunit beta, mitochondrial (P11177)	1.6 ±0.1	0.022
SLC25A3	Isoform B of Phosphate carrier protein, mitochondrial (Q00325-2)	1.8 ±0.1	0.037
XPNPEP1	Xaa-Pro aminopeptidase 1 (Q9NQW7)	2.1 ±0.2	0.030
TLR7	Toll-like receptor 7 (Q9NYK1)	2.2 ±0.1	0.014
PFDN6	Prefoldin subunit 6 (O15212)	2.7 ±0.2	0.012
CPA4	Carboxypeptidase A4 (Q9UI42)	3.1 ±0.1	0.003
MGARP	Protein MGARP (Q8TDB4)	3.8 ±0.5	0.035

Table 3.2 Quantitative differential protein expressions with at least 2 unique peptides and >1.3 fold change after 2 days treatment of baicalein (11 upregulated and 20 downregulated proteins). GN: Gene Name; Δ: Fold change (treatment/ control) (Mean ± SEM); p: p-value (n=3, paired t-test); proteins highlighted in red are the proteins selected for further discussion.

GN	Protein (UniProt Accession)	Δ	*p*
RPL37A	60S ribosomal protein L37a (P61513)	0.3 ±0.1	0.013
COPS5	COP9 signalosome complex subunit 5 (Q92905)	0.4 ±0.1	0.023
AHSG	Alpha-2-HS-glycoprotein (P02765)	0.4 ±0.1	0.041
FDXR	NADPH:adrenodoxin oxidoreductase, mitochondrial (P22570)	0.5 ±0.1	0.015
ALB	Serum albumin (P02768)	0.5 ±0.1	0.033
SOD1	Superoxide dismutase [Cu-Zn] (P00441)	0.5 ±0.1	0.045
CFAP100	Cilia- and flagella-associated protein 100 (Q494V2)	0.6 ±0.0	0.006
BASP1	Brain acid soluble protein 1 (P80723)	0.6 ±0.0	0.004
CLIC4	Chloride intracellular channel protein 4 (Q9Y696)	0.6 ±0.0	0.009
EMC4	Isoform 3 of ER membrane protein complex subunit 4 (Q5J8M3-3)	0.6 ±0.1	0.024
NAGK	N-acetyl-D-glucosamine kinase (Q9UJ70)	0.7 ±0.1	0.040
AP2A1	AP-2 complex subunit alpha-1 (O95782)	0.7 ±0.1	0.026
SMPD4	Isoform 4 of Sphingomyelin phosphodiesterase 4 (Q9NXE4-4)	0.7 ±0.1	0.049
NMT1	Glycylpeptide N-tetradecanoyltransferase 1 (P30419)	0.7 ±0.1	0.026
PURA	Transcriptional activator protein Pur-alpha (Q00577)	0.7 ±0.0	0.003
SCRN1	Secernin-1 (Q12765)	0.7 ±0.1	0.040
TMSB4X	Thymosin beta-4 (P62328)	0.7 ±0.0	0.022
IRGQ	Immunity-related GTPase family Q protein (Q8WZA9)	0.7 ±0.1	0.047
PRKCSH	Glucosidase 2 subunit beta (P14314)	0.7 ±0.0	0.007
GAP43	Neuromodulin (P17677)	0.7 ±0.0	0.022
MTHFD1	C-1-tetrahydrofolate synthase, cytoplasmic (P11586)	1.3 ±0.1	0.048
SORBS2	Isoform 11 of Sorbin and SH3 domain-containing protein 2 (O94875-11)	1.3 ±0.0	0.008
DLG1	Disks large homolog 1 (Q12959)	1.3 ±0.1	0.042
AP1M1	Isoform 2 of AP-1 complex subunit mu-1 (Q9BXS5-2)	1.3 ±0.1	0.038
SERBP1	Plasminogen activator inhibitor 1 RNA-binding protein (Q8NC51)	1.3 ±0.0	0.014
AOC3	Membrane primary amine oxidase (Q16853)	1.3 ±0.0	0.004
ARSB	Arylsulfatase B (P15848)	1.3 ±0.0	0.009
P3H1	Prolyl 3-hydroxylase 1 (Q32P28)	1.4 ±0.1	0.024
RTRAF	RNA transcription, translation and transport factor protein (Q9Y224)	2.7 ±0.2	0.012
AGPAT1	1-acyl-sn-glycerol-3-phosphate acyltransferase alpha (Q99943)	3.1 ±0.1	0.003
EFTUD2	116 kDa U5 small nuclear ribonucleoprotein component (Q15029)	3.8 ±0.5	0.035

In order to understand the potential underlying pathways involved in baicalein treatment, the iTRAQ protein database with at least 2 unique peptides was analyzed by ingenuity pathway analysis (IPA). The analysis was conducted with filter set for human with a $p<0.05$. Upstream regulator and ingenuity canonical pathways were predicted by IPA. A total of 190 and 170 upstream regulators were found after 3 hours and 2 days treatment of baicalein, respectively ($p<0.05$ for both time points). Based on the suggested guidelines on IPA Upstream Regulator Analysis, *p*-value and activation z-score were considered in the analysis. The *p*-value (Fisher's Exact Test) measures the significance of overlapping between our dataset genes with the genes potentially regulated by transcriptional regulator. Calculated z-score reflects the overall predicted activation state of the regulator (<0: inhibited, >0: activated). The potential upstream regulators were considered significant according to the whitepaper of upstream regulator analysis in IPA with a *p*-value less than 0.01 and an activation z-score less than -2 or greater than 2. Our results identified eight upstream regulators for the 2-day treatment time point (**Table 3.3**) while no upstream regulator fulfilled our selection criteria for the 3-hour treatment time point.

Transforming growth factor beta 1 (TGFB1) was the top upstream regulator (activation z-score = -2.94, $p<0.001$). As shown in **Figure 3.15**, 29 downstream

molecules were associated with their upstream regulator (TGFB1). The predicted relationships between downstream molecules and upstream regulator are connected by lines of different colors. We observed that TGFB1 downregulated the expressions of most of the downstream molecules. A full list of protein expression changes and *p*-value are listed in **Supplementary Table 3**.

Table 3.3 The eight upstream regulators predicted from IPA after 2 days treatment of baicalein. (PAS represents the Predicted Activation State; z represents the activation z-score; *p* represents the *p*-value; # represents the number of downstream proteins).

Upstream Regulator	Molecule Type	PAS	z	*p*	#
Transforming growth factor beta-1(TGFB1)	Growth factor	Inhibited	-2.94	0.000	29
Interleukin-4 (IL4)	Cytokine	Inhibited	-2.53	0.008	13
Pituitary adenylate cyclase-activating polypeptide(ADCYAP1)	Other	Inhibited	-2.45	0.005	6
Hepatocyte nuclear factor 4-alpha(HNF4A)	Transcription regulator	Inhibited	-2.43	0.001	29
X-box-binding protein 1(XBP1)	Transcription regulator	Inhibited	-2.35	0.000	9
MAP kinase-interacting serine/threonine-protein kinase 1(MKNK1)	Kinase	Inhibited	-2.24	0.001	5
E3 ubiquitin-protein ligase synoviolin (SYVN1)	Transporter	Inhibited	-2.24	0.004	5
Insulin-like growth factor 1 receptor (IGF1R)	Transmembrane receptor	Inhibited	-2.22	0.002	7

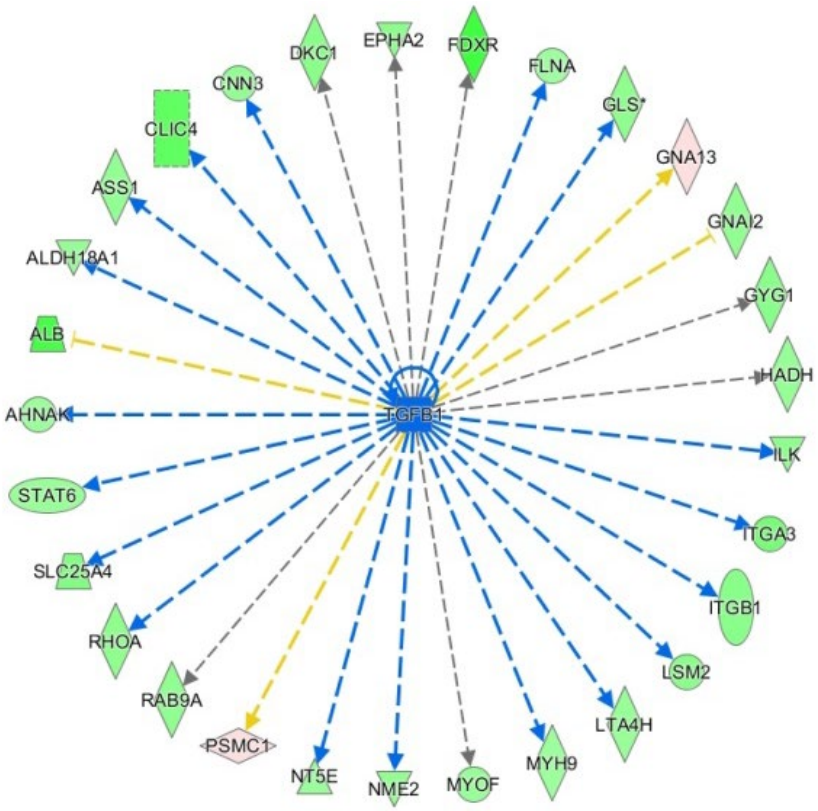

Figure 3.15 Relationship between upstream regulator (TGFB1) and downstream protein targets generated by IPA software after 2 days of baicalein treatment. Blue, yellow and grey lines represent inhibition, inconsistent relationships with different state of downstream molecules and no predicted effects. A full list of proteins with altered expression is presented in **Supplementary Table 3**.

Based on IPA analysis, a number of ingenuity canonical pathways were identified from our protein expression results. We obtained 26 and 66 predicted pathways after baicalein treatment for 3 hours and 2 days, respectively (p<0.05). As shown in **Table 3.4**, there were five common pathways after 3 hours and 2 days treatment of baicalein- namely oxidative phosphorylation, clathrin-mediated endocytosis signaling, mitochondrial dysfunction, regulation of actin-based motility by Rho, and γ-linolenate

biosynthesis II (Animals). Among them, only oxidative phosphorylation was anticipated to downregulate (p<0.01, z-score: -0.447) after 2 days baicalein treatment.

Table 3.4 The five common pathways predicted from the IPA canonical pathway analysis after 3 hours and 2 days baicalein treatment (p represented the p-value; z represented the activation z-score; # represented the number of targeted proteins).

Ingenuity Canonical Pathways	**3 hours**			**2 days**		
	p	**z**	**#**	***p***	**z**	**#**
Oxidative Phosphorylation	0.038	⁄	2	0.001	-0.447	5
Clathrin-mediated Endocytosis Signaling	0.003	⁄	4	0.005	⁄	6
Mitochondrial Dysfunction	0.013	⁄	3	0.002	⁄	6
Regulation of Actin-based Motility by Rho	0.025	⁄	2	0.025	⁄	3
γ-linolenate Biosynthesis II (Animals)	0.048	⁄	1	0.007	⁄	2

Taken together, a total of 47 and 119 proteins were significantly regulated after 3 hours and 2 days baicalein treatment, respectively. Among all differentially expressed proteins, we selected arylsulfatase B (ARSB), proliferation-associated protein 2G4 (PA2G4) and pyruvate dehydrogenase E1 component subunit beta (PDHB) for validation by qPCR because they were among the top regulated proteins that might be involved in cell migration, proliferation or ECM remodeling.

3.2.6 Validation of MS results by qPCR

Pyruvate dehydrogenase E1 beta subunit (PDHB) and proliferation-associated protein 2G4 (PA2G4) were among the top upregulated proteins with >1.5 fold change in the 3-hour time point treatment group. Based upon the upstream regulator predicted by IPA software, PDHB and PA2G4 were the related downstream proteins. Both PDHB and PA2G4 have previously been implicated in the pathogenesis of glaucoma (Bailey et al., 2014, Sacca et al., 2016). For 3 hours of baicalein treatment, baicalein upregulated the expression of PDHB protein by 61 ±9%. The qPCR results also found a 7 ±9% increase in mRNA; however, the effect was not statistically significant (n=3, p=0.229, paired t-test). Moreover, baicalein caused a significant upregulation of PA2G4 protein by 51 ±7% after 3 hours treatment. As opposed to the protein changes observed, mRNA was not significantly affected (n=3, p>0.05, paired t-test).

In addition, after baicalein treatment for 2 days, arylsulfatase B (ARSB) was found to be significantly upregulated. ARSB had previously been reported to regulate RhoA activities, cell migration and ECM deposit in colonic epithelial cells (Bhattacharyya and Tobacman, 2009), potentially accounting for its effects on hTM cells. For 2 days baicalein treatment, the protein expression of ARSB was shown to increase by 32

±3%. Consistent with the protein profile, mRNA expression increased by 18 ±6% (n=3, $p<0.05$, paired t-test).

3.3 *In vivo* study

From the above mentioned *in vitro* and *ex vivo* studies, baicalein was shown to regulate hTM cell volume, contractility, and migratory properties, potentially contributing, at least in part, to the observed increase in AH drainage in mouse eyes. Therefore, the ocular hypotensive effects of baicalein via different routes of drug administration including intraperitoneal injection, topical administration and intravitreal injection were studied. Comparison of three different baicalein administration approaches for lowering IOP was made.

3.3.1 Effect of intraperitoneal injection of baicalein on IOP in SD rats

As a starting point, we studied the effect of intraperitoneal administration of baicalein on IOP *in vivo*. Prior to the experiments, IOP was monitored daily for at least 3 days until a stable reading was achieved. Afterwards, baicalein was injected intraperitoneally once daily in the treatment group while vehicle was used in the

control group. In the first 2 weeks, 4 mg/kg of baicalein was used and the concentration of baicalein was increased to 40 mg/kg in the following two weeks.

Before drug treatment, the baseline IOP in the treatment and control groups were 14.7 ±0.5 mmHg and 14.5 ±0.4 mmHg, respectively. No significant IOP differences was found between treatment and control groups ($p>0.05$, unpaired t-test). The relative change of IOP between treatment and control groups (treatment – control) over time is illustrated in **Figure 3.16.** Intraperitoneal administration of baicalein (4 mg/kg) caused a significant IOP reduction of 1.2 ±0.4 mmHg after two weeks of treatment (9%, $p<0.05$). When baicalein concentration increased to 40 mg/kg following a period of two weeks, baicalein had an IOP-lowering effect of 2.7 ±0.5 mmHg on day 28 when compared with baseline IOP taken on day 0 (20%, $p<0.001$). These results suggest that baicalein, when applied intraperitoneally, lowered IOP in a concentration-dependent manner.

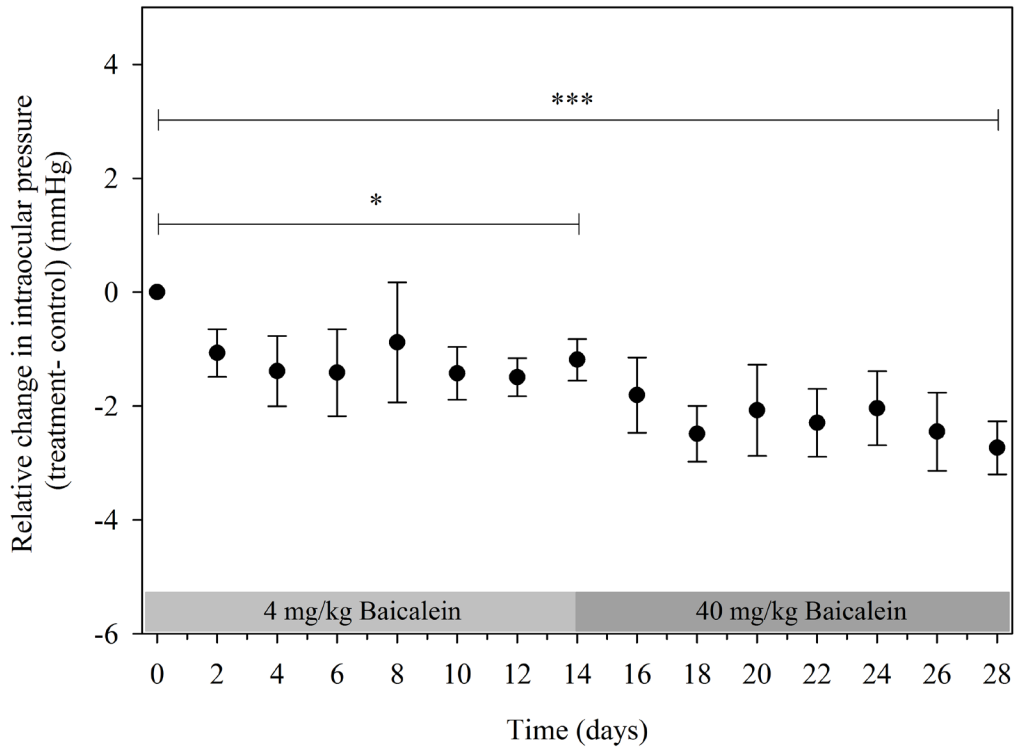

Figure 3.16 Effects of daily intraperitoneal injection of baicalein (4 mg/kg and 40 mg/kg) on IOP in SD rats. Relative IOP changes between treatment and control groups throughout the experimental period are presented (with 4 mg/kg baicalein during the initial two weeks followed by 40 mg/kg in the subsequent two weeks). Results are expressed as Mean ±SEM (n=8). *p<0.05, ***p<0.001 (one-way repeated measures ANOVA, followed by Bonferroni t-test).

3.3.2 Effect of topical administration of baicalein on IOP in SD rats and C57 mice

Given that the ocular hypotensive effect observed with intraperitoneal injection of baicalein was in the range of 2-3 mmHg after 4 weeks, we investigated whether direct administration of baicalein via topical application triggered any detectable changes of

IOP. The acute IOP changes during daytime and nighttime in both SD rats and C57 mice were monitored.

3.3.2.1 Effect of topical administration of baicalein on IOP in SD rats

Baseline IOP was monitored for at least 3 days before drug treatment and was found to be comparable between baicalein-treated and vehicle-treated eyes of the same animal ($p>0.05$, paired t-test). For the daytime group, baseline IOPs were taken during the daytime and were found to be 12.2 ±0.2 and 11.8 ±0.2 mmHg for the treatment and control eyes, respectively. For the nighttime group, baseline IOPs were taken at night and were found to be 21.7 ±0.3 and 21.5 ±0.3 mmHg for the treatment and control eyes, respectively. Topical administration of baicalein and vehicle was applied to the treatment and control eyes of the SD rats and the IOP was monitored at 1.5, 3, 6, 24, 48 and 72 hours after treatment.

For the daytime group, the IOP changes in baicalein-treated and vehicle-treated eyes over a three-day period are summarized in **Figure 3.17 A**. Our results showed a significant IOP reduction after topical baicalein by 0.7 ±0.1 mmHg (6%, $p<0.05$), 1.1 ±0.2 mmHg (10%, $p<0.001$) and 0.9±0.2 mmHg (8%, $p<0.001$) after 1.5 hours, 3

hours and 6 hours, respectively. For the nighttime group (**Figure 3.17 B**), baicalein lowered the IOP by 2.3 ±0.4 mmHg (11%, $p<0.001$), 1.9 ±0.3 mmHg (9%, $p<0.001$), and 1.1 ±0.2 mmHg (5%, $p<0.01$) at 1.5, 3 and 6 hours post treatment. There was no significant IOP difference between treatment and control eyes from 24 to 72 hours after treatment in both the daytime and nighttime groups of SD rats. Overall, our results showed that baicalein had a larger ocular hypotensive effect during the nighttime than daytime.

A. Daytime

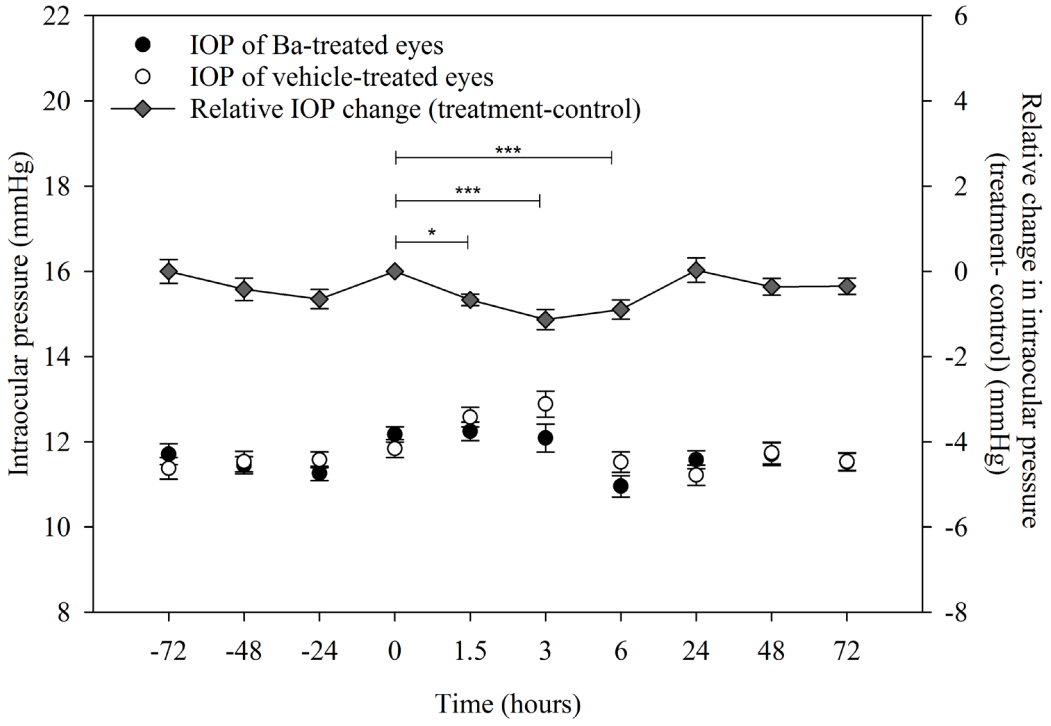

B. Nighttime

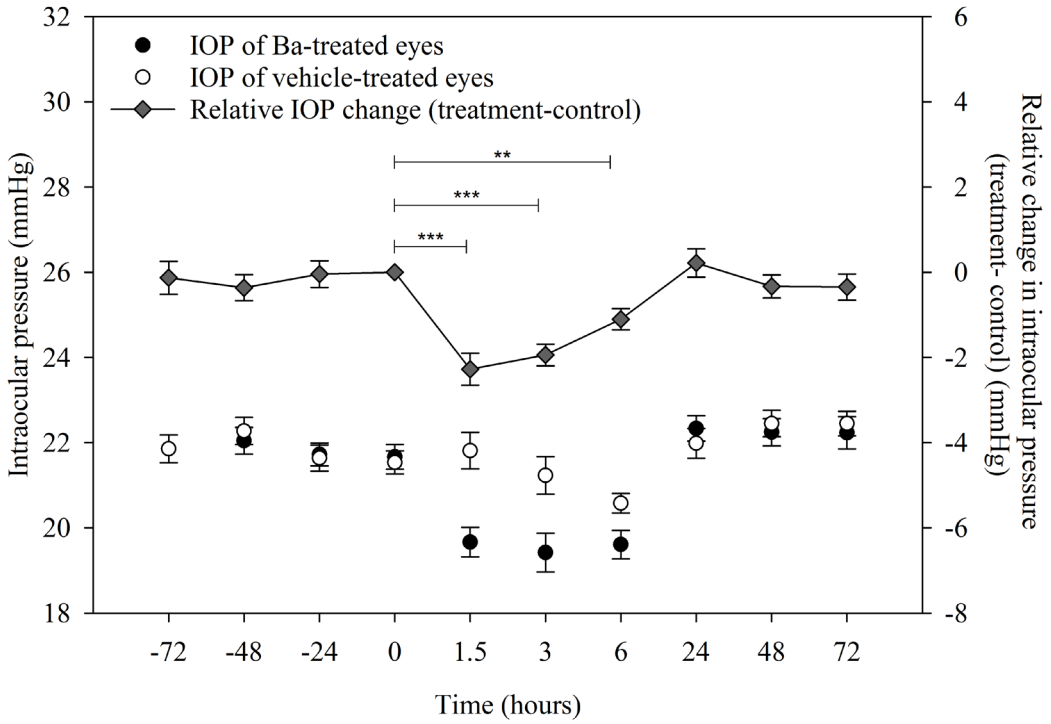

Figure 3.17 Effects of topical baicalein (10 mM) on IOP in SD rats during **A**) daytime and **B**) nighttime, respectively. Baicalein and vehicle (2 x 20 µl separated by 10 minutes) were applied to the treatment and control eyes, respectively, of the same animal. Data are expressed as Mean ±SEM (n=23, **p*<0.05, ***p*<0.01, ****p*<0.001, one-way repeated measures ANOVA).

3.3.2.2 Effect of topical administration of baicalein on IOP in C57 mice

To test whether baicalein acted across species, the effect of topical application of baicalein on IOP in C57 mice was studied. Similar to the experiments with SD rats, IOP was monitored in two separate groups, i.e. daytime and nighttime groups. For the daytime group, the baseline IOP of the treatment and control eyes were 18.2 ±0.2 mmHg and 18.1 ±0.3 mmHg, respectively. For the nighttime group, the baseline IOP

of the treatment and control eyes were 22.1 ±0.2 mmHg and 22.0 ±0.2 mmHg, respectively. There was no significant IOP difference between treatment and control eyes before drug treatment in both groups (p>0.05). Similar to the results of SD rats, significant IOP reduction was observed after baicalein treatment for at least six hours under daytime (**Figure 3.18 A**) and nighttime (**Figure 3.18 B**) in C57 mice. The maximum IOP-lowering effect was found to be 1.6 ±0.3 mmHg (9%, p<0.001), at 3 hours after baicalein treatment in the daytime group. For the nighttime group, the maximum IOP reduction was 2.3 ±0.4 mmHg (11%, p<0.001), at 1.5-hour post treatment. Again, no ocular hypotensive effect was shown from 24 hours to 72 hours after baicalein treatment (p>0.05). Our results suggest that baicalein acted across species and lowered IOP in both species.

A. Daytime

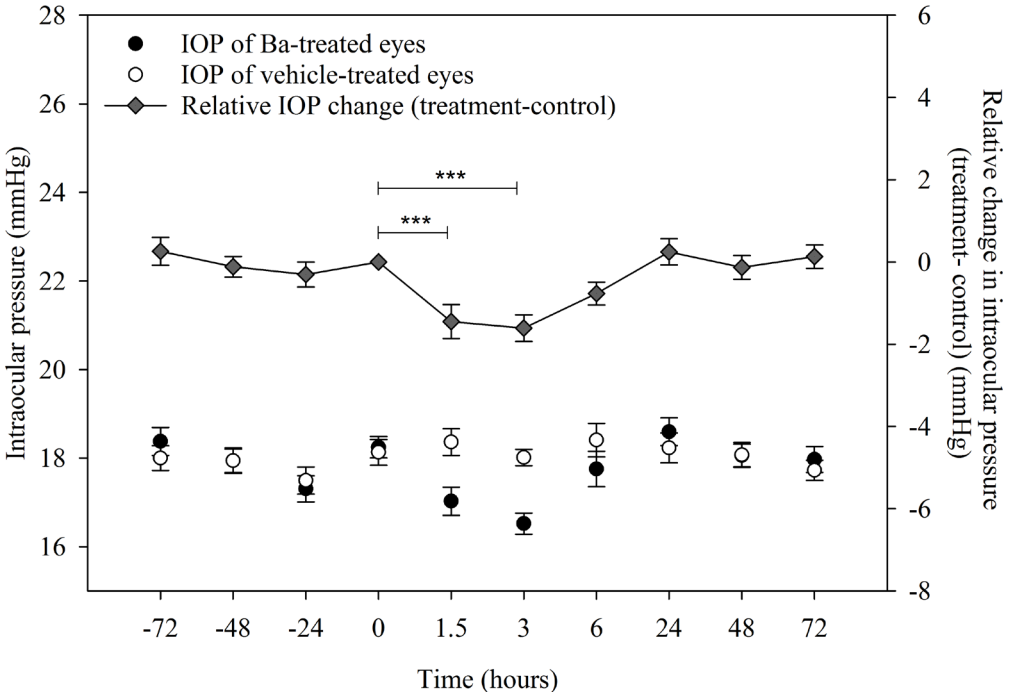

B. Nighttime

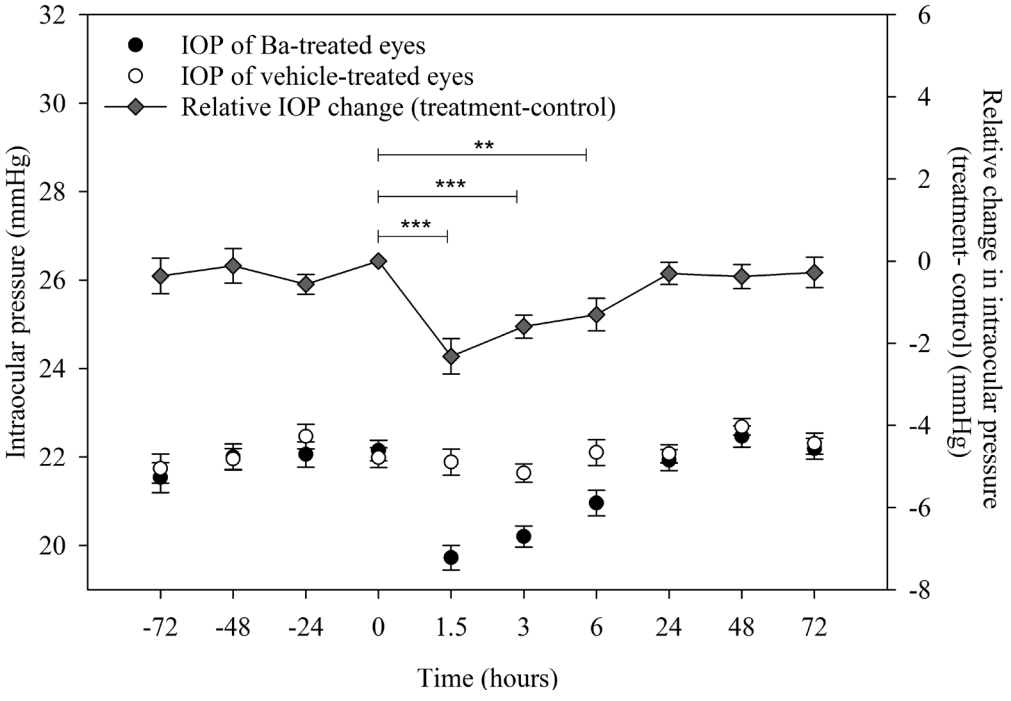

Figure 3.18 Effects of topical baicalein (10 mM) on IOP in C57 mice during **A**) daytime and **B**) nighttime, respectively. Baicalein and vehicle (2 x 20 µl separated by 10 minutes) were applied to the treatment and control eyes, respectively, of the same animal. Data are expressed as Mean ±SEM (n=23, $^{**}p<0.01$, $^{***}p<0.001$, one-way repeated measures ANOVA).

3.3.2.3 Bioavailability of baicalein in the aqueous humor after topical drug administration in C57 mice

It appeared that baicalein, when given topically, had a significant yet small IOP-lowering effect of ~10% in both SD rats and C57 mice. To address whether permeability of the cornea to baicalein (drug penetration) limited its IOP lowering efficacy, we determined the concentration of baicalein in the AH after topical application of baicalein.

As before, baicalein and vehicle were applied topically in C57 mice. The AH was collected from the mouse eyes 1.5 hours after drug treatment. Because of the limited volume of AH in the anterior chamber, AH from 3 mice were pooled together as one sample for analysis. The concentration of baicalein in the AH was measured by MRM-MS. **Figure 3.19** shows the results as measured by the MRM-MS system. After drug treatment, baicalein concentrations were 0.030 ±0.009 μM and 0.007 ±0.003 μM in the baicalein-treated and vehicle-treated eyes, respectively ($p<0.05$, paired t-test), accounting for a 4.3-fold increase in concentration in the baicalein-treated eye. The relationship between mean IOP reduction and increase in baicalein concentration after topical administration was plotted and analyzed by linear regression, as shown in **Figure 3.20**. We found that the observed IOP reduction (mean

IOP reduction of 3 mice from the same sample) was directly proportional to the increased baicalein concentration in the AH with a R^2 of 0.941. Our results suggested that the mean ocular hypotensive effect was directly proportional to the increase in baicalein concentration in the AH, although the absolute concentration was found to be relatively low (~0.0003%) compared with the stock baicalein concentration.

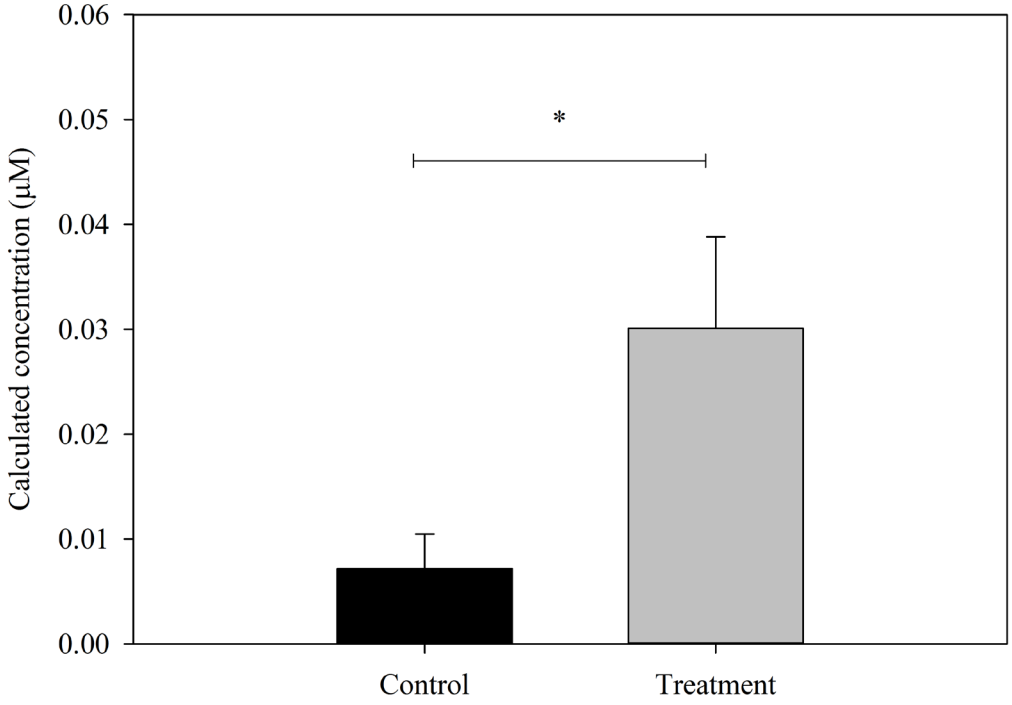

Figure 3.19 Concentration of baicalein in the aqueous humor 1.5 hours after topical administration (10 mM) in C57 mice. Baicalein and vehicle (2 x 20 μl) were applied to the treatment and control eyes, respectively. Data are expressed as Mean ±SEM (n=4, each sample was pooled from aqueous humor of 3 mice) (*p<0.05, paired t-test).

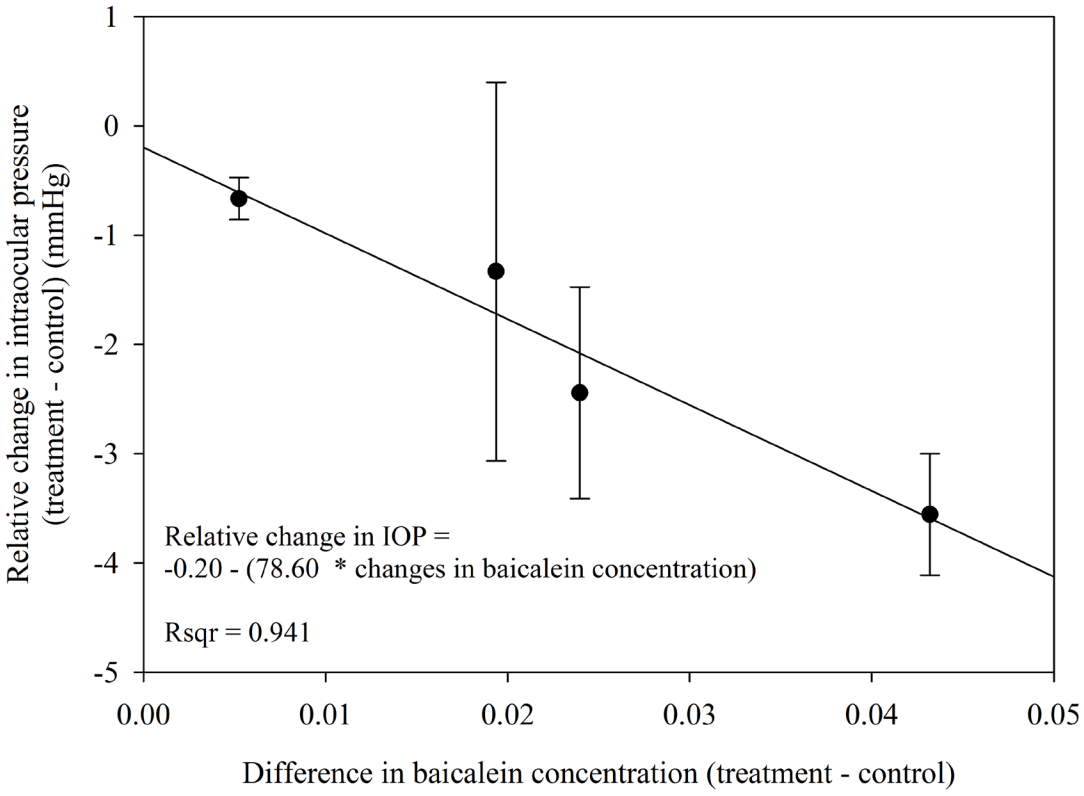

Figure 3.20 Linear regression plot showing the relationship between mean IOP reduction and increase of baicalein concentration in the aqueous humor.

3.3.3 Effect of intravitreal injection of baicalein on IOP and retinal thickness in SD rats

Based on the above results, it was shown that baicalein significantly lowers IOP when administered topically. Despite that, the maximum IOP reduction was limited to 2 to 3 mmHg within 6 hours post treatment. This might reflect a limited penetration of baicalein across intact cornea. As a result, we studied whether intravitreal injection of baicalein provided more efficacious ocular hypotensive effects. SD rats were used because it has a relatively larger eyeball for performing intravitreal injection.

This experiment consisted of two parts. In the first part, baicalein (at various concentrations) or vehicle was injected intravitreally and IOP was monitored for a period of 9 days post treatment. The changes in IOP of both experimental (either baicalein or vehicle injected) and control (untreated) eyes are summarized in **Figure 3.21**. No significant IOP difference between the experimental and untreated control eyes was detected in vehicle-treated, and (7.5 and 75 μM) baicalein-treated groups after intravitreal injection. However, the 750 μM baicalein-treated eye had a significant IOP reduction by 2.8 ±1.2 mmHg (p<0.01) 3 days after intravitreal injection. No significant IOP difference was observed at other time points.

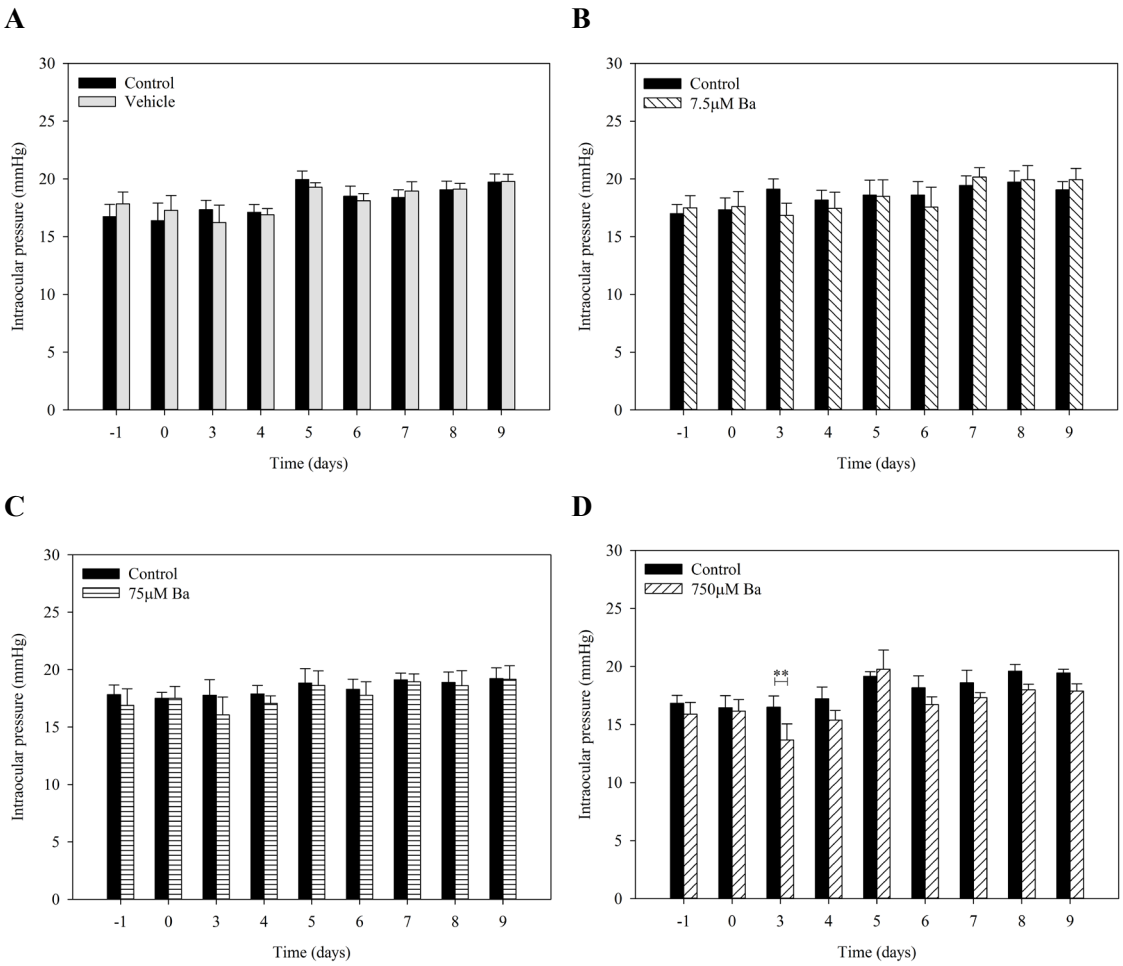

Figure 3.21 Intravitreal injection of baicalein/vehicle on IOP in both experimental and control eyes. **A**) vehicle-treated; **B**) 7.5 μM baicalein-treated; **C**) 75 μM baicalein-treated; and **D**) 750 μM baicalein-treated group in SD rats (n=6 in each group). Results are expressed as Mean ±SEM (**p<0.01; two-way repeated measures ANOVA followed by Bonferroni t-test).

To examine whether intravitreal injection of baicalein affect retinal physiology and morphology, the effect of baicalein on total retinal thickness was investigated. The central retinal thickness around the optic disc was measured by SD-OCT. No significant difference in total retinal thickness was observed between experimental and control eyes in all groups before drug treatment (p>0.05, two-way ANOVA).

Figure 3.22 summarizes changes in total retinal thickness after nine days of

intravitreal injection of baicalein or vehicle. Our results showed that intravitreal application of baicalein had no effects on total retinal thickness between all baicalein-treated and their contralateral control eyes (p>0.05, two-way ANOVA) suggesting that baicalein had minimal effect on retinal thickness after intravitreal drug administration.

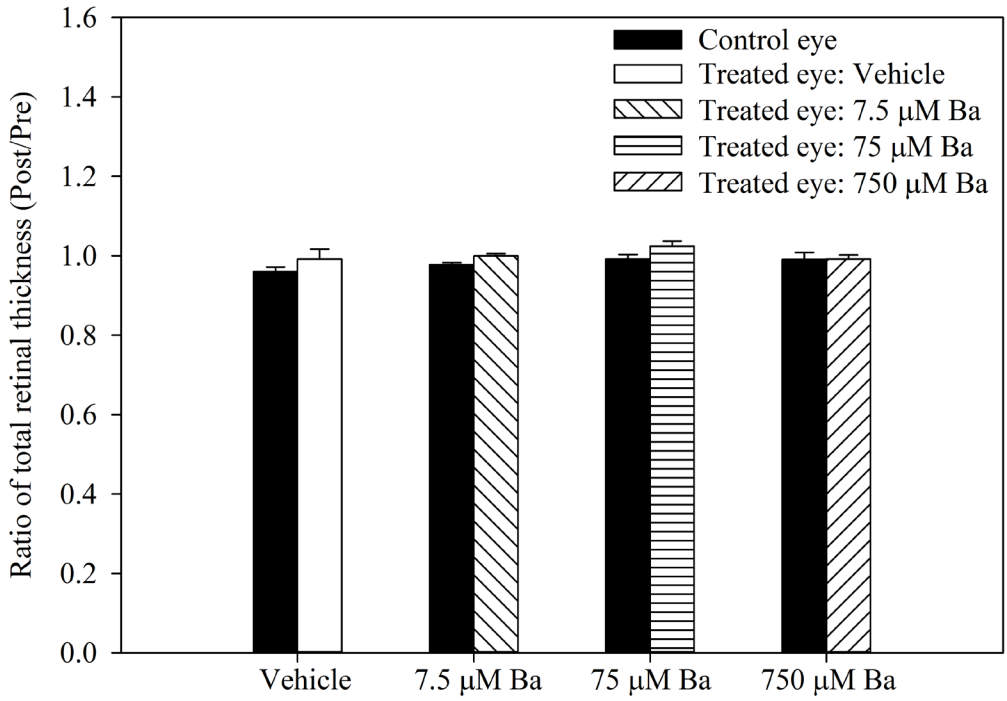

Figure 3.22 Changes in total retinal thickness (post-/pre-treatment) of SD rats after intravitreal injection in both experimental (either vehicle-treated or baicalein-treated) and untreated control eyes. Vehicle, 7.5 μM baicalein, 75 μM baicalein, and 750 μM baicalein (n=6 in each case). Results are expressed as Mean ±SEM (p>0.05, two-way ANOVA).

In the second part, we further looked into the ocular hypotensive effect exerted by baicalein. As before, 750 μM of baicalein or vehicle was injected intravitreally to the

experimental eye while the fellow untreated eye was used as the control. IOP was monitored every 12 hours for a period of 3-4 days. **Figure 3.23** presents ocular hypotensive effects of baicalein compared to the untreated fellow eye. There was no significant difference in baseline IOP between experimental and control eyes under daytime and nighttime in vehicle-treated and baicalein-treated groups ($p>0.05$). For the vehicle-treated group, there was no significant difference between experimental and control eyes at all time points ($p>0.05$). For the baicalein-treated group, baicalein produced a sustained IOP-lowering effect during both daytime and nighttime. The maximum IOP reductions were found to be 2.4 ±0.5 mmHg (22%, $p<0.01$) and 9.3 ±1.6 mmHg (51%, $p<0.01$), under daytime and nighttime, respectively. Our results suggested that baicalein had a significant IOP-lowering effect when administered intravitreally, as opposed to topical application.

A. Vehicle-treated group

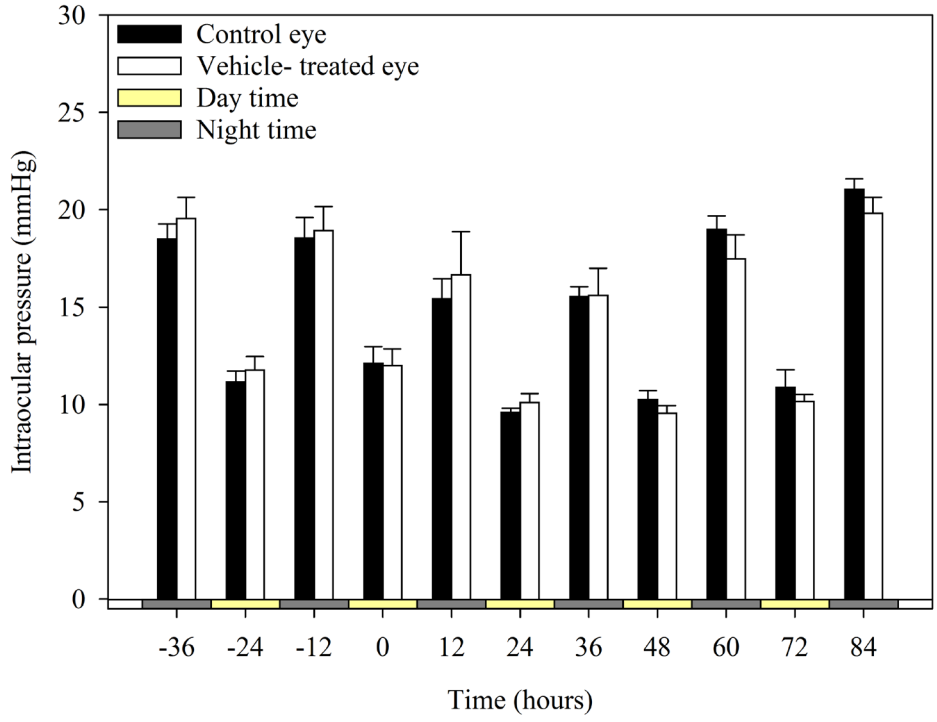

B. 750 µM baicalein-treated group

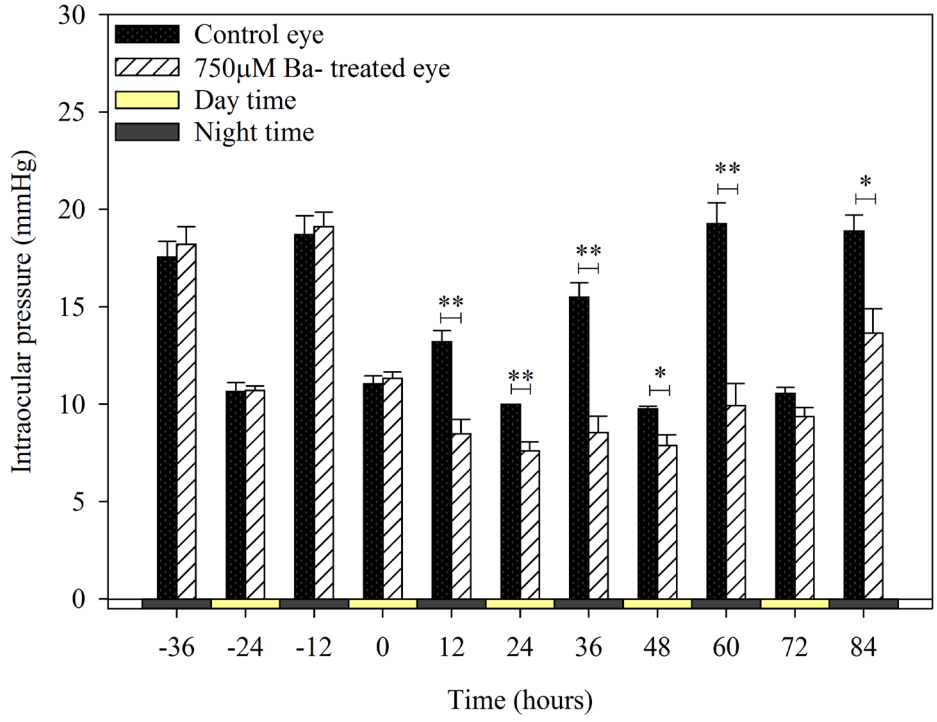

Figure 3.23 Changes in IOP of both experimental and control eyes following intravitreal injection in SD rats. **A**) vehicle-treated; and **B**) 750 µM baicalein-treated groups (n=6 in each group). Results are expressed as Mean ±SEM (*p<0.05, **p<0.01, paired t-test)

Chapter 4 Discussion

4.1 Rationale of the study

Glaucoma is a common, age-related optic neuropathy characterized by the progressive loss of sight, and ultimately, total blindness. It is often called "the silent thief of sight" as glaucoma can remain asymptomatic until it has reached an advanced stage. Despite tremendous efforts toward studying the mechanisms underlying glaucoma, its complete pathogenesis remains unclear. Elevated intraocular pressure (IOP) is the major and perhaps the only modifiable risk factor for progression among others. Thus, IOP-lowering therapy continues to be the first-line treatment to retard its development and progression (Collaborative Normal-Tension Glaucoma Study Group, 1998a, The AGIS Investigators, 2000). To date, glaucoma remains incurable; thus, requires lifelong care. As such, the importance of good patient compliance and adherence to therapy should not be overlooked as they affect treatment outcomes (Reardon et al., 2011). Many anti-glaucoma agents have significant contraindications, limitations, and long-term side effects (Lee and Higginbotham, 2005, Detry-Morel, 2006). For these reasons, our initial objective warrants the need to explore a novel agent with long-lasting actions and fewer unwanted side effects. This can bring profound clinical implications for future glaucoma management.

IOP levels are governed by the dynamics balancing AH inflow- secreted by the ciliary epithelium, and AH outflow- mainly through the conventional TM route. Elevated IOP in glaucoma patients is believed to stem primarily from an impeded fluid drainage through the TM. Currently, most existing medications used in glaucoma therapy act by either reducing AH secretion or facilitating AH drainage via uveoscleral outflow. Research on agents facilitating fluid drainage through the conventional TM outflow pathway represents an appealing approach as TM is the diseased tissue responsible for increased IOP (Vranka et al., 2015, Tektas and Lütjen-Drecoll, 2009). Most recently, ROCK inhibitors targeting TM outflow have been successfully developed for clinical use (Pan et al., 2013). Two ROCK inhibitors have been approved as IOP-lowering agents: Netarsudil (AR-13324) in the United States and Ripasudil (K-115) in Japan (Hoy, 2018, Garnock-Jones, 2014). Despite this success, no dual-action medication has been developed targeting both secretion and drainage of AH simultaneously. Such medication targeting both inflow and outflow may greatly improve treatment efficacy for the prevention of glaucoma.

Baicalein is a natural flavonoid originally derived from the root of *Scutellaria baicalensis*, and is often found in fruits and vegetables (Ren et al., 2001). Baicalein has been frequently used in traditional Chinese medicine because it is safe and well

tolerated by patients (Li et al., 2014, Pang et al., 2016). The therapeutic potential of baicalein has been associated with its anti-inflammatory, anti-oxidative, and anti-apoptotic properties (Gasiorowski et al., 2011, Huang et al., 2005, Schweiger et al., 2007). Although not yet fully explored, several studies have proposed that baicalein may have therapeutic significance in treating ocular diseases (Majumdar and Srirangam, 2010, Xiao et al., 2014). A number of reports have demonstrated that baicalein protects neurons from ischemic and oxidative damage in different models of neuropathy (Maher and Hanneken, 2005, Chao et al., 2013, Hanneken et al., 2006), indicating its potential significance for the prevention of glaucomatous optic neuropathy.

Our previous study evaluating baicalein's effects on AH inflow have demonstrated that baicalein inhibits Cl^- and fluid secretion across porcine ciliary epithelium (Xiao, 2015). We hypothesized that these effects were likely mediated by the inhibition of $I_{Cl,swell}$ in NPE cells, potentially leading to a suppression of AH production. To date, the precise physiological mechanisms on how conventional outflow is regulated are not fully clear. Previous studies have suggested that regulations of TM cell volume, contractility, ECM synthesis and remodeling all contribute to the maintenance of outflow resistance (Stamer, 2012). Baicalein has been shown to exert its effects on

cell contractility (Chen et al., 1999, Huang et al., 2004), ion and fluid secretion (Ko et al., 2002, Xue et al., 2018) and ECM remodeling (Sun et al., 2010, Gao et al., 2013) in other cell types. Whether or not baicalein modulates conventional TM outflow and IOP, as well as its mechanistic actions are yet to be established. In addition, loss of TM cells has been reported in glaucoma patients (Alvarado et al., 1984). This may cause a reduced degradation of ECM materials, resulting in an increase in outflow resistance (Gabelt and Kaufman, 2005). Several studies have reported that baicalein demonstrates the anti-inflammatory, anti-oxidative, and anti-apoptotic properties, suggesting that it may be a good candidate for strengthening and restoring the functions of TM cells, eventually improving the outflow resistance of glaucomatous eyes. Given that baicalein may act through multiple pathways, a comprehensive exploration of the protein profile and signaling cascades responsible for baicalein-induced responses was warranted.

4.2 Facilitation of conventional outflow facility by baicalein

The conventional outflow facility was determined by constant-pressure perfusion approach in *ex vivo* mouse eyes. C57BL/6J mice was chosen as experimental animals for the following reasons: 1) mouse eyes were more readily available for experiments than human eyes; 2) lack of washout effect was reported in mice; 3) mice eye had

similar anatomical outflow structures as humans; and 4) mouse eyes responded to anti-glaucoma agents similar to humans (Lei et al., 2011, Millar et al., 2011, Boussommier Calleja et al., 2012). As shown in **Figure 3.1** and **Figure 3.2**, baicalein elicited an acute concentration-dependent increase in conventional outflow facility in freshly enucleated mouse eyes. At 0.1 μM, baicalein had no significant effect on outflow facility in paired eyes. When treated with 1 and 10 μM, baicalein, we found an increase in outflow facility by 37% and 89%, respectively. The magnitude of AH outflow increase was comparable to the previous studies with ROCK inhibitors. For example, studies have shown that Y27632 increases outflow facility by 40-80% in porcine (Rao et al., 2001), bovine (Lu et al., 2008), and human eyes (Yang et al., 2013). Consistent with these findings, we found that Y39983 (50 μM) increased the outflow facility by 74% compared with the vehicle-treated control. These results support the notion that baicalein may be as effective as ROCK inhibitors in enhancing AH drainage. It was reported that Y39983, an analog of Y27632, was more potent as it had an IC_{50} ~30 times lower than Y27632 in inhibiting ROCK activity; thereby, triggering a larger reduction of IOP (Tokushige et al., 2007). Our results are also in agreement with a recent study in which Netarsudil increased outflow facility by 56% in C57 mice (Li et al., 2016). In that study, a five-day topical administration of Netarsudil lowered the IOP by 5.2 mmHg (Li et al., 2016). Similarly, perfusion with

Netarsudil-M1, an active metabolite of Netarsudil, increased the outflow facility by 51% when compared to paired controls in human eyes (Ren et al., 2016).

In addition to ROCK inhibitors, perfusion of NO donors such as S-nitroso-N-acetylpenicillamine (100 μM) and Diethylenetriamine/nitric oxide adduct (100 μM) increased the outflow facility by 62% and 97%, respectively (Chang et al., 2015a, Ge et al., 2016). In our study, it was found that baicalein, when perfused at 10 μM, increased conventional outflow to a similar extent. Generally, a lower concentration of drug is preferred because of reduced risks of cytotoxicity and ocular side effects. Comparatively, even at 1 μM, we observed a nearly 40% increase in outflow facility. Our results are consistent with the hypothesis that baicalein enhances conventional TM outflow, in addition to its inhibitory effect on AH secretion, as observed previously. This suggests that baicalein may potentially be a good candidate for lowering IOP because of its dual actions on both AH secretion and drainage.

4.3 Effects of baicalein on viability and proliferation in hTM cells

The effects of baicalein on cell viability and proliferation in hTM cells were investigated before studying its potential mechanisms of actions in enhancing TM

outflow. Our results showed that baicalein (1 to 100 μM) and vehicle had no significant effects on cell viability after 2- and 4-day treatment. Similarly, it was found that baicalein did not exert any effects on TM cell proliferation. Our results are in line with published findings reported in other cell types. For instance, baicalein (1 to 5 μM) did not affect cell viability nor proliferation in mouse macrophages (Cheng et al., 2007). At higher concentrations (e.g. 10 to 100 μM), it was reported that baicalein did not exhibit adverse effects on cell viability in rat heart myoblasts (Oh et al., 2012) and human LNCaP cells (Lee et al., 2008). Our results also accord with these observations, which showed that baicalein has minimal cytotoxicity and is safe to use.

4.4 Potential mechanisms involved in the regulation of aqueous humor outflow

As discussed before, the precise mechanisms by which conventional outflow is regulated are still unclear. The regulation is complicated, involving at least four different mechanisms including the modulations of 1) TM cell volume; 2) TM cell contractility; 3) ECM remodeling; and 4) funneling effect between JCT and the inner wall of SC (Stamer, 2012). Regulations of TM cell volume and contractility may trigger acute changes in outflow resistance, as the modulations of cell volume and

contractility are relatively fast. Conversely, alterations of ECM composition usually take a few hours to several days for structural remodeling in the outflow pathway to take place (Crosson et al., 2005). Current anti-glaucoma medications targeted at TM outflow act by modulating, at least in part, TM cell relaxation (Ramachandran et al., 2011, Dismuke et al., 2014), volume regulation (Dismuke et al., 2008) and ECM remodeling by inhibiting the matrix cross-linking (Yang et al., 2016). It is likely that these mechanisms are inter-related, mutually influencing the resultant outflow resistance.

4.4.1 Effect of baicalein on cell volume regulation in hTM cells

According to our data, it was found that baicalein triggers a significant increase in outflow facility over a period of 2-3 hours. These findings suggest that baicalein may exert acute effect(s) on TM cells. Outflow resistance in TM cells can be modulated by cell volume regulation (Gual et al., 1997, Al-Aswad et al., 1999). A number of K^+, Cl^- channels and ion transporters have been identified in the TM cells responsible for volume regulation (Dismuke and Ellis, 2009, Comes et al., 2006, O'Donnell et al., 1995, Mitchell et al., 2002). It is likely that fluctuation of AH's osmolarity may trigger swelling- and stretch-activated channels in TM cells, leading to an alteration of outflow facility (Mitchell et al., 2002, Gasull et al., 2003, Carreon et al., 2017). In the

isotonic bathing solution, we did not observe any changes of cell volume by baicalein at all concentrations (1, 10 and 100 μM) tested over a period of 30 minutes. Subsequently, when subjected to hypotonic stimulation, baicalein triggered a concentration-dependent inhibition of RVD. After 30 minutes of hypotonic challenge, a significant inhibition of RVD was observed with 10 and 100 μM baicalein when compared to vehicle-treated cells respectively. At 1 μM, baicalein had a subtle effect on RVD. Generally, the effects of volume regulation on outflow facility are fast and transient, then return to the baseline level over a few hours (Soto et al., 2004, Comes et al., 2006, Dismuke et al., 2008). It has previously been shown that bumetanide (a blocker of Na^+-K^+-$2Cl^-$), NS1619 (a BK_{Ca} activator), and Cl^- replacement cause a shrinkage of TM cells and increase outflow facility under isosmotic conditions (Al-Aswad et al., 1999, Dismuke and Ellis, 2009). In addition, it has been shown that NO donor diethylenetriamine reduces TM cell volume and increases outflow facility in a concentration-dependent manner (Dismuke et al., 2008). In our study, baicalein did not elicit any detectable change in cell volume under isosmotic condition, indicating that baicalein did not influence baseline steady-state cell volume homeostasis, unlike other channel inhibitors.

On the other hand, baicalein inhibited the RVD upon hypotonicity, potentially leading to a reduction of outflow resistance. Our data are consistent with that of Banerjee et al. in which inhibition of anoctamin-6 (a swelling-activated Cl^- channel) has been found to modulate $I_{Cl,swell}$ and RVD in TM cells, potentially reducing outflow resistance (Banerjee et al., 2017). It has been shown that ATP release increases in human TM cells following hypotonic cell swelling (Fleischhauer et al., 2003). Cell swelling resulting from RVD inhibition also stimulates ATP release and activates A1 adenosine receptors (A1ARs) (Li et al., 2011a), subsequently facilitating AH drainage and IOP reduction (Crosson et al., 2005, Crosson, 2001, Crosson, 1995). The ATP release stimulated by cell swelling is subjected to purinergic regulation via pannexin-1, connexin hemichannels, and P2X7 receptors (Li et al., 2012). It has been revealed that ATP alters ecto-enzymatic delivery of adenosine to A1ARs, which in turn modulates cytoskeletal remodeling through MMP-2 and MMP-9 secretion (Li et al., 2011a). In contrast, dexamethasone is known to increase outflow resistance (Leung et al., 2003, Overby et al., 2014b). Dexamethasone has been found to accelerate RVD following hypotonic treatment in TM cells, subsequently inhibiting ATP release and A1AR-triggered MMP secretion (Li et al., 2011a). Our results support the notion that baicalein retards RVD in hTM cells, potentially regulating subsequent cytoskeletal remodeling through MMP secretion, leading to an increased outflow facility.

4.4.2 Effect of baicalein on hTM cell relaxation

In addition to cell volume regulation, we hypothesized that baicalein regulates the contractility of TM cells. TM cells display smooth muscle-like properties (Wiederholt et al., 2000). The increase of outflow facility following treatment with ROCK inhibitors can be explained, at least in part, by the relaxation of TM cells (Honjo et al., 2001, Rao et al., 2001, Rosenthal et al., 2005). Using collagen gel contraction assay, we demonstrated that baicalein mediated a concentration-dependent relaxation of TM cells over a period of 6 hours. At 100 μM, baicalein triggered a significant TM cell relaxation by 10% after both 3-hour and 6-hour treatment. No statistically significant effects were observed at 1 and 10 μM. On the other hand, carbachol (5 μM) stimulated TM cell contraction by ~10-15% after a 3-hour and 6-hour treatment, which is consistent with previous work (Rosenthal et al., 2005).

It is likely that the relaxation effect of baicalein may be related to its inhibitory activity on ROCK and protein kinase C (PKC) (Somlyo and Somlyo, 2000), as demonstrated in cardiac myoblast cells (Oh et al., 2012) and vascular smooth muscle (Chen et al., 1999). In cardiac myoblast cells, baicalein triggers a concentration-dependent inhibition of PKC activities and ROCK activities with reduced phosphorylation of MLC (Oh et al., 2012). Similarly, baicalein (30 to 300

μM) has been shown to induce a relaxation of arterial smooth muscle by inhibiting PKC activity (Chen et al., 1999). It has been suggested that PKC inhibits actin binding action between caldesmon and calponin (Menice et al., 1997). This may facilitate the binding between actin and myosin for MLC phosphorylation and cell contraction through the mitogen-activated protein kinase pathway (Thieme et al., 1999, Harnett and Biancani, 2003).

It has been demonstrated that contractility of TM cells can be altered by agents including endothelin-1 (Rosenthal et al., 2005, Dismuke et al., 2014), nitric oxide (Dismuke et al., 2014), ROCK inhibitors (Rosenthal et al., 2005, Koga et al., 2006), and TGFB1 (Nakamura et al., 2002). In addition, TM cells exhibit a Ca^{2+}-independent contractile mechanism which is linked to RhoA and PKC (Thieme et al., 2000). Nitric oxide donor diethylenetriamine / nitric oxide adduct is shown to trigger a concentration-dependent inhibition of MLC phosphorylation with a maximum relaxation of 63% in TM cells (Dismuke et al., 2014). In contrast, Dismuke et al. have reported that endothelin-1 elicits TM cell contraction along with an increase of MLC phosphorylation (Dismuke et al., 2014). This further supports the functional importance of MLC phosphorylation in regulating contractility of TM cells. Similarly, Ramachandran et al. have shown that Y27632 inhibits the phosphorylation of MLC

and can produce a maximum cell relaxation by 50% (Ramachandran et al., 2011). Our results indicate that baicalein can significantly relax hTM cells in a dose-dependent manner, which is consistent with the baicalein-mediated increase in outflow facility. Comparing the maximum TM cell relaxation exerted by nitric oxide donors (Dismuke et al., 2014) and ROCK inhibitor (Ramachandran et al., 2011), the effects of baicalein on TM cell relaxation is relatively small. This is also supported by the subtle changes detected in MLC phosphorylation (**Figure 3.8**). Our findings imply that baicalein triggers a relaxation of TM cells, potentially contributing to the observed increase in outflow facility. However, its effect was not as strong as nitric oxide and ROCK inhibitors.

4.4.3 Effect of baicalein on cell migration in hTM cells

In contrast to the acute responses of cell volume regulation and cell contractility, the modulation of TM cell migration on outflow facility can take place over a relatively long period of time. We observed that baicalein produced a concentration-dependent inhibition of TM cell migration up to nearly 80% after 4 days. At 1 μM, significant inhibition of cell migration was only evident after 4 days. At 10 and 100 μM, inhibition of cell migration was observed in both 2- and 4-day post treatment. Our results are consistent with previous findings demonstrating baicalein's inhibitory

properties on cell migration in other cell types (Liu et al., 2003, Wang et al., 2010a, Chiu et al., 2011). Consistent with the findings of baicalein treatment, we found that Y39983 (1 μM) inhibited TM cell migration by 37%. This is in alignment with a previous study where ROCK inhibitor reduces the migration rate in glioblastoma cells (Zohrabian et al., 2009). TM cell migration has been implicated in the pathogenesis of glaucoma for the following reasons. First, TM cells collected from POAG patients have been shown to have a higher migration rate compared to normal TM cells (Hogg et al., 2000). Second, the levels of myocilin and fibronectin, which have been found to be elevated in glaucomatous eyes, cause an increase in TM cell migration and outflow resistance (Kwon and Tomarev, 2011, Calthorpe and Grierson, 1990, Fautsch et al., 2006, Li et al., 2004). Third, cell migration is found to alter the substrate modulus of TM, increasing the stiffness in glaucomatous TM (Provenzano et al., 2008, Last et al., 2011, Gabelt and Kaufman, 2005). These findings support the important role of TM cell migration in the regulation of outflow facility and IOP.

It has been previously shown that administration of noladin ether, an endocannabinoid ligand selective for cannabinoid CB1 receptor, increases outflow facility (Njie et al., 2006), leading to IOP reduction (Laine et al., 2002). Similar to the effect of baicalein, noladin ether has been shown to trigger a dose-dependent inhibition of TM cell

migration which is blocked by CB1 antagonist SR141716A (Kumar and Song, 2006). The inhibition of TM cell migration is possibly mediated by a decrease of actin stress fibers and focal adhesions (Kumar and Song, 2006). Nevertheless, it has been found that ROCK inhibitor, Y27632, elicits an increased TM cell migration (Koga et al., 2006, Honjo et al., 2001). In our experiments, we observed that baicalein triggered a concentration-dependent inhibition of TM migration concomitant with a parallel increase in outflow facility. In parallel with the results of baicalein, Y39983 was found to inhibit hTM cell migration. The exact reason(s) for this discrepancy is not clear. This might be due to the differences in ROCK inhibitors and experimental conditions used. It has been shown that ROCK inhibitors may have different affinities to the binding pocket residues of ROCKs and inhibitory activities (Wheeler and Ridley, 2004, Pan et al., 2013). Also, ROCK inhibitors might elicit multiple cellular effects in TM cells, attributing to the resultant observed changes in outflow facility. In addition, there might be other non-specific effects modulating TM cell migration that are independent of ROCK inhibition. Further studies are needed to confirm this hypothesis.

It has been proposed that the inhibition of cell migration by baicalein is associated with the decreased activities of MMP-2 and MMP-9 (Liu et al., 2003, Wang et al.,

2010a). Studies have shown that MMPs can inhibit extensive cell proliferation and migration (Larkins et al., 2006). It has also been found that baicalein reduces the activities of MMP-2 and MMP-9 induced by benzo(a)pyrene in Swiss albino mice (Chandrashekar et al., 2012). MMPs serve as important modulators of outflow resistance and IOP through continuous remodeling of ECM (De Groef et al., 2013). However, in the TM of glaucomatous eyes, the activities of MMPs have been shown to be inhibited (De Groef et al., 2013). We cannot exclude the possibility that baicalein may have inhibited MMP-2 and MMP-9 activities in hTM cells. However, it is unlikely because downregulations of MMP-2 and MMP-9 are expected to trigger a reduction, rather than an increase of outflow facility (Bradley et al., 1998).

The inhibition of cell migration induced by baicalein could also be attributed to the inhibitory effects on swelling-activated Cl^- channels (Xue et al., 2018). Studies have demonstrated that regulation of volume-activated Cl^- channels is involved in the migration on HeLa cells (Mao et al., 2009). It has been shown that the inhibition of volume-activated Cl^- channels reduces the migration rate of carcinoma cells (Mao et al., 2007). Since baicalein is shown to modulate RVD by potentially inhibiting $I_{Cl,swell}$ in hTM cells, additional studies are required to elucidate the precise relationship

between cell migration and volume regulation, and its relationship to outflow resistance.

4.5 Effect of baicalein on protein profile in hTM cells

To better delineate the functional significance of baicalein, proteomic approaches were employed to study the protein expression profile after baicalein treatment in hTM cells. It was likely that baicalein acted through multiple pathways; therefore, conventional methods of targeting candidate proteins provided only a limited view of its mechanism of action. Quantitative proteomics is the core research technology underlying high-throughput protein profiling in the post-genomic era (Lao et al., 2014, Lin et al., 2014, Wilhelm et al., 2014). This approach allowed us to better understand the differential protein expressions and the potential signaling pathways involved in the regulation of outflow facility.

In this study, hTM cells were treated with baicalein under two time points: i.e. 3 hours and 2 days. The rationale of studying 3-hour post-treatment was to identify protein changes and early cellular signals responsible for the acute effects (e.g. hTM cell volume and contractility) exerted by baicalein. For the 2-day treatment, it allowed us

to have a better understanding of the proteins involved in cell migration and ECM homeostasis.

Based on our results, there were 47 and 119 differentially expressed proteins after 3 hours and 2 days baicalein treatment, respectively. These differentially expressed proteins were analyzed by PANTHER classification system. Our results suggested that baicalein significantly regulated the catalytic and binding activities at both time points. In addition, cellular process, metabolic process and cellular component organization or biogenesis were the top biological processes regulated by baicalein. With both the IPA software and STRING analysis, we identified a number of the potential upstream regulators and ingenuity canonical pathways following baicalein treatment.

4.5.1 Potential protein candidates regulating conventional outflow facility

Within the physiological IOP range, TM accounts for more than 70% of outflow resistance in human eyes (Van Buskirk, 1977, Rosenquist et al., 1989). Various ECM components such as collagens and laminin are commonly found in the TM. ECM not only serves as a structural protein, but also influences different cellular processes and

functions such as cell contraction, cytoskeletal tension, cell migration, cell-cell and ECM adhesion (Acott and Kelley, 2008).

As shown in **Figure 3.9**, a concentration-dependent inhibition of hTM cell migration was observed after baicalein treatment. This inhibition was possibly mediated by changes in cytoskeletal rearrangement and ECM remodeling. Consistent with the migration results, we revealed a number of related proteins with altered expressions after baicalein treatment at both time points. For 3-hour treatment, baicalein was shown to upregulate cathepsin B (CTSB; P07858; $p<0.01$) by 51%. CTSB belongs to cysteine cathepsins under the C1 papain family of cysteine proteases, which is involved in numerous processes including cell adhesion, cell motility, and ECM degradation (Obermajer et al., 2008). It has been shown that increase of CTSB may facilitate ECM degradation via caveolae-mediated endocytosis (Cavallo Medved et al., 2009). This finding is consistent with a previous study that an upregulation of CTSB were demonstrated after a phagocytic challenge to E. coli and collagen I-coated bead, and that was found to be associated with the regulation of cell-matrix interactions and ECM remodeling in TM cells (Porter et al., 2013). Recently, it has been shown that CTSB expression is inhibited in the TM of glaucoma patients (Porter et al., 2015). Recent evidence demonstrating CTSB's role on attenuating fibrosis and ECM

deposition in TM cells further suggests CTSB upregulation by baicalein may contribute to ECM homeostasis (Nettesheim et al., 2021).

Likewise, D-dopachrome decarboxylase (DDT; P30046; $p<0.05$) and pre-B-cell leukemia homeobox interacting protein 1 (PBXIP1; Q96AQ6; $p<0.05$) were reduced by 42% and 60%, respectively. DDT is the homologue of macrophage migration inhibitory factor MIF and has been regarded as the MIF-like cytokine responsible for inflammatory response (Sonesson et al., 2003). Knockdown of DDT was found to inhibit the migration and proliferation of human cancer cells (Wang et al., 2017). PBXIP is a co-repressor of pre-B-cell leukemia homeobox 1 involved in cell migration, proliferation, growth and differentiation (Manavathi et al., 2012, Abramovich et al., 2002). It has previously been shown that PBXIP1 can promote cell migration in gastric (Feng et al., 2015), thyroid (Wang et al., 2015a) and human alveolar basal epithelial cells (Pan et al., 2016), through the PI3K/AKT signaling pathway. Besides, actin-related protein 2/3 complex subunit 1A (ARPC1A; Q92747; $p<0.05$) was reduced by 35% after 3 hours. Actin-related protein 2/3 complex played a crucial role in actin cytoskeletal functions (Machesky and Gould, 1999). Although there was limited evidence on ARPC1A, a study demonstrated that silencing of actin-related protein 2/3 complex subunit 5 significantly reduced the cell migration in

squamous cell carcinoma cell lines (Kinoshita et al., 2012). In our study, the upregulation of CTSB along with the downregulation of PBXIP1, DDT and ARPC1A may serve as an early signal for the subsequent inhibition of hTM cell migration.

After 2 days of baicalein treatment, we found a number of proteins with altered expressions, which may contribute to the slower rate of cell migration. Baicalein increased the expression of arylsulfatase B (ARSB; P15848; $p<0.01$) by 32%. This was confirmed by an increase in mRNA expression by 18% ($p<0.05$). ARSB is a lysosomal enzyme commonly found in epithelial or endothelial cells (Mitsunaga-Nakatsubo et al., 2009, Prabhu et al., 2011). It has been reported that an increase of ARSB retarded the migration rate by nearly 40% in primary colonic epithelial cells (Bhattacharyya and Tobacman, 2009). Overexpression of ARSB resulted in reduced MMP-9, activated RhoA and cell migration while silencing of ARSB led to opposite effects (Bhattacharyya and Tobacman, 2009). Increased RhoA expression may also enhance the migration rate in human umbilical vein endothelial cells (Zhao et al., 2006). This finding is in good agreement with our results corresponding to a significant downregulation of RhoA (13%; $p<0.05$) after 2 days of baicalein treatment. Moreover, ARSB deficiency is associated with shallow anterior chamber depth and angle-closure glaucoma due to glycosaminoglycan deposit in the TM (Ashworth et al., 2006, Veerappan et al., 2017). Similar findings have been

reported in human bronchial and colonic epithelial cells that ARSB activity is found to be inversely proportional to the amount of cellular sulfated glycosaminoglycans (Bhattacharyya and Tobacman, 2012). Our results suggest that increase of ARSB may reduce ECM deposit and cell contractility in the TM; thus, facilitating AH drainage.

In addition to ARSB, baicalein reduced the expressions of Cl^- intracellular channel protein 4 (CLIC4; Q9Y696, $p<0.01$) by 39%. It has previously been demonstrated that CLIC4 plays a crucial role in cytoskeletal organization in which CLIC4 downregulation has been shown to reduce cell migration via MMP-9 downregulation (Chiang et al., 2013). Recently, it has been found that CLIC4 acts as a matrix microenvironment modulator by regulating the matrix degradation of MMP-14; thereby, influencing focal adhesion and ECM remodeling in human RPE cells (Hsu et al., 2019). Likewise, baicalein significantly reduced the expressions of secernin-1 (SCRN1; Q12765; $p<0.05$) and thymosin beta-4 (TMSB4X; P62328; $p<0.05$) by 26% in both. Increased protein expressions of SCRN1 and TMSB4X have been found to correlate with increased cell migration via upregulation of MMP activities (Lin et al., 2015, Malinda et al., 1997, Malinda et al., 1999, Qiu et al., 2007). This is in agreement with previous studies that baicalein reduced MMPs expression and

activities in chondrocytes (Chen et al., 2015) and lung cells (Chandrashekar et al., 2012).

Different ECM proteins including laminin, fibronectin, and collagen are highly expressed in sheath-derived plaques in the JCT region of TM (Ueda et al., 2002). Excessive ECM deposition has been found to be associated with higher outflow resistance in glaucomatous TM (Tektas and Lütjen-Drecoll, 2009). In relation to ECM proteins, we observed an 18% reduction of laminin subunit beta-1 (LAMB1, P07942, $p<0.01$), an ECM component, after baicalein treatment. Increased expression and activities of MMPs has been found to trigger ECM degradation through an IOP homeostasis feedback mechanism (De Groef et al., 2013). There are approximately 25 types of MMPs discovered (Zitka et al., 2010, Lindsey, 2018). Most are secreted-type MMPs, including MMP-2 and MMP-9, while MMP-14 is a membrane-anchored type enzyme (Yang et al., 2007, Shiomi et al., 2010). The increase of MMP expressions, particularly MMP-2 and MMP-9, has been thought to enhance ECM digestion; hence, outflow facility (Yang et al., 2016, Keller et al., 2009). Our results also showed a 14% increase in MMP-14 expression after the 3-hour treatment ($p<0.05$). Other MMPs were; however, not detected in our MS results. The exact reason for this difference is not apparent. This could be due to the fact that only TM cells were used by proteomic

studies. As a result, it may have limited the detection of secreted proteins such as MMP-2 and MMP-9. Our findings are in parallel with a previous study where MMP-14 enhanced ECM digestion in isolated human skin tropoelastin and elastin (Miekus et al., 2019). In TM cells, MMP-14 was found to be upregulated under mechanical stress (Bradley et al., 2003). More recently, it has been demonstrated that genipin, an agent to induce matrix cross-linking, reduced outflow facility in porcine and human anterior segments, which may have been mediated by a reduction of MMP-14 (Yang et al., 2016). Taken together, baicalein potentially triggered ECM remodeling, which may account for increase in outflow facility by reducing the resistance to fluid drainage.

4.5.2 Other properties of baicalein in potentially regulating TM functions

4.5.2.1 Anti-oxidative properties of baicalein

Baicalein has been shown to display anti-oxidative property by reducing oxidative stress against cellular damage (Su et al., 2000, Liu et al., 2013). Oxidative stress has been implicated in the pathogenesis of glaucoma because elevated ROS has been found in the TM, AH, and RGCs of glaucomatous eyes (Saccà et al., 2005, Ghanem et al., 2010, Wax and Tezel, 2009). Based on the STRING analysis, a total of 8 and 22

proteins related to oxidation-reduction process were differentially expressed after baicalein treatment for 3 hours and 2 days, respectively. This supported the notion that baicalein was involved in the regulation of oxidation-reduction process in hTM cells, consistent with earlier reports for other cell types. After 3 hours baicalein treatment, peroxiredoxin-1 (Prdx1; Q06830; $p<0.05$) was upregulated by 20%. Prdx1 is an abundant antioxidant protein found in erythrocytes to scavenge excessive ROS (Neumann et al., 2009). Prdx1 also serves as an intracellular messenger for H_2O_2 homeostasis by reducing the intracellular level of H_2O_2 (Rhee et al., 2003). Prdx1 has been shown to inhibit oxidant-induced damages to cellular DNA, lipids, and proteins (Mu et al., 2002). Previous study has shown that ROS level increased in red blood cells of Prdx1 knockout (Prdx1-/-) mice. Significant increase in DNA damage has been found in the brain, liver and spleen of Prdx1-/- mice (Egler et al., 2005). Suppression of H_2O_2-induced DNA damage has been reported after baicalein treatment by reducing DNA double-strand breaks; thereby, increasing cell viability in Chinese hamster lung fibroblast (Kim et al., 2012) and human vestibular schwannoma cells (Park et al., 2019).

In addition to Prdx1, baicalein has been found to prevent ROS-induced mitochondrial dysfunction by increasing mitochondrial activities and inhibiting apoptotic-related

changes in mitochondria (de Oliveira et al., 2015). In our experiment, pyruvate dehydrogenase E1 component subunit beta (PDHB; P11177; $p<0.05$) was upregulated by 61% after 3 hours of treatment. PDHB has been found to be a major subunit of pyruvate dehydrogenase complex (PDHC), which plays an important role in aerobic energy metabolism (Martin et al., 2005). The covalent catalysis with thiamin diphosphate induced by PDHB has been suggested to be the rate-limiting step in PDHC catalysis (Balakrishnan et al., 2012). Therefore, upregulation of PDHB by baicalein is expected to enhance mitochondrial activities. An increase in lipid peroxidation in the mitochondria, which is induced by ROS has been reported in various neurodegenerative diseases including Alzheimer's disease (Pocernich and Butterfield, 2003) and POAG (Aslan et al., 2008). Patients with POAG have been found to have lower levels of ATP production and mitochondrial potentials in the TM (He et al., 2008). In neurodegenerative diseases, baicalein has also been found to inhibit lipid peroxidation and increase cell viability in PC12 (Zhang et al., 2010) and SH-SY5Y cells (Wang et al., 2013). These findings are consistent with our results where an upregulation of PDHB by baicalein can potentially reduce ROS-induced mitochondrial dysfunction in hTM cells.

After 2 days treatment of baicalein, we found that superoxide dismutase [Cu-Zn] (SOD1; P00441; $p<0.05$) was downregulated by 50%. SOD1 is an antioxidant enzyme reducing oxygen-derived cytotoxicity (Kobayashi et al., 2019). SOD1 has been considered a clinical biomarker of oxidative stress in renal (Pawlak et al., 2005) and eye diseases (Ferreira et al., 2004, Ghanem et al., 2010). It has been reported that the activity of superoxide dismutase increased by >50% in the AH of POAG patients compared to controls (Ferreira et al., 2004, Ghanem et al., 2010). Our results are in good agreement with previous *in vitro* studies whereby baicalein significantly attenuated oxidative stress by scavenging ROS and reduced apoptotic cell death in cardiomyocytes (Shao et al., 1999), fibroblasts (Gao et al., 1998), retinal pigment epithelium cells (Liu et al., 2010b) of different species. For *in vivo* studies, baicalein has also been found to alleviate cognitive and motor impairments by reducing mitochondrial ROS; thereby, protecting brain mitochondria against chronic cerebral hypoperfusion-induced oxidative damage (He et al., 2009). Likewise, an association of cardiomyocyte apoptosis with excessive ROS and baicalein has been found to ameliorate doxorubicin-induced cardiotoxicity in mice (Sahu et al., 2016).

4.5.2.2 Anti- inflammatory properties of baicalein

In our experiments, several proteins related to inflammation were significantly altered in expression after baicalein treatment. For example, macrophage migration inhibitory factor (MIF; P14174; $p<0.05$) were downregulated by 33% after 3 hours of incubation. As mentioned above, DDT, a MIF-like cytokine, was reduced in expression by 42% ($p<0.001$) after baicalein treatment. It has been previously suggested that MIF act as a regulator on the production of different cytokines and initiators of inflammatory response (Bucala, 1996). Upon UV exposure, inflammatory responses such as increased expressions in protein and mRNA of IL-8 and tumor necrosis factor TNF-α has been found in human blister fluid (Strickland et al., 1997). Similarly, a later study also revealed an increase of MIF and DDT activities in human blister fluid compared to non-irradiated skin after UVB irradiation (Sonesson et al., 2003). The injection of anti-MIF antibodies in BALB/c mice significantly inhibits T-cell proliferation and IL-2 production (Bacher et al., 1996). Injection of anti-MIF antibodies in atherosclerosis apolipoprotein E-deficient mice model significantly reduced the levels of MIF, IL-6 and IL-12 (Burger Kentischer et al., 2006). In addition, reduced MIF has been found to be associated with the suppression of inflammatory response such as reduced accumulation of neutrophils and macrophages in the wound (Ashcroft et al., 2003). Merk et al. reported that intraperitoneal injection of anti-DDT antibodies

significantly reduced the expressions of IL-6, IL-1β and TNF-α in the serum of mice (Merk et al., 2011). Our results imply that downregulations of MIF and DDT may be mediated by the anti-inflammatory property of baicalein.

Elevated levels of IL-8 and TGFB1 have been observed in the AH of POAG patients (Kuchtey et al., 2010, Takai et al., 2012). In the TM of POAG patients, TGFB1, IL-6, IL-1β and TNF-α levels have been found to be significantly higher than normal subjects (Taurone et al., 2015). The potential anti-inflammatory response of baicalein found in our study was consistent with the properties reported in previous studies. Lee et al. found that baicalein suppressed both the production of pro-inflammatory cytokines TNF-α and lipopolysaccharide-mediated inflammatory responses of IL-6 in human umbilical vein endothelial cells (Lee et al., 2015). Similar results have also been found in IL-1β and TNF-α activated mast cells in which baicalein inhibited the production of IL-6, IL-8, and monocyte chemotactic protein 1 (Hsieh et al., 2007). Moreover, it has been shown that rats receiving controlled cortical impact injury can recover their motor function and balance following baicalein treatment. The effects were likely mediated by the inhibition of inflammatory responses related to IL-6, IL-1β, and TNF-α (Chen et al., 2008). These findings are in good alignment with the

anti-inflammatory properties of baicalein, which may potentially play an important role in modulating TM cell functions.

It is worth noting that in our STRING analyses, we demonstrated a correlation with Parkinson's and Huntington's diseases with a FDR of <0.001. Parkinson's and Huntington's diseases are neurodegenerative disorders that are related to neuroinflammation, similar to glaucoma (Przedborski, 2010, Chang et al., 2015b, Vohra et al., 2013). Our results suggest that regulation of TM cell function by the anti-inflammatory properties of baicalein may share similar signaling cascades as reported in other neurodegenerative diseases.

4.5.2.3 Anti- apoptotic properties of baicalein

Loss of TM cellularity has been observed in patents with POAG (Alvarado et al., 1984), which may be a result of increased TM cell death. It has been shown that apoptotic cell death induced by microRNA-93 was upregulated in glaucomatous TM cells (Wang et al., 2016), suggesting that the anti-apoptotic properties of baicalein may be important for the maintenance of normal functions and viability of hTM cells. Based on the STRING analysis of significantly regulated proteins, there were 19 proteins that were related to the apoptosis process with FDR <0.05.

After 3 hours treatment of baicalein, the expression of proliferation-associated protein 2G4 (PA2G4; Q9UQ80; $p<0.05$) significantly increased by 51%. ErbB3 receptor-binding protein (Ebp1) has been found to be a human member of PA2G4 family (Kowalinski et al., 2007). Two isoforms of Ebp1, p48 and p42, have been isolated as important in regulating cell survival and differentiation. For example, p48 has been found to inhibit apoptotic cell depth while p42 suppresses cell proliferation in PC12 cells (Liu et al., 2006b). Depletion of Ebp1 has been found to induce a 50% increase of cell apoptosis in PC12 cells (Okada et al., 2007). Reduced expression of PA2G4 has been shown in aging retina with glaucoma (Sacca et al., 2016). In a study on episcleral vein occlusion in SD rats, a significant loss of RGCs and downregulation of PA2G4 expression have been observed in aged rats receiving cauterization at 47 weeks when compared with controls (Anders et al., 2018). In view of that, elevated PA2G4 expression after baicalein treatment may lead to an anti-apoptotic effect on TM cells.

Additionally, isoform 3 of SUMO-activating enzyme subunit 1 (SAE1; Q9UBE0-3; $p<0.01$) and programmed cell death protein 6 (PDCD6; O75340; $p<0.05$) were downregulated for 53% and 57%, respectively, after 3 hours. As reported by Gareau and Lima (2010), SAE1 belonged to a family of small ubiquitin-related modifier

(SUMO) and was responsible for regulating cellular process involving nuclear transport and DNA repair (Gareau and Lima, 2010). Overexpression of SUMO is shown to correlate with the neuronal apoptosis in Huntington's disease (Dorval and Fraser, 2007). PDCD6 is found as a Ca^{2+}- binding modulator protein regulating cell apoptosis (Vito et al., 1996). Rao et al. reported that inhibition of PDCD6 resulted in a reduction of endoplasmic reticulum stress-induced cell death in mouse embryonic fibroblasts (Rao et al., 2004). Our results suggested that downregulations of SAE1 and PDCD6 and upregulation of PA2G4 by baicalein may potentially exert anti-apoptotic effects on hTM cells.

Additionally, after baicalein treatment for 2 days, plasminogen activator inhibitor 1 RNA-binding protein (SERBP1; Q8NC51; $p<0.05$) was significantly upregulated by 29%. SERBP1 has been found to regulate and maintain mRNA stability (Heaton et al., 2001). Apart from that, SERBP1 plays an important role in DNA repairing. For example, SERBP1 depletion has been reported to impair DNA repairing process by affecting strand-binding protein phosphorylation; thereby, reducing cell survival (Ahn et al., 2015). Therefore, upregulation of SERBP1 after baicalein treatment may help maintain mRNA stability and DNA repairing process in hTM cells.

It is likely that there are protein candidates displaying multiple functional properties. For example, Prdx1 was found to exhibit anti-oxidative effects in erythrocytes (Neumann et al., 2009). In addition to that, knockdown of Prdx1 led to a higher phosphorylated level of apoptosis signal-regulating kinase 1 (ASK1) and p38 upon H_2O_2 treatment in HeLa cells (Kim et al., 2008). Both ASK1 and p38 were involved in the activation of apoptosis (Kim et al., 2008). Overexpression of Prdx1/2 has been found to significantly suppress the H_2O_2-induced ASK1/p38 signaling pathway and apoptosis (Lu et al., 2019), further supporting the role of Prdx1 in inhibiting the oxidative stress-induced apoptosis. Other studies have also demonstrated protective effects of baicalein against apoptosis. For example, it has been demonstrated that baicalein protects against H_2O_2-induced intracellular ROS production and apoptosis in PC12 cells (Zhang et al., 2010). This was supported by a study in which baicalein reduces apoptosis induced by 6-hydroxydopamine in human neuroblastoma cells (Mu et al., 2009).

Table 4.1 summarizes all the differentially expressed proteins mentioned in the discussion. In our study, we focused primarily on the effects of baicalein on normal healthy TM cells. Further investigations are needed to determine the anti-oxidative,

anti-inflammatory and anti-apoptotic properties of baicalein in glaucomatous TM in order to address our hypothesis.

Table 4.1 Summary of the differentially expressed proteins mentioned in the discussion (GN: Gene name; Δ: percentage changes).

		Proteins	GN	Δ (%)	References
Reduced cell migration/ increased cell relaxation	3 hours	D-dopachrome decarboxylase	DDT	-42	(Wang et al., 2017)
		Pre-B-cell leukemia homeobox interacting protein 1	PBXIP1	-60	(Feng et al., 2015, Wang et al., 2015a, Pan et al., 2016)
		Actin-related protein 2/3 complex subunit 1A	ARPC1A	-35	(Kinoshita et al., 2012)
	2 days	Arylsulfatase B	ARSB	+32	(Bhattacharyya and Tobacman, 2009, Zhao et al., 2006).
		Transforming protein RhoA	RhoA	+13	(Zhao et al., 2006).
		Chloride intracellular channel protein 4	CLIC4	-39	(Chiang et al., 2013)
		Secernin-1	SCRN1	-26	(Lin et al., 2015)
		Thymosin beta-4	TMSB4X	-26	(Malinda et al., 1997, Malinda et al., 1999, Qiu et al., 2007)
Increased ECM degradation/ reduced ECM deposition	3 hours	Laminin subunit beta-1	LAMB1	-18	(Stamer et al., 2011, Zhao et al., 2004)
		Matrix metalloproteinase-14	MMP14	+14	(Yang et al., 2016, Miekus et al., 2019).
		Cathepsin B	CTSB	-51	(Obermajer et al., 2008, Cavallo Medved et al., 2009, Porter et al., 2013, Nettesheim et al., 2021)
	2 days	Arylsulfatase B	ARSB	+32	(Ashworth et al., 2006, Veerappan et al., 2017, Bhattacharyya and Tobacman, 2012)
		Chloride intracellular channel protein 4	CLIC4	-39	(Hsu et al., 2019)

Anti-oxidation	3 hours	Peroxiredoxin-1	Prdx1	+20	(Rhee et al., 2003, Neumann et al., 2009, Mu et al., 2002, Egler et al., 2005, Kim et al., 2012, Park et al., 2019).
		Pyruvate dehydrogenase E1 component subunit beta	PDHB	+61	(Zhang et al., 2010, Wang et al., 2013)
	2 days	Superoxide dismutase [Cu-Zn]	SOD1	-50	(Pawlak et al., 2005, Ferreira et al., 2004, Ghanem et al., 2010)
Anti-inflammation	3 hours	Macrophage migration inhibitory factor	MIF	-33	(Bucala, 1996, Sonesson et al., 2003, Burger Kentischer et al., 2006).
		D-dopachrome decarboxylase	DDT	-42	(Sonesson et al., 2003, Merk et al., 2011).
Anti-apoptosis	3 hours	Proliferation-associated protein 2G4	PA2G4	+51	(Liu et al., 2006b, Okada et al., 2007)
		SUMO-activating enzyme subunit 1	SAE1	-53	(Gareau and Lima, 2010, Dorval and Fraser, 2007)
		Programmed cell death protein 6	PDCD6	-57	(Vito et al., 1996, Rao et al., 2004)
	2 days	Plasminogen activator inhibitor 1 (PAI-1) RNA-binding protein	SERBP1	+29	(Heaton et al., 2001, Ahn et al., 2015, Lu et al., 2019)

4.5.3 Potential upstream regulators

In addition to the differentially expressed proteins found in the dataset, TGFB1 was identified to be the most significant potential upstream regulator. Leveraging the Upstream Regulator Analysis of IPA software, an inhibition of TGFB1 was predicted (z-score= -2.9, p<0.001). Our results suggest that TGFB1 inhibition may be a potential regulator responsible for the observed changes in protein expressions after

baicalein treatment. This finding is in line with the significant inhibition of transforming growth factor beta-1-induced transcript 1 protein (TGFI1; O432294; $p<0.05$) by 41%.

TGFB1 has been shown to play an important role in the pathogenesis of glaucoma as an elevated level of TGFB1 was reported in AH and TM of POAG patients (Takai et al., 2012, Taurone et al., 2015). Overexpression of TGFB1 has been reported to increase IOP in rats (Robertson et al., 2010). Similar to the results of baicalein, the ocular hypotensive effect of TGFB1 was believed to be mediated by regulating different cellular processes including cell proliferation, apoptosis and ECM production (Prendes et al., 2013, Shi and Massagué, 2003).

TGFB1 has been shown to induce contraction in rat peritubular cells (Ailenberg et al., 1990). Nakamura et al. found a concentration-dependent contraction of bovine TM cells accompanied by a reorganization of actin cytoskeleton after TGFB1 treatment (Nakamura et al., 2002). Similarly, TGFB1 significantly induced the expression of α-smooth muscle actin in both monkey and human TM cells (Tamm et al., 1996). Cell contraction induced by TGFB1 can be suppressed by ROCK inhibition (Nakamura et al., 2002).

Similar results has been shown in human tenon fibroblasts whereby TGFB1 triggered cell contraction through ROCK activation (Meyer-ter-Vehn et al., 2006). In addition, numerous evidence have shown that TGFB1 promoted cell migration, via the activation of NF-κB, in human pulmonary (Fong et al., 2009) and lens epithelial (Zhang and Huang, 2018) cells. It has been demonstrated that TGFB1 increases the expressions of fibronectin (Calthorpe and Grierson, 1990, Welge-Lüßen et al., 2000), ECM cross-linking lysyl oxidase (Sethi et al., 2011), connective tissue growth factor and tissue transglutaminase (tTgase) (Chudgar et al., 2006, Welge-Lüßen et al., 2000) in TM cells, potentially leading to an increased outflow resistance. Therefore, inhibition of TGFB1 is expected to trigger a reduction of outflow resistance and IOP.

4.5.4 Potential ingenuity canonical pathway

With the core analysis in IPA software, the potential ingenuity canonical pathways were determined by analyzing all identified proteins in the database. This enabled us to determine the potential signaling pathways mediated by baicalein in influencing TM cell functions. We identified five common pathways ($p<0.05$) that were involved at both time points: namely oxidative phosphorylation, clathrin-mediated endocytosis signaling, mitochondrial dysfunction, γ-linolenate biosynthesis II (animals), and regulation of actin-based motility by Rho following baicalein treatment. Oxidative

phosphorylation was the only pathway provided with a calculated z-score after the 2-day treatment, suggesting that baicalein likely mediated its effects by inhibiting oxidative phosphorylation.

Oxidative phosphorylation (OXPHOS) is the key reaction in mitochondria for adenosine triphosphate (ATP) synthesis during aerobic respiration (Senior, 1988, Schmidt-Rohr, 2020, Tahara et al., 2009). Although OXPHOS is important for energy production in metabolism, excessive production of ROS can lead to mitochondrial dysfunction (Martin et al., 2005) and DNA damages (Yu and Anderson, 1997), eventually accelerating cell apoptosis (Kannan and Jain, 2000). Mitochondrial dysfunction, as regulated by OXPHOS pathway, has been found in neurodegenerative diseases including Parkinson's disease, Huntington's disease, and autosomal dominant optic atrophy (Federico et al., 2012). Our results suggest that downregulation of OXPHOS pathway by baicalein may potentially reduce mitochondrial dysfunction and DNA damage, as reflected by a significant downregulation of SOD1.

4.6 Ocular hypotensive effect of baicalein

Based on the encouraging results obtained from both *in vitro* and *ex vivo* studies, we evaluated the IOP-lowering effects of baicalein in rodents using various routes of drug administration. SD rats and C57 mice were chosen as they are the commonly used animal species for glaucoma studies (Izzotti et al., 2003, Ruiz-Ederra and Verkman, 2006, Lin and Liu, 2010, Morgan and Tribble, 2015). The time- and dose-dependent responses were determined for pre-clinical evaluation.

As a proof of concept, we determined the longitudinal changes of IOP after daily intraperitoneal injection of baicalein in SD rats. Two concentrations of baicalein (i.e. 4 mg/kg for two weeks followed by 40 mg/kg for additional two weeks) were used to determine whether there is a concentration-dependent ocular hypotensive response. We observed that, at 4 mg/kg, baicalein lowered the IOP by 1.2 mmHg (equivalent to 9% of baseline IOP) after 2 weeks. Subsequently, increasing the dosage to 40 mg/kg triggered a 2.7 mmHg reduction (equivalent to 20% of baseline IOP). The dosages were chosen according to a previous study using similar drug administration approach (Li et al., 2014).

However, the absolute change in IOP observed at the higher baicalein dosage is relatively small compared to the expected IOP reduction generated by a 90% increase in outflow facility. One possible reason for this discrepancy is that only a limited amount of baicalein could reach the anterior segment of the eye, resulting in a reduced IOP response. In addition, it is noted that both IOP measurements and intraperitoneal injections were conducted under anesthesia; therefore, the observed IOP responses might have been affected by anesthetic agents, which are known to lower IOP (Ding et al., 2011, Jia et al., 2000). In order to address that, we conducted a separate set of experiments to determine whether topical administration of baicalein triggered a direct IOP reduction without anesthesia.

To better understand the precise ocular hypotensive actions of baicalein *in vivo*, the effects of topical application of baicalein on IOP were studied using both SD rats and C57 mice. IOP measurements were conducted under awake conditions to minimize IOP artifacts that could be caused by anesthetic agents. Our results showed that baicalein lowers IOP substantially in both SD rats and C57 mice, suggesting that baicalein can act across different animal species. After a single dose of topical baicalein administration, the ocular hypotensive effects lasted for a period of six hours during both daytime and nighttime. The maximum IOP-lowering effects were found

to be 1.1 mmHg and 2.3 mmHg under daytime and nighttime in SD rats. Similarly, baicalein triggered a maximum reduction of IOP by 1.6 mmHg and 2.3 mmHg during daytime and nighttime in C57 mice. Consistent with the results obtained from intraperitoneal injection, our findings suggest that topical baicalein causes a significant IOP reduction. In addition, we determined the concentration of baicalein in the AH following baicalein treatment. A positive correlation between baicalein concentration in the AH and IOP-lowering effect was observed. We showed that the concentration of baicalein increased by approximately 4 to 5 fold when compared with the control eye after topical baicalein treatment. However, the absolute concentration of baicalein in the AH was found to be 0.0003% compared to the stock concentration applied topically, suggesting that the bioavailability of baicalein was low in the eye. This might be due to limited penetration across an intact cornea as well as fast clearance from the anterior chamber. Given that the concentration of baicalein is low in the eye, the precise IOP-lowering effect of baicalein remains unclear. To further estimate the actual ocular hypotensive effects triggered by baicalein, we investigated the effects of intravitreal administration of baicalein on IOP.

Intravitreal administration provides a direct access of baicalein to the target sites, enabling more precise evaluation of its drug actions. SD rats were used because it was easier to conduct intravitreal injection. Our results showed that intravitreal injection of baicalein had no significant effect on the total retinal thickness at all concentrations tested, suggesting the absence of retinal toxicity. Evaluating the retinal thickness would provide a better understanding of whether there is any potential toxicity of chemicals used (Ekinci et al., 2014, Wild et al., 2006).

After intravitreal injection, baicalein elicited a dose-dependent IOP reduction under both daytime and nighttime. The maximum ocular hypotensive effects were found to be 2.4 mmHg (22%) and 9.3 mmHg (51%) under daytime and nighttime. In addition, we observed that the ocular hypotensive effect lasted for at least 3 to 4 days. The maximum IOP reduction triggered by baicalein is in good agreement with the IOP-lowering effects shown by clinically available anti-glaucoma drugs (Aspberg et al., 2018, Lindén et al., 2018). Apart from the maximum IOP reduction, baicalein demonstrates a more potent IOP-lowering response at nighttime. It has been well documented that POAG patients display a greater IOP diurnal fluctuation than normal individuals (Sehi et al., 2005, Sihota et al., 2005, Agnifili et al., 2015, Srinivasan et al., 2016). POAG patients who have abnormal and irregular diurnal IOP variations are

more prone to have faster progression of vision deterioration (Martínez-Belló et al., 2000, Zeimer et al., 1991). Since baicalein has a more significant ocular hypotensive effect when the IOP is high, baicalein may help reduce IOP swing observed in glaucoma patients.

According to the modified Goldmann equation:

$$IOP = \frac{Fin - Fu}{C} + Pe \quad (1)$$

where *IOP* = intraocular pressure; Fin = aqueous humor formation rate; Fu = uveoscleral outflow rate; C = outflow facility and Pe = episcleral venous pressure before drug treatment. Rearranging the modified Goldmann equation, the ratio change of Fin' after drug treatment can be derived by the following expression:

$$\frac{Fin'}{Fin} = \frac{(IOP' - Pe') \times C' + Fu'}{(IOP - Pe) \times C + Fu} \quad (2)$$

where IOP′ = intraocular pressure; Fin′ = aqueous humor formation rate; Fu′ = uveoscleral outflow rate; C′ = outflow facility and Pe′ = episcleral venous pressure after drug treatment. We have made the following assumptions: 1) baicalein does not

affect Pe and Fu, and 2) the maximum IOP reduction is about 50% with a baseline IOP of 22 mmHg, 3) C′ and C are 0.047 and 0.026 µl/min/mmHg, respectively; and 4) Pe and Fu are 5.4 mmHg and 0.0012 µl/min (Millar et al., 2011). As a result, a 37% inhibition of AH secretion is expected after baicalein treatment, which is comparable with the actual results obtained from the inhibition of fluid movement (i.e. 31% inhibition) across porcine ciliary epithelium (Xiao, 2015). This result suggests that the ocular hypotensive effect of baicalein is mediated by the dual action on both AH secretion and drainage. The main action is possibly caused by an increase in conventional outflow facility.

Chapter 5 Conclusion

Although there have been tremendous efforts to elucidate the mechanisms underlying glaucoma, its pathophysiology remains unclear. It has been demonstrated that increase in outflow resistance of TM may be the major cause of IOP elevation in glaucoma (Rohen et al., 1989). Therefore, developing anti-glaucoma agent targeted at the conventional outflow pathway is an appealing approach for the prevention of glaucomatous blindness because TM is the diseased tissue responsible for elevated IOP. In this study, we have demonstrated that baicalein enhances conventional outflow facility by ~90%. In addition, we have shown that baicalein 1) inhibits RVD in hTM cells, 2) triggers relaxation of hTM cells via MLC phosphorylation, 3) reduces hTM cell migration, 4) alters expression of ECM-associated proteins in hTM cells, and 5) produces a significant reduction of IOP in rodents following baicalein treatment through various drug administration routes. We conducted a proteomic study to identify the novel and potential cellular targets responsible for mediating the baicalein-induced physiological changes and the potential signaling pathways associated with its anti-apoptotic, anti-inflammatory, and anti-oxidative properties. The elucidation of these signaling cascades provide new insight into developing novel and disease modifying targets for restoration of normal functions of TM cells. The potential mechanisms of baicalein affecting the outflow pathway and IOP are

summarized in **Figure 5.1**. In addition, it provides a basis for future studies. For example, we have yet to determine the underlying mechanisms whereby baicalein alters the expression of ECM proteins and their relationship to the regulation of outflow resistance.

Our work has supported a potential biomedical significance of baicalein in regulating AH dynamics. Clinically, it is of great importance to develop anti-glaucoma agents that are potent, long-lasting, and well-tolerated by patients. Baicalein appears to have a combination of actions that impact both the secretion and drainage of AH, leading to a reduction of IOP. Currently, there is no anti-glaucoma drug that has dual actions on both AH inflow and outflow pathways. Further studies are required to confirm whether the primary effect of baicalein is mediated by a facilitation of conventional outflow facility. This can be done by adopting a recently developed technique that can measure all AH hydrodynamic parameters simultaneously in a single experiment (Millar et al., 2011). The new technique will greatly facilitate a concurrent evaluation of pharmacologic actions on both AH inflow and outflow. Also, baicalein could be used in combination with other existing anti-glaucoma agents, such as prostaglandin analogs, beta-blockers, and carbonic anhydrase inhibitors, as these agents lower IOP by other mechanisms.

Baicalein is a hydrophobic flavonoid and has limited water solubility (Liu et al., 2006a, Huang et al., 2014). Further studies on improving baicalein's solubility, stability and bioavailability in the eye are also important for the future development of a more potent IOP-lowering agent. For instance, lipid-based nanocarriers have been shown to improve the stability and penetration ability of baicalein (Tsai et al., 2012). It has been shown that lipid nanoparticles can greatly enhance drug bioavailability and transcorneal penetration because of its tiny size (Alvarez Trabado et al., 2017).

Baicalein has been demonstrated to protect RGCs from ischemic insult and oxidative damage (Maher and Hanneken, 2005, Chao et al., 2013, Hanneken et al., 2006), indicating that baicalein could potentially be used as a neuroprotectant in the treatment of glaucoma. Currently, little is known about the therapeutic potential of baicalein as a neuroprotective agent against glaucoma and ocular hypertension. Therefore, it is also crucial to establish whether baicalein improves the dysfunctional retinal response and preserves RGC survival after ocular hypertension. As of now, there is no neuroprotectant proven to be effective for glaucoma treatment. Baicalein may be a new therapeutic agent that targets both IOP reduction and neuroprotection.

Figure 5.1 The potential mechanisms of baicalein influencing outflow pathway and intraocular pressure.

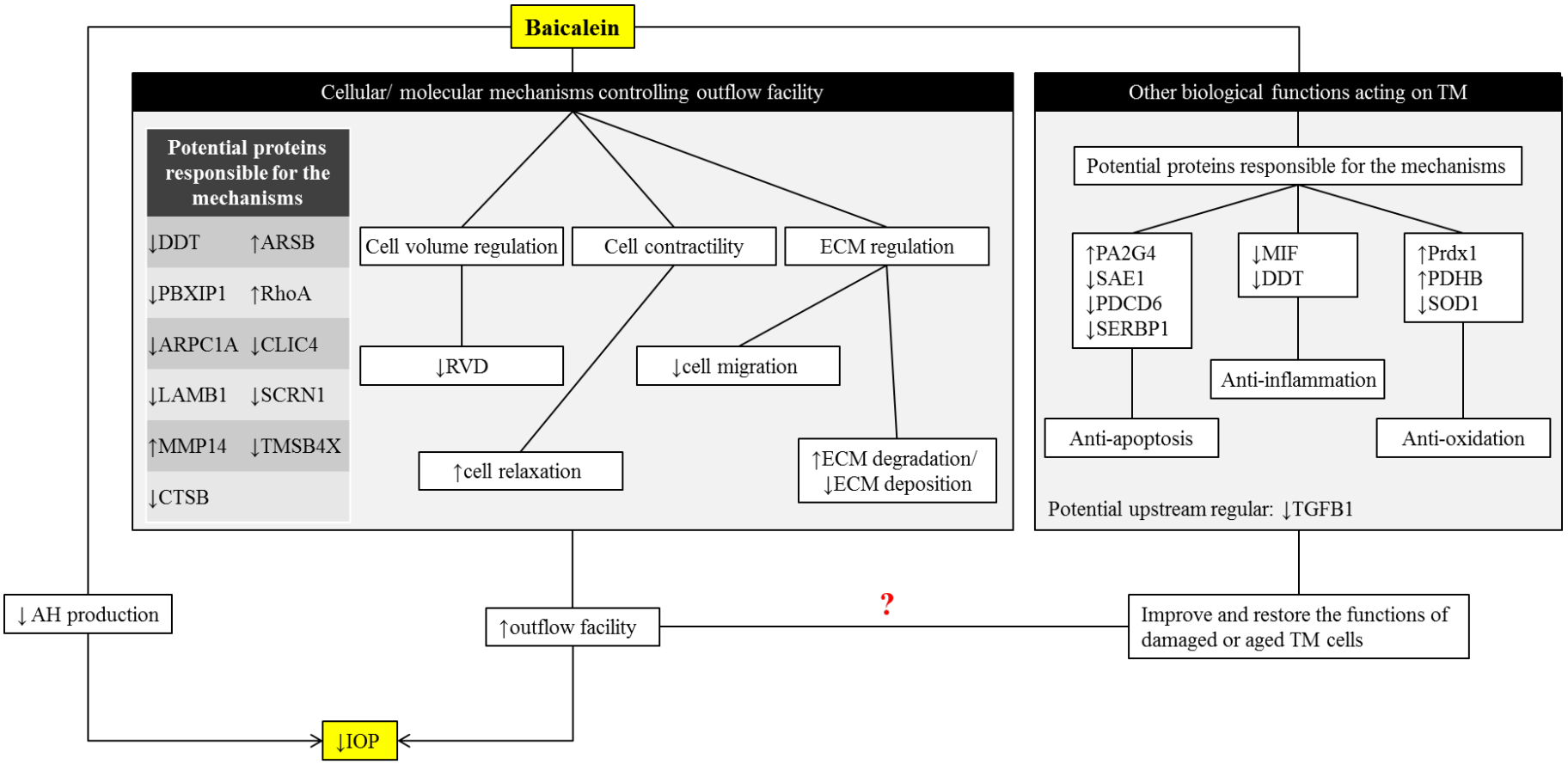

References

ABRAMOVICH, C., CHAVEZ, E. A., LANSDORP, P. M. & HUMPHRIES, R. K. 2002. Functional characterization of multiple domains involved in the subcellular localization of the hematopoietic Pbx interacting protein (HPIP). *Oncogene,* 21**,** 6766-6771.

ACOTT, T. S. & KELLEY, M. J. 2008. Extracellular matrix in the trabecular meshwork. *Experimental Eye Research,* 86**,** 543-561.

ACOTT, T. S., KINGSLEY, P. D., SAMPLES, J. R. & VAN BUSKIRK, E. M. 1988. Human trabecular meshwork organ culture: morphology and glycosaminoglycan synthesis. *Investigative Ophthalmology & Visual Science,* 29**,** 90-100.

AGNIFILI, L., MASTROPASQUA, R., FREZZOTTI, P., FASANELLA, V., MOTOLESE, I., PEDROTTI, E., IORIO, A. D., MATTEI, P. A., MOTOLESE, E. & MASTROPASQUA, L. 2015. Circadian intraocular pressure patterns in healthy subjects, primary open angle and normal tension glaucoma patients with a contact lens sensor. *Acta Ophthalmologica,* 93**,** e14-e21.

AGUDO, M., PÉREZ-MARÍN, M. C., SOBRADO-CALVO, P., LÖNNGREN, U., SALINAS-NAVARRO, M., CÁNOVAS, I., NADAL-NICOLÁS, F. M., MIRALLES-IMPERIAL, J., HALLBÖÖK, F. & VIDAL-SANZ, M. 2009. Immediate upregulation of proteins belonging to different branches of the apoptotic cascade in the retina after optic nerve transection and optic nerve crush. *Investigative Ophthalmology & Visual Science,* 50**,** 424-431.

AHN, J. W., KIM, S., NA, W., BAEK, S. J., KIM, J. H., MIN, K., YEOM, J., KWAK, H., JEONG, S. & LEE, C. 2015. SERBP1 affects homologous recombination-mediated DNA repair by regulation of CtIP translation during S phase. *Nucleic Acids Research,* 43**,** 6321-6333.

AILENBERG, M., TUNG, P. S. & FRITZ, I. B. 1990. Transforming growth factor-β elicits shape changes and increases contractility of testicular peritubular cells. *Biology of Reproduction,* 42**,** 499-509.

AKARSU, C. & BILGILI, M. Y. K. 2004. Color Doppler imaging in ocular hypertension and open-angle glaucoma. *Graefe's Archive for Clinical and Experimental Ophthalmology,* 242**,** 125-129.

AL-ASWAD, L. A., GONG, H., LEE, D., O'DONNELL, M. E., BRANDT, J. D., RYAN, W. J., SCHROEDER, A. & ERICKSON, K. A. 1999. Effects of Na-K-2Cl cotransport regulators on outflow facility in calf and human eyes in Vitro. *Investigative Ophthalmology & Visual Science,* 40**,** 1695-1701.

ALVARADO, J., MURPHY, C. & JUSTER, R. 1984. Trabecular meshwork mellularity in primary open-angle glaucoma and nonglaucomatous normals. *Ophthalmology,* 91**,** 564-579.

ALVAREZ TRABADO, J., DIEBOLD, Y. & SANCHEZ, A. 2017. Designing lipid nanoparticles for topical ocular drug delivery. *International Journal of Pharmaceutics,* 532**,** 204-217.

ANDERS, F., MANN, C., LIU, A., TEISTER, J., FUNKE, S., THANOS, S., GRUS, F., PFEIFFER, N. & PROKOSCH, V. 2018. Correlation of Crystallin Expression and RGC Susceptibility in Experimental Glaucoma Rats of Different Ages. *Current Eye Research,* 43**,** 1267-1273.

ANDERSON, D. R. & HENDRICKSON, A. 1974. Effect of intraocular pressure on rapid axoplasmic transport in monkey optic nerve. *Investigative Ophthalmology & Visual Science,* 13**,** 771-783.

ARITA, R., ITOH, K., MAEDA, S., MAEDA, K., FURUTA, A., TOMIDOKORO, A., AIHARA, M. & AMANO, S. 2012. Effects of long-term topical anti-glaucoma medications on meibomian glands. *Graefe's Archive for Clinical and Experimental Ophthalmology,* 250**,** 1181-1185.

ASHCROFT, G. S., MILLS, S. J., LEI, K., GIBBONS, L., JEONG, M. J., TANIGUCHI, M., BUROW, M., HORAN, M. A., WAHL, S. M. & NAKAYAMA, T. 2003. Estrogen modulates cutaneous wound healing by downregulating macrophage migration inhibitory factor. *The Journal of Clinical Investigation,* 111**,** 1309-1318.

ASHWORTH, J., BISWAS, S., WRAITH, E. & LLOYD, I. 2006. The ocular features of the mucopolysaccharidoses. *Eye,* 20**,** 553.

ASLAN, M., CORT, A. & YUCEL, I. 2008. Oxidative and nitrative stress markers in glaucoma. *Free Radical Biology and Medicine,* 45**,** 367-376.

ASPBERG, J., HEIJL, A., JÓHANNESSON, G., LINDÉN, C., ANDERSSON-GEIMER, S. & BENGTSSON, B. 2018. Intraocular Pressure Lowering Effect of Latanoprost as First-line Treatment for Glaucoma. *Journal of Glaucoma,* 27**,** 976-980.

BABIZHAYEV, M. A. & BRODSKAYA, M. W. 1989. Fibronectin detection in drainage outflow system of human eyes in ageing and progression of open-angle glaucoma. *Mechanisms of Ageing and Development,* 47**,** 145-57.

BACHER, M., METZ, C. N., CALANDRA, T., MAYER, K., CHESNEY, J., LOHOFF, M., GEMSA, D., DONNELLY, T. & BUCALA, R. 1996. An essential regulatory role for macrophage migration inhibitory factor in T-cell activation. *Proceedings of the National Academy of Sciences,* 93**,** 7849-7854.

BAILEY, J. N. C., YASPAN, B. L., PASQUALE, L. R., HAUSER, M. A., KANG, J. H., LOOMIS, S. J., BRILLIANT, M., BUDENZ, D. L., CHRISTEN, W. G. & FINGERT, J. 2014. Hypothesis-independent pathway analysis implicates GABA and acetyl-CoA

metabolism in primary open-angle glaucoma and normal-pressure glaucoma. *Human Genetics,* 133**,** 1319-1330.

BALAIYA, S., EDWARDS, J., TILLIS, T., KHETPAL, V. & CHALAM, K. V. 2011. Tumor necrosis factor-alpha (TNF-α) levels in aqueous humor of primary open angle glaucoma. *Clinical Ophthalmology (Auckland, NZ),* 5**,** 553.

BALAKRISHNAN, A., NEMERIA, N. S., CHAKRABORTY, S., KAKALIS, L. & JORDAN, F. 2012. Determination of pre-steady-state rate constants on the Escherichia coli pyruvate dehydrogenase complex reveals that loop movement controls the rate-limiting step. *Journal of the American Chemical Society,* 134**,** 18644-18655.

BANERJEE, J., LEUNG, C. T., LI, A., PETERSON-YANTORNO, K., OUYANG, H., STAMER, W. D. & CIVAN, M. M. 2017. Regulatory Roles of Anoctamin-6 in Human Trabecular Meshwork Cells. *Invest Ophthalmol Vis Sci,* 58**,** 492-501.

BÁRÁNY, E. H. 1962. The mode of action of pilocarpine on outflow resistance in the eye primate (Cercopithecus ethiops). *Investigative Ophthalmology & Visual Science,* 1**,** 712-727.

BECKER, B. 1960. Hypothermia and aqueous humor dynamics of the rabbit eye. *Transactions of the American Ophthalmological Society,* 58**,** 337.

BERGEÅ, B., BODIN, L. & SVEDBERGH, B. 1999. Impact of intraocular pressure regulation on visual fields in open-angle glaucoma. *Ophthalmology,* 106**,** 997-1004.

BHATTACHARYYA, S. & TOBACMAN, J. K. 2009. Arylsulfatase B regulates colonic epithelial cell migration by effects on MMP9 expression and RhoA activation. *Clinical & Experimental Metastasis,* 26**,** 535-545.

BHATTACHARYYA, S. & TOBACMAN, J. K. 2012. Hypoxia reduces arylsulfatase B activity and silencing arylsulfatase B replicates and mediates the effects of hypoxia. *PloS one,* 7.

BILL, A. 1975. Blood circulation and fluid dynamics in the eye. *Physiological Reviews,* 55**,** 383-417.

BILL, A. & PHILLIPS, C. I. 1971. Uveoscleral drainage of aqueous humour in human eyes. *Experimental Eye Research,* 12**,** 275-281.

BOUSSOMMIER CALLEJA, A., BERTRAND, J., WOODWARD, D. F., ETHIER, C. R., STAMER, W. D. & OVERBY, D. R. 2012. Pharmacologic Manipulation of Conventional Outflow Facility in Ex Vivo Mouse EyesManipulation of Outflow Facility in Mouse Eyes. *Investigative Ophthalmology & Visual Science,* 53**,** 5838-5845.

BOUSSOMMIER CALLEJA, A., LI, G., WILSON, A., ZISKIND, T., SCINTEIE, O. E., ASHPOLE, N. E., SHERWOOD, J. M., FARSIU, S., CHALLA, P. & GONZALEZ,

P. 2015. Physical factors affecting outflow facility measurements in mice. *Investigative Ophthalmology & Visual Science,* 56**,** 8331-8339.

BRADLEY, J., VRANKA, J., COLVIS, C. M., CONGER, D. M., ALEXANDER, J. P., FISK, A. S., SAMPLES, J. R. & ACOTT, T. S. 1998. Effect of matrix metalloproteinases activity on outflow in perfused human organ culture. *Investigative Ophthalmology & Visual Science,* 39**,** 2649-2658.

BRADLEY, J. M. B., KELLEY, M. J., ROSE, A. & ACOTT, T. S. 2003. Signaling Pathways Used in Trabecular Matrix Metalloproteinase Response to Mechanical Stretch. *Investigative Ophthalmology & Visual Science,* 44**,** 5174-5181.

BRADLEY, J. M. B., KELLEY, M. J., ZHU, X., ANDERSSOHN, A. M., ALEXANDER, J. P. & ACOTT, T. S. 2001. Effects of Mechanical Stretching on Trabecular Matrix Metalloproteinases. *Investigative Ophthalmology & Visual Science,* 42**,** 1505-1513.

BRYAN, A. K., ENGLER, A., GULATI, A. & MANALIS, S. R. 2012. Continuous and long-term volume measurements with a commercial Coulter counter. *PloS one,* 7**,** e29866.

BUCALA, R. 1996. MIF rediscovered: cytokine, pituitary hormone, and glucocorticoid-induced regulator of the immune response. *The FASEB Journal,* 10**,** 1607-1613.

BURGER KENTISCHER, A., GÖBEL, H., KLEEMANN, R., ZERNECKE, A., BUCALA, R., LENG, L., FINKELMEIER, D., GEIGER, G., SCHAEFER, H. E. & SCHOBER, A. 2006. Reduction of the aortic inflammatory response in spontaneous atherosclerosis by blockade of macrophage migration inhibitory factor (MIF). *Atherosclerosis,* 184**,** 28-38.

CAI, Y. Z., SUN, M., XING, J., LUO, Q. & CORKE, H. 2006. Structure–radical scavenging activity relationships of phenolic compounds from traditional Chinese medicinal plants. *Life Sciences,* 78**,** 2872-2888.

CALTHORPE, C. M. & GRIERSON, I. 1990. Fibronectin induces migration of bovine trabecular meshwork cells in vitro. *Experimental Eye Research,* 51**,** 39-48.

CARREON, T. A., CASTELLANOS, A., GASULL, X. & BHATTACHARYA, S. K. 2017. Interaction of cochlin and mechanosensitive channel TREK-1 in trabecular meshwork cells influences the regulation of intraocular pressure. *Scientific Reports,* 7**,** 1-11.

CAVALLO MEDVED, D., RUDY, D., BLUM, G., BOGYO, M., CAGLIC, D. & SLOANE, B. F. 2009. Live-cell imaging demonstrates extracellular matrix degradation in association with active cathepsin B in caveolae of endothelial cells during tube formation. *Experimental Cell Research,* 315**,** 1234-1246.

CHAN-LING, T., HUGHES, S., BAXTER, L., ROSINOVA, E., MCGREGOR, I., MORCOS, Y., VAN NIEUWENHUYZEN, P. & HU, P. 2007. Inflammation and breakdown of the blood–retinal barrier during "physiological aging" in the rat retina: a model for CNS aging. *Microcirculation,* 14**,** 63-76.

CHANDRASHEKAR, N., SELVAMANI, A., SUBRAMANIAN, R., PANDI, A. & THIRUVENGADAM, D. 2012. Baicalein inhibits pulmonary carcinogenesis-associated inflammation and interferes with COX-2, MMP-2 and MMP-9 expressions in-vivo. *Toxicology and Applied Pharmacology,* 261**,** 10-21.

CHANG, J. Y., STAMER, W. D., BERTRAND, J., READ, A. T., MARANDO, C. M., ETHIER, C. R. & OVERBY, D. R. 2015a. Role of nitric oxide in murine conventional outflow physiology. *American Journal of Physiology-Cell Physiology,* 309**,** C205-C214.

CHANG, K. H., WU, Y. R., CHEN, Y. C. & CHEN, C. M. 2015b. Plasma inflammatory biomarkers for Huntington's disease patients and mouse model. *Brain, Behavior, and Immunity,* 44**,** 121-127.

CHAO, H. M., CHUANG, M. J., LIU, J. H., LIU, X. Q., HO, L. K., PAN, W. H., ZHANG, X. M., LIU, C. M., TSAI, S. K. & KONG, C. W. 2013. Baicalein protects against retinal ischemia by antioxidation, antiapoptosis, downregulation of HIF-1α, VEGF, and MMP-9 and upregulation of HO-1. *Journal of Ocular Pharmacology and Therapeutics,* 29**,** 539-549.

CHAUHAN, B. C., PAN, J., ARCHIBALD, M. L., LEVATTE, T. L., KELLY, M. E. M. & TREMBLAY, F. O. 2002. Effect of Intraocular Pressure on Optic Disc Topography, Electroretinography, and Axonal Loss in a Chronic Pressure-Induced Rat Model of Optic Nerve Damage. *Investigative Ophthalmology & Visual Science,* 43**,** 2969-2976.

CHEN, S. F., HSU, C. W., HUANG, W. H. & WANG, J. Y. 2008. Post-injury baicalein improves histological and functional outcomes and reduces inflammatory cytokines after experimental traumatic brain injury. *British Journal of Pharmacology* 155**,** 1279-1296.

CHEN, W. P., XIONG, Y., HU, P. F., BAO, J. P. & WU, L. D. 2015. Baicalein inhibits MMPs expression via a MAPK-dependent mechanism in chondrocytes. *Cellular Physiology and Biochemistry,* 36**,** 325-333.

CHEN, Z. Y., SU, Y. L., LAU, C. W., LAW, W. I. & HUANG, Y. 1999. Endothelium-dependent contraction and direct relaxation induced by baicalein in rat mesenteric artery. *European Journal of Pharmacology,* 374**,** 41-47.

CHENG, A. K., CIVAN, M. M., TO, C. H. & DO, C. W. 2016. cAMP stimulates transepithelial short-circuit current and fluid transport across porcine ciliary epithelium. *Investigative Ophthalmology & Visual Science,* 57**,** 6784-6794.

CHENG, P. Y., LEE, Y. M., WU, Y. S., CHANG, T. W., JIN, J. S. & YEN, M. H. 2007. Protective effect of baicalein against endotoxic shock in rats in vivo and in vitro. *Biochemical pharmacology,* 73**,** 793-804.

CHIANG, P. C., CHOU, R. H., CHIEN, H. F., TSAI, T. & CHEN, C. T. 2013. Chloride intracellular channel 4 involves in the reduced invasiveness of cancer cells treated by photodynamic therapy. *Lasers in Surgery and Medicine,* 45**,** 38-47.

CHIU, Y. W., LIN, T. H., HUANG, W. S., TENG, C. Y., LIOU, Y. S., KUO, W. H., LIN, W. L., HUANG, H. I., TUNG, J. N., HUANG, C. Y., LIU, J. Y., WANG, W. H., HWANG, J. M. & KUO, H. C. 2011. Baicalein inhibits the migration and invasive properties of human hepatoma cells. *Toxicology and Applied Pharmacology,* 255**,** 316-326.

CHU, T. C. & CANDIA, O. A. 1988. Active transport of ascorbate across the isolated rabbit ciliary epithelium. *Investigative Ophthalmology & Visual Science,* 29**,** 594-599.

CHUDGAR, S. M., DENG, P., MADDALA, R., EPSTEIN, D. L. & RAO, P. V. 2006. Regulation of connective tissue growth factor expression in the aqueous humor outflow pathway. *Molecular Vision,* 12**,** 1117-1126.

COCA-PRADOS, M., GHOSH, S., GILULA, N. B. & KUMAR, N. M. 1992. Expression and cellular distribution of the al gap junction gene product in the ocular pigmented ciliary epithelium. *Current Eye Research,* 11**,** 113-122.

COLE, D. 1969. Evidence for active transport of chloride in ciliary epithelium of the rabbit. *Experimental Eye Research,* 8**,** 5-15.

COLEMAN, A. L. & MIGLIOR, S. 2008. Risk factors for glaucoma onset and progression. *Survey of Ophthalmology,* 53**,** S3-S10.

COLLABORATIVE NORMAL-TENSION GLAUCOMA STUDY GROUP 1998a. Comparison of glaucomatous progression between untreated patients with normal-tension glaucoma and patients with therapeutically reduced intraocular pressures. *American Journal of Ophthalmology,* 126**,** 487-497.

COLLABORATIVE NORMAL-TENSION GLAUCOMA STUDY GROUP 1998b. The effectiveness of intraocular pressure reduction in the treatment of normal-tension glaucoma. *American Journal of Ophthalmology,* 126**,** 498-505.

COMES, N., ABAD, E., MORALES, M., BORRÁS, T., GUAL, A. & GASULL, X. 2006. Identification and functional characterization of ClC-2 chloride channels in trabecular meshwork cells. *Experimental Eye Research,* 83**,** 877-889.

CONLON, R., SAHEB, H. & AHMED, I. I. K. 2017. Glaucoma treatment trends: a review. *Canadian Journal of Ophthalmology,* 52**,** 114-124.

COUNILLON, L., TOURET, N., BIDET, M., PETERSON-YANTORNO, K., COCA-PRADOS, M., STUART-TILLEY, A., WILHELM, S., ALPER, S. & CIVAN, M. 2000. Na+/H+ and Cl–/HCO 3–-antiporters of bovine pigmented ciliary epithelial cells. *Pflügers Archiv,* 440**,** 667-678.

CROSSON, C. E. 1995. Adenosine receptor activation modulates intraocular pressure in rabbits. *Journal of Pharmacology and Experimental Therapeutics,* 273**,** 320-326.

CROSSON, C. E. 2001. Intraocular pressure responses to the adenosine agonist cyclohexyladenosine: evidence for a dual mechanism of action. *Investigative Ophthalmology & Visual Science,* 42**,** 1837-1840.

CROSSON, C. E., SLOAN, C. F. & YATES, P. W. 2005. Modulation of conventional outflow facility by the adenosine A1 agonist N6-cyclohexyladenosine. *Investigative Ophthalmology & Visual Science,* 46**,** 3795-3799.

DE GROEF, L., VAN HOVE, I., DEKEYSTER, E., STALMANS, I. & MOONS, L. 2013. MMPs in the Trabecular Meshwork: Promising Targets for Future Glaucoma Therapies? *Investigative Ophthalmology & Visual Science,* 54**,** 7756-7763.

DE OLIVEIRA, M. R., NABAVI, S. F., HABTEMARIAM, S., ORHAN, I. E., DAGLIA, M. & NABAVI, S. M. 2015. The effects of baicalein and baicalin on mitochondrial function and dynamics: A review. *Pharmacological Research,* 100**,** 296-308.

DETRY-MOREL, M. 2006. Side effects of glaucoma medications. *Bulletin de la Société belge d'ophtalmologie,* 299**,** 27.

DINDA, B., DINDA, S., DASSHARMA, S., BANIK, R., CHAKRABORTY, A. & DINDA, M. 2017. Therapeutic potentials of baicalin and its aglycone, baicalein against inflammatory disorders. *European Journal of Medicinal Chemistry,* 131**,** 68-80.

DING, C., WANG, P. & TIAN, N. 2011. Effect of general anesthetics on IOP in elevated IOP mouse model. *Experimental Eye Research,* 92**,** 512-520.

DISMUKE, W. M. & ELLIS, D. Z. 2009. Activation of the BKCa channel increases outflow facility and decreases trabecular meshwork cell volume. *Journal of Ocular Pharmacology and Therapeutics,* 25**,** 309-314.

DISMUKE, W. M., LIANG, J., OVERBY, D. R. & STAMER, W. D. 2014. Concentration-related effects of nitric oxide and endothelin-1 on human trabecular meshwork cell contractility. *Experimental Eye Research,* 120**,** 28-35.

DISMUKE, W. M., MBADUGHA, C. C. & ELLIS, D. Z. 2008. NO-induced regulation of human trabecular meshwork cell volume and aqueous humor outflow facility involve the BKCa ion channel. *American Journal of Physiology-Cell Physiology,* 294**,** C1378-C1386.

DO, C. W. & CIVAN, M. M. 2004. Basis of chloride transport in ciliary epithelium. *The Journal of Membrane Biology,* 200**,** 1-13.

DO, C. W., LU, W., MITCHELL, C. H. & CIVAN, M. M. 2005. Inhibition of swelling-activated Cl- currents by functional anti-ClC-3 antibody in native bovine non-pigmented ciliary epithelial cells. *Investigative Ophthalmology & Visual Science,* 46**,** 948-55.

DO, C. W. & TO, C. H. 2000. Chloride secretion by bovine ciliary epithelium: a model of aqueous humor formation. *Investigative Ophthalmology & Visual Science,* 41**,** 1853-1860.

DON, M. 2003. The Coulter principle: foundation of an industry. *Journal of the Association for Laboratory Automation,* 8**,** 72-81.

DORVAL, V. & FRASER, P. E. 2007. SUMO on the road to neurodegeneration. *Biochimica et Biophysica Acta (BBA)-Molecular Cell Research,* 1773**,** 694-706.

DVORIANTCHIKOVA, G., DEGTEREV, A. & IVANOV, D. 2014. Retinal ganglion cell (RGC) programmed necrosis contributes to ischemia–reperfusion-induced retinal damage. *Experimental Eye Research,* 123**,** 1-7.

EGLER, R. A., FERNANDES, E., ROTHERMUND, K., SEREIKA, S., DE SOUZA-PINTO, N., JARUGA, P., DIZDAROGLU, M. & PROCHOWNIK, E. V. 2005. Regulation of reactive oxygen species, DNA damage, and c-Myc function by peroxiredoxin 1. *Oncogene,* 24**,** 8038.

EKINCI, M., CEYLAN, E., KELEŞ, S., ÇAĞATAY, H. H., APIL, A., TANYıLDıZ, B. & ULUDAG, G. 2014. Toxic effects of chronic mercury exposure on the retinal nerve fiber layer and macular and choroidal thickness in industrial mercury battery workers. *Medical Science Monitor: International Medical Journal of Experimental and Clinical Research,* 20**,** 1284.

ERGORUL, C., RAY, A., HUANG, W., WANG, D. Y., BEN, Y., CANTUTI-CASTELVETRI, I. & GROSSKREUTZ, C. L. 2010. Hypoxia Inducible Factor-1α (HIF-1α) and Some HIF-1 Target Genes are Elevated in Experimental Glaucoma. *Journal of Molecular Neuroscience,* 42**,** 183-191.

ETHIER, C. R. & CHAN, D. W.-H. 2001. Cationic ferritin changes outflow facility in human eyes whereas anionic ferritin does not. *Investigative Ophthalmology & Visual Science,* 42**,** 1795-1802.

EVANGELHO, K., MOGILEVSKAYA, M., LOSADA-BARRAGAN, M. & VARGAS-SANCHEZ, J. K. 2019. Pathophysiology of primary open-angle glaucoma from a neuroinflammatory and neurotoxicity perspective: a review of the literature. *International Ophthalmology,* 39**,** 259-271.

EVERS, D. L., CHAO, C.-F., WANG, X., ZHANG, Z., HUONG, S.-M. & HUANG, E.-S. 2005. Human cytomegalovirus-inhibitory flavonoids: studies on antiviral activity and mechanism of action. *Antiviral Research,* 68**,** 124-134.

FAN, G. W., ZHANG, Y., JIANG, X., ZHU, Y., WANG, B., SU, L., CAO, W., ZHANG, H. & GAO, X. 2013. Anti-inflammatory activity of baicalein in LPS-stimulated RAW264. 7 macrophages via estrogen receptor and NF-κB-dependent pathways. *Inflammation,* 36**,** 1584-1591.

FAUTSCH, M. P., BAHLER, C. K., VRABEL, A. M., HOWELL, K. G., LOEWEN, N., TEO, W. L., POESCHLA, E. M. & JOHNSON, D. H. 2006. Perfusion of His-Tagged Eukaryotic Myocilin Increases Outflow Resistance in Human Anterior Segments in

the Presence of Aqueous Humor. *Investigative Ophthalmology & Visual Science,* 47**,** 213-221.

FECHTNER, R. D. & WEINREB, R. N. 1994. Mechanisms of optic nerve damage in primary open angle glaucoma. *Survey of ophthalmology,* 39**,** 23-42.

FEDERICO, A., CARDAIOLI, E., DA POZZO, P., FORMICHI, P., GALLUS, G. N. & RADI, E. 2012. Mitochondria, oxidative stress and neurodegeneration. *Journal of the neurological sciences,* 322**,** 254-262.

FENG, Y., LI, L., ZHANG, X., ZHANG, Y., LIANG, Y., LV, J., FAN, Z., GUO, J., HONG, T. & JI, B. 2015. Hematopoietic pre-B cell leukemia transcription factor interacting protein is overexpressed in gastric cancer and promotes gastric cancer cell proliferation, migration, and invasion. *Cancer science,* 106**,** 1313-1322.

FERREIRA, S. M., LERNER, S. F., BRUNZINI, R., EVELSON, P. A. & LLESUY, S. F. 2004. Oxidative stress markers in aqueous humor of glaucoma patients. *American Journal of Ophthalmology,* 137**,** 62-69.

FIRUZI, O., MIRI, R., TAVAKKOLI, M. & SASO, L. 2011. Antioxidant therapy: current status and future prospects. *Current Medicinal Chemistry,* 18**,** 3871-3888.

FLAMMER, J., ORGÜL, S., COSTA, V. P., ORZALESI, N., KRIEGLSTEIN, G. K., SERRA, L. M., RENARD, J.-P. & STEFÁNSSON, E. 2002. The impact of ocular blood flow in glaucoma. *Progress in retinal and eye research,* 21**,** 359-393.

FLEISCHHAUER, J. C., MITCHELL, C. H., STAMER, W. D., KARL, M. O., PETERSON-YANTORNO, K. & CIVAN, M. M. 2003. Common actions of adenosine receptor agonists in modulating human trabecular meshwork cell transport. *The Journal of Membrane Biology,* 193**,** 121-36.

FONG, Y. C., HSU, S. F., WU, C. L., LI, T. M., KAO, S. T., TSAI, F. J., CHEN, W. C., LIU, S. C., WU, C. M. & TANG, C. H. 2009. Transforming growth factor-β1 increases cell migration and β1 integrin up-regulation in human lung cancer cells. *Lung Cancer,* 64**,** 13-21.

FOTI, M., PIATTELLI, M., BARATTA, M. T. & RUBERTO, G. 1996. Flavonoids, coumarins, and cinnamic acids as antioxidants in a micellar system. Structure− activity relationship. *Journal of Agricultural and Food Chemistry,* 44**,** 497-501.

FREDDO, T. F., CIVAN, M. & GONG, H. 2020. Aqueous Humor and the Dynamics of Its Flow: Mechanisms and Routes of Aqueous Humor Drainage. *Albert and Jakobiec's Principles and Practice of Ophthalmology***,** 1-45.

GABELT, B. A. T. & KAUFMAN, P. L. 2005. Changes in aqueous humor dynamics with age and glaucoma. *Progress in Retinal and Eye Research,* 24**,** 612-637.

GAO, D., TAWA, R., MASAKI, H., OKANO, Y. & SAKURAI, H. 1998. Protective effects of baicalein against cell damage by reactive oxygen species. *Chemical and Pharmaceutical Bulletin,* 46**,** 1383-1387.

GAO, Y., LU, J., ZHANG, Y., CHEN, Y., GU, Z. & JIANG, X. 2013. Baicalein attenuates bleomycin-induced pulmonary fibrosis in rats through inhibition of miR-21. *Pulmonary Pharmacology & Therapeutics,* 26**,** 649-654.

GAO, Y., SNYDER, S. A., SMITH, J. N. & CHEN, Y. C. 2016. Anticancer properties of baicalein: a review. *Medicinal Chemistry Research,* 25**,** 1515-1523.

GAO, Z., HUANG, K., YANG, X. & XU, H. 1999. Free radical scavenging and antioxidant activities of flavonoids extracted from the radix of Scutellaria baicalensis Georgi. *Biochimica et Biophysica Acta (BBA)-General Subjects,* 1472**,** 643-650.

GAREAU, J. R. & LIMA, C. D. 2010. The SUMO pathway: emerging mechanisms that shape specificity, conjugation and recognition. *Nature reviews Molecular cell biology,* 11**,** 861-871.

GARNOCK-JONES, K. P. 2014. Ripasudil: first global approval. *Drugs,* 74**,** 2211-2215.

GASIOROWSKI, K., LAMER-ZARAWSKA, E., LESZEK, J., PARVATHANENI, K., YENDLURI, B. B., BLACH-OLSZEWSKA, Z. & ALIEV, G. 2011. Flavones from root of Scutellaria baicalensis Georgi: drugs of the future in neurodegeneration? *CNS Neurol Disord Drug Targets,* 10**,** 184-91.

GASULL, X., FERRER, E., LLOBET, A., CASTELLANO, A., NICOLÁS, J. M., PALÉS, J. & GUAL, A. 2003. Cell Membrane Stretch Modulates the High-Conductance Ca2+-Activated K+ Channel in Bovine Trabecular Meshwork Cells. *Investigative Ophthalmology & Visual Science,* 44**,** 706-714.

GE, P., NAVARRO, I. D., KESSLER, M. M., BERNIER, S. G., PERL, N. R., SARNO, R., MASFERRER, J., HANNIG, G. & STAMER, W. D. 2016. The soluble guanylate cyclase stimulator IWP-953 increases conventional outflow facility in mouse eyes. *Investigative Ophthalmology & Visual Science,* 57**,** 1317-1326.

GEHR, B. T., WEISS, C. & PORZSOLT, F. 2006. The fading of reported effectiveness. A meta-analysis of randomised controlled trials. *BMC Medical Research Methodology,* 6**,** 25.

GHANEM, A. A., ARAFA, L. F. & EL-BAZ, A. 2010. Oxidative stress markers in patients with primary open-angle glaucoma. *Current Eye Research,* 35**,** 295-301.

GLYNN, I. M. 2002. A hundred years of sodium pumping. *Annual Review of Physiology,* 64**,** 1-18.

GOEL, M., PICCIANI, R. G., LEE, R. K. & BHATTACHARYA, S. K. 2010. Aqueous humor dynamics: a review. *The Open Ophthalmology Journal,* 4**,** 52.

GONG, H., TRIPATHI, R. C. & TRIPATHI, B. J. 1996. Morphology of the aqueous outflow pathway. *Microscopy Research and Technique,* 33**,** 336-67.

GONG, H. & YANG, C. Y. C. 2014. Morphological and hydrodynamic correlations with increasing outflow facility by rho-kinase inhibitor Y-27632. *Journal of Ocular Pharmacology and Therapeutics,* 30**,** 143-153.

GOULD, S. & SCOTT, R. C. 2005. 2-Hydroxypropyl-β-cyclodextrin (HP-β-CD): A toxicology review. *Food and Chemical Toxicology,* 43**,** 1451-1459.

GUAL, A., LLOBET, A., GILABERT, R., BORRAS, M., PALES, J., BERGAMINI, M. & BELMONTE, C. 1997. Effects of time of storage, albumin, and osmolality changes on outflow facility (C) of bovine anterior segment in vitro. *Investigative Ophthalmology & Visual Science,* 38**,** 2165-2171.

HALD, A. & LOTHARIUS, J. 2005. Oxidative stress and inflammation in Parkinson's disease: is there a causal link? *Experimental Neurology,* 193**,** 279-290.

HANNEKEN, A., LIN, F. F., JOHNSON, J. & MAHER, P. 2006. Flavonoids protect human retinal pigment epithelial cells from oxidative-stress-induced death. *Investigative Ophthalmology & Visual Science,* 47**,** 3164-77.

HARNETT, K. M. & BIANCANI, P. 2003. Calcium-dependent and calcium-independent contractions in smooth muscles. *The American Journal of Medicine,* 115**,** 24-30.

HE, X. L., WANG, Y. H., GAO, M., LI, X. X., ZHANG, T. T. & DU, G. H. 2009. Baicalein protects rat brain mitochondria against chronic cerebral hypoperfusion-induced oxidative damage. *Brain Research,* 1249**,** 212-221.

HE, Y., LEUNG, K. W., ZHANG, Y. H., DUAN, S., ZHONG, X. F., JIANG, R. Z., PENG, Z., TOMBRAN-TINK, J. & GE, J. 2008. Mitochondrial complex I defect induces ROS release and degeneration in trabecular meshwork cells of POAG patients: protection by antioxidants. *Investigative Ophthalmology & Visual Science,* 49**,** 1447-1458.

HEATON, J. H., DLAKIC, W. M., DLAKIC, M. & GELEHRTER, T. D. 2001. Identification and cDNA cloning of a novel RNA-binding protein that interacts with the cyclic nucleotide-responsive sequence in the Type-1 plasminogen activator inhibitor mRNA. *Journal of Biological Chemistry,* 276**,** 3341-3347.

HOARE, M. J., GRIERSON, I., BROTCHIE, D., POLLOCK, N., CRACKNELL, K. & CLARK, A. F. 2009. Cross-linked actin networks (CLANs) in the trabecular meshwork of the normal and glaucomatous human eye in situ. *Investigative Ophthalmology & Visual Science,* 50**,** 1255-63.

HOFFMANN, E. K., LAMBERT, I. H. & PEDERSEN, S. F. 2009. Physiology of cell volume regulation in vertebrates. *Physiological Reviews,* 89**,** 193-277.

HOGG, P., CALTHORPE, M., BATTERBURY, M. & GRIERSON, I. 2000. Aqueous humor stimulates the migration of human trabecular meshwork cells in vitro. *Investigative Ophthalmology & Visual Science,* 41**,** 1091-1098.

HOLMSTRÖM, K. M. & FINKEL, T. 2014. Cellular mechanisms and physiological consequences of redox-dependent signalling. *Nature reviews Molecular cell biology,* 15**,** 411.

HONJO, M., TANIHARA, H., INATANI, M., KIDO, N., SAWAMURA, T., YUE, B. Y. J. T., NARUMIYA, S. & HONDA, Y. 2001. Effects of rho-associated protein kinase inhibitor Y-27632 on intraocular pressure and outflow facility. *Investigative Ophthalmology & Visual Science,* 42**,** 137-144.

HONJO, M., TANIHARA, H., KAMEDA, T., KAWAJI, T., YOSHIMURA, N. & ARAIE, M. 2007. Potential role of Rho-associated protein kinase inhibitor Y-27632 in glaucoma filtration surgery. *Investigative Ophthalmology & Visual Science,* 48**,** 5549-5557.

HOY, S. M. 2018. Netarsudil ophthalmic solution 0.02%: first global approval. *Drugs,* 78**,** 389-396.

HSIEH, C. J., HALL, K., HA, T., LI, C., KRISHNASWAMY, G. & CHI, D. S. 2007. Baicalein inhibits IL-1β-and TNF-α-induced inflammatory cytokine production from human mast cells via regulation of the NF-κB pathway. *Clinical and Molecular Allergy,* 5**,** 5.

HSU, K. S., OTSU, W., LI, Y., WANG, H. C., CHEN, S., TSANG, S. H., CHUANG, J. Z. & SUNG, C. H. 2019. CLIC4 regulates late endosomal trafficking and matrix degradation activity of MMP14 at focal adhesions in RPE cells. *Scientific Reports,* 9**,** 1-17.

HUANG, H. L., WANG, Y. J., ZHANG, Q. Y., LIU, B., WANG, F. Y., LI, J. J. & ZHU, R. Z. 2012. Hepatoprotective effects of baicalein against CCl4-induced acute liver injury in mice. *World Journal of Gastroenterology,* 18**,** 6605.

HUANG, P., QI, Y., XU, Y. S., LIU, J., LIAO, D., ZHANG, S. S. M. & ZHANG, C. 2010. Serum cytokine alteration is associated with optic neuropathy in human primary open angle glaucoma. *Journal of Glaucoma,* 19**,** 324-330.

HUANG, Y., TSANG, S. Y., YAO, X. & CHEN, Z. Y. 2005. Biological properties of baicalein in cardiovascular system. *Current Drug Targets - Cardiovascular & Haematological Disorders,* 5**,** 177-84.

HUANG, Y., WONG, C. M., LAU, C.-W., YAO, X., TSANG, S. Y., SU, Y. L. & CHEN, Z. Y. 2004. Inhibition of nitric oxide/cyclic GMP-mediated relaxation by purified flavonoids, baicalin and baicalein, in rat aortic rings. *Biochemical Pharmacology,* 67**,** 787-794.

HUANG, Y., ZHANG, B., GAO, Y., ZHANG, J. & SHI, L. 2014. Baicalein–nicotinamide cocrystal with enhanced solubility, dissolution, and oral bioavailability. *Journal of Pharmaceutical Sciences,* 103**,** 2330-2337.

ICHHPUJANI, P. & KUMAR, S. 2019. What's New in Pathogenesis of Glaucoma. *Glaucoma.* Springer.

INOUE, K. 2014. Managing adverse effects of glaucoma medications. *Clinical Ophthalmology (Auckland, NZ),* 8**,** 903.

IZZOTTI, A., BAGNIS, A. & SACCÀ, S. C. 2006. The role of oxidative stress in glaucoma. *Mutation Research/Reviews in Mutation Research,* 612**,** 105-114.

IZZOTTI, A., SACCÀ, S. C., CARTIGLIA, C. & DE FLORA, S. 2003. Oxidative deoxyribonucleic acid damage in the eyes of glaucoma patients. *The American Journal of Medicine,* 114**,** 638-646.

IZZOTTI, A., SACCÀ, S. C., LONGOBARDI, M. & CARTIGLIA, C. 2010. Mitochondrial damage in the trabecular meshwork of patients with glaucoma. *Archives of Ophthalmology,* 128**,** 724-730.

JAFFER, U., WADE, R. & GOURLAY, T. 2010. Cytokines in the systemic inflammatory response syndrome: a review. *HSR Proceedings in Intensive Care & Cardiovascular Anesthesia,* 2**,** 161.

JIA, L., CEPURNA, W. O., JOHNSON, E. C. & MORRISON, J. C. 2000. Effect of general anesthetics on IOP in rats with experimental aqueous outflow obstruction. *Investigative Ophthalmology & Visual Science,* 41**,** 3415-3419.

JIN, G., ARAI, K., MURATA, Y., WANG, S., STINS, M. F., LO, E. H. & VAN LEYEN, K. 2008. Protecting against cerebrovascular injury: contributions of 12/15-lipoxygenase to edema formation after transient focal ischemia. *Stroke,* 39**,** 2538-43.

JOHNSON, M. 2006. What controls aqueous humour outflow resistance? *Experimental Eye Research,* 82**,** 545-557.

KANG, K. A., ZHANG, R., PIAO, M. J., CHAE, S., KIM, H. S., PARK, J. H., JUNG, K. S. & HYUN, J. W. 2012. Baicalein inhibits oxidative stress-induced cellular damage via antioxidant effects. *Toxicology and Industrial Health,* 28**,** 412-421.

KANNAN, K. & JAIN, S. K. 2000. Oxidative stress and apoptosis. *Pathophysiology,* 7**,** 153-163.

KAPETANAKIS, V. V., CHAN, M. P., FOSTER, P. J., COOK, D. G., OWEN, C. G. & RUDNICKA, A. R. 2016. Global variations and time trends in the prevalence of primary open angle glaucoma (POAG): a systematic review and meta-analysis. *British Journal of Ophthalmology,* 100**,** 86-93.

KELLER, K. E. & ACOTT, T. S. 2013. The juxtacanalicular region of ocular trabecular meshwork: a tissue with a unique extracellular matrix and specialized function. *Journal of ocular biology,* 1**,** 3.

KELLER, K. E., AGA, M., BRADLEY, J. M., KELLEY, M. J. & ACOTT, T. S. 2009. Extracellular matrix turnover and outflow resistance. *Experimental Eye Research,* 88**,** 676-682.

KELLER, K. E., BHATTACHARYA, S. K., BORRÁS, T., BRUNNER, T. M., CHANSANGPETCH, S., CLARK, A. F., DISMUKE, W. M., DU, Y., ELLIOTT, M. H. & ETHIER, C. R. 2018. Consensus recommendations for trabecular meshwork cell isolation, characterization and culture. *Experimental eye research,* 171**,** 164-173.

KIM, K. C., LEE, I. K., KANG, K. A., KIM, H. S., KANG, S. S. & HYUN, J. W. 2012. Baicalein (5, 6, 7-trihydroxyflavone) reduces oxidative stress-induced DNA damage by upregulating the DNA repair system. *Cell Biology and Toxicology,* 28**,** 421-433.

KIM, S. Y., KIM, T. J. & LEE, K. Y. 2008. A novel function of peroxiredoxin 1 (Prx-1) in apoptosis signal-regulating kinase 1 (ASK1)-mediated signaling pathway. *FEBS letters,* 582**,** 1913-1918.

KINOSHITA, T., NOHATA, N., WATANABE-TAKANO, H., YOSHINO, H., HIDAKA, H., FUJIMURA, L., FUSE, M., YAMASAKI, T., ENOKIDA, H. & NAKAGAWA, M. 2012. Actin-related protein 2/3 complex subunit 5 (ARPC5) contributes to cell migration and invasion and is directly regulated by tumor-suppressive microRNA-133a in head and neck squamous cell carcinoma. *International Journal of Oncology,* 40**,** 1770-1778.

KO, W. H., LAW, V., YIP, W., YUE, G., LAU, C. W., CHEN, Z. Y. & HUANG, Y. 2002. Stimulation of chloride secretion by baicalein in isolated rat distal colon. *American Journal of Physiology-Gastrointestinal and Liver Physiology,* 282**,** G508-G518.

KOBAYASHI, Y., NOJIMA, Y., SAKAMOTO, T., IWABUCHI, K., NAKAZATO, T., BONO, H., TOYODA, A., FUJIYAMA, A., KANOST, M. R. & TABUNOKI, H. 2019. Comparative analysis of seven types of superoxide dismutases for their ability to respond to oxidative stress in Bombyx mori. *Scientific Reports,* 9**,** 1-12.

KODAMA, T., REDDY, V. & MACRI, F. 1985. Pharmacological study on the effects of some ocular hypotensive drugs on aqueous humor formation in the arterially perfused enucleated rabbit eye. *Ophthalmic Research,* 17**,** 120-124.

KOGA, T., KOGA, T., AWAI, M., TSUTSUI, J. I., YUE, B. Y. J. T. & TANIHARA, H. 2006. Rho-associated protein kinase inhibitor, Y-27632, induces alterations in adhesion, contraction and motility in cultured human trabecular meshwork cells. *Experimental Eye Research,* 82**,** 362-370.

KONG, C. W., LI, K. K. & TO, C. H. 2006. Chloride secretion by porcine ciliary epithelium: new insight into species similarities and differences in aqueous humor formation. *Investigative Ophthalmology & Visual Science,* 47**,** 5428-5436.

KONG, G. Y., VAN BERGEN, N. J., TROUNCE, I. A. & CROWSTON, J. G. 2009. Mitochondrial dysfunction and glaucoma. *Journal of Glaucoma,* 18**,** 93-100.

KOWALINSKI, E., BANGE, G., BRADATSCH, B., HURT, E., WILD, K. & SINNING, I. 2007. The crystal structure of Ebp1 reveals a methionine aminopeptidase fold as binding platform for multiple interactions. *FEBS letters,* 581**,** 4450-4454.

KRUPIN, T., REINACH, P. S., CANDIA, O. A. & PODOS, S. M. 1984. Transepithelial electrical measurements on the isolated rabbit iris-ciliary body. *Experimental Eye Research,* 38**,** 115-123.

KUBISTA, M., ANDRADE, J. M., BENGTSSON, M., FOROOTAN, A., JONÁK, J., LIND, K., SINDELKA, R., SJÖBACK, R., SJÖGREEN, B. & STRÖMBOM, L. 2006. The real-time polymerase chain reaction. *Molecular Aspects of Medicine,* 27**,** 95-125.

KUCHTEY, J., REZAEI, K. A., JARU-AMPORNPAN, P., STERNBERG, P. & KUCHTEY, R. W. 2010. Multiplex cytokine analysis reveals elevated concentration of interleukin-8 in glaucomatous aqueous humor. *Investigative Ophthalmology & Visual Science,* 51**,** 6441-6447.

KUMAR, A. & SONG, Z. H. 2006. CB1 cannabinoid receptor-mediated changes of trabecular meshwork cellular properties. *Molecular Vision,* 12**,** 290-297.

KWON, H. S. & TOMAREV, S. I. 2011. Myocilin, a glaucoma-associated protein, promotes cell migration through activation of integrin-focal adhesion kinase-serine/threonine kinase signaling pathway. *Journal of Cellular Physiology,* 226**,** 3392-3402.

LAINE, K., JÄRVINEN, K., MECHOULAM, R., BREUER, A. & JÄRVINEN, T. 2002. Comparison of the enzymatic stability and intraocular pressure effects of 2-arachidonylglycerol and noladin ether, a novel putative endocannabinoid. *Investigative Ophthalmology & Visual Science,* 43**,** 3216-3222.

LAO, Y., WANG, X., XU, N., ZHANG, H. & XU, H. 2014. Application of proteomics to determine the mechanism of action of traditional Chinese medicine remedies. *Journal of Ethnopharmacology,* 155**,** 1-8.

LAPCHAK, P., MAHER, P., SCHUBERT, D. & ZIVIN, J. 2007. Baicalein, an antioxidant 12/15-lipoxygenase inhibitor improves clinical rating scores following multiple infarct embolic strokes. *Neuroscience,* 150**,** 585-591.

LARKINS, T. L., NOWELL, M., SINGH, S. & SANFORD, G. L. 2006. Inhibition of cyclooxygenase-2 decreases breast cancer cell motility, invasion and matrix metalloproteinase expression. *BMC Cancer,* 6**,** 181.

LAST, J. A., PAN, T., DING, Y., REILLY, C. M., KELLER, K., ACOTT, T. S., FAUTSCH, M. P., MURPHY, C. J. & RUSSELL, P. 2011. Elastic modulus determination of normal and glaucomatous human trabecular meshwork. *Investigative Ophthalmology & Visual Science,* 52**,** 2147-2152.

LEBEAU, A., ESCLAIRE, F., ROSTÈNE, W. & PÉLAPRAT, D. 2001. Baicalein protects cortical neurons from β-amyloid (25-35) induced toxicity. *Neuroreport,* 12**,** 2199-2202.

LEE, D. A. & HIGGINBOTHAM, E. J. 2005. Glaucoma and its treatment: a review. *American Journal of Health-System Pharmacy,* 62**,** 691-699.

LEE, D. H., KIM, C., ZHANG, L. & LEE, Y. J. 2008. Role of p53, PUMA, and Bax in wogonin-induced apoptosis in human cancer cells. *Biochemical Pharmacology,* 75**,** 2020-2033.

LEE, W., KU, S. K. & BAE, J. S. 2015. Anti-inflammatory effects of Baicalin, Baicalein, and Wogonin in vitro and in vivo. *Inflammation,* 38**,** 110-125.

LEI, Y., OVERBY, D. R., BOUSSOMMIER-CALLEJA, A., STAMER, W. D. & ETHIER, C. R. 2011. Outflow physiology of the mouse eye: pressure dependence and washout. *Investigative Ophthalmology & Visual Science,* 52**,** 1865-1871.

LEUNG, Y. F., TAM, P., LEE, W. S., LAM, D., YAM, H. F., FAN, B. J., THAM, C., CHUA, J. & PANG, C. P. 2003. The dual role of dexamethasone on anti-inflammation and outflow resistance demonstrated in cultured human trabecular meshwork cells. *Molecular Vision,* 9**,** 425-39.

LI, A., LEUNG, C. T., PETERSON-YANTORNO, K., STAMER, W. D. & CIVAN, M. M. 2011a. Cytoskeletal dependence of adenosine triphosphate release by human trabecular meshwork cells. *Investigative Ophthalmology & Visual Science,* 52**,** 7996-8005.

LI, A., LEUNG, C. T., PETERSON-YANTORNO, K., STAMER, W. D., MITCHELL, C. H. & CIVAN, M. M. 2012. Mechanisms of ATP release by human trabecular meshwork cells, the enabling step in purinergic regulation of aqueous humor outflow. *Journal of Cellular Physiology,* 227**,** 172-182.

LI, A. F., TANE, N. & ROY, S. 2004. Fibronectin overexpression inhibits trabecular meshwork cell monolayer permeability. *Molecular Vision,* 10**,** 750-7.

LI, C., LIN, G. & ZUO, Z. 2011b. Pharmacological effects and pharmacokinetics properties of Radix Scutellariae and its bioactive flavones. *Biopharmaceutics & Drug Disposition,* 32**,** 427-445.

LI, G., LUNA, C., LITON, P. B., NAVARRO, I., EPSTEIN, D. L. & GONZALEZ, P. 2007. Sustained stress response after oxidative stress in trabecular meshwork cells. *Molecular Vision,* 13**,** 2282-2288.

LI, G., MUKHERJEE, D., NAVARRO, I., ASHPOLE, N. E., SHERWOOD, J. M., CHANG, J., OVERBY, D. R., YUAN, F., GONZALEZ, P. & KOPCZYNSKI, C. C. 2016. Visualization of conventional outflow tissue responses to netarsudil in living mouse eyes. *European Journal of Pharmacology,* 787**,** 20-31.

LI, H. B. & CHEN, F. 2005. Isolation and purification of baicalein, wogonin and oroxylin A from the medicinal plant Scutellaria baicalensis by high-speed counter-current chromatography. *Journal of Chromatography. A,* 1074**,** 107-110.

LI, M., SHI, A., PANG, H., XUE, W., LI, Y., CAO, G., YAN, B., DONG, F., LI, K., XIAO, W., HE, G., DU, G. & HU, X. 2014. Safety, tolerability, and pharmacokinetics of a single ascending dose of baicalein chewable tablets in healthy subjects. *Journal of Ethnopharmacology,* 156**,** 210-215.

LI, Y., ZHAO, J. & HOLSCHER, C. 2017. Therapeutic Potential of Baicalein in Alzheimer's Disease and Parkinson's Disease. *CNS Drugs,* 31**,** 639-652.

LIANG, W., HUANG, X. & CHEN, W. 2017. The Effects of Baicalin and Baicalein on Cerebral Ischemia: A Review. *Aging and Disease,* 8**,** 850-867.

LIN, J. S. & LIU, J. H. K. 2010. Circadian Variations in Intracranial Pressure and Translaminar Pressure Difference in Sprague-Dawley Rats. *Investigative Ophthalmology & Visual Science,* 51**,** 5739-5743.

LIN, S., JIANG, T., YU, Y., TANG, H., LU, S., PENG, Z. & FAN, J. 2015. Secernin-1 contributes to colon cancer progression through enhancing matrix metalloproteinase-2/9 exocytosis. *Disease Markers,* 2015.

LIN, S. Y., HSU, W. H., LIN, C. C. & CHEN, C. J. 2014. Mass spectrometry-based proteomics in Chest Medicine, Gerontology, and Nephrology: subgroups omics for personalized medicine. *Biomedicine (Taipei),* 4**,** 25.

LINDÉN, C., HEIJL, A., JÓHANNESSON, G., ASPBERG, J., ANDERSSON GEIMER, S. & BENGTSSON, B. 2018. Initial intraocular pressure reduction by mono-versus multi-therapy in patients with open-angle glaucoma: results from the Glaucoma Intensive Treatment Study. *Acta Ophthalmologica,* 96**,** 567-572.

LINDSEY, M. L. 2018. Assigning matrix metalloproteinase roles in ischaemic cardiac remodelling. *Nature Reviews Cardiology,* 15**,** 471-479.

LIU, C., WU, J., XU, K., CAI, F., GU, J., MA, L. & CHEN, J. 2010a. Neuroprotection by baicalein in ischemic brain injury involves PTEN/AKT pathway. *Journal of Neurochemistry,* 112**,** 1500-12.

LIU, H., DONG, Y., GAO, Y., DU, Z., WANG, Y., CHENG, P., CHEN, A. & HUANG, H. 2016. The fascinating effects of baicalein on cancer: a review. *International Journal of Molecular Sciences,* 17**,** 1681.

LIU, J., QIU, L., GAO, J. & JIN, Y. 2006a. Preparation, characterization and in vivo evaluation of formulation of baicalein with hydroxypropyl-β-cyclodextrin. *International Journal of Pharmaceutics,* 312**,** 137-143.

LIU, J. H., WANN, H., CHEN, M. M., PAN, W. T., CHEN, Y. C., LIU, C. M., YEH, M. Y., TSAI, S. K., YOUNG, M. S., CHUANG, H. Y., CHAO, F. P. & CHAO, H. M. 2010b. Baicalein Significantly Protects Human Retinal Pigment Epithelium Cells Against H 2 O 2 -Induced Oxidative Stress by Scavenging Reactive Oxygen Species and Downregulating the Expression of Matrix Metalloproteinase-9 and Vascular Endothelial Growth Factor. *Journal of Ocular Pharmacology and Therapeutics,* 26**,** 421-429.

LIU, J. J., HUANG, T. S., CHENG, W. F. & LU, F. J. 2003. Baicalein and baicalin are potent inhibitors of angiogenesis: inhibition of endothelial cell proliferation, migration and differentiation. *International Journal of Cancer,* 106**,** 559-565.

LIU, P. F., HAN, F. G., DUAN, B. B., DENG, T. S., HOU, X. L. & ZHAO, M. Q. 2013. Purification and antioxidant activities of baicalin isolated from the root of huangqin

(Scutellaria baicalensis gcorsi). *Journal of Food Science and Technology,* 50**,** 615-619.

LIU, Z., AHN, J. Y., LIU, X. & YE, K. 2006b. Ebp1 isoforms distinctively regulate cell survival and differentiation. *Proceedings of the National Academy of Sciences,* 103**,** 10917-10922.

LLOBET, A., GASULL, X. & GUAL, A. 2003. Understanding trabecular meshwork physiology: a key to the control of intraocular pressure? *News in Physiological Sciences,* 18**,** 205-9.

LU, Y., ZHANG, X. S., ZHOU, X. M., GAO, Y. Y., CHEN, C. L., LIU, J. P., YE, Z. N., ZHANG, Z. H., WU, L. Y. & LI, W. 2019. Peroxiredoxin 1/2 protects brain against H2O2-induced apoptosis after subarachnoid hemorrhage. *The FASEB Journal,* 33**,** 3051-3062.

LU, Z., OVERBY, D. R., SCOTT, P. A., FREDDO, T. F. & GONG, H. 2008. The mechanism of increasing outflow facility by rho-kinase inhibition with Y-27632 in bovine eyes. *Experimental Eye Research,* 86**,** 271-281.

LUNA, C., LI, G., HUANG, J., QIU, J., WU, J., YUAN, F., EPSTEIN, D. L. & GONZALEZ, P. 2012. Regulation of trabecular meshwork cell contraction and intraocular pressure by miR-200c. *PloS one,* 7**,** e51688.

LUTJEN-DRECOLL, E., FUTA, R. & ROHEN, J. W. 1981. Ultrahistochemical studies on tangential sections of the trabecular meshwork in normal and glaucomatous eyes. *Investigative Ophthalmology & Visual Science,* 21**,** 563-73.

MÄÄTTÄ, M., TERVAHARTIALA, T., HARJU, M., AIRAKSINEN, J., AUTIO-HARMAINEN, H. & SORSA, T. 2005. Matrix metalloproteinases and their tissue inhibitors in aqueous humor of patients with primary open-angle glaucoma, exfoliation syndrome, and exfoliation glaucoma. *Journal of Glaucoma,* 14**,** 64-69.

MACHESKY, L. M. & GOULD, K. L. 1999. The Arp2/3 complex: a multifunctional actin organizer. *Current Opinion In Cell Biology,* 11**,** 117-121.

MÄEPEA, O. & BILL, A. 1989. The pressures in the episcleral veins, Schlemm's canal and the trabecular meshwork in monkeys: effects of changes in intraocular pressure. *Experimental Eye Research,* 49**,** 645-663.

MAHER, P. & HANNEKEN, A. 2005. Flavonoids protect retinal ganglion cells from oxidative stress-induced death. *Investigative Ophthalmology & Visual Science,* 46**,** 4796-803.

MAHMOOD, T. & YANG, P.-C. 2012. Western blot: technique, theory, and trouble shooting. *North American Journal of Medical Sciences,* 4**,** 429.

MAJUMDAR, S. & SRIRANGAM, R. 2010. Potential of the bioflavonoids in the prevention/treatment of ocular disorders. *Journal of Pharmacy and Pharmacology,* 62**,** 951-965.

MALINDA, K., GOLDSTEIN, A. & KLEINMAN, H. 1997. Thymosin beta 4 stimulates directional migration of human umbilical vein endothelial cells. *The FASEB Journal,* 11**,** 474-481.

MALINDA, K. M., KLEINMAN, H. K., SIDHU, G. S., MANI, H., BANAUDHA, K., MAHESHWARI, R. K. & GOLDSTEIN, A. L. 1999. Thymosin β4 Accelerates Wound Healing. *Journal of Investigative Dermatology,* 113**,** 364-368.

MANAVATHI, B., LO, D., BUGIDE, S., DEY, O., IMREN, S., WEISS, M. J. & HUMPHRIES, R. K. 2012. Functional regulation of pre-B-cell leukemia homeobox interacting protein 1 (PBXIP1/HPIP) in erythroid differentiation. *Journal of Biological Chemistry,* 287**,** 5600-5614.

MAO, J., CHEN, L., XU, B., WANG, L., WANG, W., LI, M., ZHENG, M., LI, H., GUO, J., LI, W., JACOB, T. J. C. & WANG, L. 2009. Volume-activated chloride channels contribute to cell-cycle-dependent regulation of HeLa cell migration. *Biochemical Pharmacology,* 77**,** 159-168.

MAO, J., WANG, L., FAN, A., WANG, J., XU, B., JACOB, T. & CHEN, L. 2007. Blockage of volume-activated chloride channels inhibits migration of nasopharyngeal carcinoma cells. *Cellular Physiology and Biochemistry,* 19**,** 249-258.

MARSHALL, W. S., BRYSON, S. E. & GARG, D. 1993. Alpha 2-adrenergic inhibition of Cl-transport by opercular epithelium is mediated by intracellular Ca2+. *Proceedings of the National Academy of Sciences,* 90**,** 5504-5508.

MARTIN, E., ROSENTHAL, R. E. & FISKUM, G. 2005. Pyruvate dehydrogenase complex: metabolic link to ischemic brain injury and target of oxidative stress. *Journal of Neuroscience Research,* 79**,** 240-247.

MARTÍNEZ-BELLÓ, C., CHAUHAN, B. C., NICOLELA, M. T., MCCORMICK, T. A. & LEBLANC, R. P. 2000. Intraocular pressure and progression of glaucomatous visual field loss. *American Journal of Ophthalmology,* 129**,** 302-308.

MATTSON, M. P. 2000. Apoptosis in neurodegenerative disorders. *Nature Reviews Molecular Cell Biology,* 1**,** 120-130.

MAYNE, S. T. 2003. Antioxidant nutrients and chronic disease: use of biomarkers of exposure and oxidative stress status in epidemiologic research. *The Journal of Nutrition,* 133**,** 933S-940S.

MEDEIROS, F. A., ALENCAR, L. M., ZANGWILL, L. M., SAMPLE, P. A. & WEINREB, R. N. 2009. The relationship between intraocular pressure and progressive retinal nerve fiber layer loss in glaucoma. *Ophthalmology,* 116**,** 1125-1133. e3.

MENICE, C. B., HULVERSHORN, J., ADAM, L. P., WANG, C.-L. A. & MORGAN, K. G. 1997. Calponin and mitogen-activated protein kinase signaling in differentiated vascular smooth muscle. *Journal of Biological Chemistry,* 272**,** 25157-25161.

MERK, M., ZIEROW, S., LENG, L., DAS, R., DU, X., SCHULTE, W., FAN, J., LUE, H., CHEN, Y. & XIONG, H. 2011. The D-dopachrome tautomerase (DDT) gene product is a cytokine and functional homolog of macrophage migration inhibitory factor (MIF). *Proceedings of the National Academy of Sciences,* 108**,** E577-E585.

MEYER-TER-VEHN, T., SIEPRATH, S., KATZENBERGER, B., GEBHARDT, S., GREHN, F. & SCHLUNCK, G. N. 2006. Contractility as a prerequisite for TGF-β–induced myofibroblast transdifferentiation in human tenon fibroblasts. *Investigative Ophthalmology & Visual Science,* 47**,** 4895-4904.

MIEKUS, N., LUISE, C., SIPPL, W., BACZEK, T., SCHMELZER, C. E. & HEINZ, A. 2019. MMP-14 degrades tropoelastin and elastin. *Biochimie,* 165**,** 32-39.

MILLAR, J. C., CLARK, A. F. & PANG, I.-H. 2011. Assessment of aqueous humor dynamics in the mouse by a novel method of constant-flow infusion. *Investigative Ophthalmology & Visual Science,* 52**,** 685-694.

MILLARD, L. H., WOODWARD, D. F. & STAMER, W. D. 2011. The role of the prostaglandin EP4 receptor in the regulation of human outflow facility. *Investigative Ophthalmology & Visual Science,* 52**,** 3506-13.

MIN, L. W. 2009. New therapeutic aspects of flavones: the anticancer properties of Scutellaria and its main active constituents Wogonin, Baicalein and Baicalin. *Cancer Treatment Reviews,* 35**,** 57-68.

MITCHELL, C. H., FLEISCHHAUER, J. C., STAMER, W. D., PETERSON-YANTORNO, K. & CIVAN, M. M. 2002. Human trabecular meshwork cell volume regulation. *American Journal of Physiology-Cell Physiology,* 283**,** C315-C326.

MITSUNAGA-NAKATSUBO, K., KUSUNOKI, S., KAWAKAMI, H., AKASAKA, K. & AKIMOTO, Y. 2009. Cell-surface arylsulfatase A and B on sinusoidal endothelial cells, hepatocytes, and Kupffer cells in mammalian livers. *Medical Molecular Morphology,* 42**,** 63-69.

MOON, Y. J., WANG, X. & MORRIS, M. E. 2006. Dietary flavonoids: effects on xenobiotic and carcinogen metabolism. *Toxicology in Vitro,* 20**,** 187-210.

MORGAN, J. E. & TRIBBLE, J. R. 2015. Microbead models in glaucoma. *Experimental Eye Research,* 141**,** 9-14.

MORGAN, W. H., YU, D. Y., COOPER, R. L., ALDER, V. A., CRINGLE, S. J. & CONSTABLE, I. J. 1995. The influence of cerebrospinal fluid pressure on the lamina cribrosa tissue pressure gradient. *Investigative Ophthalmology & Visual Science,* 36**,** 1163-1172.

MOSMANN, T. 1983. Rapid colorimetric assay for cellular growth and survival: application to proliferation and cytotoxicity assays. *Journal of Immunological Methods,* 65**,** 55-63.

MOZAFFARIEH, M., GRIESHABER, M. C. & FLAMMER, J. 2008. Oxygen and blood flow: players in the pathogenesis of glaucoma. *Molecular Vision,* 14**,** 224.

MU, X., HE, G., CHENG, Y., LI, X., XU, B. & DU, G. 2009. Baicalein exerts neuroprotective effects in 6-hydroxydopamine-induced experimental parkinsonism in vivo and in vitro. *Pharmacology Biochemistry and Behavior,* 92**,** 642-648.

MU, Z. M., YIN, X. Y. & PROCHOWNIK, E. V. 2002. Pag, a putative tumor suppressor, interacts with the Myc Box II domain of c-Myc and selectively alters its biological function and target gene expression. *Journal of Biological Chemistry,* 277**,** 43175-84.

NAKAJIMA, E., NAKAJIMA, T., MINAGAWA, Y., SHEARER, T. R. & AZUMA, M. 2005. Contribution of ROCK in contraction of trabecular meshwork: proposed mechanism for regulating aqueous outflow in monkey and human eyes. *Journal of Pharmaceutical Sciences,* 94**,** 701-708.

NAKAMURA, Y., HIRANO, S., SUZUKI, K., SEKI, K., SAGARA, T. & NISHIDA, T. 2002. Signaling Mechanism of TGF-β1–Induced Collagen Contraction Mediated by Bovine Trabecular Meshwork Cells. *Investigative Ophthalmology & Visual Science,* 43**,** 3465-3472.

NCBI, N. C. F. B. I. *Nucleotide* [Online]. Available: https://www.ncbi.nlm.nih.gov/nucleotide/ [Accessed 2019].

NCBI, N. C. F. B. I. *Primer- BLAST* [Online]. Available: https://www.ncbi.nlm.nih.gov/tools/primer-blast/ [Accessed 2019].

NETTESHEIM, A., SHIM, M. S., DIXON, A., RAYCHAUDHURI, U., GONG, H. & LITON, P. B. 2021. Cathepsin B Localizes in the Caveolae and Participates in the Proteolytic Cascade in Trabecular Meshwork Cells. Potential New Drug Target for the Treatment of Glaucoma. *Journal of Clinical Medicine,* 10**,** 78.

NEUMANN, C. A., CAO, J. & MANEVICH, Y. 2009. Peroxiredoxin 1 and its role in cell signaling. *Cell Cycle,* 8**,** 4072-4078.

NJIE, Y. F., KUMAR, A., QIAO, Z., ZHONG, L. & SONG, Z. H. 2006. Noladin ether acts on trabecular meshwork cannabinoid (CB1) receptors to enhance aqueous humor outflow facility. *Investigative Ophthalmology & Visual Science,* 47**,** 1999-2005.

O'DONNELL, M. E., BRANDT, J. D. & CURRY, F. 1995. Na-K-Cl cotransport regulates intracellular volume and monolayer permeability of trabecular meshwork cells. *American Journal of Physiology-Cell Physiology,* 268**,** C1067-C1074.

OBERMAJER, N., JEVNIKAR, Z., DOLJAK, B. & KOS, J. 2008. Role of cysteine cathepsins in matrix degradation and cell signalling. *Connective Tissue Research,* 49**,** 193-196.

OH, K. S., OH, B. K., PARK, C. H., MUN, J., WON, S. H. & LEE, B. H. 2012. Baicalein potently inhibits Rho kinase activity and suppresses actin stress fiber formation in

angiotensin II-stimulated H9c2 cells. *Biological and Pharmaceutical Bulletin,* 35**,** 1281-1286.

OKADA, M., JANG, S. W. & YE, K. 2007. Ebp1 association with nucleophosmin/B23 is essential for regulating cell proliferation and suppressing apoptosis. *Journal of Biological Chemistry,* 282**,** 36744-36754.

ONG, E. S. & LEN, S. M. 2003. Pressurized hot water extraction of berberine, baicalein and glycyrrhizin in medicinal plants. *Analytica Chimica Acta,* 482**,** 81-89.

OVERBY, D. R., BERTRAND, J., SCHICHT, M., PAULSEN, F., STAMER, W. D. & LÜTJEN-DRECOLL, E. 2014a. The structure of the trabecular meshwork, its connections to the ciliary muscle, and the effect of pilocarpine on outflow facility in mice. *Investigative Ophthalmology & Visual Science,* 55**,** 3727-3736.

OVERBY, D. R., BERTRAND, J., TEKTAS, O. Y., BOUSSOMMIER-CALLEJA, A., SCHICHT, M., ETHIER, C. R., WOODWARD, D. F., STAMER, W. D. & LÜTJEN-DRECOLL, E. 2014b. Ultrastructural changes associated with dexamethasone-induced ocular hypertension in mice. *Investigative Ophthalmology & Visual Science,* 55**,** 4922-4933.

OVERBY, D. R., STAMER, W. D. & JOHNSON, M. 2009. The changing paradigm of outflow resistance generation: towards synergistic models of the JCT and inner wall endothelium. *Experimental Eye Research,* 88**,** 656-670.

PAN, J., QIN, Y. & ZHANG, M. 2016. HPIP promotes non-small cell lung cancer cell proliferation, migration and invasion through regulation of the Sonic hedgehog signaling pathway. *Biomedicine & Pharmacotherapy,* 77**,** 176-181.

PAN, P., SHEN, M., YU, H., LI, Y., LI, D. & HOU, T. 2013. Advances in the development of Rho-associated protein kinase (ROCK) inhibitors. *Drug Discovery Today,* 18**,** 1323-1333.

PANG, H., XUE, W., SHI, A., LI, M., LI, Y., CAO, G., YAN, B., DONG, F., XIAO, W., HE, G., DU, G., HU, X. & CHENG, G. 2016. Multiple-Ascending-Dose Pharmacokinetics and Safety Evaluation of Baicalein Chewable Tablets in Healthy Chinese Volunteers. *Clinical Drug Investigation,* 36**,** 713-724.

PANG, I. H. & CLARK, A. F. 2008. Outflow Signaling Mechanisms and New Therapeutic Strategies for the Control of Intraocular Pressure. *In:* CIVAN, M. M. (ed.) *The Eye's Aqueous Humor.* San Diego: Academic Press.

PARK, C., CHOI, E. O., KIM, G. Y., HWANG, H. J., KIM, B. W., YOO, Y. H., PARK, H. T. & CHOI, Y. H. 2019. Protective effect of baicalein on oxidative stress-induced DNA damage and apoptosis in RT4-D6P2T schwann cells. *International Journal of Medical Sciences,* 16**,** 8.

PARK, C. Y., LEE, J. K., KAHOOK, M. Y., SCHULTZ, J. S., ZHANG, C. & CHUCK, R. S. 2016. Revisiting ciliary muscle tendons and their connections with the trabecular

meshwork by two photon excitation microscopic imaging. *Investigative Ophthalmology & Visual Science,* 57**,** 1096-1105.

PAWLAK, K., PAWLAK, D. & MYSLIWIEC, M. 2005. Cu/Zn superoxide dismutase plasma levels as a new useful clinical biomarker of oxidative stress in patients with end-stage renal disease. *Clinical Biochemistry,* 38**,** 700-705.

PENA, J. D., AGAPOVA, O., B'ANN, T. G., LEVIN, L. A., LUCARELLI, M. J., KAUFMAN, P. L. & HERNANDEZ, M. R. 2001. Increased elastin expression in astrocytes of the lamina cribrosa in response to elevated intraocular pressure. *Investigative Ophthalmology & Visual Science,* 42**,** 2303-2314.

PEREZ, C. A., WEI, Y. & GUO, M. 2009. Iron-binding and anti-Fenton properties of baicalein and baicalin. *Journal of Inorganic Biochemistry,* 103**,** 326-332.

PLANGE, N., KAUP, M., AREND, O. & REMKY, A. 2006. Asymmetric visual field loss and retrobulbar haemodynamics in primary open-angle glaucoma. *Graefe's Archive for Clinical and Experimental Ophthalmology,* 244**,** 978-983.

PO, L. S., CHEN, Z. Y., TSANG, D. S. & LEUNG, L. K. 2002. Baicalein and genistein display differential actions on estrogen receptor (ER) transactivation and apoptosis in MCF-7 cells. *Cancer Letters,* 187**,** 33-40.

POCERNICH, C. B. & BUTTERFIELD, D. A. 2003. Acrolein inhibits NADH-linked mitochondrial enzyme activity: implications for Alzheimer's disease. *Neurotoxicity Research,* 5**,** 515-519.

PORTER, K., HIRT, J., STAMER, W. D. & LITON, P. B. 2015. Autophagic dysregulation in glaucomatous trabecular meshwork cells. *Biochimica et Biophysica Acta (BBA)-Molecular Basis of Disease,* 1852**,** 379-385.

PORTER, K., LIN, Y. & LITON, P. B. 2013. Cathepsin B is up-regulated and mediates extracellular matrix degradation in trabecular meshwork cells following phagocytic challenge. *PloS one,* 8**,** e68668.

PRABHU, S. V., BHATTACHARYYA, S., GUZMAN-HARTMAN, G., MACIAS, V., KAJDACSY-BALLA, A. & TOBACMAN, J. K. 2011. Extra-lysosomal localization of arylsulfatase B in human colonic epithelium. *Journal of Histochemistry & Cytochemistry,* 59**,** 328-335.

PRENDES, M. A., HARRIS, A., WIROSTKO, B. M., GERBER, A. L. & SIESKY, B. 2013. The role of transforming growth factor β in glaucoma and the therapeutic implications. *British Journal of Ophthalmology,* 97**,** 680-686.

PROVENZANO, P. P., INMAN, D. R., ELICEIRI, K. W., TRIER, S. M. & KEELY, P. J. 2008. Contact guidance mediated three-dimensional cell migration is regulated by Rho/ROCK-dependent matrix reorganization. *Biophysical Journal,* 95**,** 5374-5384.

PRZEDBORSKI, S. 2010. Inflammation and Parkinson's disease pathogenesis. *Movement Disorders,* 25**,** S55-S57.

QIU, P., KURPAKUS-WHEATER, M. & SOSNE, G. 2007. Matrix metalloproteinase activity is necessary for thymosin beta 4 promotion of epithelial cell migration. *Journal of Cellular Physiology,* 212**,** 165-173.

RAMACHANDRAN, C., PATIL, R. V., COMBRINK, K., SHARIF, N. A. & SRINIVAS, S. P. 2011. Rho-Rho kinase pathway in the actomyosin contraction and cell-matrix adhesion in immortalized human trabecular meshwork cells. *Molecular Vision,* 17**,** 1877-1890.

RANKIN, S. J., WALMAN, B. E., BUCKLEY, A. R. & DRANCE, S. M. 1995. Color Doppler imaging and spectral analysis of the optic nerve vasculature in glaucoma. *American Journal of Ophthalmology,* 119**,** 685-693.

RAO, P. V., DENG, P. F., KUMAR, J. & EPSTEIN, D. L. 2001. Modulation of Aqueous Humor Outflow Facility by the Rho Kinase–Specific Inhibitor Y-27632. *Investigative Ophthalmology & Visual Science,* 42**,** 1029-1037.

RAO, P. V., DENG, P., SASAKI, Y. & EPSTEIN, D. L. 2005. Regulation of myosin light chain phosphorylation in the trabecular meshwork: role in aqueous humour outflow facility. *Experimental Eye Research,* 80**,** 197-206.

RAO, R. V., POKSAY, K. S., CASTRO-OBREGON, S., SCHILLING, B., ROW, R. H., DEL RIO, G., GIBSON, B. W., ELLERBY, H. M. & BREDESEN, D. E. 2004. Molecular components of a cell death pathway activated by endoplasmic reticulum stress. *Journal of Biological Chemistry,* 279**,** 177-187.

REARDON, G., KOTAK, S. & SCHWARTZ, G. F. 2011. Objective assessment of compliance and persistence among patients treated for glaucoma and ocular hypertension: a systematic review. *Patient Preference and Adherence,* 5**,** 441.

REN, H., BAO, H., ENDO, H. & HAYASHI, T. 2001. Antioxidative and antimicrobial activities and flavonoid contents of organically cultivated vegetables. *Journal of the Japanese Society for Food Science and Technology (Japan)*.

REN, R., LI, G., LE, T. D., KOPCZYNSKI, C., STAMER, W. D. & GONG, H. 2016. Netarsudil increases outflow facility in human eyes through multiple mechanisms. *Investigative Ophthalmology & Visual Science,* 57**,** 6197-6209.

RHEE, S. G., CHANG, T. S., BAE, Y. S., LEE, S. R. & KANG, S. W. 2003. Cellular regulation by hydrogen peroxide. *Journal of the American Society of Nephrology,* 14**,** S211-S215.

RICE-EVANS, C. A., MILLER, N. J. & PAGANGA, G. 1996. Structure-antioxidant activity relationships of flavonoids and phenolic acids. *Free radical biology and medicine,* 20**,** 933-956.

ROBERTSON, J. V., GOLESIC, E., GAULDIE, J. & WEST-MAYS, J. A. 2010. Ocular gene transfer of active TGF-β induces changes in anterior segment morphology and elevated IOP in rats. *Investigative Ophthalmology & Visual Science,* 51**,** 308-318.

ROHEN, J. W., KAUFMAN, P. L., EICHHORN, M., GOECKNER, P. A. & BITO, L. Z. 1989. Functional morphology of accommodation in the raccoon. *Experimental Eye Research,* 48**,** 523-7.

ROSENQUIST, R., EPSTEIN, D., MELAMED, S., JOHNSON, M. & GRANT, W. M. 1989. Outflow resistance of enucleated human eyes at two different perfusion pressures and different extents of trabeculotomy. *Current Eye Research,* 8**,** 1233-1240.

ROSENTHAL, R., CHORITZ, L., SCHLOTT, S., BECHRAKIS, N. E., JAROSZEWSKI, J., WIEDERHOLT, M. & THIEME, H. 2005. Effects of ML-7 and Y-27632 on carbachol- and endothelin-1-induced contraction of bovine trabecular meshwork. *Experimental Eye Research,* 80**,** 837-845.

ROY CHOWDHURY, U., HANN, C. R., STAMER, W. D. & FAUTSCH, M. P. 2015. Aqueous humor outflow: dynamics and disease. *Investigative Ophthalmology & Visual Science,* 56**,** 2993-3003.

RUIZ-EDERRA, J. & VERKMAN, A. S. 2006. Mouse model of sustained elevation in intraocular pressure produced by episcleral vein occlusion. *Experimental Eye Research,* 82**,** 879-884.

SABANAY, I., B'ANN, T. G., TIAN, B., KAUFMAN, P. L. & GEIGER, B. 2000. H-7 effects on the structure and fluid conductance of monkey trabecular meshwork. *Archives of Ophthalmology,* 118**,** 955-962.

SACCA, S. C., GANDOLFI, S., BAGNIS, A., MANNI, G., DAMONTE, G., TRAVERSO, C. E. & IZZOTTI, A. 2016. From DNA damage to functional changes of the trabecular meshwork in aging and glaucoma. *Ageing Research Reviews,* 29**,** 26-41.

SACCÀ, S. C., PASCOTTO, A., CAMICIONE, P., CAPRIS, P. & IZZOTTI, A. 2005. Oxidative DNA damage in the human trabecular meshwork: clinical correlation in patients with primary open-angle glaucoma. *Archives of Ophthalmology,* 123**,** 458-463.

SAHU, B. D., KUMAR, J. M., KUNCHA, M., BORKAR, R. M., SRINIVAS, R. & SISTLA, R. 2016. Baicalein alleviates doxorubicin-induced cardiotoxicity via suppression of myocardial oxidative stress and apoptosis in mice. *Life Sciences,* 144**,** 8-18.

SAHU, B. D., KUMAR, J. M. & SISTLA, R. 2015. Baicalein, a bioflavonoid, prevents cisplatin-induced acute kidney injury by up-regulating antioxidant defenses and down-regulating the MAPKs and NF-κB pathways. *PloS one,* 10**,** e0134139.

SAIKUMAR, P., DONG, Z., MIKHAILOV, V., DENTON, M., WEINBERG, J. M. & VENKATACHALAM, M. A. 1999. Apoptosis: definition, mechanisms, and relevance to disease. *The American Journal of Medicine,* 107**,** 489-506.

SARRAFCHI, A., BAHMANI, M., SHIRZAD, H. & RAFIEIAN-KOPAEI, M. 2016. Oxidative stress and Parkinson's disease: new hopes in treatment with herbal antioxidants. *Current Pharmaceutical Design,* 22**,** 238-246.

SATO, T. & ROY, S. 2002. Effect of high glucose on fibronectin expression and cell proliferation in trabecular meshwork cells. *Investigative Ophthalmology & Visual Science,* 43**,** 170-175.

SCHEHLEIN, E. M. & ROBIN, A. L. 2019. Rho-associated kinase inhibitors: evolving strategies in glaucoma treatment. *Drugs,* 79**,** 1031-1036.

SCHLÖTZER-SCHREHARDT, U., LOMMATZSCH, J. R., KÜCHLE, M., KONSTAS, A. G. & NAUMANN, G. O. 2003. Matrix metalloproteinases and their inhibitors in aqueous humor of patients with pseudoexfoliation syndrome/glaucoma and primary open-angle glaucoma. *Investigative Ophthalmology & Visual Science,* 44**,** 1117-1125.

SCHMIDT-ROHR, K. 2020. Oxygen Is the High-Energy Molecule Powering Complex Multicellular Life: Fundamental Corrections to Traditional Bioenergetics. *ACS omega,* 5**,** 2221-2233.

SCHUMAN, J. S., CHANG, W., WANG, N., DE KATER, A. W. & ALLINGHAM, R. 1999. Excimer laser effects on outflow facility and outflow pathway morphology. *Investigative Ophthalmology & Visual Science,* 40**,** 1676-1680.

SCHWEIGER, D., FURSTENBERGER, G. & KRIEG, P. 2007. Inducible expression of 15-lipoxygenase-2 and 8-lipoxygenase inhibits cell growth via common signaling pathways. *Journal of Lipid Research,* 48**,** 553-64.

SEHI, M., FLANAGAN, J. G., ZENG, L., COOK, R. J. & TROPE, G. E. 2005. Relative change in diurnal mean ocular perfusion pressure: a risk factor for the diagnosis of primary open-angle glaucoma. *Investigative Ophthalmology & Visual Science,* 46**,** 561-567.

SENIOR, A. E. 1988. ATP synthesis by oxidative phosphorylation. *Physiological Reviews,* 68**,** 177-231.

SETHI, A., MAO, W., WORDINGER, R. J. & CLARK, A. F. 2011. Transforming growth factor–β induces extracellular matrix protein cross-linking lysyl oxidase (LOX) genes in human trabecular meshwork cells. *Investigative Ophthalmology & Visual Science,* 52**,** 5240-5250.

SHA, O. & KWONG, W. 2006. Postnatal developmental changes of vitreous and lens volumes in Sprague-Dawley rats. *Neuroembryology and Aging,* 4**,** 183-188.

SHAHIDULLAH, M., MANDAL, A. & DELAMERE, N. A. 2017. Src Family Kinase Links Insulin Signaling to Short Term Regulation of Na,K-ATPase in Nonpigmented Ciliary Epithelium. *Journal of Cellular Physiology,* 232**,** 1489-1500.

SHAHIDULLAH, M., WILSON, W. S., YAP, M. & TO, C. H. 2003. Effects of ion transport and channel-blocking drugs on aqueous humor formation in isolated bovine eye. *Investigative Ophthalmology & Visual Science,* 44**,** 1185-1191.

SHAO, Z. H., LI, C. Q., VANDEN HOEK, T. L., BECKER, L. B., SCHUMACKER, P. T., WU, J. A., ATTELE, A. S. & YUAN, C.-S. 1999. Extract from Scutellaria

baicalensis Georgi Attenuates Oxidant Stress in Cardiomyocytes. *Journal of Molecular and Cellular Cardiology,* 31**,** 1885-1895.

SHI, Y. & MASSAGUÉ, J. 2003. Mechanisms of TGF-β signaling from cell membrane to the nucleus. *Cell,* 113**,** 685-700.

SHIOMI, T., LEMAÎTRE, V., D'ARMIENTO, J. & OKADA, Y. 2010. Matrix metalloproteinases, a disintegrin and metalloproteinases, and a disintegrin and metalloproteinases with thrombospondin motifs in non-neoplastic diseases. *Pathology International,* 60**,** 477-496.

SIHOTA, R., SAXENA, R., GOGOI, M., SOOD, A., GULATI, V. & PANDEY, R. 2005. A comparison of the circadian rhythm of intraocular pressure in primary chronic angle closure glaucoma, primary open angle glaucoma and normal eyes. *Indian Journal of Ophthalmology,* 53**,** 243.

SLATER, B. J., MEHRABIAN, Z., GUO, Y., HUNTER, A. & BERNSTEIN, S. L. 2008. Rodent anterior ischemic optic neuropathy (rAION) induces regional retinal ganglion cell apoptosis with a unique temporal pattern. *Investigative Ophthalmology & Visual Science,* 49**,** 3671-3676.

SMITH, R. S., ZABALETA, A., SAVINOVA, O. V. & JOHN, S. W. 2001. The mouse anterior chamber angle and trabecular meshwork develop without cell death. *BMC Developmental Biology,* 1**,** 1-14.

SOMLYO, A. P. & SOMLYO, A. V. 2000. Signal transduction by G-proteins, rho-kinase and protein phosphatase to smooth muscle and non-muscle myosin II. *The Journal of Physiology,* 522**,** 177-185.

SOMMER, A., TIELSCH, J. M., KATZ, J., QUIGLEY, H. A., GOTTSCH, J. D., JAVITT, J. & SINGH, K. 1991. Relationship between intraocular pressure and primary open angle glaucoma among white and black Americans: the Baltimore Eye Survey. *Archives of ophthalmology,* 109**,** 1090-1095.

SONESSON, B., ROSENGREN, E., HANSSON, A. S. & HANSSON, C. 2003. UVB-induced inflammation gives increased d-dopachrome tautomerase activity in blister fluid which correlates with macrophage migration inhibitory factor. *Experimental Dermatology,* 12**,** 278-282.

SOTO, D., COMES, N., FERRER, E., MORALES, M., ESCALADA, A., PALÉS, J., SOLSONA, C., GUAL, A. & GASULL, X. 2004. Modulation of aqueous humor outflow by ionic mechanisms involved in trabecular meshwork cell volume regulation. *Investigative Ophthalmology & Visual Science,* 45**,** 3650-3661.

SOWNDHARARAJAN, K., DEEPA, P., KIM, M., PARK, S. J. & KIM, S. 2017. Baicalein as a potent neuroprotective agent: A review. *Biomedicine & Pharmacotherapy,* 95**,** 1021-1032.

SRINIVASAN, S., CHOUDHARI, N., BASKARAN, M., GEORGE, R., SHANTHA, B. & VIJAYA, L. 2016. Diurnal intraocular pressure fluctuation and its risk factors in angle-closure and open-angle glaucoma. *Eye,* 30**,** 362.

STAMER, W. D. 2012. The cell and molecular biology of glaucoma: mechanisms in the conventional outflow pathway. *Investigative Ophthalmology & Visual Science,* 53**,** 2470-2472.

STAMER, W. D. & ACOTT, T. S. 2012. Current understanding of conventional outflow dysfunction in glaucoma. *Current Opinion in Ophthalmology,* 23**,** 135-143.

STAMER, W. D., BRAAKMAN, S. T., ZHOU, E. H., ETHIER, C. R., FREDBERG, J. J., OVERBY, D. R. & JOHNSON, M. 2015. Biomechanics of Schlemm's canal endothelium and intraocular pressure reduction. *Progress in Retinal and Eye Research,* 44**,** 86-98.

STAMER, W. D., HOFFMAN, E., LUTHER, J., HACHEY, D. & SCHEY, K. 2011. Protein profile of exosomes from trabecular meshwork cells. *Journal of Proteomics,* 74**,** 796-804.

STAMER, W. D., ROBERTS, B. C., EPSTEIN, D. L. & ALLINGHAM, R. R. 2000. Isolation of primary open-angle glaucomatous trabecular meshwork cells from whole eye tissue. *Current Eye Research,* 20**,** 347-350.

STAMER, W. D., SEFTOR, R. E., WILLIAMS, S. K., SAMAHA, H. A. & SNYDER, R. W. 1995. Isolation and culture of human trabecular meshwork cells by extracellular matrix digestion. *Current Eye Research,* 14**,** 611-617.

STEVE ROZEN, A. U., MAIDO REMM, TRIINU KORESSAAR AND HELEN SKALETSKY. *primer3web suite* [Online]. Available: http://primer3.ut.ee/ [Accessed 2019].

STEWART, W. C. & GARRISON, P. M. 1998. β-Blocker–Induced Complications and the Patient With Glaucoma: Newer Treatments to Help Reduce Systemic Adverse Events. *Archives of Internal Medicine,* 158**,** 221-226.

STRICKLAND, I., RHODES, L. E., FLANAGAN, B. F. & FRIEDMANN, P. S. 1997. TNF-α and IL-8 are upregulated in the epidermis of normal human skin after UVB exposure: correlation with neutrophil accumulation and E-selectin expression. *Journal of Investigative Dermatology,* 108.

STROBER, W. 2015. Trypan blue exclusion test of cell viability. *Current Protocols in Immunology,* 111**,** A3. B. 1-A3. B. 3.

STUMPFF, F., QUE, Y., BOXBERGER, M., STRAUSS, O. & WIEDERHOLT, M. 1999. Stimulation of maxi-K channels in trabecular meshwork by tyrosine kinase inhibitors. *Investigative Ophthalmology & Visual Science,* 40**,** 1404-1417.

SU, Y. L., LEUNG, L. K., BI, Y. R., HUANG, Y. & CHEN, Z. Y. 2000. Antioxidant activity of flavonoids isolated from Scutellaria rehderiana. *Journal of the American Oil Chemists' Society,* 77**,** 807-813.

SUGRUE, M. F. 2000. Pharmacological and ocular hypotensive properties of topical carbonic anhydrase inhibitors. *Progress in Retinal and Eye Research,* 19**,** 87-112.

SUMIDA, G. M. & STAMER, W. D. 2010. Sphingosine-1-phosphate enhancement of cortical actomyosin organization in cultured human Schlemm's canal endothelial cell monolayers. *Investigative Ophthalmology & Visual Science,* 51**,** 6633-8.

SUN, H., CHE, Q. M., ZHAO, X. & PU, X. P. 2010. Antifibrotic effects of chronic baicalein administration in a CCl4 liver fibrosis model in rats. *European Journal of Pharmacology,* 631**,** 53-60.

SWAMINATHAN, S. S., OH, D. J., KANG, M. H. & RHEE, D. J. 2014. Aqueous outflow: segmental and distal flow. *Journal of Cataract & Refractive Surgery,* 40**,** 1263-1272.

TAHARA, E. B., NAVARETE, F. D. & KOWALTOWSKI, A. J. 2009. Tissue-, substrate-, and site-specific characteristics of mitochondrial reactive oxygen species generation. *Free Radical Biology and Medicine,* 46**,** 1283-1297.

TAKAI, Y., TANITO, M. & OHIRA, A. 2012. Multiplex cytokine analysis of aqueous humor in eyes with primary open-angle glaucoma, exfoliation glaucoma, and cataract. *Investigative Ophthalmology & Visual Science,* 53**,** 241-247.

TAMM, E. R. 2009. The trabecular meshwork outflow pathways: structural and functional aspects. *Experimental Eye Research,* 88**,** 648-655.

TAMM, E. R., SIEGNER, A., BAUR, A. & LÜTJEN-DRECOLL, E. 1996. Transforming growth factor-β1 induces α-smooth muscle-actin expression in cultured human and monkey trabecular meshwork. *Experimental Eye Research,* 62**,** 389-398.

TANIHARA, H., INOUE, T., YAMAMOTO, T., KUWAYAMA, Y., ABE, H., SUGANAMI, H. & ARAIE, M. 2015. Additive intraocular pressure–lowering effects of the Rho kinase inhibitor ripasudil (K-115) combined with timolol or latanoprost: a report of 2 randomized clinical trials. *JAMA Ophthalmology,* 133**,** 755-761.

TAURONE, S., RIPANDELLI, G., PACELLA, E., BIANCHI, E., PLATEROTI, A. M., DE VITO, S., PLATEROTI, P., GRIPPAUDO, F. R., CAVALLOTTI, C. & ARTICO, M. 2015. Potential regulatory molecules in the human trabecular meshwork of patients with glaucoma: immunohistochemical profile of a number of inflammatory cytokines. *Molecular Medicine Reports,* 11**,** 1384-1390.

TEKTAS, O. Y. & LÜTJEN-DRECOLL, E. 2009. Structural changes of the trabecular meshwork in different kinds of glaucoma. *Experimental Eye Research,* 88**,** 769-775.

TEZEL, G. L. N., LI, L. Y., PATIL, R. V. & WAX, M. B. 2001. TNF-α and TNF-α receptor-1 in the retina of normal and glaucomatous eyes. *Investigative Ophthalmology & Visual Science,* 42**,** 1787-1794.

THAM, Y. C., LI, X., WONG, T. Y., QUIGLEY, H. A., AUNG, T. & CHENG, C. Y. 2014. Global prevalence of glaucoma and projections of glaucoma burden through 2040: a systematic review and meta-analysis. *Ophthalmology,* 121**,** 2081-2090.

THE AGIS INVESTIGATORS 2000. The Advanced Glaucoma Intervention Study (AGIS): 7. The relationship between control of intraocular pressure and visual field deterioration. *American Journal of Ophthalmology,* 130**,** 429-40.

THIEME, H., NASS, J. U., NUSKOVSKI, M., BECHRAKIS, N. E., STUMPFF, F., STRAUSS, O. & WIEDERHOLT, M. 1999. The Effects of Protein Kinase C on Trabecular Meshwork and Ciliary Muscle Contractility. *Investigative Ophthalmology & Visual Science,* 40**,** 3254-3261.

THIEME, H., NUSKOVSKI, M., NASS, J. U., PLEYER, U., STRAUSS, O. & WIEDERHOLT, M. 2000. Mediation of calcium-independent contraction in trabecular meshwork through protein kinase C and rho-A. *Investigative Ophthalmology & Visual Science,* 41**,** 4240-4246.

TO, C. H., KONG, C. W., CHAN, C. Y., SHAHIDULLAH, M. & DO, C. W. 2002. The mechanism of aqueous humour formation. *Clinical and Experimental Optometry,* 85**,** 335-349.

TOKUSHIGE, H., INATANI, M., NEMOTO, S., SAKAKI, H., KATAYAMA, K., UEHATA, M. & TANIHARA, H. 2007. Effects of topical administration of y-39983, a selective rho-associated protein kinase inhibitor, on ocular tissues in rabbits and monkeys. *Investigative Ophthalmology & Visual Science,* 48**,** 3216-3222.

TORIS, C. B., B'ANN, T. G. & KAUFMAN, P. L. 2008. Update on the mechanism of action of topical prostaglandins for intraocular pressure reduction. *Survey of Ophthalmology,* 53**,** S107-S120.

TORIS, C. B. & CAMRAS, C. B. 1998. Aqueous Humor Dyamics II Clinical Studies. *In:* CIVAN, M. M. (ed.) *The eye's aqueous humor : from secretion to glaucoma.* San Diego: Academic Press.

TORIS, C. B., YABLONSKI, M. E., WANG, Y.-L. & CAMRAS, C. B. 1999. Aqueous humor dynamics in the aging human eye. *American Journal of Ophthalmology,* 127**,** 407-412.

TOWNSEND, D. J. & BRUBAKER, R. F. 1980. Immediate effect of epinephrine on aqueous formation in the normal human eye as measured by fluorophotometry. *Investigative Ophthalmology & Visual Science,* 19**,** 256-66.

TSAI, M. J., WU, P. C., HUANG, Y. B., CHANG, J. S., LIN, C. L., TSAI, Y. H. & FANG, J. Y. 2012. Baicalein loaded in tocol nanostructured lipid carriers (tocol NLCs) for enhanced stability and brain targeting. *International Journal of Pharmaceutics,* 423**,** 461-470.

TU, B., LI, R. R., LIU, Z. J., CHEN, Z. F., OUYANG, Y. & HU, Y. J. 2016. Structure-activity relationship study between baicalein and wogonin by spectrometry, molecular docking and microcalorimetry. *Food Chemistry,* 208**,** 192-198.

TURNER, M. D., NEDJAI, B., HURST, T. & PENNINGTON, D. J. 2014. Cytokines and chemokines: at the crossroads of cell signalling and inflammatory disease. *Biochimica et Biophysica Acta (BBA)-Molecular Cell Research,* 1843**,** 2563-2582.

UEDA, J., WENTZ-HUNTER, K. & YUE, B. Y. 2002. Distribution of myocilin and extracellular matrix components in the juxtacanalicular tissue of human eyes. *Investigative Ophthalmology & Visual Science,* 43**,** 1068-1076.

UEDA, J. & YUE, B. Y. 2003. Distribution of myocilin and extracellular matrix components in the corneoscleral meshwork of human eyes. *Investigative Ophthalmology & Visual Science,* 44**,** 4772-9.

VALDERRAMA, C. M., LI, R. & LIU, J. H. 2008. Direct effect of light on 24-h variation of aqueous humor protein concentration in Sprague–Dawley rats. *Experimental Eye Research,* 87**,** 487-491.

VAN BUSKIRK, E. 1977. Trabeculotomy in the immature, enucleated human eye. *Investigative Ophthalmology & Visual Science,* 16**,** 63-66.

VECINO, E., GALDÓS, M., BAYÓN, A., RODRÍGUEZ, F., MICÓ, C. & SHARMA, S. 2015. Elevated intraocular pressure induces ultrastructural changes in the trabecular meshwork. *Journal of Cytology & Histology,* 3**,** 1.

VEERAPPAN, M., CHAK, G., SHIEH, C. & CHALLA, P. 2017. Atypical presentation of acute angle-closure glaucoma in Maroteaux-Lamy mucopolysaccharidosis with patent prophylactic laser peripheral Iridotomy: A case report. *The Permanente Journal,* 21.

VITO, P., LACANA, E. & D'ADAMIO, L. 1996. Interfering with apoptosis: Ca2+-binding protein ALG-2 and Alzheimer's disease gene ALG-3. *Science,* 271**,** 521-525.

VOHRA, R., TSAI, J. C. & KOLKO, M. 2013. The role of inflammation in the pathogenesis of glaucoma. *Survey of Ophthalmology,* 58**,** 311-320.

VRANKA, J. A., KELLEY, M. J., ACOTT, T. S. & KELLER, K. E. 2015. Extracellular matrix in the trabecular meshwork: intraocular pressure regulation and dysregulation in glaucoma. *Experimental Eye Research,* 133**,** 112-125.

WANG, L., LING, Y., CHEN, Y., LI, C. L., FENG, F., YOU, Q. D., LU, N. & GUO, Q. L. 2010a. Flavonoid baicalein suppresses adhesion, migration and invasion of MDA-MB-231 human breast cancer cells. *Cancer Letters,* 297**,** 42-48.

WANG, N., XIE, X., YANG, D., XIAN, J., LI, Y., REN, R., PENG, X., JONAS, J. B. & WEINREB, R. N. 2012. Orbital cerebrospinal fluid space in glaucoma: the Beijing intracranial and intraocular pressure (iCOP) study. *Ophthalmology,* 119**,** 2065-2073. e1.

WANG, P., HENNING, S. M. & HEBER, D. 2010b. Limitations of MTT and MTS-Based Assays for Measurement of Antiproliferative Activity of Green Tea Polyphenols. *PloS one,* 5**,** e10202.

WANG, Q., WEI, Y. & ZHANG, J. 2017. Combined knockdown of D-dopachrome tautomerase and migration inhibitory factor inhibits the proliferation, migration, and invasion in human cervical cancer. *International Journal of Gynecologic Cancer,* 27**,** 634-642.

WANG, S. C., CHAI, D. S., CHEN, C. B., WANG, Z. Y. & WANG, L. 2015a. HPIP promotes thyroid cancer cell growth, migration and EMT through activating PI3K/AKT signaling pathway. *Biomedicine & Pharmacotherapy,* 75**,** 33-39.

WANG, S. Y., WANG, H. H., CHI, C. W., CHEN, C. F. & LIAO, J. F. 2004. Effects of baicalein on β-amyloid peptide-(25–35)-induced amnesia in mice. *European Journal of Pharmacology,* 506**,** 55-61.

WANG, W., ZHOU, P. H., XU, C. G., ZHOU, X. J., HU, W. & ZHANG, J. 2015b. Baicalein attenuates renal fibrosis by inhibiting inflammation via down-regulating NF-κB and MAPK signal pathways. *Journal of Molecular Histology,* 46**,** 283-290.

WANG, Y., LI, F. & WANG, S. 2016. MicroRNA‐93 is overexpressed and induces apoptosis in glaucoma trabecular meshwork cells. *Molecular Medicine Reports,* 14**,** 5746-5750.

WANG, Y. H., YU, H. T., PU, X. P. & DU, G. H. 2013. Baicalein prevents 6-hydroxydopamine-induced mitochondrial dysfunction in SH-SY5Y cells via inhibition of mitochondrial oxidation and up-regulation of DJ-1 protein expression. *Molecules,* 18**,** 14726-14738.

WAX, M. B. & TEZEL, G. 2009. Immunoregulation of retinal ganglion cell fate in glaucoma. *Experimental Eye Research,* 88**,** 825-830.

WEINREB, R. N., AUNG, T. & MEDEIROS, F. A. 2014. The pathophysiology and treatment of glaucoma: a review. *JAMA Ophthalmology,* 311**,** 1901-1911.

WEINREB, R. N. & KHAW, P. T. 2004. Primary open-angle glaucoma. *The Lancet,* 363**,** 1711-1720.

WELGE-LÜßEN, U., MAY, C. A. & LÜTJEN-DRECOLL, E. 2000. Induction of tissue transglutaminase in the trabecular meshwork by TGF-β1 and TGF-β2. *Investigative Ophthalmology & Visual Science,* 41**,** 2229-2238.

WHEELER, A. P. & RIDLEY, A. J. 2004. Why three Rho proteins? RhoA, RhoB, RhoC, and cell motility. *Experimental Cell Research,* 301**,** 43-49.

WIEDERHOLT, M., BIELKA, S., SCHWEIG, F., LÜTJEN-DRECOLL, E. & LEPPLE-WIENHUES, A. 1995. Regulation of outflow rate and resistance in the perfused anterior segment of the bovine eye. *Experimental Eye Research,* 61**,** 223-234.

WIEDERHOLT, M., GROTH, J. & STRAUSS, O. 1998. Role of protein tyrosine kinase on regulation of trabecular meshwork and ciliary muscle contractility. *Investigative Ophthalmology & Visual Science,* 39**,** 1012-1020.

WIEDERHOLT, M., THIEME, H. & STUMPFF, F. 2000. The regulation of trabecular meshwork and ciliary muscle contractility. *Progress in Retinal and Eye Research,* 19**,** 271-295.

WILD, J. M., ROBSON, C. R., JONES, A. L., CUNLIFFE, I. A. & SMITH, P. E. 2006. Detecting vigabatrin toxicity by imaging of the retinal nerve fiber layer. *Investigative Ophthalmology & Visual Science,* 47**,** 917-924.

WILHELM, J. & PINGOUD, A. 2003. Real-time polymerase chain reaction. *Chembiochem,* 4**,** 1120-1128.

WILHELM, M., SCHLEGL, J., HAHNE, H., MOGHADDAS GHOLAMI, A., LIEBERENZ, M., SAVITSKI, M. M., ZIEGLER, E., BUTZMANN, L., GESSULAT, S., MARX, H., MATHIESON, T., LEMEER, S., SCHNATBAUM, K., REIMER, U., WENSCHUH, H., MOLLENHAUER, M., SLOTTA-HUSPENINA, J., BOESE, J. H., BANTSCHEFF, M., GERSTMAIR, A., FAERBER, F. & KUSTER, B. 2014. Mass-spectrometry-based draft of the human proteome. *Nature,* 509**,** 582-7.

WILLCOX, J. K., ASH, S. L. & CATIGNANI, G. L. 2004. Antioxidants and prevention of chronic disease. *Critical Reviews in Food Science and Nutrition,* 44**,** 275-295.

WORLD HEALTH ORGANIZATION. 2020. *Vision impairment and blindness* [Online]. Available: https://www.who.int/en/news-room/fact-sheets/detail/blindness-and-visual-impairment [Accessed 24/11/20 2020].

XIAO, J. 2015. *The effects of baicalein on chloride transport and aqueous humour formation of porcine ciliary epithelium.* Degree of Doctor of Philosophy, The Hong Kong Polytechnic University

XIAO, J. R., DO, C. W. & TO, C. H. 2014. Potential therapeutic effects of baicalein, baicalin, and wogonin in ocular disorders. *Journal of Ocular Pharmacology and Therapeutics,* 30**,** 605-614.

XUE, Y., LI, H., ZHANG, Y., HAN, X., ZHANG, G., LI, W., ZHANG, H., LIN, Y., CHEN, P. & SUN, X. 2018. Natural and synthetic flavonoids, novel blockers of the volume-regulated anion channels, inhibit endothelial cell proliferation. *Pflügers Archiv-European Journal of Physiology,* 470**,** 1473-1483.

YANAGI, M., KAWASAKI, R., WANG, J. J., WONG, T. Y., CROWSTON, J. & KIUCHI, Y. 2011. Vascular risk factors in glaucoma: a review. *Clinical & Experimental Ophthalmology,* 39**,** 252-258.

YANG, C. Y. C., LIU, Y., LU, Z., REN, R. & GONG, H. 2013. Effects of Y27632 on Aqueous Humor Outflow Facility With Changes in Hydrodynamic Pattern and

Morphology in Human Eyes. *Investigative Ophthalmology & Visual Science,* 54**,** 5859-5870.

YANG, J., ZHANG, Z., LIN, J., LU, J., LIU, B. F., ZENG, S. & LUO, Q. 2007. Detection of MMP activity in living cells by a genetically encoded surface-displayed FRET sensor. *Biochimica et Biophysica Acta (BBA) - Molecular Cell Research,* 1773**,** 400-407.

YANG, Y. F., SUN, Y. Y., ACOTT, T. S. & KELLER, K. E. 2016. Effects of induction and inhibition of matrix cross-linking on remodeling of the aqueous outflow resistance by ocular trabecular meshwork cells. *Scientific Reports,* 6**,** 30505.

YANTORNO, R. E., COCA-PRADOS, M., KRUPIN, T. & CIVAN, M. M. 1989. Volume regulation of cultured, transformed, non-pigmented epithelial cells from human ciliary body. *Experimental Eye Research,* 49**,** 423-437.

YEE, A. J., AKENS, M., YANG, B. L., FINKELSTEIN, J., ZHENG, P. S., DENG, Z. & YANG, B. 2007. The effect of versican G3 domain on local breast cancer invasiveness and bony metastasis. *Breast Cancer Research,* 9**,** 1-11.

YU, T. W. & ANDERSON, D. 1997. Reactive oxygen species-induced DNA damage and its modification: a chemical investigation. *Mutation Research/Fundamental and Molecular Mechanisms of Mutagenesis,* 379**,** 201-210.

YUE, G. G. L., YIP, T. W. N., HUANG, Y. & KO, W. H. 2004. Cellular mechanism for potentiation of Ca2+-mediated Cl–secretion by the flavonoid baicalein in intestinal epithelia. *Journal of Biological Chemistry,* 279**,** 39310-39316.

ZEIMER, R. C., WILENSKY, J. T., GIESER, D. K. & VIANA, M. A. 1991. Association between intraocular pressure peaks and progression of visual field loss. *Ophthalmology,* 98**,** 64-69.

ZHANG, S., YE, J. & DONG, G. 2010. Neuroprotective effect of baicalein on hydrogen peroxide-mediated oxidative stress and mitochondrial dysfunction in PC12 cells. *Journal of Molecular Neuroscience,* 40**,** 311-320.

ZHANG, X., YANG, Y., DU, L., ZHANG, W. & DU, G. 2017. Baicalein exerts anti-neuroinflammatory effects to protect against rotenone-induced brain injury in rats. *International Immunopharmacology,* 50**,** 38-47.

ZHANG, Y. & HUANG, W. 2018. Transforming Growth Factor β1 (TGF-β1)-Stimulated Integrin-Linked Kinase (ILK) Regulates Migration and Epithelial-Mesenchymal Transition (EMT) of Human Lens Epithelial Cells via Nuclear Factor κB (NF-κB). *Medical Science Monitor,* 24**,** 7424-7430.

ZHAO, L., XU, G., ZHOU, J., XING, H., WANG, S., WU, M., LU, Y. P. & MA, D. 2006. The effect of RhoA on human umbilical vein endothelial cell migration and angiogenesis in vitro. *Oncology Reports,* 15**,** 1147-1152.

ZHAO, Q., CHEN, X. Y. & MARTIN, C. 2016. Scutellaria baicalensis, the golden herb from the garden of Chinese medicinal plants. *Science Bulletin,* 61**,** 1391-1398.

ZHAO, X., RAMSEY, K. E., STEPHAN, D. A. & RUSSELL, P. 2004. Gene and protein expression changes in human trabecular meshwork cells treated with transforming growth factor-β. *Investigative Ophthalmology & Visual Science,* 45**,** 4023-4034.

ZHOU, L., LI, Y. & YUE, B. Y. 1999. Oxidative stress affects cytoskeletal structure and cell-matrix interactions in cells from an ocular tissue: The trabecular meshwork. *Journal of Cellular Physiology,* 180**,** 182-189.

ZHOU, L., TAN, S., SHAN, Y. L., WANG, Y. G., CAI, W., HUANG, X. H., LIAO, X. Y., LI, H. Y., ZHANG, L. & ZHANG, B. J. 2016. Baicalein improves behavioral dysfunction induced by Alzheimer's disease in rats. *Neuropsychiatric Disease and Treatment,* 12**,** 3145.

ZITKA, O., KUKACKA, J., KRIZKOV, S., HUSKA, D., ADAM, V., MASARIK, M., PRUSA, R. & KIZEK, R. 2010. Matrix metalloproteinases. *Current Medicinal Chemistry,* 17**,** 3751-3768.

ZOHRABIAN, V. M., FORZANI, B., CHAU, Z., MURALI, R. & JHANWAR-UNIYAL, M. 2009. Rho/ROCK and MAPK signaling pathways are involved in glioblastoma cell migration and proliferation. *Anticancer Research,* 29**,** 119-123.

Supplementary Tables

Supplementary Table 1. A full list of proteins with altered expression after baicalein treatment for 3 hours (47 proteins in total).

GN	Protein (UniProt Accession)	Δ	*p*
NAGA	Alpha-N-acetylgalactosaminidase (P17050)	0.2 ±0.0	0.001
PBXIP1	Pre-B-cell leukemia transcription factor-interacting protein 1 (Q96AQ6)	0.4 ±0.1	0.018
SAE1	Isoform 3 of SUMO-activating enzyme subunit 1 (Q9UBE0-3)	0.4 ±0.0	0.004
BCAP29	Isoform 2 of B-cell receptor-associated protein 29 (Q9UHQ4-2)	0.5 ±0.1	0.022
AKR1B10	Aldo-keto reductase family 1 member B10 (O60218)	0.5 ±0.1	0.027
PSMD10	26S proteasome non-ATPase regulatory subunit 10 (O75832)	0.5 ±0.0	0.005
PDCD6	Programmed cell death protein 6 (O75340)	0.5 ±0.1	0.011
XRCC6	X-ray repair cross-complementing protein 6 (P12956)	0.6 ±0.1	0.048
DDT	D-dopachrome decarboxylase (P30046)	0.6 ±0.0	0.000
MANF	Mesencephalic astrocyte-derived neurotrophic factor (P55145)	0.6 ±0.1	0.015
ARPC1A	Actin-related protein 2/3 complex subunit 1A (Q92747)	0.6 ±0.1	0.044
MIF	Macrophage migration inhibitory factor (P14174)	0.7 ±0.0	0.015
KLC1	Isoform I of Kinesin light chain 1 (Q07866-9)	0.7 ±0.1	0.038
DAB2	Disabled homolog 2 (P98082)	0.7 ±0.1	0.050
CYB5R3	NADH-cytochrome b5 reductase 3 (P00387)	0.8 ±0.0	0.009
GMFB	Glia maturation factor beta (P60983)	0.8 ±0.0	0.000
PRDX4	Peroxiredoxin-4 (Q13162)	0.8 ±0.0	0.001
LAMB1	Laminin subunit beta-1 (P07942)	0.8 ±0.0	0.001
USP9X	Probable ubiquitin carboxyl-terminal hydrolase FAF-X (Q93008)	0.9 ±0.0	0.009
PSMA3	Proteasome subunit alpha type-3 (P25788)	0.9 ±0.0	0.017
DLD	Dihydrolipoyl dehydrogenase, mitochondrial (P09622)	1.0 ±0.0	0.021
UQCRC2	Cytochrome b-c1 complex subunit 2, mitochondrial (P22695)	1.0 ±0.0	0.035
NNMT	Nicotinamide N-methyltransferase (P40261)	1.1 ±0.0	0.014
DLST	Dihydrolipoyllysine-residue succinyltransferase component of 2-oxoglutarate dehydrogenase complex, mitochondrial (P36957)	1.1 ±0.0	0.013
RPL23A	60S ribosomal protein L23a (P62750)	1.1 ±0.0	0.010
MMP14	Matrix metalloproteinase-14 (P50281)	1.1 ±0.0	0.031
OXSR1	Serine/threonine-protein kinase OSR1 (O95747)	1.2 ±0.0	0.010
PRDX1	Peroxiredoxin-1 (Q06830)	1.2 ±0.0	0.022
LIMA1	LIM domain and actin-binding protein 1 (Q9UHB6)	1.2 ±0.0	0.023

HIST1H2BK	Histone H2B type 1-K (O60814)	1.2 ±0.0	0.013
AHCYL1	S-adenosylhomocysteine hydrolase-like protein 1 (O43865)	1.3 ±0.0	0.030
TUFM	Elongation factor Tu, mitochondrial (P49411)	1.3 ±0.1	0.038
ATP5O	ATP synthase subunit O, mitochondrial (P48047)	1.3 ±0.1	0.048
EML4	Echinoderm microtubule-associated protein-like 4 (Q9HC35)	1.3 ±0.1	0.032
RUVBL2	RuvB-like 2 (Q9Y230)	1.3 ±0.1	0.031
RBMX	RNA-binding motif protein, X chromosome (P38159)	1.3 ±0.1	0.042
ACTA2	Actin, aortic smooth muscle (P62736)	1.4 ±0.0	0.006
CTSB	Cathepsin B (P07858)	1.5 ±0.0	0.009
PA2G4	Proliferation-associated protein 2G4 (Q9UQ80)	1.5 ±0.1	0.018
CARS	Isoform 3 of Cysteine--tRNA ligase, cytoplasmic (P49589-3)	1.5 ±0.1	0.047
PDHB	Pyruvate dehydrogenase E1 component subunit beta, mitochondrial (P11177)	1.6 ±0.1	0.022
SLC25A3	Isoform B of Phosphate carrier protein, mitochondrial (Q00325-2)	1.8 ±0.1	0.037
XPNPEP1	Xaa-Pro aminopeptidase 1 (Q9NQW7)	2.1 ±0.2	0.030
TLR7	Toll-like receptor 7 (Q9NYK1)	2.2 ±0.1	0.014
PFDN6	Prefoldin subunit 6 (O15212)	2.7 ±0.2	0.012
CPA4	Carboxypeptidase A4 (Q9UI42)	3.1 ±0.1	0.003
MGARP	Protein MGARP (Q8TDB4)	3.8 ±0.5	0.035

GN: Gene Name; Δ: Fold change (treatment/ control) (Mean ± SEM); p: p-value.

Supplementary Table 2. A full list of proteins with altered expression after baicalein treatment for 2 days (119 proteins in total).

GN	Protein (UniProt Accession)	Δ	*p*
RPL37A	60S ribosomal protein L37a (P61513)	0.3 ±0.1	0.013
COPS5	COP9 signalosome complex subunit 5 (Q92905)	0.4 ±0.1	0.023
AHSG	Alpha-2-HS-glycoprotein (P02765)	0.4 ±0.1	0.041
FDXR	NADPH:adrenodoxin oxidoreductase, mitochondrial (P22570)	0.5 ±0.1	0.015
ALB	Serum albumin (P02768)	0.5 ±0.1	0.033
SOD1	Superoxide dismutase [Cu-Zn] (P00441)	0.5 ±0.1	0.045
CCDC37	Cilia- and flagella-associated protein 100 (Q494V2)	0.6 ±0.0	0.006
BASP1	Brain acid soluble protein 1 (P80723)	0.6 ±0.0	0.004
CLIC4	Chloride intracellular channel protein 4 (Q9Y696)	0.6 ±0.0	0.009
EMC4	Isoform 3 of ER membrane protein complex subunit 4 (Q5J8M3-3)	0.6 ±0.1	0.024
NAGK	N-acetyl-D-glucosamine kinase (Q9UJ70)	0.7 ±0.1	0.040
AP2A1	AP-2 complex subunit alpha-1 (O95782)	0.7 ±0.1	0.026
SMPD4	Isoform 4 of Sphingomyelin phosphodiesterase 4 (Q9NXE4-4)	0.7 ±0.1	0.049
NMT1	Glycylpeptide N-tetradecanoyltransferase 1 (P30419)	0.7 ±0.1	0.026
PURA	Transcriptional activator protein Pur-alpha (Q00577)	0.7 ±0.0	0.003
SCRN1	Secernin-1 (Q12765)	0.7 ±0.1	0.040
TMSB4X	Thymosin beta-4 (P62328)	0.7 ±0.0	0.022
IRGQ	Immunity-related GTPase family Q protein (Q8WZA9)	0.7 ±0.1	0.047
PRKCSH	Glucosidase 2 subunit beta (P14314)	0.7 ±0.0	0.007
GAP43	Neuromodulin (P17677)	0.7 ±0.0	0.022
RAB14	Ras-related protein Rab-14 (P61106)	0.8 ±0.0	0.018
TMOD2	Tropomodulin-2 (Q9NZR1)	0.8 ±0.0	0.026
SLC25A4	ADP/ATP translocase 1 (P12235)	0.8 ±0.0	0.004
BAG3	BAG family molecular chaperone regulator 3 (O95817)	0.8 ±0.0	0.043
SLC25A3	Isoform B of Phosphate carrier protein, mitochondrial (Q00325-2)	0.8 ±0.0	0.032
LMAN2	Vesicular integral-membrane protein VIP36 (Q12907)	0.8 ±0.0	0.022
RPL28	60S ribosomal protein L28 (P46779)	0.8 ±0.0	0.025
RPS12	40S ribosomal protein S12 (P25398)	0.8 ±0.0	0.014
GDI2	Rab GDP dissociation inhibitor beta (P50395)	0.8 ±0.0	0.022
TPI1	Triosephosphate isomerase (P60174)	0.8 ±0.0	0.035
PDIA3	Protein disulfide-isomerase A3 (P30101)	0.8 ±0.0	0.025
DKC1	H/ACA ribonucleoprotein complex subunit DKC1 (O60832)	0.8 ±0.0	0.017
TUBB	Tubulin beta chain (P07437)	0.8 ±0.0	0.041

EPHA2	Ephrin type-A receptor 2 (P29317)	0.8 ±0.0	0.047
LSM2	U6 snRNA-associated Sm-like protein LSm2 (Q9Y333)	0.8 ±0.0	0.017
GYG1	Glycogenin-1 (P46976)	0.8 ±0.0	0.005
ITGB1	Integrin beta-1 (P05556)	0.8 ±0.0	0.013
PRDX6	Peroxiredoxin-6 (P30041)	0.8 ±0.0	0.024
ILK	Integrin-linked protein kinase (Q13418)	0.8 ±0.0	0.044
UPF1	Regulator of nonsense transcripts 1 (Q92900)	0.8 ±0.0	0.016
FKBP11	Peptidyl-prolyl cis-trans isomerase FKBP11 (Q9NYL4)	0.8 ±0.0	0.042
BDH2	3-hydroxybutyrate dehydrogenase type 2 (Q9BUT1)	0.8 ±0.0	0.048
NDUFB10	NADH dehydrogenase [ubiquinone] 1 beta subcomplex subunit 10 (O96000)	0.8 ±0.0	0.005
HINT2	Histidine triad nucleotide-binding protein 2, mitochondrial (Q9BX68)	0.9 ±0.0	0.024
PDIA4	Protein disulfide-isomerase A4 (P13667)	0.9 ±0.0	0.009
RPLP0	60S acidic ribosomal protein P0 (P05388)	0.9 ±0.0	0.035
ATP5A1	ATP synthase subunit alpha, mitochondrial (P25705)	0.9 ±0.0	0.000
CD151	CD151 antigen (P48509)	0.9 ±0.0	0.026
RHOA	Transforming protein RhoA (P61586)	0.9 ±0.0	0.019
HADHA	Trifunctional enzyme subunit alpha, mitochondrial (P40939)	0.9 ±0.0	0.044
NME1-NME2	Isoform 3 of Nucleoside diphosphate kinase B (P22392-2)	0.9 ±0.0	0.041
RAB9A	Ras-related protein Rab-9A (P51151)	0.9 ±0.0	0.047
CNN3	Calponin-3 (Q15417)	0.9 ±0.0	0.036
PSMA1	Proteasome subunit alpha type-1 (P25786)	0.9 ±0.0	0.044
SF3B1	Splicing factor 3B subunit 1 (O75533)	0.9 ±0.0	0.032
HSPA4	Heat shock 70 kDa protein 4 (P34932)	0.9 ±0.0	0.007
CYB5R3	NADH-cytochrome b5 reductase 3 (P00387)	0.9 ±0.0	0.001
ASS1	Argininosuccinate synthase (P00966)	0.9 ±0.0	0.036
ALDH18A1	Delta-1-pyrroline-5-carboxylate synthase (P54886)	0.9 ±0.0	0.038
BAG2	BAG family molecular chaperone regulator 2 (O95816)	0.9 ±0.0	0.046
UBA1	Ubiquitin-like modifier-activating enzyme 1 (P22314)	0.9 ±0.0	0.033
ATP6V1A	V-type proton ATPase catalytic subunit A (P38606)	0.9 ±0.0	0.033
DCTN4	Dynactin subunit 4 (Q9UJW0)	0.9 ±0.0	0.010
MYOF	Myoferlin (Q9NZM1)	0.9 ±0.0	0.019
GAPDHS	Glyceraldehyde-3-phosphate dehydrogenase, testis-specific (O14556)	0.9 ±0.0	0.013
HADH	Hydroxyacyl-coenzyme A dehydrogenase, mitochondrial (Q16836)	0.9 ±0.0	0.029
STAT6	Signal transducer and activator of transcription 6 (P42226)	0.9 ±0.0	0.013
DNM2	Dynamin-2 (P50570)	0.9 ±0.0	0.022
ERP44	Endoplasmic reticulum resident protein 44 (Q9BS26)	0.9 ±0.0	0.050

LTA4H	Leukotriene A-4 hydrolase (P09960)	1.0 ±0.0	0.013
RPL27	60S ribosomal protein L27 (P61353)	1.0 ±0.0	0.036
ACSL4	Long-chain-fatty-acid--CoA ligase 4 (O60488)	1.0 ±0.0	0.037
ATP5J	ATP synthase-coupling factor 6, mitochondrial (P18859)	1.0 ±0.0	0.048
SLC16A2	Monocarboxylate transporter 8 (P36021)	1.0 ±0.0	0.006
GAPDH	Glyceraldehyde-3-phosphate dehydrogenase (P04406)	1.0 ±0.0	0.038
NT5E	5'-nucleotidase (P21589)	1.0 ±0.0	0.020
RPN1	Dolichyl-diphosphooligosaccharide--protein glycosyltransferase subunit 1 (P04843)	1.0 ±0.0	0.008
QDPR	Dihydropteridine reductase (P09417)	1.0 ±0.0	0.008
AHNAK	Neuroblast differentiation-associated protein AHNAK (Q09666)	1.0 ±0.0	0.037
CPPED1	Serine/threonine-protein phosphatase CPPED1 (Q9BRF8)	1.0 ±0.0	0.034
MYH9	Myosin-9 (P35579)	1.0 ±0.0	0.037
FLNA	Isoform 2 of Filamin-A (P21333-2)	1.0 ±0.0	0.037
AP2B1	AP-2 complex subunit beta (P63010)	1.0 ±0.0	0.037
COPB2	Coatomer subunit beta' (P35606)	1.0 ±0.0	0.037
AARS	Alanine--tRNA ligase, cytoplasmic (P49588)	1.0 ±0.0	0.038
OAT	Ornithine aminotransferase, mitochondrial (P04181)	1.0 ±0.0	0.036
AMPD3	AMP deaminase 3 (Q01432)	1.0 ±0.0	0.008
CAP2	Adenylyl cyclase-associated protein 2 (P40123)	1.1 ±0.0	0.004
WASF2	Wiskott-Aldrich syndrome protein family member 2 (Q9Y6W5)	1.1 ±0.0	0.028
H2AFV	Histone H2A.V (Q71UI9)	1.1 ±0.0	0.031
COX5B	Cytochrome c oxidase subunit 5B, mitochondrial (P10606)	1.1 ±0.0	0.004
ALDH1L2	Mitochondrial 10-formyltetrahydrofolate dehydrogenase (Q3SY69)	1.1 ±0.0	0.037
DDRGK1	DDRGK domain-containing protein 1 (Q96HY6)	1.1 ±0.0	0.035
GNA13	Guanine nucleotide-binding protein subunit alpha-13 (Q14344)	1.1 ±0.0	0.047
PSMC6	26S proteasome regulatory subunit 10B (P62333)	1.1 ±0.0	0.042
LYPLA2	Acyl-protein thioesterase 2 (O95372)	1.1 ±0.0	0.023
TMEM14C	Transmembrane protein 14C (Q9P0S9)	1.1 ±0.0	0.034
LMNB1	Lamin-B1 (P20700)	1.1 ±0.0	0.040
UQCRH	Cytochrome b-c1 complex subunit 6, mitochondrial (P07919)	1.2 ±0.0	0.046
NSF	Vesicle-fusing ATPase (P46459)	1.2 ±0.0	0.027
EIF3I	Eukaryotic translation initiation factor 3 subunit I (Q13347)	1.2 ±0.0	0.036
NAGA	Alpha-N-acetylgalactosaminidase (P17050)	1.2 ±0.0	0.014
SLC25A5	ADP/ATP translocase 2 (P05141)	1.2 ±0.0	0.033
PTMS	Parathymosin (P20962)	1.2 ±0.0	0.012

PSMC1	26S proteasome regulatory subunit 4 (P62191)	1.2 ±0.0	0.001
CCDC154	Coiled-coil domain-containing protein 154 (A6NI56)	1.2 ±0.0	0.034
PRKDC	DNA-dependent protein kinase catalytic subunit (P78527)	1.2 ±0.0	0.025
YKT6	Synaptobrevin homolog YKT6 (O15498)	1.2 ±0.0	0.029
MTHFD1	C-1-tetrahydrofolate synthase, cytoplasmic (P11586)	1.3 ±0.1	0.048
SORBS2	Isoform 11 of Sorbin and SH3 domain-containing protein 2 (O94875-11)	1.3 ±0.0	0.008
DLG1	Disks large homolog 1 (Q12959)	1.3 ±0.1	0.042
AP1M1	Isoform 2 of AP-1 complex subunit mu-1 (Q9BXS5-2)	1.3 ±0.1	0.038
SERBP1	Plasminogen activator inhibitor 1 RNA-binding protein (Q8NC51)	1.3 ±0.0	0.014
AOC3	Membrane primary amine oxidase (Q16853)	1.3 ±0.0	0.004
ARSB	Arylsulfatase B (P15848)	1.3 ±0.0	0.009
LEPRE1	Prolyl 3-hydroxylase 1 (Q32P28)	1.4 ±0.1	0.024
C14orf166	RNA transcription, translation and transport factor protein (Q9Y224)	1.5 ±0.1	0.024
AGPAT1	1-acyl-sn-glycerol-3-phosphate acyltransferase alpha (Q99943)	1.9 ±0.2	0.047
EFTUD2	116 kDa U5 small nuclear ribonucleoprotein component (Q15029)	2.3 ±0.3	0.045

GN: Gene Name; Δ: Fold change (treatment/ control) (Mean ± SEM); *p*: *p*-value.

Supplementary Table 3. A list of downstream molecules associated with upstream regulator (TGFB1) of hTM cells after baicalein treatment (29 proteins in total).

GN	Protein (UniProt Accession)	Δ	*p*
PSMC1	26S proteasome regulatory subunit 4 (P62191)	1.2 ±0.0	0.001
GNA13	Guanine nucleotide-binding protein subunit alpha-13 (Q14344)	1.1 ±0.0	0.047
FLNA	Isoform 2 of Filamin-A (P21333-2)	1.0 ±0.0	0.037
MYH9	Myosin-9 (P35579)	1.0 ±0.0	0.037
AHNAK	Neuroblast differentiation-associated protein AHNAK (Q09666)	1.0 ±0.0	0.037
NT5E	5'-nucleotidase (P21589)	1.0 ±0.0	0.020
LTA4H	Leukotriene A-4 hydrolase (P09960)	1.0 ±0.0	0.013
STAT6	Signal transducer and activator of transcription 6 (P42226)	0.9 ±0.0	0.013
HADH	Hydroxyacyl-coenzyme A dehydrogenase, mitochondrial (Q16836)	0.9 ±0.0	0.029
MYOF	Myoferlin (Q9NZM1)	0.9 ±0.0	0.019
ALDH18A1	Delta-1-pyrroline-5-carboxylate synthase (P54886)	0.9 ±0.0	0.038
ASS1	Argininosuccinate synthase (P00966)	0.9 ±0.0	0.036
GNAI2	Guanine nucleotide-binding protein G(i) subunit alpha-2 (P04899)	0.9 ±0.0	0.052
CNN3	Calponin-3 (Q15417)	0.9 ±0.0	0.036
RAB9A	Ras-related protein Rab-9A (P51151)	0.9 ±0.0	0.047
NME2	Isoform 3 of Nucleoside diphosphate kinase B (P22392-2)	0.9 ±0.0	0.041
GLS	Isoform 3 of Glutaminase kidney isoform, mitochondrial (O94925)	0.9 ±0.0	0.060
RHOA	Transforming protein RhoA (P61586)	0.9 ±0.0	0.019
ILK	Integrin-linked protein kinase (Q13418)	0.8 ±0.0	0.044
ITGB1	Integrin beta-1 (P05556)	0.8 ±0.0	0.013
GYG1	Glycogenin-1 (P46976)	0.8 ±0.0	0.005
LSM2	U6 snRNA-associated Sm-like protein LSm2 (Q9Y333)	0.8 ±0.0	0.017
EPHA2	Ephrin type-A receptor 2 (P29317)	0.8 ±0.0	0.047
DKC1	H/ACA ribonucleoprotein complex subunit DKC1 (O60832)	0.8 ±0.0	0.017
SLC25A4	ADP/ATP translocase 1 (P12235)	0.8 ±0.0	0.004
ITGA3	Integrin alpha-3 (P26006)	0.7 ±0.1	0.051
CLIC4	Chloride intracellular channel protein 4 (Q9Y696)	0.6 ±0.0	0.009
ALB	Serum albumin (P02768)	0.5 ±0.1	0.033
FDXR	NADPH:adrenodoxin oxidoreductase, mitochondrial (P22570)	0.5 ±0.1	0.015

GN: Gene Name; Δ: Fold change (treatment/ control) (Mean ± SEM); *p*: *p*-value.